



<https://theses.gla.ac.uk/>

Theses Digitisation:

<https://www.gla.ac.uk/myglasgow/research/enlighten/theses/digitisation/>

This is a digitised version of the original print thesis.

Copyright and moral rights for this work are retained by the author

A copy can be downloaded for personal non-commercial research or study, without prior permission or charge

This work cannot be reproduced or quoted extensively from without first obtaining permission in writing from the author

The content must not be changed in any way or sold commercially in any format or medium without the formal permission of the author

When referring to this work, full bibliographic details including the author, title, awarding institution and date of the thesis must be given

Enlighten: Theses

<https://theses.gla.ac.uk/>
research-enlighten@glasgow.ac.uk

**Control of endoderm development in
*Caenorhabditis elegans***

Caroline Clucas

Wellcome Centre for Molecular Parasitology
Anderson College
University of Glasgow
56 Dumbarton Road
Glasgow
G11 6NU

This Thesis is presented in submission for the degree of Doctor of Philosophy
in the faculty of Veterinary Medicine

January 2003

ProQuest Number: 10390757

All rights reserved

INFORMATION TO ALL USERS

The quality of this reproduction is dependent upon the quality of the copy submitted.

In the unlikely event that the author did not send a complete manuscript and there are missing pages, these will be noted. Also, if material had to be removed, a note will indicate the deletion.



ProQuest 10390757

Published by ProQuest LLC (2017). Copyright of the Dissertation is held by the Author.

All rights reserved.

This work is protected against unauthorized copying under Title 17, United States Code
Microform Edition © ProQuest LLC.

ProQuest LLC.
789 East Eisenhower Parkway
P.O. Box 1346
Ann Arbor, MI 48106 – 1346

GLASGOW
UNIVERSITY
LIBRARY

12957
copy. 2

Declaration

I declare that the work presented in this thesis is my own except where otherwise stated. This thesis contains unique work and will not be submitted for any other degree, diploma or qualification at any other university.

Caroline Clucas

January 2003

Acknowledgements

I would like to thank Dr. Iain Johnstone, my supervisor, for all of his help and encouragement over the last few years. I would also like to thank other members of the worm lab, both past in present, and in particular Dr. Brett Roberts and Dr. Laura McMahon. I also acknowledge my assessors Prof. Eileen Devancy and Dr Collette Britton and thank them for their advice. I also wish to thank people from the 'non-worm' lab for their chats.

I would like to thank members of the Schnabel lab for their help in the cell lineage analysis. I also acknowledge Mario deBono for the ICB4 antibody, Joel Rothman for JR1838 strain, Jim McGhee for the plasmid pJM67 and Neville Ashcroft for discussing unpublished work.

Above all, I would like to thank my husband Iain for all his hugs and support and daughter Gemma, who always makes me smile on a rainy day. Special thanks also to all my friends and family for the baby-sitting duties (especially both mums, Pauline and Karen) and my parents, who have always encouraged me.

Abbreviations

APC	adenomatous polypolis coli protein
CE	<i>C. elegans</i>
CB	<i>C. briggsae</i>
cdc	cell-division cycle
Cdk	cyclin-dependent kinase
DIC	differential interference contrast
DNA	deoxyribonucleic acid
ds	double stranded
Df	Deficiency
EMS	Ethyl methanesulphonate
GFP	green fluorescent protein
GSK3 β	glycogen synthase kinase 3 β
mRNA	messenger ribonucleic acid
NLK	Nemo-like kinase
PCR	polymerase chain reaction
RNA	ribonucleic acid
RNAi	RNA-mediated interference
rpm	revolutions per minute
RT-PCR	reverse transcription polymerase chain reaction
ss	single stranded
STS	sequence-tagged site
ts	temperature sensitive
UV	ultraviolet
UTR	untranslated region
YAC	yeast artificial chromosome

Measurements

bp	base pair
cm	centimetre
kb	kilobase
kDa	kilodalton
Mb	megabase
mg	milligram
μ g	microgram
ng	nanogram
mm	millimetre
μ m	micrometre
nm	nanometre
h	hour
min	minute
L	litre
ml	millilitre
μ l	microlitre
M	Molar
mM	milliMolar
nM	nanoMolar
V	volt

Contents

Declaration	i
Acknowledgements	ii
Abbreviations	iii
Contents	iv
Abstract	xii

Chapter 1

General introduction

1.1.	The Phylum Nematoda	1
1.2.	<i>C.elegans</i> biology	2
1.2.1.	The life-cycle of <i>C. elegans</i>	2
1.2.2.	The cell lineage of <i>C. elegans</i>	2
1.2.3.	The genetics of <i>C. elegans</i>	3
1.2.4.	The anatomy of <i>C.elegans</i>	4
1.2.5.	The <i>C.elegans</i> physical map and genomic sequence	6
1.2.6.	<i>C.elegans</i> as an experimental system	7
1.3.	Embryogenesis	8
1.3.1	Specification of endoderm	10
1.3.2.	The roles of the maternal proteins, SKN-1, PIE-1 and PAL-1	11
1.3.3.	Wnt signalling	11
1.3.4.	GATA factors and the E-cell cycle	15
1.3.5.	Post-embryonic development of the intestine	16
1.4.	Project aims and objectives	16

Figures for Chapter 1

Figure 1.1	Cartoon representation of the anatomy of <i>C.elegans</i>	1
Figure 1.2	Summary of events during embryogenesis	9
Figure 1.3	Early cell lineage tree	9
Figure 1.4	Wild type E-cell lineage	10
Figure 1.5	Wnt signalling in the early <i>C.elegans</i> embryo	14

Chapter 2

Materials and Methods

2.1.	Chemical abbreviations	17
2.2.	Commonly used stocks, solutions and media	18
2.3.	<i>C. elegans</i> and bacterial strains	21
2.3.1.	<i>C.elegans</i> strains	21
2.3.2	Bacterial strains	23
2.4.	Vectors and Clones	24
2.4.1.	Plasmid vectors	24
2.4.2	Clones	25
2.4.2.1.	Plasmid clones	25
2.5	Culture maintenance	26
2.5.1.	Bacterial Culture	26
2.5.1.1.	Bacterial Culture on solid media	26
2.5.1.2.	Liquid Culture of Bacteria	26
2.6.	General Molecular Biology Techniques	26

2.6.1.	Agarose gel electrophoresis of DNA	26
2.6.2.	Restriction Endonuclease Digests	27
2.6.3.	Ligation reactions	27
2.6.4.	Purification of PCR-amplified and gel isolated DNA fragments	27
2.6.5.	Transformation of <i>E. coli</i>	28
2.6.6.	Screening of transformed colonies	28
2.6.6.1.	Colony PCR	28
2.6.6.2.	Colony lysis	29
2.7.	DNA preparation	29
2.7.1.	Isolation of <i>C. elegans</i> genomic DNA	29
2.7.2.	Plasmid and Cosmid DNA mini preparation	30
2.8.	DNA Sequencing	30
2.8.1.	DNA sequencing of PCR fragments	30
2.8.2.	DNA Sequencing of Plasmid clones	31
2.9.	<i>C. elegans</i> Culture	31
2.9.1.	Maintenance of transgenic strains containing a free array	32
2.9.2.	Maintenance of strains carrying a sterile or lethal mutation	32
2.10.	Mutagenesis using Ethyl methanesulphonate (EMS)	32
2.10.1.	FMS Treatment	32
2.10.2.	Non-clonal F2 Mutant Screen	33
2.10.3.	Screening for mutants with intestinal lineage defects	33
2.11.	Classical Genetic mapping	33
2.11.1.	Generation of Males	33
2.11.2.	Setting up genetic crosses	34
2.11.3.	Chromosome assignment by classical mapping	34
2.11.4.	Multi-factor crosses	34
2.12.	Sequence Tagged Sites (STS) mapping	35
2.13.	Physical mapping of <i>hDf8</i> using PCR based approach	37
2.14.	Generation of <i>C. elegans</i> transgenic strains by microinjection	39
2.14.1.	Preparation of materials and worms for microinjection	39
2.15.	Gamma ray-induced integration of extrachromosomal arrays	41
2.15.1.	Identification of integrated lines	42
2.16.	RNA-mediated interference (RNAi)	42
2.16.1.	Generating the target DNA fragment using PCR	42
2.16.2.	<i>In vitro</i> transcription	44
2.16.3.	Annealing reaction	44
2.16.4.	Examination of phenocopies produced by RNAi	45
2.16.5.	RNAi administered by bacterial feeding method	45
2.17.	Microscopy of live and fixed specimens	46
2.17.1.	Nomarski and fluorescence optics used in microscopy of live and fixed specimens	46
2.17.2.	Preparation of slides for observations of living embryos, larvae and adults	46
2.17.2.1.	Preparations of slides for short term microscopy of live larvae and adults	47
2.17.2.2.	Preparation of slides for time course observations of live embryos	47
2.17.3.	Preparation of slides for immuno-fluorescence staining	47
2.17.3.1.	Permeabilisation of embryo specimens on slides by freeze-crack Method	47
2.17.3.2.	Fixation of embryos on slides	48

2.17.3.3.	DAPI staining of fixed specimens	48
2.17.3.4.	Antibody staining of fixed embryos	48
2.18.	Cell lineage analysis	49
2.19.	Transgenesis with <i>cdc-25.1(tj48)</i>	51

Tables for Chapter 2

Table 2.1	<i>C.elegans</i> strains	22
Table 2.2	Bacterial strains	23
Table 2.3	Cloning vectors	24
Table 2.4	Plasmid clones	24
Table 2.5	Cosmid clones	25
Table 2.6	PCR cocktail for colony PCR	28
Table 2.7	Cycling Parameters for Colony PCR	28
Table 2.8	Primers used for Sequencing K06A5.7a	31
Table 2.9	STS PCR reaction cocktail	35
Table 2.10	Reaction parameters for single worm/embryo PCR	35
Table 2.11	Primers used for STS mapping	36
Table 2.12	Primers for mapping left-hand breakpoint of <i>hDf8</i>	38
Table 2.13	Transformation material	40
Table 2.14	Components of reaction mix for generating template for <i>in vitro</i> transcription	42
Table 2.15	Cycling parameters for PCR for generating template for <i>in vitro</i> transcription	43
Table 2.16	Primers used to generate DNA template for <i>in vitro</i> transcription	43
Table 2.17	Sequence and position of primers for RNAi K06A5.7a by feeding	46
Table 2.18	Antibodies used in immunofluorescence microscopy	49
Table 2.19	Primers designed for transgenesis with <i>cdc-25.1</i>	51
Table 2.20	Reaction parameters for amplifying <i>cdc-25.1</i>	51

Chapter 3

A genetic screen to identify genes involved in the execution of the E-cell lineage in *Caenorhabditis elegans*

3.1.	Introduction	52
3.2.	Background to E-cell specification and development	54
3.3.	Aims and Experimental approach	58
3.4.	Vector construction	60
3.5.	Generation of <i>C.elegans</i> lines containing <i>cpr-5</i> reporter constructs	64
3.5.1.	Transgenic lines of pCC5	64
3.5.2.	Transgenic lines of pCC7, pCC8 and pCC16	66
3.6.	Using excess genomic DNA as a carrier to prevent transgene silencing	66
3.7.	Isolation of integrated lines	67
3.8.	Characterisation of <i>cpr-5::GFP</i> expression in integrated lines	68
3.9.	Background to STS mapping	70
3.10.	Chromosomal assignment of <i>tjIs10</i>	71
3.11.	Generation of mutants using EMS	71
3.12.	Characterisation of intestinal mutants	72
3.12.1.	Class I. putative E lineage defect	72

3.12.2	Class II: mutant with mononucleate intestinal cells	75
3.12.2.1.	Mapping of <i>ij51</i>	78
3.12.3	Class III: Mutants with multinucleate cells	80
3.12.4.	Class IV: Mutant with abnormal gut morphology	83
3.13.	Discussion	86

Tables for Chapter 3

Table 3.1	Primers used in the amplification of <i>cpr-5</i> 5' flanking region	60
Table 3.2	Genotypes of integrated lines	67
Table 3.3	STS Chromosome assignment of <i>ijIs10</i>	71
Table 3.4	Classes of mutants identified	71
Table 3.5	STS chromosome assignment of the dominant allele <i>ij48</i>	72
Table 3.6	STS chromosome assignment of the recessive allele <i>ij52</i>	72
Table 3.7	STS Chromosome assignment of <i>ij51</i>	79
Table 3.8	Tabulated data of proposed recombination events between <i>ij51</i> and RW7000	79
Table 3.9	STS Chromosome assignment of <i>ij53</i>	85
Table 3.10	Tabulated data of proposed recombination events between <i>ij53</i> and RW7000	85

Figures for Chapter 3

Figure 3.1	Wild type E-cell lineage	55
Figure 3.2	Cartoon representation of the <i>C.elegans</i> intestine	57
Figure 3.3	Strategy for cloning of 1kb PCR-amplified <i>cpr-5</i> promoter fragment into pPD95.67 and pPD96.04	62
Figure 3.4	Strategy for cloning of 3kb PCR-amplified <i>cpr-5</i> promoter fragment into pPD96.04	63
Figure 3.5	Transgenic worms of pCC5 and pCC7	65
Figure 3.6	L4 and adult gut nuclei	69
Figure 3.7	Characterisation of <i>lin-60(ij48)</i>	73
Figure 3.8	Characterisation of <i>lin-62(ij52)</i>	74
Figure 3.9	Characterisation of <i>ij51</i>	77
Figure 3.10	Representative gel of STS mapping of <i>ij51</i> using chromosome III markers	79
Figure 3.11	Proposed recombination events between RW7000 and <i>ij51</i>	79
Figure 3.12	Characterisation of <i>ij49</i>	81
Figure 3.13	Characterisation of <i>ij50</i>	82
Figure 3.14	Characterisation of <i>ij53</i>	84
Figure 3.15	Representative gel of STS mapping of <i>ij53</i> using chromosome I markers	85
Figure 3.16	Proposed recombination events between RW7000 and <i>ij53</i>	85

Chapter 4.

Characterisation of *lin-60* and *lin-62*

4.1.	Introduction	91
4.2.	Phenotypic characterisation of <i>lin-60(ij48)</i>	92
4.2.1.	Gross phenotype of <i>lin-60(ij48)</i>	92
4.2.2.	Characterisation using terminally differentiated intestinal GFP markers	92

4.2.3.	Characterisation of <i>lin-60(ij48)</i> with MH27	93
4.2.4.	The E-cell lineage of <i>lin-60(ij48)</i> mutant embryos	95
4.2.5.	Characterisation of <i>lin-60(ij48)</i> using non-intestinal markers	100
4.3.	Genetic characterisation of the <i>ij48</i> allele	102
4.3.1.	The <i>ij48</i> allele identifies a maternal gene and is semi-dominant over wild-type	102
4.3.2.	Characterisation of <i>ij48</i> over the deficiencies <i>hDf8</i> and <i>qDf16</i>	104
4.4.	Mapping of <i>lin-60(ij48)</i>	108
4.4.1.	Linkage of <i>lin-60(ij48)</i> to chromosome I	108
4.4.2.	Multi-factor mapping of <i>lin-60(ij48)</i>	109
4.4.2.1.	<i>lin-60(ij48)/unc-73(e936) dpy-5(e61)</i> and <i>lin-60(ij48)/dpy-5(e61) unc-87(e1216)</i>	109
4.4.2.2.	<i>lin-60(ij48)/dpy-5(e61) air-1(h289) unc-13(e450)</i>	110
4.4.2.3.	<i>dpy-5(e61) let-607(h402) unc-13(e450)/lin-60(ij48)</i>	111
4.4.2.4.	<i>dpy-5(e61) let-602(h283) unc-13/lin-60(ij48)</i>	111
4.4.2.5.	<i>dpy-5(e61) let-382(h82) unc-13(e450)/lin-60(ij48)</i>	112
4.4.2.6.	<i>dpy-5(e61) let-608(h706)unc-13(e450)/lin-60(ij48)</i>	112
4.4.2.7.	<i>dpy-5(e61) let-604(h293) unc-13(e450)/lin-60(ij48)</i>	113
4.4.2.8.	Conclusion of the genetic mapping of <i>lin-60(ij48)</i>	113
4.5.	Characterisation of <i>lin-62(ij52)</i>	115
4.5.1.	Gross phenotype and genetics of <i>lin-62(ij52)</i>	115
4.5.2.	Characterisation of <i>lin-62(ij52)</i> using intestinal terminal differentiation markers	118
4.5.3.	Characterisation of <i>lin-62(ij52)</i> with ICB4	120
4.5.4.	E-Cell lineage of <i>lin-62(ij52)</i>	120
4.5.5.	Germline of <i>lin-62(ij52)</i>	120
4.6.	STS mapping of <i>lin-62(ij52)</i>	123
4.7.	Three-factor mapping of <i>lin-62(ij52)</i>	123
4.7.1.	<i>lin-62(ij52)/unc-5(e53) bli-6(sc16)</i>	123
4.7.2.	<i>lin-62(ij52)/bli-6(sc16) unc-24(e138)</i>	123
4.8.	Characterisation of <i>lin-62(ij52)/Df</i>	125
4.8.1.	<i>lin-62(ij52)/stDf7</i>	126
4.8.2.	<i>lin-62(ij52)/stDf8</i>	127
4.8.3.	<i>lin-62(ij52)/eDf18</i>	128
4.8.4.	<i>lin-62(ij52)/eDf19</i>	128
4.8.5.	Conclusion on the genetics of <i>lin-62(ij52)</i>	128
4.9.	Discussion	131

Tables for Chapter 4

Table 4.1	Analysis of phenotypes of F1 broods from <i>+/ij48</i> hermaphrodites	103
Table 4.2	Analysis of genotypes of F1 broods from <i>+/ij48</i> hermaphrodites	103
Table 4.3	Relationship between zygotic genotype and phenotype of progeny from <i>+/ij48</i> hermaphrodites	104
Table 4.4	% Phenotypes of total progeny from <i>lin-60(ij48)/hDf8</i>	105
Table 4.5	% Phenotypes of total progeny from <i>lin-60(ij48)/qDf16</i>	105
Table 4.6	Relating phenotype to zygotic genotype of F1 progeny from <i>lin-60(ij48)/hDf8</i> parent	106
Table 4.7	Relating phenotype to zygotic genotype of F1 progeny from <i>lin-60(ij48)/hDf8</i>	106

Table 4.8	Relating phenotype to zygotic genotype of F1 progeny from <i>lin-60(ij48)/qDf16</i> parent	106
Table 4.9	Relating phenotype to zygotic genotype of F1 progeny from <i>lin-60 (ij48)/qDf16</i> parent	106
Table 4.10	Multi-factor data for <i>dpy-5(e61) unc-87(e1216)/lin-60(ij48)</i>	109
Table 4.11	Multi-factor data for <i>unc-73(e936) dpy-5(e61)/lin-60(ij48)</i>	109
Table 4.12	Map positions of various lethal mutations used for mapping of <i>lin-60(ij48)</i>	110
Table 4.13	Multifactor data for <i>dpy-5(e61) air-1(h289) unc-13(e450)/lin-60(ij48)</i>	110
Table 4.14	Multifactor data for <i>dpy-5(e61) let-607(h402) unc-13(e450)/(lin-60(ij48)</i>	111
Table 4.15	Multifactor data for <i>dpy-5(e61) let-602(h283) unc-13(e450)/lin-60(ij48)</i>	111
Table 4.16	Multifactor data for <i>dpy-5(e61) let-382(h82) unc-13(e450)/lin-60(ij48)</i>	112
Table 4.17	Multifactor data for <i>dpy-5(e61) let-608(h706) unc-13(e450)/lin-60(ij48)</i>	112
Table 4.18	Multifactor data for <i>dpy-5(e61) let-604(h293) unc-13/lin-60(ij48)</i>	113
Table 4.19	Approximate map positions of <i>lin-60(ij48)</i> calculated from multi-factor data	113
Table 4.20	% death of F1 progeny of homozygotic <i>lin-62(ij52)</i> hermaphrodites	116
Table 4.21	Analysis of distribution of phenotypes from <i>+/lin-62(ij52)</i> heterozygotes	118
Table 4.22	Tabulated data of recombination events between <i>lin-62(ij52)</i> and RW7000	124
Table 4.23	Three-factor data for <i>lin-62(ij52)/unc-5(e53) bli-6(sc16)</i>	123
Table 4.24	Three-factor data for <i>lin-62(ij52)/bli-6(sc16) unc-24(e138)</i>	125
Table 4.25	Analysis of progeny from <i>lin-62(ij52)</i> X RW1324	126
Table 4.26	Analysis of progeny from <i>lin-62(ij52)</i> X RW1333	127
Table 4.27	Analysis of progeny from <i>lin-62(ij52)</i> X CB3823	128
Table 4.28	Analysis of progeny from <i>lin-62(ij52)</i> X CB3824	128

Figures for Chapter 4

Figure 4.1	Characterisation of <i>lin-60(ij48)</i>	94
Figure 4.2	The E-cell lineage in wild-type and <i>lin-60(ij48)</i>	97
Figure 4.3	E-cell lineage of <i>lin-60(ij48)</i>	98
Figure 4.4	Seam cells in <i>lin-60(ij48)</i>	101
Figure 4.5	The <i>lin-62(ij52)</i> gonad	101
Figure 4.6	Map position of <i>lin-60(ij48)</i>	114
Figure 4.7	Tails of <i>lin-62(ij52)</i>	117
Figure 4.8	Characterisation of <i>lin-62(ij52)</i>	119
Figure 4.9	E-cell lineage of <i>lin-62(ij52)</i>	121
Figure 4.10	<i>lin-62(ij52)</i> gonads	122
Figure 4.11	Representative gel of STS mapping of <i>lin-62(ij52)</i>	124
Figure 4.12	Proposed recombination events between <i>lin-62(ij52)</i> and RW7000	124
Figure 4.13	Map position of <i>lin-62(ij52)</i>	130

Chapter 5.

The cloning of *lin-60(ij48)*

5.1.	Introduction	136
5.2.	Mapping the left breakpoint of <i>hDf8</i>	139
5.3.	Positioning of <i>let-604(h293)</i> onto the <i>C. elegans</i> physical map	141
5.4.	RNA interference of genes in the <i>lin-60(ij48)</i> interval to suppress the <i>lin-60(ij48)</i> phenotype	145
5.4.1.	Background to RNA interference	145
5.4.2.	RNA interference of genes in the <i>lin-60(ij48)</i> region	147
5.5.	Sequencing of <i>cdc-25.1</i> from the <i>lin-60(ij48)</i> , wild-type and IA109 backgrounds	153
5.5.1.	Sequencing of <i>cdc-25.1</i> from the <i>lin-60(ij48)</i> background	153
5.5.2.	Sequencing of <i>cdc-25.1</i> in wild type and IA109 backgrounds	156
5.6.	A <i>HinFI</i> polymorphism is present in <i>lin-60(ij48)</i>	156
5.7.	Substitution of C→T at base 137 creates a predicted Ser→Phe amino acid change	158
5.8.	Ser ₄₆ is contained within a conserved domain	158
5.9.	DNA transformations with mutant <i>cdc-25.1(ij48)</i>	159
5.10.	Characterisation of RNAi of <i>cdc-25.1</i>	163
5.10.1.	Analysis of intestinal and hypodermal cell number from <i>cdc-25.1</i> RNAi lethal embryos	164
5.10.2.	Analysis of germline development in <i>cdc-25.1</i> RNAi	168
5.11.	Analysis of CDC-25.1 protein distribution on wild-type and <i>lin-60(ij48)</i>	170
5.12.	RNAi with <i>wee 1.1</i> and <i>wee 1.3</i>	173
5.13.	Discussion	174

Tables for Chapter 5

Table 5.1.	Number of predicted genes in <i>lin-60</i> interval	139
Table 5.2.	Restriction enzymes and predicted sizes of digested products of cosmids used to rescue <i>let-604</i>	144
Table 5.3.	Suppression of the <i>lin-60(ij48)</i> phenotype following injection with dsRNA corresponding to genes in the <i>lin-60(ij48)</i> area	149
Table 5.4	% of Dpy and Let phenotype following injection with F57B10.1 dsRNA	150
Table 5.5	Analysis of dead embryos and survivors following injection with <i>cdc-25.1</i> dsRNA	151
Table 5.6	Combinations of DNA fragments and primers used for sequencing <i>cdc-25.1</i>	154
Table 5.7	Predicted sizes of fragments from a PCR-amplified fragment containing <i>cdc-25.1</i> genomic sequence from N2 and IA123 DNA, following digestion with <i>HinFI</i>	157
Table 5.8	Transgenesis with <i>cdc-25.1(ij48)</i> fragment	161
Table 5.9.	Number of intestinal cells following <i>cdc-25.1</i> RNAi	164
Table 5.10.	Number of hypodermal cells following <i>cdc-25.1</i> RNAi	166

Figures for Chapter 5

Figure 5.1	Cosmid map of the <i>let-602/let-607</i> interval	138
Figure 5.2	Mapping left-hand breakpoint of <i>hDf8</i>	140

Figure 5.3	Positional information for <i>let-604(h293)</i>	143
Figure 5.4	Restriction digests of cosmids used in positioning <i>let-604</i> onto physical map	144
Figure 5.5	Agarose gel of RNA products from <i>in vitro</i> transcription	148
Figure 5.6	Dead embryo from F57B10.1 RNAi injections in <i>lin-60(ij48)</i> background	152
Figure 5.7	Dead embryo from K06A5.7a (<i>cdc-25.1</i>) RNAi injections in <i>lin-60(ij48)</i> background	152
Figure 5.8	Schematic diagram of <i>cdc-25.1</i> coding sequence showing positions and directions of sequencing primers	154
Figure 5.9	Sequencing trace from wild-type and <i>lin-60(ij48)</i>	155
Figure 5.10	<i>Hin</i> FI polymorphism present in <i>cdc-25.1</i> in <i>lin-60(ij48)</i> DNA	157
Figure 5.11	<i>Hin</i> FI restriction analysis	157
Figure 5.12.	Sequence comparison of the amino terminal regions of CDC-25.1 and CDC25.2 of <i>C.elegans</i> and CDC-25.1 of <i>C.briggsae</i>	159
Figure 5.13	Microscopy of rescued lines	162
Figure 5.14	Intestinal cells in embryos of wild-type, <i>lin-60(ij48)</i> and <i>cdc-25.1</i> RNAi	165
Figure 5.15	Hypodermal cells in embryos of wild-type and <i>cdc-25.1</i> RNAi	167
Figure 5.16	Gonads of adult hermaphrodites treated with <i>cdc-25.1</i> RNAi	169
Figure 5.17	Detection of the CDC-25.1 protein	172
Figure 5.18	The vertebrate cell cycle	176

Chapter 6.

Final discussion

6.1.	Summary of Results	179
6.2.	Lineage mutations causing defective E-cell lineage	179
6.2.1.	<i>lin-60(ij48)</i> is a maternal gene and identifies the cell cycle gene CDC-25.1	179
6.2.2.	The site of the <i>cdc-25.1(ij48)</i> lesion identifies a conserved motif which may be involved in its regulation	181
6.2.3	Other roles and functions of CDC25	184
6.2.3.	E-cell development of <i>cdc-25.1(ij48)</i> and <i>lin-62(ij52)</i> must be correctly coordinated with developmental cues	185
6.3.	Future Work	187
6.3.1.	Further genetic screens to identify mutants with an altered E-lineage	187
6.3.2.	Characterisation and cloning of mutants with mononucleate and binucleate cells	187
6.3.3.	Identification of molecules that bind to the SRDSG motif in CDC25	187
6.3.4.	The role of POP-1 in the E-cell lineage	188
6.3.5.	Cloning the gene identified by <i>lin-62(ij52)</i>	188
References		189
Appendix 1	Published paper containing work described in this thesis.	

Abstract

The intestine (or gut) of *Caenorhabditis elegans* consists of 20 cells and is exclusively derived from the E-cell blastomere, by a precise pattern of cell divisions. During post-embryonic development no cell divisions occur in the E-lineage. Instead a nuclear division occurs, such that most cells are binucleate. In addition, endoreduplication occurs once during each larval stage, resulting in a DNA content of 32C in adult intestinal cell nuclei. Although much research has focussed on E-cell specification, not much is known about genes involved in the execution of the E-cell lineage. In this thesis, I have identified and characterised 4 classes of mutants with various E-cell lineage defects. These are mutants with an altered E-cell lineage, a mutant that fails to execute the L1 nuclear division, mutants that undergo additional post-embryonic nuclear divisions, and a mutant with an abnormal gut morphology. Most of the work in this thesis focussed on the class with an altered E-cell lineage. Two independent genes were identified in this class, *lin-60(ij48)* and *lin-62(ij52)*, the behaviour of these mutant alleles is genetically very distinct. *lin-60* is a maternal gene and *ij48* is a gain-of-function allele whereas *lin-62* is a zygotic gene and *ij52* is a loss-of-function allele. By cell lineage analysis, I showed that extra intestinal cells were generated from the E blastomere in each mutant. Additionally, I have shown that the *ij48* lesion creates deregulation of the cell cycle in the E-cell lineage, resulting in a hyperplasia of intestinal cells, while other aspects of intestinal cell function are retained. Using a novel RNA-mediated interference (RNAi) approach, I cloned the wild-type copy of the gene identified by *lin-60(ij48)* and found that it encoded a previously identified homologue of the cell cycle control gene, Cdc25 (*cdc-25.1*). While gain of *cdc-25.1* created intestinal hyperplasia, loss of the wild-type *cdc-25.1* by RNAi caused a failure of proliferation of intestinal and other cell types. I found that the site of the *cdc-25.1* mutation in *ij48* mutants identifies a conserved motif. However, the distribution of CDC-25.1 protein in *ij48* animals does not explain the intestinal hyperplasia.

Chapter 1.

General introduction

1.1. The Phylum Nematoda

1998 was a landmark year in the history of biological research as the genomic sequence of the first multicellular organism, *Caenorhabditis elegans*, was completed. This milestone was achieved in a joint collaboration between The Sanger Institute and the St. Louis Genome Sequencing Centre. The *C. elegans* genome encodes over 19,000 proteins, many of which are homologues of proteins involved in human disease and development.

C. elegans (Figure 1.1), a free-living nematode, belongs to the Rhabditida order and the Rhabditidae family of the phylum Nematoda. Nematodes live almost anywhere, from the tropics to the polar regions and inhabit all types of marine and terrestrial environments. Out of every five animals on the planet, four are nematodes (Platt, 1994). Many adopt a parasitic lifestyle, forming relationships with both animals and plants. Although nematodes live in variable habitats and conditions, they are composed of the same basic body plan; two concentric tubes separated by a space, the pseudocoelom. The inner tube is the intestine. The outer tube consists of a collagenous cuticle, epidermis (known as the hypodermis in *C. elegans*), muscle and nerve cells. The gonads of adult worms are contained in the pseudocoelomic space.

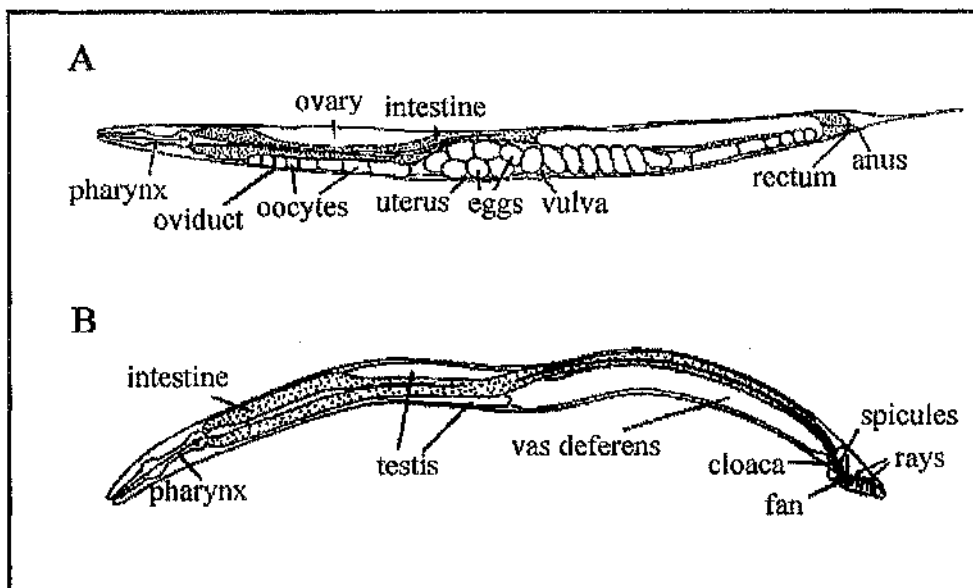


Figure 1.1 Cartoon representation of the anatomy of *C. elegans*. (A) is hermaphrodite, (B) is male. Adapted from Riddle *et al.*, 1997.

1.2. *C. elegans* biology

The simple anatomy, biology and genetics of *C. elegans* all attribute to the attractiveness of *C. elegans* as a model organism. There are two sexes of *C. elegans*, self-fertilising hermaphrodites and males (Figure 1.1). Both sexes are approximately 1mm in length and 70 μ m in diameter at adult and can be easily distinguished and manipulated under a dissecting microscope. The egg shell of *C. elegans* embryos and the body wall of *C. elegans* is transparent, thus developmental processes can be observed at the cellular level. *C. elegans* also has a short life cycle, 3 days at optimal temperatures thereby generating fast results from genetic crosses. Although the natural habitat of this nematode is soil, *C. elegans* can be easily cultured in the laboratory on solid or liquid media using *E.coli* as a food source (Brenner, 1974).

1.2.1. The life-cycle of *C. elegans*

As stated above, the life cycle of *C. elegans* is around 3 days. Embryogenesis, from fertilisation to hatching takes around 14 hours at 22°C, where 550 cells are generated by a precise pattern of divisions (Sulston *et al.*, 1983). This increases to 959 in the mature adult hermaphrodite and 1031 in the mature adult male (Sulston and Horvitz, 1977). Once hatched, *C. elegans* precedes through four larval stages, termed L1 through L4. Transition between each larval stage, termed molt, is characterised by the secretion of a new cuticle and subsequent shedding of the old one. These cuticles are different, both structurally and molecularly. As a means of dispersal and long-term survival, an alternative L3 larval stage termed dauer or "enduring" is entered in response to starvation (Riddle, 1988). If food becomes available, the dauer larva molts to become an L4, which resumes normal development.

1.2.2. The cell lineage of *C. elegans*

Another attractive feature of *C. elegans* is that the entire cell lineage, that is the timing, locations and ancestral relationships of all cell divisions during the development of *C. elegans*, is known and is largely invariant (Sulston and Horvitz, 1977; Sulston *et al.*, 1983). Thus, a constant number of cells in the same position are generated during *C. elegans* development. This has allowed the biology of *C. elegans* to be studied at the cellular level, resulting in an accurate description of events during the embryonic and postembryonic stages.

Laser ablation studies have given some insight into the degree of cell autonomy that is involved in determining the pattern of cell divisions and differentiations that occur. Generally it seems that, in *C. elegans*, cells behave fairly autonomously during development, although there are several well-defined instances where regulative cell-cell interactions have been demonstrated (Sulston and White, 1980; Kimble, 1981).

1.2.3. The genetics of *C. elegans*

The wild-type metaphase karyotype of *C. elegans* consists of 12 chromosomes in hermaphrodites, consisting of 5 pairs of autosomes and two sex chromosomes. Males have 11 chromosomes consisting of 5 pairs of autosomes and a single sex chromosome. The classical genetic procedures for gene mapping in *C. elegans* were developed by Brenner (1974), who identified approximately 100 genes by mutation, and subsequently placed them onto the six linkage groups. Hermaphrodites make up the vast majority of *C. elegans* animals in a normal population; males arise by the non-disjunction of the X chromosome during meiosis (Wood, 1988). Genetic crosses can be set up by mating males with hermaphrodites. When the sperm from a male enters the spermatheca of a young hermaphrodite, which already has hundreds of her own sperm, male sperm outcompete hermaphrodite sperm and preferentially fertilises oocytes (Ward and Carrell, 1979).

Due to the short life cycle and mode of reproduction, mutants can be generated with relative ease in *C. elegans*. The generation of mutants has allowed large-scale functional analysis of genes essential for growth and development in *C. elegans*. Due to the hermaphrodite mode of reproduction, mutagenised populations can be screened in the F1 for dominant mutations, and F2 for homozygotic recessive mutants of interest. Mutations can be generated by chemical or radiation means (see Chapter 3). The self-fertilising hermaphrodite mode of reproduction also allows easy propagation of sterile and lethal mutations; for zygotic lethal mutations (sterile, embryonic or larval), two thirds of the viable or fertile progeny of a heterozygote will also be heterozygous for the lethal mutation, whereas the remaining one third will be homozygous wild-type.

Many genes have been identified by mutation and placed onto the genetic map. This map represents the combination of data from a large volume of 2-factor and multi-factor mapping experiments. The genetic map of *C. elegans* is an invaluable tool for the *C. elegans* researcher, for example, in positioning a mutant allele relative to other genes during the process of cloning a gene identified by a mutant allele. The availability of the genome map has also allowed investigation of issues such as the rates of recombination per

physical distance and gene density across chromosomes. The recombination frequency varies between each chromosome, and along the length of a single chromosome. Most recombination occurs in gene-poor regions and it has been proposed that recombination-promoting sequences exist at high density along chromosome arms (Barnes *et al.*, 1995).

In addition to genes identified via mutant phenotype, chromosomal rearrangements have also been isolated and placed onto the genetic map. These include deletions, translocations, inversions and free duplications. These have been used as tools for mapping and characterising mutant alleles of interests, and can also be used as genetic balancers of lethal mutations. The modes of transmission of chromosomal rearrangements have been used to study mitosis and meiosis. *C. elegans*, like many organisms including some plants, protozoa, insects and other nematodes have diffuse kinetochores. The metaphase chromosomes lack any visible constriction, which commonly marks the centromere or kinetochore in monocentric chromosomes (Herman, 1988). Microtubule attachment is distributed along the chromosome, and the chromosomes move broadside on toward the spindle poles during segregation.

The ease of obtaining mutants and setting up crosses has permitted genes to be ordered in functional pathways. A classic example of this is in the vulval induction pathway, where genetic epistasis experiments led to a genetic pathway of vulval induction. Molecular analysis of the genes involved in vulval induction revealed its genetic pathway corresponded to the well-conserved Ras-mediated signal transduction pathway (Sundaram and Han, 1996).

1.2.4. The anatomy of *C. elegans*

The complete anatomy of *C. elegans* has been reconstructed using electron micrographs of serial sections and combined with the cell lineage data to produce a more complete picture (Sulston *et al.*, 1983; White, 1988).

The cuticle is the worms' exoskeleton; it functions as a barrier between the worm and its environment and maintains the shape of the worm. The cuticle is made up of collagen and is synthesised and secreted by the external epithelium, the hypodermis. There are a series of indentations (annuli) that run circumferentially along the length of the cuticle. Two elevated longitudinal ridges termed alae run along the lateral surfaces of the cuticles of the L1 and adult. These alae are synthesised and secreted by a specialised set of hypodermal cells termed seam cells. A basement membrane lies on the basolateral side of the cells between the hypodermis and the underlying body wall muscles.

The nervous system is the most complex organ of *C. elegans*, accounting for 37% and 46% of somatic nuclei in hermaphrodites and males, respectively (Chalfie and White, 1988). All connections and positions of the nerves in the nervous system have been reconstructed from electron micrographs of serial sections (White *et al.*, 1986). Neurons have simple morphologies with few, if any, branches. Processes from neurons run in defined positions within bundles of parallel processes and synaptic connections are made between adjacent neural processes within bundles. Process bundles are arranged longitudinally (including the dorsal and ventral nerve cord) and circumferentially (the nerve ring) and are often adjacent to ridges of hypodermis. Neurons are generally highly locally connected, thus make synaptic connections with many of their neighbours.

The alimentary canal consists of the pharynx, intestine and rectum. The pharynx comprises the largest organ at birth, almost 50% of the body length, but grows more slowly than other organs during larval development, so that in the adult, the pharynx is less than 20% of the body length. The pharynx is a self-contained system of muscles, epithelial cells and nerves. The pharynx functions to ingest, concentrate and process food prior to pumping it into the intestine. The pharynx is connected to the intestine via the pharyngeal-intestinal valve.

A more detailed description of the anatomy of the intestine is given in Chapter 3, but to summarise, the intestine is a tube containing a quartet of cells at the anterior (int-1) followed by eight pairs of cells (int-2 to int-9). The four cells of int-1 represent the point of attachment of the intestine to the cells of the pharyngeal-intestinal valve. During post-embryonic development, the *C. elegans* intestine is a major organ, involved not only in digestion but also in storage and macromolecular synthesis. Yolk proteins, the vitellogenins, are synthesised by the intestine and function in the nurture of germ cells.

The rectum is connected to the posterior of the intestine via the intestinal-rectal valve, a very similar structure to the pharyngeal-intestinal valve. The rectum has 3 sets of associated muscles that control excretion. They are coupled together through gap junctions and innervated by a single neuron.

As the animal grows during larval development, the most substantial changes occur in the germline. The hermaphrodite and male gonads are very different structures. The *C. elegans* adult hermaphrodite gonad consists of two equivalent U-shaped gonad arms. Each arm of the gonad can be divided into the distal ovary, the loop, the oviduct, the spermatheca, the spermathecal valve, and the uterus. The distal portion of each gonad arm contains syncytial germline nuclei surrounded by incomplete membranes (Hirsh *et al.*,

1976). Although technically a syncytium, each germline nucleus and its associated cytoplasm are referred to as a germ cell. The axial polarity of the gonad is determined by a specialised somatic cell termed the distal tip cell (Kimble and White, 1981). Mitotic germ cells are located near the distal tip of the gonad arm in the ovary. As germline nuclei progress more proximally, away from the distal tip cell, they exit the mitotic cell cycle and enter meiosis. The first germ cells to complete cellularisation within the proximal gonad differentiate as spermatocytes that complete meiosis to form approximately 160 sperm (Hirsh *et al.*, 1976; Ward and Carrell, 1979). Further germ cells differentiate as oocytes instead of sperm (Hirsh *et al.*, 1976) which remain in diakinesis of prophase I in the oviduct prior to under-going meiotic maturation and ovulation. Fertilisation occurs within the spermatheca, which contains amoeboid sperm (Ward and Carrell, 1979; McCarter *et al.*, 1997). The meiotic maturation divisions of the oocytes are completed in the uterus (McCarter *et al.*, 1999) and embryogenesis begins. The uterus opens to the outside via a vulva protruding from the ventral surface of the hermaphrodite.

The male gonad is a single lobed, U-shaped structure that consists of the testis, the seminal vesicle and the vas deferens. It begins in the central region of the worm that extends anteriorly before turning dorsally and running posteriorly until it reaches the cloaca in the specialised reproductive structures of the male tail. At the end distal to the cloaca, the germ cells are mitotic, which become meiotic and advance through the various stages of meiosis, as they travel proximally to the seminal vesicle. The sperm are stored in the seminal vesicle until copulation, where they are released via the vas deferens and cloaca. The male tail is organised into a copulatory bursa that consists of many specialised neurons, muscles and hypodermal structure required for mating.

A detailed description of the *C. elegans* anatomy is given in White (1988).

1.2.5. The *C. elegans* physical map and genomic sequence

The *C. elegans* physical map consists of overlapping cosmids, YACs and fosmids that have been placed into overlapping sets by restriction analysis and sequencing. The alignment of the physical and genetic maps allows fast positional cloning of mutant alleles.

The *C. elegans* genomic sequence has revolutionised *C. elegans* biology. Together with genetic, developmental and anatomical data, it also provides a powerful resource for research in other systems. The 100-megabase genomic sequence of the nematode *C. elegans* reveals over 19,000 genes. (*C. elegans* sequencing consortium, 1998; Wormbase 2002).

More than 40% of the predicted protein products find significant matches in other organisms (*C. elegans* sequencing consortium, 1998) and many have been implicated in human disease (Rubin *et al.*, 2000). Many human and *C. elegans* predicted genes are uncharacterised. Thus, *C. elegans* continues to play a key role in helping to assign function to novel genes.

1.2.6. *C. elegans* as an experimental system

In addition to the short life cycle, low maintenance and the genetically tractable system *C. elegans* offers, there are various tools available to *C. elegans* biology that make it an attractive experimental system. Methods have been developed to create transgenic strains via microinjection (Stinchcomb *et al.*, 1985; Fire, 1986; Mello *et al.*, 1991). This has permitted the introduction of GFP and/or *lacZ* gene fusions allowing the spatial and temporal expression patterns of genes of interest to be elucidated. Transgenic strains can also be used phenotypically to rescue genetic mutations in *C. elegans* by supplying a wild-type copy of a mutant gene. The correlation of mutant phenotypes and transforming DNA renders these mutations accessible for cloning.

The physical and genetic map have also been aligned in various regions of the genome, where large-scale experiments have been used to rescue lethal mutations (for example, McDowall and Rose, 1997). These cosmid rescue experiments integrate the genetic and physical maps by placing genetically mapped lethal mutations on the cosmid contig map.

Recently, the technique of injecting dsRNA, commonly known as RNA-mediated interference (RNAi) has been developed in *C. elegans* (Fire *et al.*, 1998; Tabara *et al.*, 1998; Timmons and Fire, 1998). This technique allows specific targeted gene disruption and is thus a very useful tool for investigating the function of a gene, beginning with only genomic sequence. dsRNA has also been shown to suppress expression of specific genes in plants (Waterhouse *et al.*, 1998), *Trypanosoma brucei* (Ngo *et al.*, 1998) and *Drosophila* (Kennerdell and Carthew, 1998). In *C. elegans*, targeted gene disruption by RNAi has been performed in all genes on chromosome I (Fraser *et al.*, 2000) and chromosome III (Gonczy *et al.*, 2000). At present, only about 10% of the genes in *C. elegans* have been identified by mutation (Johnsen and Baillie, 1997). Thus these genomic wide RNAi screens have assigned function to genes that have not been identified via mutation. Moreover, they have demonstrated that conserved genes are significantly more likely to have an RNAi phenotype than genes with no conservation (Fraser *et al.*, 2000), again enhancing the use

of *C. elegans* as a model organism. For a more detailed description of RNAi, see Chapter 5.

1.3. Embryogenesis

The process of embryogenesis can be conveniently considered in three major stages: zygote formation and establishment of embryonic axes, gastrulation and morphogenesis (Figure 1.2). Following fertilisation and during the first four cleavages of the embryo, five cells or blastomeres are produced that generate distinct sets of somatic tissues. These blastomeres, termed AB, MS, E, C and D generate ectodermal (nervous tissue and hypodermis) and pharyngeal tissue, mesoderm, endoderm, muscle and hypodermal tissue and body wall muscle respectively, are often referred to as somatic founder cells. The sister of D is the P4 blastomere and is the precursor of the germline (Figure 1.3). Gastrulation commences at the 26-cell stage by the inward movement of Ea and Ep. It is during gastrulation that organogenesis is initiated and most of the cell divisions occur. Organogenesis and cell differentiation are essentially complete prior to the process of elongation, where the embryo changes from an almost spherical ball of cells to a thin cylindrical worm, four times the original length.

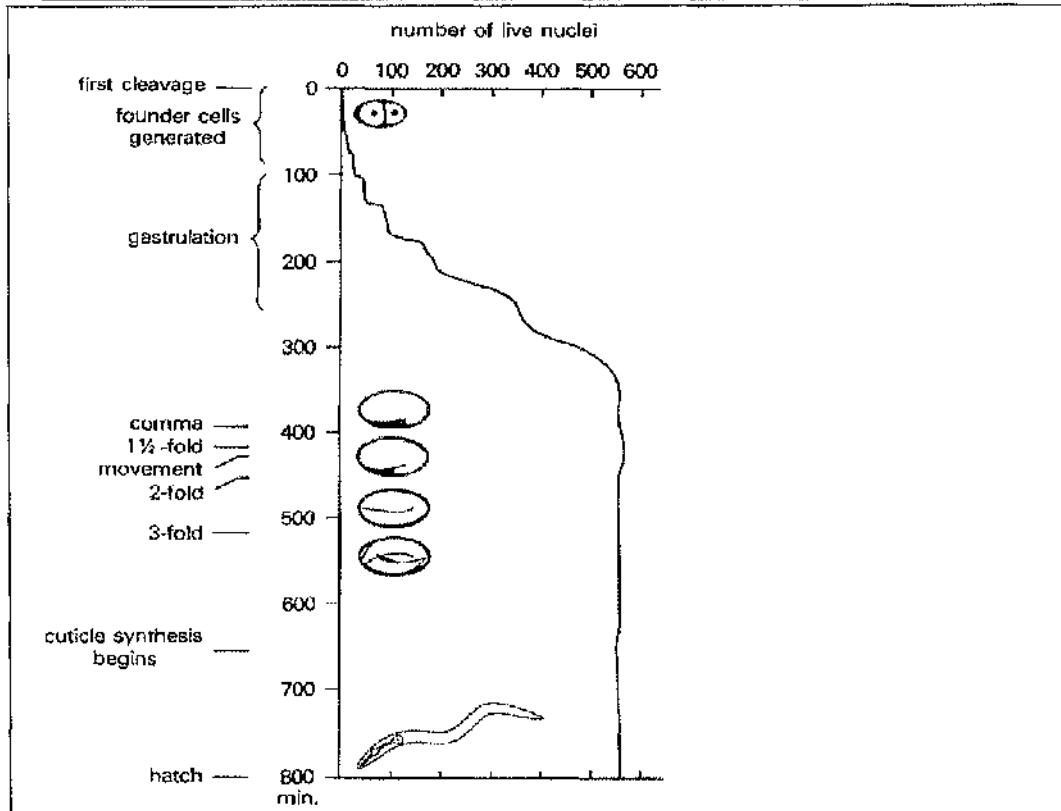


Figure 1.2 Summary of events during embryogenesis. The timing of key events and stages of elongation (at 20°C) are shown on the left axis. Time is from first cleavage. The number of nuclei generated at each stage is shown on the right. Adapted from Kempthues & Strome, 1997

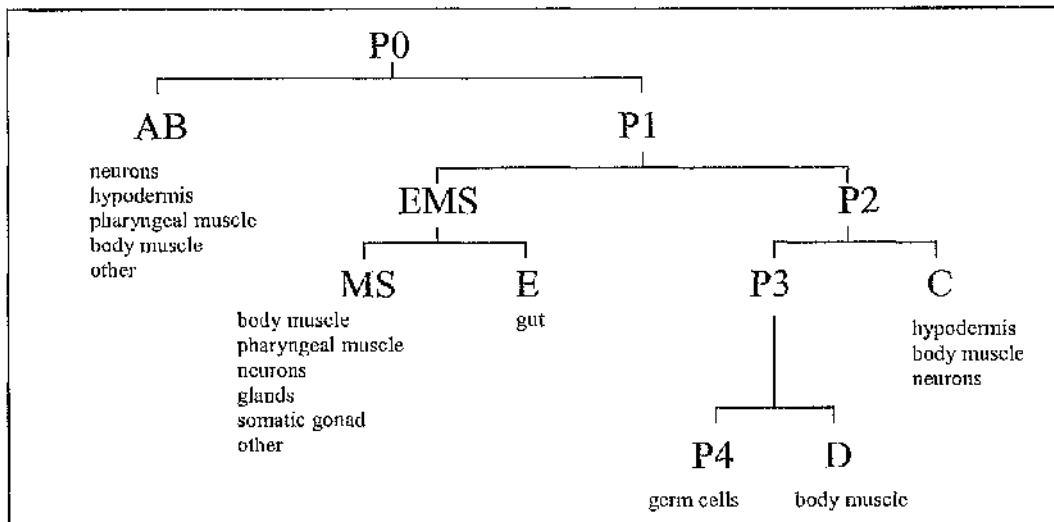


Figure 1.3 Early cell lineage tree. The cleavage patterns that give rise to the five somatic founder cells (AB, MS, E, C, and D) and the germ cell precursor (P4). The tissues generated by each founder cell are shown. The F blastomere generates exclusively intestine. Adapted from Sulston *et al.*, 1983.

1.3.1. Specification of endoderm

A lot of research has focussed on characterising genes that specify the fate of the individual cells in the early embryo (for a recent review refer to Schnabel and Priess, 1997). There clearly must be differences to distinguish the fates of the blastomeres. Asymmetric cell division, in which one cell divides to give rise to two dissimilar daughter cells serves as a fundamental mechanism for generating cell diversity. In some cases, the daughter cells are equivalent when born but they subsequently develop distinctive properties in response to differences in external cues. In other cases, cell polarisation events prior to cell division cause cell fate determinants to become differentially segregated to the daughter cells. This ultimately must involve activation of tissue specific genes and repression of genes that function in other tissues. *C. elegans* uses both of these modes in specifying the fate of cells in the early embryo.

The main focus of my thesis is in the control of the E-cell lineage, which produces exclusively intestine, or gut, in *C. elegans*. The remainder of this chapter will focus on E-cell development. I will summarise what makes the progenitor of E, EMS, different from other blastomeres. Next I will review E-cell specification and discuss what specifies the difference between E and its sister blastomere, MS. Finally I will evaluate genes implicated in the terminal differentiation of the intestine. The advantage of using *C. elegans* as a model system has permitted the generation of mutants of these processes and analysis of mutant alleles has permitted genetic pathways to be elucidated.

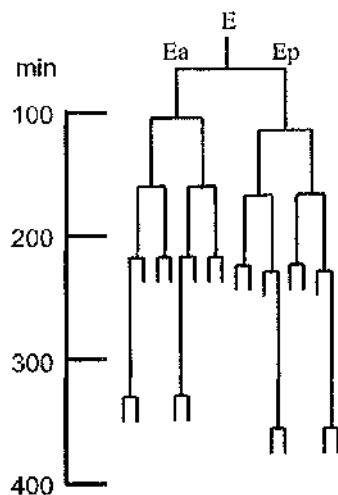


Figure 1.4 Wild type E-cell lineage. The divisions shown are during embryogenesis, time (min) from the first cleavage. Adapted from Sulston *et al.*, 1983.

1.3.2. The roles of the maternal proteins, SKN-1, PIE-1 and PAL-1

The bZIP/homeodomain transcription factor SKN-1 is required for both E and MS fates (Bowerman *et al.*, 1992). The sister blastomere of EMS is P2, which divides to generate the blastomeres C and P3. In *skn-1(-)* mutants, EMS adopts a fate reminiscent of the C blastomere, which produces ectodermal and body muscle (Bowerman *et al.*, 1993) (Bowerman *et al.*, 1992a). Though SKN-1 is present at comparable levels in both EMS and P2, it is able to activate transcription in EMS only, owing to a general transcription inhibitor PIE-1, which is differentially segregated to the P2 cell during the first two cell divisions (Mello *et al.*, 1996; Tenenhaus *et al.*, 1998; Batchelder *et al.*, 1999). The C-like fate is produced in EMS in *skn-1(-)* mutants owing to the presence of PAL-1, a CAUDAL-like homeoprotein, which is required for the generation of body muscle from the C and D blastomere (Hunter and Kenyon, 1996).

Two immediate transcriptional targets of maternal SKN-1 are the zygotic genes, MED-1 and MED-2. These encode GATA-like transcription factors and although on different chromosomes, they are almost identical and are generally described together as MED-1, -2. Loss of MED-1, -2 by RNAi resembles loss of SKN-1 (Maduro *et al.*, 2001). The C-promoting activity of PAL-1 is blocked by MED-1, -2 and SGG-1 kinase, a GSK-3 β homologue in EMS. In the C blastomere, SGG-1 kinase prevents SKN-1 from activating the MED-1, -2 genes in C and thus specifies an EMS-like fate. In the absence of both SGG-1 and PAL-1, the daughters of C, Ca and Cp, adopt a MS and E-like fate respectively.

Interestingly, in *pie-1(-)* mutants, the P2 cell has an EMS-like fate and also produces a gut lineage from one daughter cell. Thus gut fate is segregated to one daughter independently of cell contact (i.e. cell autonomously), yet the normal EMS cell requires a cell-cell specification in one daughter (see below) (Goldstein, 1995). The *pie-1* gene product is believed to repress SKN-1 activity in the P2 cell, preventing P2 developing as an EMS-like fate. In *pie-1(-)* mutant embryos, P2 generally develops as EMS, thus *pie-1(-)* mutant embryos produce two EMS-like lineages.

1.3.3. Wnt signalling

From the entry of sperm defining the cleavage pattern of the first division, asymmetric cell divisions are generated in *C. elegans*. Many early *C. elegans* embryonic divisions occur in an anterior-posterior division plane, usually producing sister cells with

different fates (Sulston *et al.*, 1983). Several experimental studies have focussed on how the fate of E is specified during early embryogenesis. The E cell is born when there are only 7 cells in the embryo and is the posterior daughter of the EMS blastomere. Interestingly, once specified, E cell differentiation appears to be autonomous to the E cell and in the absence of other blastomeres, E can give rise to a full set of differentiated intestinal cells and even structural elements of a fully formed intestine (Priess and Thomson, 1987; Leung *et al.*, 1999)

Two inductions by P2 at the four cell stage serve to elaborate the anterior-posterior axis of the *C. elegans* embryo: on the ventral side E and MS and on the dorsal side, ABa and ABp, due to the P2-ABp interaction (Bowerman *et al.*, 1992b; Mango *et al.*, 1994; Moskowitz *et al.*, 1994; Mello *et al.*, 1994; Hutter and Schnabel, 1995). The E blastomere fate depends on a P2-EMS cell-cell interaction polarising EMS (Goldstein, 1992; Goldstein, 1993). In the absence of gut induction, E loses its distinctive cell lineage timing and takes on an early lineage timing of an MS-like lineage (Goldstein, 1992, 1993). Gut differentiation does not occur from EMS cells isolated early in the four-cell stage, but contact with a P2 cell will rescue gut differentiation. Both sides of EMS are competent to respond to the inducing signals (Goldstein, 1993) but when presented with signals on both sides, only one generally forms gut lineage.

By examining mutants identified as having more mesoderm (*mom*), generated by an E to MS fate, it has been shown that signalling from the P2 blastomere promotes asymmetric division of the MS blastomere to produce an anterior MS fate and a posterior E fate. This polarised induction involves a Wnt signalling pathway and a MAP kinase cascade. These signalling pathways act in a posterior dependent manner to induce and orient the asymmetric cell division of EMS cell (Goldstein, 1993; Thorpe *et al.*, 1997). Both of these pathways converge to ultimately downregulate POP-1/TCF activity of maternally supplied POP-1 in the posterior E blastomere (Lin *et al.*, 1995; Lin *et al.*, 1998) (Figure 1.5). POP-1 is a member of the TCF/LEF class of HMG box proteins, which serve as the terminal transcription factors in Wnt signalling pathways (Brunner *et al.*, 1997). Members of the TCF/LEF family of transcription factors have been shown to play roles in multiple biological processes including cell fate determination, pattern formation and differentiation. The homology between POP-1 and other TCF/LEF members is restricted mainly to the HMG box, which mediates the sequence-specific DNA binding as shown for TCF/LEF-1 (Roose and Clevers, 1999). To date, POP-1 is the only protein that has been genetically identified as a suppressor of the E fate in MS descendants (Lin *et al.*, 1995).

The Wnts are a conserved family of secreted glycoproteins that function as signalling molecules in many developmental processes. However it is unclear to what extent the pathway components are shared in each Wnt-controlled pathway. E-cell specification is one of the best characterised Wnt pathways in *C. elegans*. Genetic screens have been performed to identify loci that are required to distinguish the fates of E during endoderm induction. Mutation of any of these genes causes both daughters of EMS to adopt an MS-like fate. The loci identified include 5 *mom* genes (more mesoderm), *mom-1* through *mom-5* (Rocheleau *et al.*, 1997; Thorpe *et al.*, 1997). Three *mom* genes were found to encode previously identified Wnt signal transduction pathway components: *mom-1* is similar to porcupine (*porc*), *mom-2* to wingless (*wg*) and *mom-5* to frizzled (*fz*). RNAi studies suggested that a B-catenin related gene, *wrm-1*, a tumour suppressor-related gene, *apf-1* (for APC-related) (Rocheleau *et al.*, 1997) and a glycogen synthase kinase 3 (GSK-3 β) homologue called *sgg-1* are also involved in this pathway (Schlesinger *et al.*, 1999). Interestingly, SGG-1 activity blocks endoderm formation in the C lineage (Maduro *et al.*, 2001). Thus SGG-1 is required positively for the Wnt-mediated activation of endoderm in the EMS lineage and is an inhibitor of endoderm in the C lineage. It has also been speculated that SGG-1 may be a branchpoint for endoderm specification and spindle orientation in EMS (Schlesinger *et al.*, 1999).

In addition to Wnt, components of a mitogen-activated protein kinase (MAPK) pathway including LIT-1 (Nemo-like kinase, NLK) and MOM-4 (transforming growth-factor-B-activated kinase, TAK1) have been shown to downregulate POP-1 in the E cell. The Wnt and MAPK signals are integrated at the level of complex formation between WRM-1/B-catenin and LIT-1/NLK. Consistent with this, Rocheleau *et al.*, (1999) demonstrated an interaction between LIT-1 and WRM-1/B-catenin that leads to a LIT-1 kinase domain dependent phosphorylation of LIT-1, WRM-1 and POP-1, and a redistribution of POP-1 from the nucleus to the cytoplasm when coexpressed in vertebrate tissue culture cells. Similar interactions are also likely to be conserved in vertebrates as TAK-1 and NLK can downregulate IIMG-domain-containing proteins related to POP-1 (Ishitani *et al.*, 1999). The source and nature of the signal that activates the MOM-4/LIT-1 kinase cascade in *C. elegans* is under investigation.

Inactivation of the Wnt pathway upregulates POP-1 protein level, generating an E to MS switch, whereas inactivation of *pop-1* results in both daughters adopting a posterior fate (i.e. MS to E switch) (Lin *et al.*, 1995; Lin *et al.*, 1998). This result contrasts with many

models for the Wnt signalling pathway where the WRM-1 related proteins, B-catenin have a positive role in response to Wnt signalling. In these models reviewed by (Cadigan and Nusse, 1997), B-catenin and armadillo are thought to enter the nucleus and stimulate transcriptional activation of TCF/LEF proteins. Thus loss of B-catenin and TCF/LEF would result in similar phenotypes.

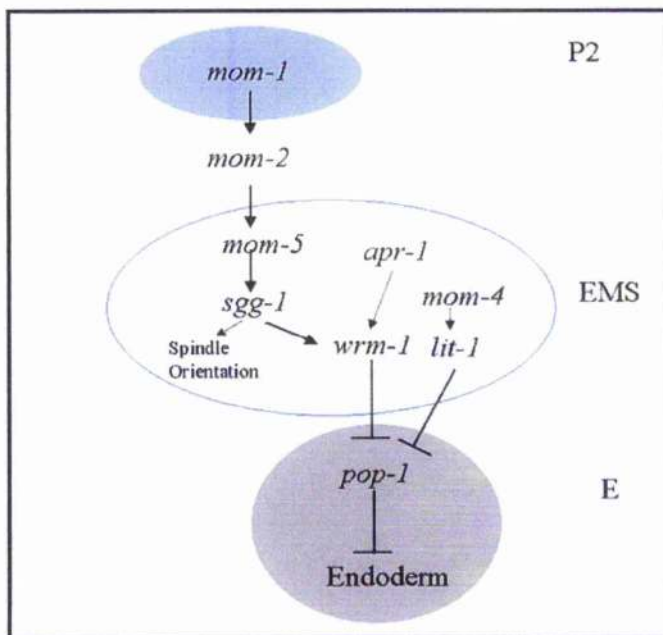


Figure 1.5 Wnt signalling in the early *C.elegans* embryo. Positive interactions are indicated by arrows, negative by truncated lines. Adapted from Thorpe *et al.*, 2000.

The histone acetyltransferase (CPB-1) and histone deacetylase (HDA-1) have been shown to have a role in endoderm development (Shi and Mello, 1998; Calvo *et al.*, 2001). In *C. elegans*, CBP-1 is essential for the execution of most differentiation programmes during embryogenesis (Shi and Mello, 1998). Endoderm differentiation is abrogated in embryos lacking CBP-1, however, differentiation can be restored by subsequent inhibition of HDA-1, suggesting that CBP-1 promotes differentiation by counteracting the repressive activity of HDA-1. Calvo *et al* (2001) proposed a molecular mechanism for the

suppression of endoderm development from the MS blastomere. They suggested that in E, the Wnt/MAPK pathways block the endoderm-repressing activity of POP-1, thus endoderm induction is induced by inactivating a repressor. The repression by POP-1 involves a complex containing the co-repressor Groucho-like molecule UNC-37 and HDA-1 resulting in repression of *end-1*, a crucial initial endoderm-determining gene whose product is sufficient to induce endoderm differentiation. (Zhu *et al.*, 1997; Zhu *et al.*, 1998). Vertebrate TCFs can also mediate repression by recruitment of histone deacetylases to promoters via Groucho family corepressors (Roose *et al.*, 1998; Chen *et al.*, 1999; Brantjes *et al.*, 2001). Recently it has been suggested that POP-1 represses target gene transcription by inhibiting the activity of a bound activator rather than preventing its binding. Activation of *end-1* and its related gene *end-3*, requires the redundant, zygotically expressed GATA factors MED-1, -2 (Maduro *et al.*, 2001). In a *pop-1(-)* mutant, MED-1, -2 are required for the endoderm that arises from both MS and E (Maduro *et al.*, 2001) suggesting that the activation by MED-1 -2, combined with the asymmetry provided by POP-1, dictates either MS fate (active MED-1, -2; high POP-1) or E fate (active MED-1, -2; low POP-1) (Maduro *et al.*, 2001). By observing protein-DNA interactions in live embryos, these authors speculated that the qualitative differences between Wnt signalled and unsignalled POP-1 are correlated with the ability of POP-1 to bind directly to the *end-1* and *end-3* promoters. The P2-EMS interaction results in a change in POP-1, which prevents the interaction between POP-1 and *end-1*, -3 in the E nucleus, permitting MED-1, -2 to activate *end-1*, -3 and thus specify an E fate.

1.3.4. GATA factors and the E-cell cycle

The GATA-like transcription factors bind to the DNA sequence motif(A/T)GATA(A/G). Downstream of MED-1, -2, lie END-1 and END-3, another pair of redundant GATA factors. These genes were identified following an attempt to obtain a zygotic lethal mutant with a 'gutless' phenotype. *end-1* and *end-3* are contained within the 'endoderm determining region' (EDR). In embryos lacking the EDR, the E blastomere adopts a C blastomere fate (similar to *skn-1(-)* mutants and RNAi of *med-1*, -2) (Zhu *et al.*, 1997). During the second cell cycle of the E-cell lineage, another pair of redundant GATA transcription factors, *elt-2* and *elt-7* are expressed (Fukushige *et al.*, 1998; Maduro and Rothman, 2002).

GATA consensus motifs are found in many genes that are expressed in the intestine such as *ges-1* (Edgar and McGhee, 1986), cysteine protease genes (*cpr-1,3,4,5*) (Larminie,

1995; Larminie and Johnstone, 1996) and the vitellogenin gene *vit-2* (Blumenthal *et al.*, 1984), and have been reported to be essential for correct gut expression (MacMorris *et al.*, 1992; Egan *et al.*, 1995; Britton *et al.*, 1998).

1.3.5. Post-embryonic development of the intestine

During post-embryonic development, no more cell divisions occur in E. However most gut nuclei under go a nuclear division during L1, producing binucleate cells. Additionally, endoreduplication (DNA synthesis without nuclear division) occurs once during each larval molt such that the DNA content in the adult gut nuclei is 32C (see Chapter 3).

1.4. Project aims and objectives

Most work to date concerning E-cell development has been with identifying genes that are implemented in E-cell specification. Little work has focussed on identifying genes that are involved in the execution of the E-cell lineage, during both embryonic and post-embryonic development. For example, in the E-cell lineage during embryogenesis, there are both symmetric and asymmetric divisions. To date, no molecules have been identified that create the cell diversity in this process. My aim in this project was to elucidate some of the molecules involved in the execution of the E-cell lineage by identifying and characterising mutants with an abnormal E-cell lineage.

Chapter 2

Materials and Methods

Unless otherwise stated, all chemicals/reagents were purchased from Fisher Scientific (Fisher Scientific UK Ltd., Loughborough, Leicestershire, UK), Invitrogen (Invitrogen Ltd., Paisley, Renfrewshire, UK), Sigma (Sigma-Aldrich Company Ltd., Poole, Dorset, UK), BDH (Merck House, Poole, Dorset, UK), Sigma-Genosys (Sigma-Genosys Biotechnologies Europe Ltd, Pampisford, Cambridgeshire), New England Biolabs (NEB Ltd., Hertfordshire, UK), Stratagene (Stratagene Europe P.O. Box 120851100 Amsterdam, The Netherlands) and ABgene (ABgene House, Epsom Surrey, UK). Restriction enzymes and DNA modifying enzymes were obtained from NEB. Custom oligonucleotide primers for Polymerase Chain Reaction (PCR) were obtained from Sigma-Genosys. DNA polymerases were supplied by AB (*Taq*), Stratagene (*Pfu Turbo*) or NEB (*Vent*).

2.1. Chemical abbreviations

BSA:	Bovine Serum Albumin
DABCO:	1, 4-Diazabicyclo[2.2.2]octane
DAPI:	4, 6-diamidino-2-phenylindole
DEPC:	Diethyl pyrocarbonate
DMF:	N, N-Dimethylformamide
Na ₂ EDTA:	ethylenediaminetetraacetate disodium salt
EMS:	Ethyl methanesulphonate
dH ₂ O:	Deionised water
IPTG:	Isopropyl β-D-thiogalactoside
NGM:	Nematode growild-typeh medium
PBS:	Phosphate buffered saline
SDS:	Sodium dodecyl sulphate
Tris-HCl:	2-amino-2-(hydroxymethyl)-1,3-propanediol-hydrochloride
Tween 20:	Polyethylene glycol sorbitan monolaurate
X-gal:	5-Bromo-4-chloro-3-indolyl β-D-galactoside

2.2. Commonly used stocks, solutions and media

Ampicillin (1000x): 100mg/ml in sterile dH₂O. Sterilised by filtration and aliquoted and stored at -20°C.

Blocking Solution (1x): 1% milk powder in 1% PBST. Made fresh before use.

Chitinase solution: 20mg/ml stock. Purchased as solid (Sigma) and dissolved in 50mM NaCl, 70mM KCl, 2.5mM MgCl₂. Aliquoted and stored at -20°C.

Diethylpyrocarbonate (DEPC)-treated dH₂O: DEPC added to dH₂O to a final concentration of 0.1%, mixed vigorously and left to stand in fumehood overnight prior to autoclaving. Stored at room temperature.

10x DNA Sample Loading Buffer: 25% Ficoll (Type 400), 20mM EDTA, 0.2% Bromophenol Blue. Stored at room temperature

Ethylmethanesulphonate (EMS) (50mM): 20µl liquid EMS added to 4ml M9 buffer and gently agitated until EMS dissolved. Made fresh prior to use.

Ethidium Bromide: 10mg/ml stock in dH₂O, final concentration 0.5µg/ml in agarose gels. Stored, protected from light, at room temperature.

Injection Mix Buffer (10x) for RNAi: 20% Polyethylene glycol (MW 6000-8000), 200mM KPO₄ (pH7.5), 30mM Potassium Citrate in DEPC treated dH₂O. Stored at 4°C.

IPTG: 0.5M stock in sterile dH₂O. Aliquoted and stored at -20°C

Kanamycin (1000x): 50mg/ml in sterile dH₂O. Sterilised by filtration, aliquoted and stored at -20°C.

L-Broth: 1% Bacto tryptone (Difco, Michican, USA) 0.5% yeast extract (Difco), 0.5% NaCl, in dH₂O. Autoclaved and stored at room temperature.

L-Broth Agar: as for L-Broth + 1.5g/100ml bacto-agar (Difco). Autoclaved then allowed to cool (antibiotics were added at this stage, if required) poured with sterile technique onto plastic plates, allowed to set, dried by inversion in flow hood and stored for short periods at 4°C.

M9 Buffer (1x): 0.3% KH₂PO₄, 0.6% Na₂HPO₄, 0.5% NaCl, 1mM MgSO₄, in dH₂O. Autoclaved and stored at room temperature.

Mounting Solution: 50% glycerol, 1XPBS, 2.5% DABCO. Made fresh prior to use

Na₂EDTA: 0.5M stock in dH₂O. adjusted to pH8 with NaOH. Autoclaved and stored at room temperature.

NGM Agar: 0.3% NaCl, 2% agar (Difco), 0.25% peptone (Difco), 0.0003% cholesterol (1ml/L of 5mg/ml stock in ethanol) in dH₂O. Autoclaved then 1ml/L of 1M CaCl₂, 1ml/L of MgSO₄ and 25ml/L of 1M Potassium Phosphate buffer pH6.0 added. Stored at room temperature.

Phenol: For DNA manipulations, purchased liquefied and equilibrated with 10 mM Tris HCl, (pH8), 1mM EDTA. For RNA manipulations, phenol was purchased liquefied and saturated with 0.1M citrate buffer, pH4.3. Stored at 4°C.

Phenol/Chloroform: Equal volumes of phenol (above) and chloroform:isoamyl alcohol 24:1 were mixed. Stored at 4°C.

Phosphate buffered saline (PBS): Purchased as Tablets (Sigma). Dissolved 1 Tablet in 200 ml water to obtain a 137 mM NaCl, 2.7 mM KCl and 10 mM phosphate buffer solution (pH 7.4 at 25°C).

PBST: As PBS with the addition of Tween-20 to a final concentration of 0.2%. Stored at room temperature.

Potassium Phosphate Buffer (1M): Prepared from 1M KH_2PO_4 and 1M K_2HPO_4 , mixed in appropriate ratio for desired pH. Autoclaved and stored at room temperature.

Proteinase K: 10mg/ml stock in sterile dH_2O . Stored at -20°C .

Sodium dodecyl sulphate solution (SDS), 10% (w/v): Stock solution in sterile dH_2O . Stored at room temperature.

Single Worm Lysis Buffer (SWLB): 50mM KCl, 10mM Tris (pH8.3), 2.5mM MgCl_2 , 0.45% Tween-20, 0.01% (w/v) gelatin. Autoclaved and stored in aliquots at -20°C . Proteinase K (Boehringer-Mannheim) added to $60\mu\text{g/ml}$ prior to use.

Single worm PCR Taq buffer (10x): 100mM Tris (pH8.3), 500mM KCl, 15mM MgCl_2 , 0.01% (w/v) gelatin. Autoclaved and stored in aliquots at -20°C .

Sodium Phosphate Buffer (1M): Prepared from 1M Na_2HPO_4 and 1M NaH_2PO_4 , mixed in appropriate ratio for desired pH. Autoclaved and stored at room temperature.

SOC medium (1L): 20g Bacto-tryptone, 5g Bacto-yeast extract, 0.5g NaCl, added to 960ml dH_2O . Allowed to dissolve. Autoclaved, then 10ml 1M MgCl_2 , 10ml 1M MgSO_4 and 20ml 20% (w/v) glucose added before use. Stored at -20°C .

TBE (10x): 0.9M Tris-HCl, 0.9M Boric acid, 25mM Na_2EDTA pH8.0 in dH_2O . Stored at room temperature.

TE: 1mM EDTA, 10mM Tris-HCl, (pH as required) in dH_2O . Autoclaved and stored at room temperature. TE at pH8.0 was used for all DNA manipulations, unless otherwise stated

Tetracycline (1000x): 12.5mg/ml in 50% sterile dH_2O and 50% ethanol. Aliquoted and stored protected from light at 4°C .

Tris-HCl: Molarity and pH as required (pH adjusted with HCl). Autoclaved and stored at room temperature.

X-Gal (100x): 2% in Dimethylformamide (DMF). Stored in aliquots protected from light at -20°C.

Note: All media and most heat insensitive solutions were autoclaved using the following conditions: 120°C, 15lbs/in² for 15 minutes. Heat sensitive solutions were sterilised by filter sterilisation.

2.3. *C. elegans* and bacterial strains

2.3.1. *C.elegans* strains

Unless indicated, strains were obtained from *Caenorhabditis* Genetics Centre (CGC), University of Minnesota, St Paul, Minnesota, USA. For details of nomenclature refer to Hodgkin, 1997.

Name	Genotype	Notes
CB61	<i>dpy-5(e61)I</i>	Obtained from the CGC (Brenner, 1974)
CB2067	<i>unc-73(e936) dpy-5(e61)I</i>	A gift from J. Hodgkin
CB3823	<i>eDf18/unc-24(e138) dpy-20(e1282)IV.</i>	Obtained from the CGC
CB3824	<i>eDf19/unc-24(e138) dpy-20(e1282)IV.</i>	Obtained from the CGC
DA740	<i>bli-6(sc16) unc-24(e138)IV</i>	Obtained from the CGC
DR96	<i>unc-76(e911)V</i>	Obtained from the CGC (Brenner, 1974)
DR438	<i>dpy-5(e61) unc-87(e1216)I</i>	Obtained from the CGC
EII135	<i>unc-44(e362) bli-6(sc16)IV.</i>	Obtained from the CGC
IA105	<i>unc-76(e911) V;dpy-7::GFP, unc-76(+)(ijIs12)</i>	A gift from I. Johnstone (generated by E. Stewart)
JK1726	<i>qDf16/dpy-5(e61) unc-15 (e1402)I</i>	Obtained from the CGC (Kadyk and Kimble, 1998)
JR1838	<i>wIs84</i>	A gift from Joel Rotlumann

Name	Genotype	Notes
KR357	<i>dpy-5(e61) let-382(h82) unc-13(e450); sDp2(I; f)</i>	Obtained from the CGC (Howell <i>et al</i> , 1987)
KR623	<i>dpy-5(e61) let-602(h283) unc-13(e450); sDp2 (I; f)</i>	Obtained from the CGC (McDowall and Rose, 1997a)
KR633	<i>dpy-5(e61) air-1*(h289) unc-13(e450); sDp2 (I; f)</i>	Obtained from the CGC (McDowall and Rose, 1997a)
KR637	<i>dpy-5(e61)let-604(h293) unc-13(e450); sDp2(I; f)</i>	Obtained from the CGC (McDowall and Rose, 1997a)
KR727	<i>dpy-5(e61) let-607(h402) unc-13(e450); sDp2(I; f)</i>	Obtained from the CGC (McDowall and Rose, 1997a)
KR1233	<i>hDf8/dpy-5 (e61)unc-13(e450)I</i>	Obtained from the CGC (McKim <i>et al</i> , 1992)
KR1347	<i>dpy-5(e61) let-608(h706) unc-13(e450); sDp2(I; f)</i>	Obtained from the CGC (McDowall and Rose 1997a)
MT5242	<i>unc-5(e53) bli-6(sc16)IV.</i>	Obtained from the CGC
N2	<i>C. elegans</i> wild-type Bristol Strain	Obtained from the CGC (Brenner, 1974)
RW1324	<i>fem-1(e1991) unc-24(e138) unc-22(s12)/stDf7 IV</i>	Obtained from the CGC (Williams and Waterston, 1994)
RW1333	<i>fem-1(e1991) unc-24(e138) unc-22(s12)/stDf8 IV</i>	Obtained from the CGC (Williams and Waterston, 1994)
RW7000	<i>C. elegans</i> wild-type, RW subclone of Bergerac BO (Tc1 pattern HCA).	Obtained from the CGC (Williams <i>et al</i> , 1992)

Table 2.1 *C.elegans* strains. **air-1* was previously known as *let-603*

2.3.2 Bacterial strains

Name	Genotype	Notes	Use
HT115 (DE3)	<i>F</i> ⁻ , <i>mcrA</i> , <i>mcrB</i> , <i>IN(rrnD-rrnE)1</i> , <i>rnc14::Tn10(DE3</i> <i>lysogen: lacUV5</i> <i>promoter -T7</i> <i>polymerase)</i> <i>(IPTG-inducible T7</i> <i>polymerase)</i> <i>(RNase III minus).</i>	A gift from CGC	Food source of <i>C.elegans</i> when administering RNAi by feeding
OP50		The strain used in our laboratory is a variant of the uracil requiring OP50 strain (Brenner, 1974) which has been transformed with a plasmid containing the Tet ^r marker (I.L.Johnstone, pers.comm.)	Food source of <i>C.elegans</i>
Novablue	<i>endA1</i> , <i>hsd17(r_{K12}⁻</i> <i>m_{K12}⁺)</i> , <i>supE44</i> , <i>thg1-1</i> , <i>recA1</i> , <i>gyrA96</i> , <i>relA1</i> , <i>lac[F'</i> , <i>proA+B+lac^aZ-</i> <i>M15::Tn10]</i>	Obtained from Novagen, Inc. via R&D systems Europe, Abingdon, UK.	Competent cells for general cloning
XL10-Gold™	Tet ^R Δ(<i>mcrA</i>)I83 Δ(<i>mcrCB-hsdSMR-</i> <i>mrr</i>)I73 <i>endA1</i> <i>supE44 thi-1 recA1</i> <i>gyrA96 relA1 lac</i> <i>Hte [F' proAB</i> <i>lac^RZAM15 Tn10</i> <i>(Tet^R) Amy Cam^R]</i>	Obtained from Stratagene Ltd., Cambridge, UK.	Competent cells for general cloning

Table 2.2 Bacterial strains

2.4. Vectors and Clones

2.4.1. Plasmid vectors

Name of vector	Notes and use
PCR-Script™	A PCR fragment cloning vector derived from pBluescript®II SK(+) phagemid. Used for cloning blunt-ended PCR fragments. Obtained from Stratagene Ltd., Cambridge, UK
pGEM®-T	A PCR fragment cloning vector derived from pGEM®-5Zf(+) phagemid. Used for cloning PCR fragments with 3'-deoxyadenosine tail. Obtained from Promega Corporation.
pTAg	pUC derived phagemid. Used as a carrier in microinjection (contains Kan and Amp resistance gene)
pPD95.67	Promoterless <i>GFP</i> fusion vector (A.Fire, pers.comm.). A gift from A.Fire.
pPD96.04	Promoterless <i>GFPlacZ</i> fusion vector (A.Fire, pers.comm.). A gift from A.Fire.

Table 2.3 Cloning vectors

2.4.2 Clones

2.4.2.1. Plasmid clones

Name of plasmid	Notes and use
pRF4	Contains the dominant <i>rol-6(su1006)</i> <i>C.elegans</i> cuticular collagen mutation (Mello <i>et al.</i> , 1991). Used as a marker for identifying and selecting transformed lines following microinjection of <i>C.elegans</i> . A gift from J. Kramer
p76-16B	Contains 10.7kb <i>Xba</i> I wild-type genomic fragment of <i>unc-76</i> . Used as a marker for identifying and selecting transformed lines following microinjection of <i>C.elegans</i> strain DR96. A gift from Laird Bloom.
pMW0002	Consists of the <i>dpy-7</i> cuticular collagen gene promoter in a translational fusion with GFP contained in the Fire vector pPD95.67 (A. Fire, pers.comm.). A gift from I.L. Johnstone
pJM67	Consists of 5144bp <i>elt-2</i> GATA-like transcription factor promoter fused with <i>GFPlacZ</i> contained in the Fire vector pPD96.04 (Fukushige <i>et al.</i> , 1998). A gift from J. McGhee.

Table 2.4 Plasmid clones

2.4.2.2. Cosmid clones

Cosmid name	Notes and use
C55B7	DNA template for PCR. A gift from J. Sulston and A.Coulson.
F37E3	DNA template for PCR. A gift from J. Sulston and A.Coulson.
F57B10	DNA template for PCR. A gift from J. Sulston and A.Coulson.
K06A5	DNA template for PCR. A gift from J. Sulston and A.Coulson.
R10A10	DNA template for PCR. A gift from J. Sulston and A.Coulson.
T23H2	DNA template for PCR. A gift from J. Sulston and A.Coulson.
W07B8	DNA template for PCR. A gift from J. Sulston and A.Coulson.

Table 2.5 Cosmid clones

2.5 Culture maintenance

2.5.1. Bacterial Culture

2.5.1.1. Bacterial Culture on solid media

All *E.coli* bacterial strains were grown at 37°C on L-Agar plates (9cm diameter plates – Greiner Labortechnik Ltd., Stonehouse, Gloucestershire, UK) supplemented with the appropriate antibiotic. The final concentrations of the antibiotics used were as follows:

E.coli strains transformed with plasmids: 100µg/ml ampicillin or
12.5µg/ml tetracycline

E.coli strains transformed with cosmids: 50µg/ml ampicillin or
25µg/ml kanamycin

2.5.1.2. Liquid Culture of Bacteria

Single colonies were transferred using sterile technique, into L-broth supplemented with the same final concentration of antibiotic as in 2.4.1.1. All liquid cultures of bacteria were grown with vigorous shaking at 37°C in an orbital shaker.

2.6. General Molecular Biology Techniques

2.6.1. Agarose gel electrophoresis of DNA

Restriction endonuclease digested DNA and PCR amplified DNA samples were electrophoresed through agarose gels, ranging from 0.7%-1.8%. Gels were prepared by dissolving the appropriate amount of agarose in 1xTBE. Samples from STS mapping were electrophoresed through 3% MetaPhor agarose (FMC corporation, via Flowgen, Lichfield, Staffordshire) to permit greater separation of smaller DNA fragments. MetaPhor agarose gels were prepared according to manufacturer's protocol. 15cm gels were generally cast using gel electrophoresis kits from GibcoBRL. The gels were generally run at a voltage equivalent to 3-10V/cm in 1xTBE. All DNA samples were loaded into the wells using 1xDNA sample buffer. Gels were post-stained by placing in a container of dH₂O plus 0.2µg/ml ethidium bromide on a moving platform for 20-40 mins, then washed with dH₂O before visualising. The electrophoresed DNA was visualised using a UV transilluminator (Appligene Oncor, Durham, UK) and a record of the gel made using a digital imaging

system (Appligene). Where necessary, the gel contained one lane of DNA size standards, either 1kb ladder or 50bp ladder (both from GibcoBRL).

The T3 and T7 transcript material for RNAi was also electrophoresed through standard 1% agarose gels. Although gels for northern blots would be run differently, this separation was used as a crude measure as to whether *in vitro* transcription had been successful and to examine whether the sense and anti-sense strands had annealed.

2.6.2. Restriction Endonuclease Digests

Digests were set up using the recommended buffer with an appropriate amount of DNA and enzyme. BSA was added (final concentration 100 μ g/ml) where recommended by manufacturer. The quantity of enzyme varied depending on the source of DNA, however, as a general rule, one unit of enzyme was added per μ g of substrate DNA in a 50 μ l reaction volume. Reaction volumes were chosen such that the glycerol content did not exceed 10%. Reactions were incubated at the recommended temperature from 3h to overnight.

2.6.3. Ligation reactions

10 μ l ligations were set up using the recommended buffer. Generally, 100ng vector was ligated with a specified amount of insert using the following equation:

$$\frac{\text{ng of vector} \times \text{size (kb) insert}}{\text{size (kb) of vector}} \times \text{desired insert:vector molar ratio} = \text{ng of insert}$$

As a general rule, a 3:1 insert:vector molar ratio was used as an initial parameter.

1U ligase (NEB) was used per ligation reaction. When ligating PCR products into commercial PCR cloning vectors, manufacturer's recommendations were applied. Ligations were performed at room temperature for 1hour or 16°C overnight.

2.6.4. Purification of PCR-amplified and gel isolated DNA fragments

PCR amplified products were purified using Qiagen QIAquick PCR Purification Kit or QIAquick Gel Extraction kits (both from Qiagen Ltd) according to manufacturer's protocol.

2.6.5. Transformation of *E. coli*

10-50ng of DNA from ligations was transformed into commercially sourced competent cells as described in section 2.3.2. using manufacturer's instructions with the following exception: 50 μ l competent cells were used in each transformation reaction and all volumes of solutions adjusted accordingly. The transformed cells were selected using the appropriate antibiotic resistance marker.

2.6.6. Screening of transformed colonies

Where applicable, blue-white *lacZ* colour screening of recombinant plasmids was applied. Thirty minutes prior to plating out transformations, 100 μ l 100mM IPTG and 100 μ l 2% X-gal was spread onto L-agar plates. White colonies were subject to colony screening by colony PCR or colony lysis.

2.6.6.1. Colony PCR

Single colonies were streaked onto an agar plate containing appropriate antibiotic and dipped into PCR cocktail shown in Table 2.6. Reactions were made to a volume of 20 μ l. Gene-specific primers were used.

Component	Final concentration
10X Taq Polymerase Buffer	1X
MgCl ₂	2.5mM
dNTPs (Promega Corporation)	0.2mM
Sense Primer	4ng/ μ l
Antisense primer	4ng/ μ l
Taq polymerase (Advanced Biotechnologies)	0.5U

Table 2.6 PCR cocktail for colony PCR

Segment	Number of Cycles	Temperature	Duration (minutes)
1	1	94°C	3
2	30	94°C	0.5
		55°C	1
		72°C	*1-3

Table 2.7. Cycling Parameters for Colony PCR * Extension time varied with size of insert, generally 1min/kb.

2.6.6.2. Colony lysis

Colony lysis was also used to screen for transformed *E.coli* colonics. The protocol is outlined below:

- (i) Isolated colonies from transformed plates were picked using a wooden toothpick and patched onto a fresh Amp plate.
- (ii) The patched colonies were grown at 37°C overnight.
- (iii) A sample from each streak was dipped, using a toothpick, into 30µl colony lysis buffer (2% Ficoll, 1% SDS, 0.2% Bromophenol Blue in 1xTBE buffer).
- (iv) Samples were incubated at room temperature for 20 min.
- (v) Samples were microfuged at 13000rpm for 25 min.
- (vi) Samples were placed at 4°C for 30 min to aid subsequent loading onto agarose gel.
- (vii) The sample supernatant was loaded onto a 1.2% agarose gel and care was taken to avoid the loose pellet.
- (viii) The gel was electrophoreses at 5V/cm and DNA visualised by standard means.

Plasmid DNA from colonics containing an inscrt were differentiated from those without, via their increased size when separated by agarose gel electrophoresis.

2.7. DNA preparation

2.7.1. Isolation of *C.elegans* genomic DNA

The method used was a modified version of a protocol used for the isolation of Chromosomal DNA from *C.elegans* (Johnstone, 1999).

- (i) Worms were grown on four 9cm NGM agarose plates and collected in M9 buffer. The worms were washed twice with M9 buffer to remove excess bacteria and pelleted in a 1.5ml eppendorf by centrifugation at 5000rpm for 5 minutes. The approximate volume of packed worms was determined.
- (ii) Six volumes of freshly made worm lysis buffer (50mM Tris-HCl pH8, 100mM NaCl, 50mM EDTA, 1% SDS, 30mM β-mercaptoethanol 100µg/ml proteinase K) was added to one volume of packed worms.
- (iii) The mixture was incubated at 65°C for 4 hours.

- (iv) Debris was removed by centrifuging the lysis mixture at 13000rpm for 5 minutes in a microfuge.
- (v) The lysed worm preparation was extracted with one volume phenol/chloroform and the phases were separated by centrifuging in a microfuge for 10 minutes at 13000rpm, according to standard procedures (Sambrook *et al*, 1989).
- (vi) The aqueous phase was removed and extracted (as above) a further three times with phenol/chloroform.
- (vii) The aqueous phase was extracted once with chloroform.
- (viii) DNA was precipitated by adding 2 volumes ice cold 100% ethanol.
- (ix) DNA was collected by centrifuging at 13000rpm for 30 min.
- (x) Pellet was washed with 70% ethanol.
- (xi) The pellet was resuspended in 1ml TE buffer and left at room temperature for 2h to allow dissolution .
- (xii) DNase-free RNaseA was added to a final concentration of 100µg/ml and the preparation incubated at 37°C for 1h .
- (xiii) The aqueous phase was extracted once with phenol/chloroform and once with chloroform.
- (xiv) DNA was precipitated by adding 0.7 vol isopropanol and $\frac{1}{25}$ vol 5M NaCl.
- (xv) DNA was collected by centrifuging at 13000g for 30 min.
- (xvi) Pellet was washed with 70% ethanol.
- (xvii) Pellet was resuspended in a suitable volume of TE.

2.7.2. Plasmid and Cosmid DNA mini preparation

All plasmid and cosmid DNA was prepared using Qiagen mini kits (Qiagen Ltd) and the method used was as instructed by the manufacturer. As a general rule, 5ml cultures were set up for plasmid DNA preparation and 9ml cultures were set up for cosmid DNA preparation. The pelleted DNA was resuspended in 20µl TE.

2.8. DNA Sequencing

2.8.1. DNA sequencing of PCR fragments

A proof-reading enzyme (*Pfu* Turbo or Vent) was generally used when generating the target DNA for sequencing. However, if poor yields of product were obtained with *Pfu* or Vent, *Taq* DNA polymerase was used. PCR amplified products were purified using Qiagen QIAquick PCR Purification Kit or QIAquick Gel Extraction kits (both from Qiagen

Ltd) according to manufacturer's protocol. The cleaned fragments were eluted in 30 μ l dH₂O and sequenced by MBSU DNA Sequencing Service, IBLS, University of Glasgow.

2.8.2. DNA Sequencing of Plasmid clones

If sequencing was not possible with PCR-amplified products, the fragments were cloned into pGEM or PCR-Script. Plasmid DNA was purified using QIAprep miniprep spin columns (Qiagen Ltd). The DNA was eluted from the column in 30 μ l dH₂O. Purified DNA was sent for sequencing to MBSU DNA Sequencing Service, IBLS, University of Glasgow

Name	Sense	5' position relative to ATG K06a5.7a	Sequence (5'→3')
k06a5.7aseq1	Sense	-100	GTGGTCAATCTCTCTCCGCG
k06a5.7aseq2	Sense	312	CGAAACTCGTCTGTCAGCTCA
k06a5.7aseq3	Sense	711	ATCAAATTTTCGCTCAACCTGC
k06a5.7aseq4	Sense	1104	GGTGGTCATGTGAAAGGAGC
k06a5.7aseq5	Anti	2221	GAGACCTGCAAAGTGTGACTC
k06a5.7aseq6	Anti	1868	GCGCTGATAGATAAGAGCTGC
k06a5.7aseq7	Anti	1401	GACGACATTCAGCAGTACTC
K06a5.7aseqA	Sense	-2	TGATGGCTACCACCGGG
T3*	N/A	N/A	AATTAACCCTCACTAAAGGG
T7*	N/A	N/A	GTAATACGACTCACTATAGGGC
SP6*	N/A	N/A	ATTTAGGTGACACTATAG

Table 2.8 Primers used for Sequencing K06A5.7a. * General sequencing primers used for sequencing plasmid clones

2.9. *C.elegans* Culture

Bristol N2 wild-type, mutant and transgenic *C.elegans* strains were grown at 20°C (Jencons LT3, Jencons Scientific Ltd., Leighton Buzzard, UK) on NGM agar plates (9cm, 5.5cm or 3.5cm diameter plates-Greiner) seeded with OP50 as food source, according to standard procedures (Sulston and Hodgkin, 1988). Starved plates (i.e those devoid of bacteria and containing dauer larvae) were stored at 15°C.

2.9.1. Maintenance of transgenic strains containing a free array

Transgenic worms identified as being roller (described in Section 2.4.2.1) were maintained by transferring the rollers (approximately 10) onto a fresh plate using a platinum wire pick. Transgenic worms identified by *unc-76* repair of phenotype were cultured by similar means, with the exception that rescued worms (i.e. worms with wild-type movement) were transferred onto fresh plates.

2.9.2. Maintenance of strains carrying a sterile or lethal mutation

Strains carrying a lethal or sterile mutation were maintained at 20°C as heterozygotes using the following method: hermaphrodites were picked clonally onto 3.5cm plates and allowed to self fertilise until the first eggs hatched. This parent hermaphrodite was then removed and the F1 brood was scored the following day(s) for the relevant phenotype. This pattern of cloning and scoring was repeated. This genetic analysis of broods was particularly important for new mutations.

2.10. Mutagenesis using Ethyl methanesulphonate (EMS)

2.10.1. EMS Treatment

A healthy mixed population of well-fed worms containing a high number of L4 hermaphrodites were subject to EMS mutagenesis using standard protocol (Sulston and Hodgkin, 1988). The worms were collected from NGM plates and washed twice with M9 buffer to remove excess bacteria. The worms were resuspended to a volume of 2ml and added to 2ml 100mM EMS (to give a final concentration EMS is 50mM), in a sterile glass universal. The worms were incubated in this solution for 4hrs at room temperature. The glass universal was gently shaken at regular intervals to increase aeration. Following incubation the worms were washed three times with M9 buffer, transferred to a fresh 9cm NGM plate and allowed to recover for one hour at 20°C. Approximately 300 L4/young adult hermaphrodites were picked onto a fresh NGM plate and incubated at 20°C overnight. All contaminated glassware and tips were soaked in 1M NaOH overnight prior to disposal.

2.10.2. Non-clonal F2 Mutant Screen

This method was adapted from a method suggested by Michael Koelle (personal communication). Eight P₀s were allowed to egg lay at 20°C until approximately 60 eggs were present on the plate (around 5 hours). These worms were then transferred onto fresh plates for a second lay and then discarded. Fifty 9cm plates were used in each lay and this number of eggs on each plate ensured that optimal conditions were met for screening; the plates were not overcrowded and the F₂s reached the adult stage before the plates were exhausted of bacteria.

2.10.3. Screening for mutants with intestinal lineage defects

Strain IA109 (refer to Section 3.6. for a description of the generation of this strain) was subject to EMS mutagenesis described above. The F₂ generation was screened using a Leica MZ12 dissecting fluorescent microscope. Mutants were identified as having an altered pattern of GFP expression. The putative mutants were picked clonally onto 3.5cm plates and allowed to self. Their broods were analysed for presence and penetrance of the mutant phenotype.

In the case of *ij51*, where the isolated mutant was sterile, heterozygotes for this mutation were required from the plate where the original mutant was obtained. Hermaphrodites were transferred in groups of five onto twenty 5.5cm plates and allowed to self. The twenty plates were then screened for the presence of mutant phenotype ('positive plates'). From one positive plate, 100 animals were cloned individually to 3.5cm plates, allowed to self and the progeny were scored for the presence of the mutant phenotype, thus identifying a heterozygotic parent.

2.11. Classical Genetic mapping

2.11.1 Generation of Males

Male worms occur at a very low frequency at around 0.2% in a wild-type population (Sulston and Hodgkin, 1988). Males were obtained by heat shock: 6 L4 hermaphrodites were transferred to 30°C for four hours and allowed to self at 20°C and males were obtained in the F₁ progeny. Male cultures were maintained by mating males with L4 hermaphrodites, a typical culture containing 10 males and 6 hermaphrodites on a 5.5cm plate with a small bacterial lawn in the centre of the agar.

2.11.2. Setting up genetic crosses

When crossing into homozygous viable strains, 6 L4 hermaphrodites and 10 L4 males were placed in a 5.5cm plate seeded with a small amount of bacteria. When crossing into strains carrying a lethal mutation, single 'old' heterozygotes (i.e. those exhausted of sperm), containing the lethal mutation were placed on a 3.5cm plate with 5 males. The number of F1 males generated determined the success of the cross - a successful cross would contain 50% males in the F1 brood.

2.11.3. Chromosome assignment by classical mapping

Chromosome assignment of new mutations was determined by standard linkage analysis using visible markers. Mutant alleles were crossed into a mapping strain e.g. MT465. MT465 contains a recessive visible mutation on chromosomes I, II and III: *dpy-5* (*e61*) on chromosome I, *bli-2* (*e768*) on chromosome II and *unc-32*(*e189*) on chromosome III. Outcrossed F1s were picked onto single 3.5cm plates and allowed to self, generating F2 recombinants of classes Dpy-non-Bli-non-Unc, Bli-non-Dpy-non-Unc and Unc-non-Dpy-non-Bli. These recombinant F2s were scored for the presence of the mutant test allele: if the test allele was not linked to a chromosome, 25% of F2s of the recombinants marking that chromosome (e.g. Dpys for chromosome I) would also be homozygous for the test allele. Linkage was detected by a reduced frequency of such double mutants. Other strains were available to assign linkage to chromosome IV and V. Mutations assigned to X chromosome can be assigned by segregation through males.

2.11.4. Multi-factor crosses

Multi-factor crosses are used to position a mutation relative to known mutations. For example, in a three-factor cross, ordering mutation *z* with respect to *x* and *y* would involve selfing a recombinant of the class $x^+ y^+ z^+$. Recombinant progeny of class X-non-Y and Y-non-X would be picked and the phenotypes and genotypes of their progeny analysed for the presence or absence of phenotype Z. There are three possible scenarios: *z* lies to the left of *x*, *z* lies between *x* and *y* or *z* lies to the right of *y*. One can use the proportion of values obtained to estimate the relative distances between *x*, *z* and *y*.

2.12. Sequence Tagged Sites (STS) mapping

STS mapping is a PCR-based mapping system that allows fast positional information of a mutation. It utilises known Tc1 insertions into the genome of the Bergerac strain, RW7000, (Williams *et al.*, 1992; Williams, 1995) that are not present in N2. The principle of STS mapping is outlined in Chapters 3 and 4.

The protocol used for STS mapping of mutant alleles was essentially the same as that described in Williams *et al.* (1992). Slight modifications were made to the PCR cocktail and PCR conditions. These are detailed in Tables 2.9 and 2.10 below. The protocol for the mapping of dominant alleles was obtained from Michael Koelle (personal communication).

Component	Final concentration
10X Taq Polymerase Buffer (as described in Williams <i>et al.</i> , 1992)	1x
dNTPs (Promega Corporation)	0.2mM
Tc1 primer 618	125pM (24ng/ μ l)
Each STS specific primer	25pM (4ng/ μ l)
Taq polymerase (Advanced Biotechnologies)	0.5U

Table 2.9 STS PCR reaction cocktail

The reactions were made up to a final volume of 25 μ l. Each worm was lysed in 2.5 μ l-10 μ l single worm lysis buffer. The PCR cocktail was mixed with the 2.5 μ l DNA from the lysis step and mineral oil was laid over the top. The reactions were carried out using a Crocodile III thermocycler (Appligene) using the conditions in Table 2.10.

Segment	Number of Cycles	Temperature	Duration (minutes)
1	1	94°C	3
2	38	94°C	0.5
		58°C	1
		72°C	1

Table 2.10 Reaction parameters for single worm/embryo PCR

Primers used for STS mapping are shown in Table 2.11 below. 10 μ l of each reaction was run on 3% MetaPhor gel as described in Section 2.6.1.

Name	Polymorphism	Chromosome	Product size	Sequence (5'-3')
618*				GAACACTGTG GTGAAGTTTC
734	<i>hP4</i>	I	130	AAATATTATCA GCACAGC
723	<i>maP1</i>	II	234	CCAATT'TCCG GAAGTT'TCG
363	<i>stP100</i>	II	198	GGAAACCAAG AACATTGGAC G
886	<i>stP36</i>	II	153	CACTGTCTTGT CGATAACC
543	<i>stP196</i>	II	133	CCAAAAGTTTA AAGGAAATGA AGC
133	<i>stP101</i>	II	118	CGCCTGATTTT TCCAGGIGC
587	<i>mgP21</i>	III	165	GGAACAAAAG TGCCTTGGG
845	<i>stP19</i>	III	216	ACAAGCGGGT CTACTGAACC
401	<i>stP127</i>	III	233	GCATCGATACA AGTGGAAAGC
548	<i>stP120</i>	III	149	AATAATCAGTG AAGCCTCATG
800	<i>stP17</i>	III	183	CTCGATGTGTC TCAATAGTTCC
653	<i>stP4</i>	IV	179	TTTCTGTTTG TGCTTAGACG
056	<i>stP51</i>	IV	281	GTTCGTTTTTA CTGGGAAGG
510	<i>stP5</i>	IV	261	GGATTATTACC GTCTTACGCA
815	<i>stP13</i>	IV	236	CCCACAACCTT TTGCTACAAC
931	<i>stP44</i>	IV	209	CCATCGTTTGT GTCTAGAGTC
536	<i>stP35</i>	IV	149	GCAGTCTCTAA TAGAGCTGC
813	<i>stP3</i>	V	153	GTCGCAIT'ICC ATTCATGCAG
440	<i>stP192</i>	V	290	GCACGCTGAG AGTAAAGTGC
997	<i>stP23</i>	V	135	TTGTCAACTAT TTTACAGCGAG
736	<i>bp1</i>	V	119	AACACATTTAG GTAATGTAGCA C

Name	Polymorphism	Chromosome	Product size	Sequence (5'-3')
998	<i>stP6</i>	V	170	TCACAATCGAT GACTAAGTACT GG
862	<i>stP18</i>	V	203	TTGAACTTCTC CCACTCCTC
438	<i>stP108</i>	V	135	AAAGATAAAC GCGCTTTTGG
439	<i>stP105</i>	V	152	GGGTAGTTGTT CATGTCTCG
652	<i>stP128</i>	V	200	GCAACGCTTTG TGGATCTG
112	<i>stP33</i>	X	260	CGTCTAGTCGT GTGTTTCC

Table 2.11 Primers used for STS mapping. *Primer 618 is the common *Tc1* primer used in every STS assay. Primers typed in **bold** are those used for chromosome assignment of mutations.

2.13. Physical mapping of *hDf8* using PCR based approach

This method was used to map the left-hand breakpoint of the deficiency *hDf8*. The method used to obtain DNA from single embryos and the PCR conditions was essentially the same as described in Williams *et al.*, 1992 with the following changes: single homozygous mutant deficiency embryos were lysed in 12.5 μ l SWLB (as opposed to 2.5 μ l) and the PCR cocktail and PCR conditions used are described in Section 2.7.1. DNA from each lysed embryo was split between four reactions, 2.5 μ l of DNA solution was used per assay. Primers were designed to amplify small genomic sequences within cosmids (Cosmid Sequence Marker, CSM) covering the *let-601- let-607* region of chromosome I. CSMs were amplified from *Df* embryos by PCR where the presence or absence of products was used to determine if an individual gene was deleted in the *Df*.

Each embryo was tested for the presence or absence of two test CSMs. In addition to the test CSM, a positive and negative control CSM were also amplified.

Name	Sequence (5'-3')	Sense	Gene amplified	Size of fragment produced
F26B1 sense	ATGATGATCAAAGTGG GAGC	sense	F26B1.	216
F26B1 anti	GAATGAGCGTACACGC AGTG	antisense		
F37E3 sense	TTATTTGCGCTGGAATT GAT	sense	F37E3.3	224
F37E3 anti	GGTACATATCTGAGTTT TGAAGGAA	antisense		
F48A9 sense	GACAGGAAAAACAGCA TTGAG	sense	F48A9.2	311
F48A9 anti	GCACTATGTACCACCA ATCCATTA	antisense		
R10A10 sense	TTATTTGCTCGTGC GGC TGA	sense	R10A10.2	229
R10A10 anti	GGGAGCAGGAGATCCA CACT	antisense		
R10A10.1 sense	AAACTTCAAAGCTTTTT CCCAC	sense	R10A10.1	102
R10A10.1 anti	GAGAAGAACATGAACA AATCACG	antisense		
T10E9 sense	TTGTTCGTGGAGTAGC TG	sense	T10E9.7	310
T10E9 anti	GTAAGTGTACGATA GTATGG	antisense		
T23H2 sense	TCGCATGCTCGATCCG TCTAGT	sense	T23H2.3	315
T23H2 anti	ATCCCGCACTGGAACA GCAG	antisense		
ZC328 sense	GAAAAGTTGTATGCA GCC	sense	ZC328.1	370
ZC328 anti	CGGAAATATGTAGAAC TACCGTA	antisense		

Table 2.12 Primers for mapping left-hand breakpoint of *hDf8*

2.14. Generation of *C. elegans* transgenic strains by microinjection

2.14.1 Preparation of materials and worms for microinjection

All plasmid and cosmid DNA used for microinjection was extracted and purified using the Qiagen Plasmid Mini or Qiagen Plasmid Midi kits as described in Section 2.7.2. Genomic DNA was purified using the protocol described in Section 2.7.1. For injections with linear DNA to generate complex arrays, plasmid and genomic DNA were digested with the appropriate restriction enzyme and purified via a Qiagen spin column (Section 2.6.4.). The concentrations of DNA used are shown in Table 2.12. Immediately before use, the injection mix was centrifuged at 15000rpm in a microcentrifuge for 20 minutes. The injection mix was first loaded onto a drawn out capillary (Clark Electromedical Instruments) using a mouth pipette (Sigma) to aid loading into the injection needle. The injection mix was transferred to the needle and care was taken to avoid touching the needle tip and forming air bubbles.

Injection pads were prepared by adding a drop of molten 2% agarose in dH₂O on a 64mm x 22mm glass coverslip (Thickness 1, BDH). A second coverslip was placed on top, flattening the agarose to a thin pad. When the agarose hardened, one coverslip was removed. The agarose pads were dried by placing in an 80°C oven for 10 minutes.

Needles for microinjection were prepared from Aluminium Silicate glass capillaries with inner filament (Clark Electromedical Instruments, Pangbourne, Reading, UK) . Needles were pulled to the desired shape using an electrode puller (Model 773, Campden Instruments Ltd., Sileby, Loughborough, UK).

Purpose of injection	Transformation material	Injection Mix	Final Concentrations (ng/ μ l)
<i>cpr-5::lacZGFP</i> transgenic lines	Plasmid DNA	p76-16B	100
		pCC7 or pCC16	10
	Linear Plasmid DNA	<i>Sma</i> I cut p76-16B	1.5
		<i>Fsp</i> I cut pCC7	2
		<i>Pvu</i> II cut genomic DNA	100
Rescue of <i>let-604</i>	Cosmid DNA	F37E3	10
		R10A10	10
		C55B7	10
		T23H2	10
		K06A5	10
		pTag	100
		pMW002	10
<i>elt-2::lacZGFP</i> expression <i>lin60(ij48)</i> mutant	Plasmid DNA	pRF4	100
		pJM67	2
Phenocopy <i>cdc25.1(ij48)</i>	Linear Plasmid DNA /PCR product	PCR K06A5.7a	2/5/10
		<i>Fsp</i> I cut pJM67	0.2
		<i>Eco</i> RV cut pRF4	2
		<i>Pvu</i> II cut genomic DNA	100

Table 2.13 Transformation material

Paraffin oil was placed on top of the dried agarose pad. Five young adult hermaphrodites were transferred to the paraffin oil using a platinum wire pick and allowed to adhere to the agarose. Once immobilised, the injection procedure commenced immediately.

The microinjection procedure and apparatus are essentially the same as that described by Mello *et al.*, (1991) and Mello and Fire (1995). The loaded needles were mounted onto the microtool collar of a Narishige MO-202 Joystick Hydraulic Micromanipulator (Narishige Co Ltd., Tokyo 157, Japan). The needles were pressurised using a compressed nitrogen source. A pressure regulator and solenoid valve was attached to the nitrogen cylinder. Pressure was delivered with a foot pedal connected to the solenoid valve. Agarose pads containing immobilised worms were taped onto the stage of a Zeiss

Axiovert 100 inverted microscope fitted with Normaski optics. The needle and agarose pad were positioned into the same focal plane using 50X magnification and the needle was opened by scratching the tip against a piece of glass on the pad. The pressure was adjusted to obtain a good flow. The syncytial gonad of the worm and needle were brought into the same focal plane using 400X magnification. Once this was achieved, the needle was forced to puncture the worm and DNA or dsRNA was released into the syncytial gonad by applying pressure to the foot peddle. After injection, the pad was placed under a dissecting microscope and a drop of M9 buffer was placed on top of the oil. This caused the worms to float from the pad. The worms were then transferred to a drop of M9 on a seeded NGM agar plate, using a platinum pick. Injected worms were allowed to recover at 20°C.

2.15. Gamma ray-induced integration of extrachromosomal arrays

The protocol used was essentially the same as that described in Mello and Fire (1995). A ^{60}Co source was used as a source of γ -radiation, instead of ^{137}Cs . Extrachromosomal lines with a low transmission frequency were chosen for integration as this allowed easier identification of integrated lines. Two lines were chosen for integration, IA099 (containing 1kb *cpr-5* promoter fused to *GFPlacZ*) and IA102 [containing 3kb *cpr-5* promoter fused to *GFPlacZ* (Section 3.6.)]

Healthy worm cultures containing a high proportion of L4 animals were irradiated with 3800 rad using ^{60}Co source (courtesy of the late Prof Tom Wheldon, Beatson Institute of Cancer Research, University of Glasgow). The P_0 worms were allowed to recover for two hours. For IA099, 5 L4 irradiated worms were picked onto each of 20 seeded 9cm plates. For IA102, 8 L4 irradiated worms were picked onto each of 20 9cm plates, and allowed to grow. The cultures were allowed to starve. A chunk of agar was transferred from each large plate onto a 5.5cm plate, as far from the bacterial lawn as possible. Worms which are *Unc-76* rescue and have wild-type locomotion, move to the bacterial lawn and are selected over the *Unc-76* non-rescued worms, which generally remain in the agar plug. For IA099, 20 *Unc-76* rescued worms (presumably F2s) from each medium plate were transferred onto single 3.5cm plates (the total number of F2s cloned was therefore 400). For IA102, 10 *Unc-76* rescued worms from each medium plate were picked to individual 3.5cm plates (the total number of F2s cloned in this case was 200). Integrated lines were selected from different F1 populations.

2.15.1. Identification of integrated lines

The F2 animals were allowed to self and the F3 progeny were screened for 100% segregation of the transgene. The lines were then outcrossed to N2 at least three times. During each round of outcrossing the absence of death was checked to ensure no extraenous chromosomal rearrangements were present.

2.16. RNA-mediated interference (RNAi)

The general protocol and information concerning RNAi can be found in the Fire lab website version 1.0, February, 1998 (also Fire *et al.*, 1998; Tabara *et al.*, 1998).

2.16.1. Generating the target DNA fragment using PCR

Specific primers were designed to each cloned or predicted gene (Table 2.16). Each of these primers had either T3 or T7 promoter sequences engineered to their 5' end so the amplified fragment could be used as a template for *in vitro* RNA synthesis. As cosmid or genomic DNA was used as a template for PCR, intronic sequences were present. As a general rule, primers were designed such that the fragment of DNA amplified contained over 500bp of exonic sequence. Reactions were made to a volume of 50 μ l with dH₂O. 3x 50 μ l reactions were set up for each primer set. The PCR components, PCR conditions and primers used are shown in Tables 2.14, 2.15, and 2.16, respectively.

Component	Final concentration
10x Taq Reaction buffer (AB)	1x
MgCl ₂	2.5mM
dNTPs	0.2mM
DNA template	4ng/ μ l
Primer Sense	4ng/ μ l
Primer Antisense	4ng/ μ l
Taq DNA Polymerase (AB)	2U

Table 2.14 Components of reaction mix for generating template for *in vitro* transcription

Segment	Number of cycles	Temperature	Duration
1	1	94°C	3 min
2	25-30*	94°C	1 min
		58°C	1 min
		72°C	1 min
3	1	72°C	10 min

Table 2.15 Cycling parameters for PCR for generating template for *in vitro* transcription. *25 cycles were performed when cosmid DNA used as template. 30 cycles were performed when genomic DNA was used as template.

Name	Sequence (5'-3')	Sense	Size of fragment produced (bp)
T3	AATTAACCCTCACTAAAGGGAGA	-	-
T7	TAAATACGACTCACTATAGGGAGA	-	-
R10A10.2S	TTATTTGCTCGTGCGGCT	sense	958
R10A10.2AS	GTGCTCAGTAAGTCAATTATTCCA	antisense	
F37E3.2S	GCGTTTTCCGGAAGAGG	sense	779
F37E3.2AS	TCTGACACATTCATTCCTTCTTG	antisense	
F37E3.3S	GAGCAATCCGCTAGCACC	sense	836
F37E3.3AS	GGATTTCTTTCATTTGGTGAGA	antisense	
T23H2.1S	ATCTACTCGTCCCGATATTGTCT	sense	1022
T23H2.1AS	GGTTTCTAGCATCCAATTATCTCC	antisense	
T23H2.2S	TGATTGCTGTCCGTGGTG	sense	856
T23H2.2AS	TCTACATTCGATCTTCTCCCTT	antisense	
T23H2.4S	GCCTCTGCTCAACCACAGGA	sense	1007
T23H2.4AS	GAATGGCGACTTTGAGGGTA	antisense	
T23H2.5S	CCCGGATGAAACATTTACAA	sense	1245
T23H2.5AS	TGCCATGACTCAAGTGTCTT	antisense	
K06A5.7aS	ACAAGGAACTGTATGACCCC	sense	874
K06A5.7aAS	CGGCGAAGCCAGTTCTT	antisense	
C55B7.2S	TTCAGAAATGTTCCCGATTTC	sense	1010
C55B7.2AS	CAACTGCTGACGAAAATTAT	antisense	
C55B7.3S	GTTACTATGAAAGTTCGAGTATGCC	sense	1006
C55B7.3AS	TGCAGAACAATGGACAACGA	antisense	

Name	Sequence (5'-3')	Sense	Size of fragment produced (bp)
C55B7.10S	GTTTATTTGCTTGTAATCAGGTGC	sense	722
C55B7.10AS	CGTAGGCTGAAAATAAGTCAATTGA	antisense	
C55B7.12S	AGGAGCAGACAGGTGTGTGG	sense	854
C55B7.12AS	GCAACGAATGATGGAAATATTC	antisense	
F57B10.1S	AAATTTTCAGTTGTTTCCGATCCAG	sense	1025
F57B10.1AS	CCCCAACTGTGCAAACACC	antisense	
wee1.1S	TGAAATATACTAACC GAAGG	sense	1014
wee1.1AS	CACCAACTGGTAAGTATTTT	antisense	
wee1.3S	ACCAACCGTTTCC AAGTTT	sense	980
wee1.3AS	CATGATATGCAAAC TCGG	antisense	

Table 2.16 Primers used to generate DNA template for *in vitro* transcription

The PCR reactions electrophoresed on 0.8% gels and amplified fragments purified as in Section 2.6.4.

2.16.2. *In vitro* transcription

The RiboMAX™ large scale RNA production systems kit (Promega Corporation) was used for T3 and T7 synthesis of RNA, using the amplified DNA as a template. The manufacturer's protocol was followed, with the exception that 50µl reactions were set up (as opposed to 100µl). The pelleted RNA was resuspended in 50µl DEPC-treated water and incubated at 65°C for 10min to aid resuspension. Once resuspended, RNA was stored at -80°C.

2.16.3. Annealing reaction

Equal amounts (10µg) of sense RNA and antisense RNA were incubated with 1x injection buffer and 80U RNAsin ribonuclease inhibitor (Promega Corporation) in a final volume of 20µl. The mix was incubated at 68°C for 10min and 37°C for 30min. Successful annealing was checked on a standard 1% agarose gel (Section 2.6.1). The injection mix was stored at -80°C. All dsRNA was injected using the same method described for microinjection of DNA (Section 2.14), at a final concentration of 1mg/ml.

2.16.4. Examination of phenocopies produced by RNAi

Injected hermaphrodites were allowed to recover for between 6h to 14h. Healthy hermaphrodites were transferred separately onto 3.5cm plates. The worms were transferred to fresh plates after 12h. F1 progeny were examined and scored for visible phenocopies such as death (embryonic/larval/sterility), dumpy (Dpy) and uncoordinated (Unc). Suppression of the *lin-60 (ij048)* phenotype was scored using GFP stereomicroscope.

2.16.5. RNAi administered by bacterial feeding method

The general method for administering RNAi in the duration of this work was by microinjection. The technique of administering RNAi by bacterial feeding was only used for certain applications of RNAi of K06A5.7a (refer to Chapter 5). PCR products containing genomic sequence were amplified from cosmid DNA with Taq DNA polymerase, using the method described in Section 2.16.1. The sequence and position of the primers are shown in Table 2.16 The amplified fragment was first cloned into pGEM-T. Colonies containing correctly sized inserts were identified by PCR. Plasmid DNA containing inserts were digested with *Spe*-I and *Nco*-I and ligated into a similarly digested L4440 vector (Timmons *et al.*, 1998). The ligated product was transformed into HT115(DE3) bacterial strain using standard procedures.

The RNAi feeding protocol was essentially as described by Fraser *et al.*, (2000) with the following exceptions: 5.5cm plates containing NGM agar with 1mM IPTG and 100µg/ml ampicillin were inoculated with bacterial cultures. The plates were incubated at room temperature for 16h to allow λ 7 polymerase induction. To isolate lethal embryos, between 10 and 15 L4 hermaphrodites were placed onto the induced plates and incubated at 25°C. These worms were removed after 16h and placed onto a fresh RNAi plate and allowed to egg lay for 24h. The process of removing the worms onto fresh induced plates was repeated once. Each plate was examined for dead eggs 16h after the removal of hermaphrodites. To isolate sterile adults, eggs were transferred to induced plates and allowed to develop on the induced plates at 25°C.

Name	Sense	5' position relative to ATG K06A5.7a	Sequence (5'→3')
K06a5.7aseq1	Sense	-100	GTGGTCAATCTCTCTCCGCG
K06a5.7aseq5	Anti	2221	GAGACCTGCAAAGTGTGACTC

Table 2.17 Sequence and position of primers for RNAi K06A5.7a by feeding

2.17. Microscopy of live and fixed specimens

2.17.1. Nomarski and fluorescence optics used in microscopy of live and fixed specimens

Live embryos, larvae and adults were viewed using a Zeiss Axioplan microscope (Carl Zeiss, Oberkochen, FRG) using appropriate magnification. The lenses used were 10x/0.3, 20x/0.5, and 40x/0.75 Plan-Neofluar, and 63x/1.4 and 100x/1.4 Plan-Apochromat. GFP fluorescence was viewed using a mercury lamp (240V 100W, Osram) UV source and filter set 09. Images were taken with a Hamamatsu C4742-95 (Hamamatsu photonics, Hamamatsu City, Japan) monochrome digital camera and Openlab 2.2.0. software. Images were processed using Adobe Photoshop version 5.5 or Openlab.

2.17.2. Preparation of slides for observations of living embryos, larvae and adults

A 0.4mm thick pad was generated by flattening a drop of 2% molten agarose in H₂O on a twin frosted microscope slide (slide A) with a second microscope slide (slide B), placed at right angles to slide A. Slide B was supported on either side of slide A with two slides (running parallel and separated by slide A), each resting on 2 layers of autoclave tape. This generated an agarose pad of approximately 0.4mm thickness and 15mm diameter. Care was taken to avoid the formation of air bubbles. Embryos were washed from an NGM plate using M9 buffer and transferred to a watchglass. A 1mm capillary (Clarke) was drawn out to a thickness of around 0.2mm and attached to a mouth pipettor. This was used to transfer embryos to the agarose pad. Embryos were placed around the surface of the pad, not too close to the edge, in a volume of around 20µl. A 22x22mm coverslip (thickness 1, BDH) was carefully laid on top of the agarose pad using a scalpel blade. The edge of the coverslip was sealed using molten white soft paraffin (Pinewood

laboratories, Clonmel, Ireland). The specimen was stored in a humid chamber at 20°C prior to viewing.

2.17.2.1. Preparations of slides for short term microscopy of live larvae and adults

Essentially the same method was used to prepare slides for microscopy of live larvae and adults as for embryos, with the exception that live worms were paralysed by adding 10mM (final concentration) sodium azide to the molten agarose. Worms were transferred onto agarose pads using a platinum wire pick and stored in the same way as for embryos.

2.17.2.2. Preparation of slides for time course observations of live embryos

Agarose pads were made in the same manner as 2.17.2 with the exception that 5% agarose was used (as opposed to 2%). Gravid hermaphrodites were transferred from plates using a worm pick into a watchglass containing 100µl M9 buffer and cut open using two 25 gauge needles (Microlance, Becton Dickinson S.A., Madrid, Spain), releasing embryos into the buffer. Embryos were transferred to the pad, a coverslip was overlaid, and the pad was sealed with white paraffin as above. In between viewings, specimens were stored in a humid chamber at 20°C.

2.17.3. Preparation of slides for immuno-fluorescence staining

Slides were cleaned with 70% ethanol and subbed by immersing the slide in 0.1% Poly- L-Lysine solution for 10 minutes then allowed the slide to dry at 60°C for 30 minutes. Embryos were transferred from plates to a watchglass containing M9 buffer to remove excess bacteria. A large amount of embryos in 20µl were transferred to the Poly-L-Lysine coated slide using a drawn out capillary attached to a mouth pipette. A 22x22 coverslip (thickness 1, BDH) was lowered over the buffer using a scalpel blade and excess buffer wicked off the edge of the coverslip using a tissue.

2.17.3.1. Permeabilisation of embryo specimens on slides by freeze-crack method

Following preparation, slides were placed on a pre-cooled aluminium block which was surrounded with dry ice. After 10 minutes, the specimen was permeabilised using the freeze-crack method (Siddiqui *et al.*, 1989), by removing the coverslip using a scalpel.

2.17.3.2. Fixation of embryos on slides

Following permeabilisation, slides were placed in Copelin jars filled with methanol pre-chilled to -20°C , and incubated at -20°C for 10 mins. Slides were then transferred to acetone at -20°C for 10 min, then rehydrated with 1xPBS.

2.17.3.3. DAPI staining of fixed specimens

Following permeabilisation, fixation and rehydration described above, $30\mu\text{l}$ of $1\mu\text{g/ml}$ DAPI (Sigma) was placed over specimen. A 22x22 coverslip (thickness 1, BDH) was lowered over the DAPI and specimen using a scalpel blade. The coverslip was sealed using nail varnish and specimen viewed immediately.

2.17.3.4. Antibody staining of fixed embryos

Refer to Table 2.17 for a description of the primary antibodies and dilutions used. The secondary antibody used for most staining was FITC (goat-anti-mouse or goat-anti-rabbit) (Sigma) at a 1:50 dilution in blocking solution (PBST + 1% dry milk). The secondary used with CDC25 antibody staining was Alex Fluor 546 goat anti-rabbit (Molecular Probes). The protocol used was a variation of a protocol obtained from J. Ahringer (pers.comm.).

- i) Following hydration, excess PBS was removed with a tissue and the slide placed in a humid chamber. Approximately $500\mu\text{l}$ of blocking solution was placed over the slide and left at 20°C for 20 min. Blocking solution was removed by tilting the slide at a 45° angle, and excess block removed with a tissue. Primary antibody, diluted in blocking solution, was added to the slide and the slide incubated in a humid chamber at 4°C overnight.
- ii) The primary antibody was removed and the slides were washed 2x15mins with 1xPBST. Washing was carried out by pipetting 1ml 1xPBST onto the slide placed flat in a humid chamber. After 15 minutes, PBST was removed by tilting the slide and draining it onto a tissue.
- iii) Excess PBST was removed from the slide by wiping a tissue around the area surrounding the embryos. $500\mu\text{l}$ of secondary antibody was added and the slide incubated in a humid chamber at 37°C for 1hr.
- iv) The secondary antibody was drained from the slide and the slide washed 2x15min with 1xPBST as in (ii), with the exception that the slide was covered with foil during the washes, to prevent exposure of the slide to light.

- v) The slides were allowed to dry completely and 15 μ l of mounting solution (50% glycerol, 1xPBS, 2.5% DABCO) was placed on top of the specimens. A 22x22 coverslip (thickness 1, BDII) was gently lowered with a scalpel blade to prevent the formation of air bubbles. The edges of the slide were sealed with clear nail varnish and the slide stored in a dark slide box at 4°C until viewing.

Antibody name	Antibody type	Localisation	Dilution used in staining	Notes and reference
ICB4	Monoclonal	Mixed (intestinal, sperm, IL2 neuron, CEM cells, pharyngeal gland, valve and sensory process in male tail)	1:2	A gift from Mario de Bono. (Okamoto and Thomson, 1985; Bowerman <i>et al.</i> , 1992b)
MH27	Monoclonal	A component of adherens junctions between hypodermal cells and within the intestine.	1:500	A gift from R. Waterson. (Francis and Waterson, 1985)
CDC25.1	Polyclonal (Anti-peptide)		1:50	Clucas <i>et al.</i> , 2002.

Table 2.18 Antibodies used in immunofluorescence microscopy

2.18. Cell lineage analysis

Cell lineage analysis was performed essentially as described by Schnabel *et al.*, 1997. Embryos were dissected from gravid *ij48* hermaphrodites and placed on 5% agarose pads. The embryos were oriented to the same axis using a fine hair. Cell divisions were examined from 2-cell stage at 20°C except with *lin-62* where cell divisions were examined at 25°C. Cell lineage was performed for all blastomeres until the 16-cell stage.

Thereafter, only E (and in one case, D lineage as a control) were examined. Recordings were taken using a 100x Neofluar objective. Attached around the objective was a copper ring, which water passed through: this permitted a constant temperature throughout the recording. 25 images, separated by a distance of 1 μ m between each focal plane, at intervals of 30-35 seconds, were taken for approximately 12h. The recordings were taken until the embryos were around 1.5-fold stage. Embryos older than this stage cannot be examined by time lapse recording due to the embryo moving. The time-lapse recordings were analysed using Biocell software.

2.19. Transgenesis with *cdc25.1(ij48)*

A fragment was amplified by *Pfu*-Turbo (Stratagene) using wild-type or *lin-60(ij48)* genomic DNA as template, and primers and reaction conditions in Tables 2.19 and 2.20 below. The primers were designed to ensure that a functional promoter and polyadenylation signals were present in *cdc25.1* gene (Ashcroft *et al.*, 1998; Ashcroft *et al.*, 1999).

Several unsuccessful attempts were made to clone these PCR-amplified fragments. I therefore injected them as linear fragments (Chapter 5).

Name	Sense	5' position relative to ATG K06A5.7a	Sequence (5'→3')
K06a5.7aWS	Sense	-3550	GAACGCCGAGTAACAATTGG
K06a5.7aWAS	Anti	+3110	ATCCGGCTTTTGGTTATTG

Table 2.19 Primers designed for transgenesis with *cdc25.1*

Segment	Number of cycles	Temperature	Duration
1	1	94°C	3 min
2	30	94°C	1 min
		54°C	1 min
		72°C	14 min
3	1	72°C	10 min

Table 2.20 Reaction parameters for amplifying *cdc25.1*

Chapter 3

A genetic screen to identify genes involved in the execution of the E-cell lineage in *Caenorhabditis elegans*

3.1. Introduction

Caenorhabditis elegans is an excellent organism for genetic analysis: the short life cycle together with the self-fertilising hermaphrodites allows the generation of large numbers of homozygous mutant animals. The generation and analysis of mutants has been the key to the success of the *C. elegans* research because much about the *in vivo* function of a gene can be inferred from an analysis of its mutant phenotype(s). A wide variety of mutant phenotypes have now been described, many of which are identifiable with a dissecting microscope. Moreover, the transparency of *C. elegans* and the largely invariant cell lineage for both embryonic development and post-embryonic development, facilitates detailed characterisation of a phenotype at the level of individual cells.

The *C. elegans* genome sequence predicts approximately 19,000 genes. Around 2000 of these have been identified in forward genetic screens for animals with mutant phenotypes. Many mutants have been identified by direct inspection of progeny of mutagenised hermaphrodites. These include, for example, mutants with neuronal defects identified by abnormal movements, skeletal defects with altered body shape, and essential genes identified by lethality. Once a mutant with a desired phenotype has been identified, one can screen for suppressors and modifiers to identify other genes in the pathway. Sophisticated genetic tools such as balancer chromosomes and free duplications can aid with saturation screens in certain regions of chromosomes. For example, saturation screens for lethal mutations have been achieved utilising the free duplication *sDp2*, in the *bli-4 unc-13* region of chromosome I (McDowall and Rose, 1997b). Cosmid rescue of these lethal mutations allowed the alignment of the genetic and physical map of chromosome I (McDowall and Rose, 1997a).

A variety of mutagenic treatments are available and choice is made depending upon the type of mutation required (e.g. point mutation versus deletion) together with the efficiency and specificity of the mutagen. Chemical treatments such as ethyl methanesulphonate (EMS), nitrosoguanidine (NTG), diethyl sulphate, N-nitroso-N-ethyl (ENU), formaldehyde, acetaldehyde, diepoxyoctane (DEO) and diepoxybutane can be used to generate point mutations and/or deletions. Radiation treatments such as γ - and X- and

ultraviolet-rays are more commonly used to create chromosomal rearrangements (Sulston and Hodgkin, 1988; Anderson, 1995). Psoralen-UV mutagenesis is now commonly used to create gene knockouts in *C. elegans*.

EMS is the most commonly used mutagen in *C. elegans* research. The frequency of loss-of-function or reduction-of-function alleles for an average sized gene is about 5×10^{-4} per mutagenised gamete. EMS generally creates G/C \rightarrow A/T transition, although around 13% of EMS induced mutations are deletions. The frequency of G/C \rightarrow A/T transitions mutations is high, approximately 7×10^{-6} to 8×10^{-6} per G/C base pair in a mutagenised genome. This has been estimated by screening for mutants of defined genes, for example amber suppressor mutations affecting tRNA^{trp} genes (Hodgkin, 1985; Kondo *et al.*, 1990). Thirty-six percent of the *C. elegans* genome is G/C (Sulston and Brenner, 1974). The haploid genome of *C. elegans* is 10×10^7 bp (*C.elegans* sequencing consortium, 1998; Wormbase, 2002), thus every mutagenised gamete contains an excess of 200 G/C \rightarrow A/T transitions. F1 progeny derived from mutagenised hermaphrodites could therefore theoretically contain over 400 mutations.

Such an excess of mutations could prove to be detrimental when studying phenotypes of interest. Each new mutant is therefore thoroughly outcrossed to a wild-type background. This will remove most, but not all unwanted base pair changes. Linked mutations can only be removed via recombination, therefore selecting recombination on both sides of the gene of interest can remove all but the closest unwanted mutations on the same chromosome. Isolating multiple alleles of a gene of interest can assist in evidence that extraneous mutations are not playing a role in the phenotype of the mutant. Also, many genes when mutated, do not show an easily identifiable mutant phenotype. Redundancy is apparent when the simultaneous inactivation of two genes results in a strong phenotype that is not seen with either single gene knockout. It is widely known that genetic redundancy exists in *C. elegans*. For example, both a Tc1 deletion mutant and RNAi of *pes-1*, a member of the fork head family of transcription factors do not show a detectible mutant phenotype. RNAi of T14G12.4, an orthologue of the *Drosophila* segmentation gene *slp-2*, produces impaired L1 movement. However, disruption of *pes-1* with T14G12.4 results in L1 larval death (Molin *et al.*, 2000). It has been estimated that only 20-35% of all *C. elegans* genes are mutable to an obvious viable phenotype or to a sterile or lethal phenotype (Johnson and Ballie, 1997; Waterston *et al.*, 1997; *C. elegans*

sequencing consortium, 1998; Hodgkin and Herman, 1998). However, the subtle effects may contribute in more significant ways in the natural environment of *C. elegans*.

With the entire genomic sequence of *C. elegans* available, many reverse genetic screens have been performed whereby the inactivation of genes of interest has been targeted. Recombination-mediated gene replacement, where a wild-type genomic copy of a gene is replaced with a mutant copy has been largely unsuccessful in *C. elegans*. However, gene knockouts can be obtained by a random deletion mutagenesis approach, by chemical or transposon means, followed by PCR screening to detect the desired genetic lesion.

3.2. Background to E-cell specification and development

The *C. elegans* intestine, or gut, is exclusively derived from the E blastomere, which gives rise to no other tissue. At the four-cell stage, the EMS blastomere undergoes an asymmetric cell division to produce MS (generating mesodermal tissues such as pharyngeal tissue and body wall muscle) and E. At this stage, the cell division patterns and differential fates of EMS are instructed by P2-originated signalling. This P2-EMS signalling event has been shown to involve a set of maternal genes, which include members of the Wnt signalling pathway (Han, 1997). If the EMS blastomere is isolated and left to develop alone, that is, in the absence of P2-EMS interaction, both of its daughter cells develop as MS and no longer produce intestinal cells (Goldstein, 1992). Moreover, the position of P2 relative to EMS determines which daughter of EMS produces intestine (Goldstein, 1993). Various maternal effect lethal mutants have been isolated from classical genetic screens that show defects in the specification of the E blastomere. For a more detailed discussion, see Chapter 1.

The E blastomere divides in a precise fashion to generate twenty gut cells (Sulston *et al*, 1983) (Figure 3.1). The pattern of cell divisions in E includes both symmetric cell divisions and asymmetric cell divisions. The first division in E, an anterior-posterior division generates two daughter cells, Ea and Ep. These cells are present on the ventral surface and contact the vitelline membrane that surrounds the embryo within the eggshell. At around the 24-cell stage of development, a basic blastocoele is formed in the centre of the embryo and at the 26-cell stage, gastrulation is initiated by the movement of Ea and Ep towards the blastocoele. This migration of Ea and Ep creates the ventral cleft, through which descendants of the other five founder cells (AB, MS, C, D and P4) subsequently migrate. During this migration, Ea and Ep divide in a left-right direction, followed by an anterior-posterior division. At this 180-cell stage, there are 8 gut cells (8E) and a gut

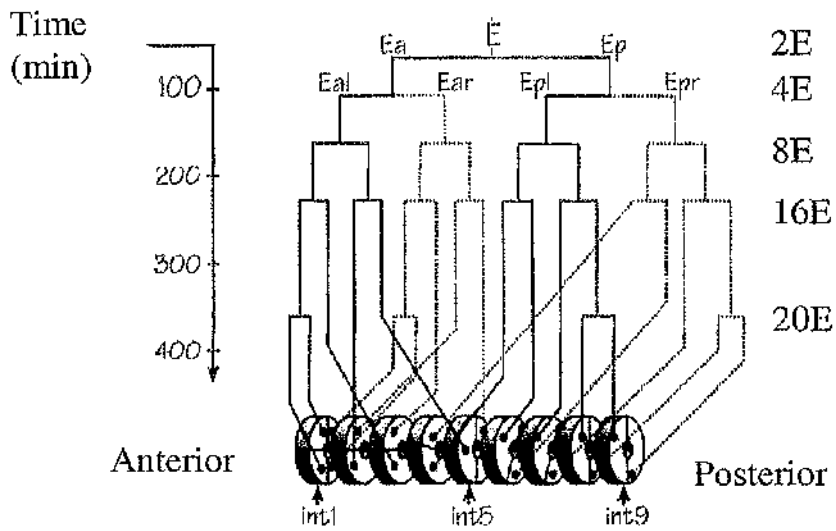


Figure 3.1 Wild type E-cell lineage. The divisions shown are during embryogenesis, time (min) from the first cleavage. The number of cells present at each division is shown to the right. No cell divisions occur during post-embryonic development. The positions of the cells relative to the 9 'int' rings are shown. Adapted from Schroeder and McGhee, 1998.

rudiment is formed. Autofluorescent gut granules are visible at this stage. By 300 minutes, the gut consists of two rows of eight cells, one on the left and one on the right. The anterior pair, Ealaa and Earaa undergo an additional dorsal-ventral division, giving rise to the four cells of int-1, which attaches to the pharyngeal-intestinal valve. The intestine of *C. elegans* is asymmetrical, a phenomenon which becomes evident during cell intercalation at 16E, where three of the anterior cells in the right row of the primordium move counterclockwise to the left, as the contralateral three left cells move simultaneously towards the right (Sulston *et al.*, 1983; Leung *et al.*, 1999). This morphogenic movement generates a left-handed twist of around 90°, which increases to 180° following attachment of the intestine to the pharyngeal-intestinal valve, by the time the larva hatches (Sulston and Horvitz, 1977). The intestinal twist requires a Notch-like signalling pathway involving the receptor LIN-12, the ligands LAG-2 and APX-1 and the nuclear protein LAG-1 (Hermann *et al.*, 2000). By hatch, the intestine consists of a tube made from a quartet of cells (int-1) followed by 8 pairs of cells (int-2 to int-9) (Figure 3.2).

During post-embryonic development, no cell divisions occur in E. However, during L1, a nuclear division occurs in most gut nuclei, except those of int-1 and int-2 (Hedgecock and White, 1985) (Figure 3.2). Additionally, the nuclear divisions in int-8 and int-9 are somewhat variable. Endoreduplication of all gut nuclei occurs once during each larval stage. This results in intestinal cells being predominantly binucleate and by adult stage, each nucleus has a ploidy of 32C.

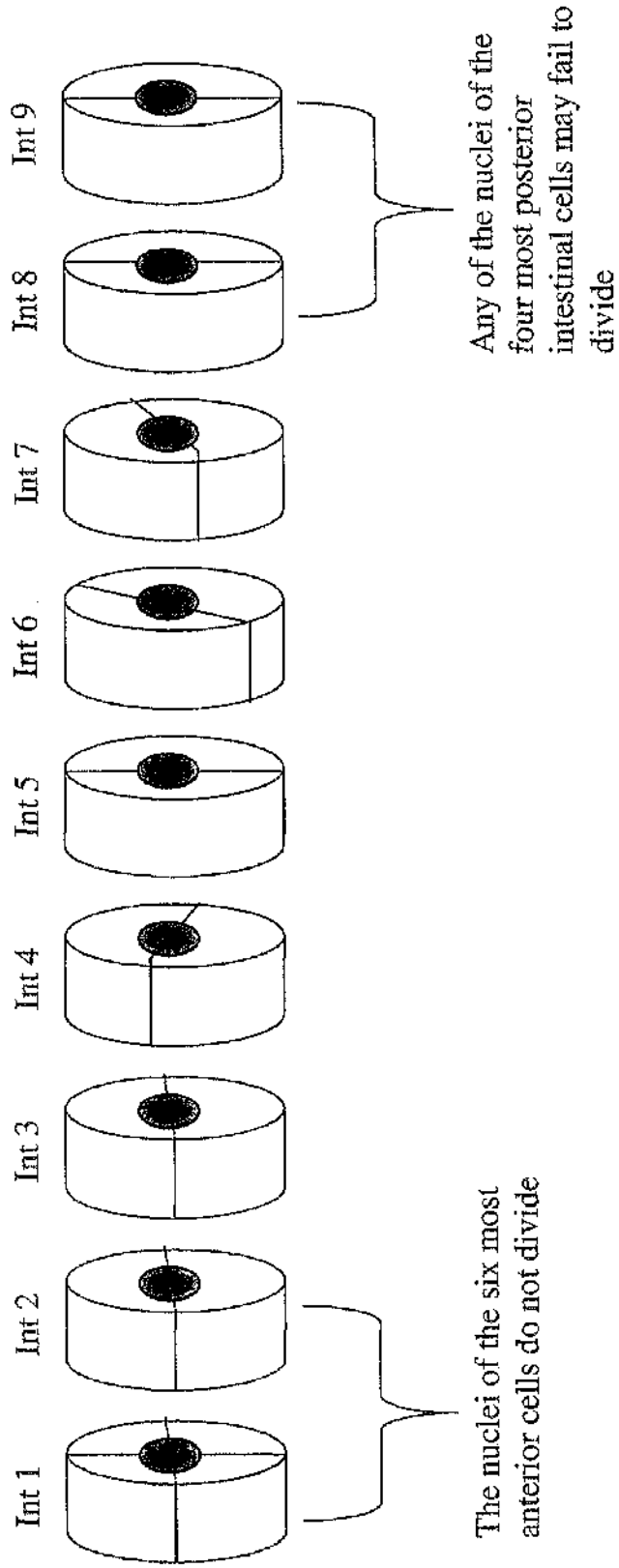


Figure 3.2 Cartoon representation of the *C. elegans* intestine. The 20 gut cells arranged into the 9 int rings. The nuclei of the six most anterior cells, that of int-1 and int-2, do not undergo the nuclear division during L1 and thus are mononucleate. The nuclei of int-8 and int-9 variably divide. Adapted from Sulston *et al.*, 1983

3.3. Aims and Experimental approach

Although the specification of E has been the subject of a considerable amount of research, very little is known about genes controlling the E cell lineage, during both embryogenesis and larval development. The developmental mechanism by which the 20 intestinal cells are generated is unknown. For example, the genes controlling the asymmetric cell divisions in the E lineage, which are critical for the generation of 20 cells rather than, for example, 16 or 32, are undefined. Genes controlling the nuclear division to a subset of intestinal cells and genes involved in the control of endoreduplication are also unknown. I performed forward genetic screens to generate mutants with an altered E cell lineage.

Screening for such mutants by standard means would have been extremely difficult. I therefore decided to use the reporter *GFP* gene fused to a gut specific promoter (*cpr-5*, see below) as a tool to assist in the initial detection and characterisation of mutant phenotype. The *GFP* gene was originally cloned from the jellyfish *Aequorea victoria* and has been used as a reporter of gene expression, a tracer in cell lineage and as a tag to monitor protein localisation in living cells. It has the advantage over other reporters such as β -galactosidase that live specimens can be visualised, thus removing the need for fixation.

Aequorea GFP is a protein of 238 amino acids with an absorbance peak of 395nm (with a small peak at 475nm) and emission of 508nm (Cubitt *et al.*, 1995). Vectors have been designed to specifically analyse gene expression in *C. elegans* (A. Fire, A. Xu, J. Ahun and G. Seydoux, pers. comm.). The GFP reporter vectors contain the mutations S65T or S65C in GFP, modifying the site of fluorochrome formation, resulting in a more rapid, stronger fluorescent signal, which has improved resistance to fading (Heim *et al.*, 1994 Heim *et al.*, 1995). The promoterless vectors used, pPD95.67 containing *GFP* and pPD96.04, containing *GFPlacZ*, both contained the S65C mutation in GFP. This mutant GFP has an excitation wavelength of 479nm and an emission wavelength of 507nm. Fire *et al.*, also introduced introns into the coding region of GFP, as previous studies with the *unc-54* promoter showed that the inclusion of introns improves the yield of protein product and thus sensitivity of the reporter. These GFP vectors also contained an SV40 nuclear localisation signal to target the GFP to the nucleus. This allows easier identification of the cells expressing the transgene. To block readthrough transcription and possible background associated with promoterless vectors, a decoy sequence is present. It consists of a short intron containing the splice donor and splice acceptor, followed by a short open reading frame with a consensus *C. elegans* translational start. The open reading frame terminates

just prior to the multiple cloning site for promoter insertion (A. Fire, A. Xu, J. Ahnn and G. Seydoux, pers. comm.). To allow correct processing of the transcript, a proportion of the *unc-54* 3' end, containing a polyadenylation signal, is placed after the reporter.

GFP and/or *lacZ* fusion transgenes have been used widely to study the spatial expression pattern of many genes in *C. elegans*. Indeed, for a number of genes, the spatial pattern generated by the transgene fusions accurately reflects the expression pattern of the endogenous gene detected by other methods such as *in-situ* hybridisation. Promoter::reporter constructs are generated by ligating the 5' flanks of genes, with or without part of the coding region, upstream of, and in frame with the reporter gene. Plasmid constructs containing these gene fusions are injected with a marker plasmid into the syncytial gonad of the hermaphrodite of *C. elegans*. Transgenic progeny are selected and the expression pattern of the reporter is analysed. The injected DNA generates a large extrachromosomal array (Mello *et al.*, 1991) made from tandem repeats of the reporter and marker plasmids. Such arrays vary in size and may contain around 80 – 300 copies of the injected plasmid (Stinchcomb *et al.*, 1985).

Extrachromosomal arrays however suffer from two main problems that may be solved to different extents by integration into chromosomes. Firstly, extrachromosomal arrays are lost from the germ line at some frequency. Maintaining a line carrying an extrachromosomal array involves constantly selecting animals at least every few generations, as transmission of the array varies from 10 to 90% of the progeny (Mello *et al.*, 1991). Exposure of the extrachromosomal transgenic lines to γ -radiation can generate integrated lines, whereby the transgene is incorporated into a chromosome. Thus, integrated lines will transmit the transgene at a 100% frequency. For this reason, it was preferable to use an integrated line for the mutant screens because with an unstable line, many mutants would have been missed due to loss of the reporter transgene.

Secondly, extrachromosomal arrays can be lost mitotically at some frequency, producing somatic mosaics. Transgenes may therefore not be expressed in a consistent manner. Integrating extrachromosomal arrays can partially solve this problem, although mosaicism has also been observed following integration of arrays into the genome (Krause *et al.*, 1994).

Although the expression of promoter::reporter constructs from integrated lines is generally more reliable than from extrachromosomal arrays, one disadvantage is that positional effects may cause problems as the transgene promoter is not integrated in its

normal chromosomal position. For example, the integrated arrays may be artificially activated or shut off in certain cells, thus may not give the same expression pattern as the endogenous promoter in its natural context. One way to resolve this problem is to examine the expression pattern with more than one integrated line, and compare this with the expression pattern obtained with extrachromosomal transgenic lines.

3.4. Vector construction

Primers A, B and C (Table 3.1) were designed to amplify two regions of approximately 1kb and 3kb upstream of *cpr-5* ATG translational start. Restriction sites were engineered into the 5' sequence of each primer to facilitate cloning into the polylinker of vectors pPD95.67 or pPD96.04. Primer 'C' was designed to link the ATG translational start of *cpr-5* with *GFPlacZ*, generating a translational fusion between *cpr-5* and *GFPlacZ*.

Fragments were amplified using proof-reading Vent DNA polymerase. Cosmid W07B8 was used as the DNA template for the 1kb fragment and wild-type N2 genomic DNA was used as the DNA template for amplifying the 3kb fragment. Amplified products were first subcloned into pGEM-T (Promega Corporation). This is a vector system for the cloning of PCR products. This system utilises the addition of 3'-terminal deoxyadenosines added to a significant proportion of PCR products by thermostable DNA polymerases such as *Taq*. Thermostable polymerases with proofreading activity such as Vent and *Pfu* Turbo generally form blunt-ended PCR products. These products can be 'A-tailed' by incubating with *Taq* and dATP at 72°C for 15 minutes. The T-overhang vector was incubated with the A-tailed PCR product in a standard ligation reaction. The ligated products were transformed into Novablue competent cells and colonies were screened using colony PCR, using the appropriate gene specific primer combinations. DNA from at least four positive colonies was isolated. The integrity of the insert was examined by digesting with the restriction sites engineered onto the primers and analysing the size of products released.

Name of Primer	Sequence (5'→3')	Restriction site engineered onto 5' end	Position of 5' end with respect to ATG
A	TGTAGCATG CTTGCATACAGTTATCGAACA	<i>Sph</i> I	-3020
B	TAAAGTCGACGTGGAATTGACATGCACTCC	<i>Sa</i> II	-986
C	TTACGGATCCATTATGAGAGAAGTGTCTGCG	<i>Ba</i> mHI	+2

Table 3.1. Primers used in the amplification of *cpr-5* 5' flanking region. Bold denotes sequence of restriction site engineered onto primers

To sub-clone the 1kb fragment into the vectors pPD95.67 (*GFP*) or pPD96.04 (*GFPlacZ*), the 1kb amplified product (Fragment X) in pGEM (pCC1) was released by digesting with *Bam*HI and *Sal*I (Figure 3.3.) and gel purified. Vectors pPD95.67 and pPD96.04 were also digested with *Bam*HI and *Sal*I (present in the polylinker) and the digested product was gel purified. Digested pPD95.67 and pPD96.04 were ligated with Fragment X (Figure 3.3) and the ligated products transformed into Novablue competent cells. Colonies were screened by colony PCR using primers B and C (Table 3.1). Plasmid DNA was prepared from two colonies for each ligation, which generated the correct size of PCR product. The integrity of the insert was examined by digesting with *Sal*I and *Bam*HI and analysing the size of products released. Two sub-clones from each ligation were found to contain the correct insert. These were termed pCC5 and pCC6 with pPD95.67 and pCC7 and pCC8 with pPD96.04.

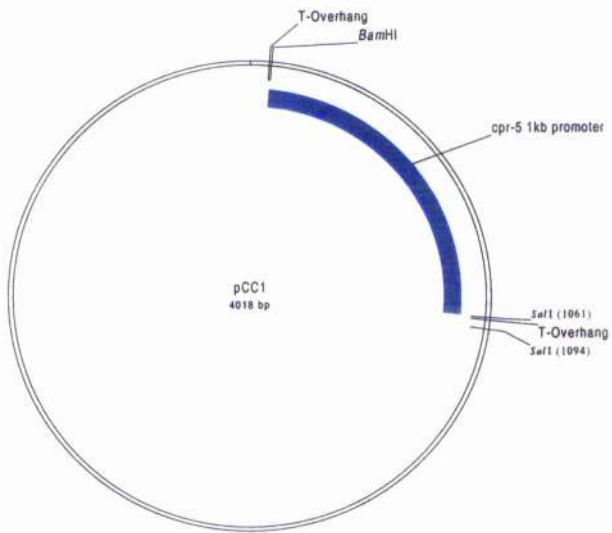
An additional step was required when subcloning the 3kb fragment into pPD96.04, as in addition to the *Bam*HI site engineered on primer C, an internal *Bam*HI site was present in the amplified product (Figure 3.4). The 3kb fragment was amplified using primer combinations A and C and first cloned into pGEM as before, generating pCC13. This clone was digested with *Sph*I and *Sal*I yielding fragment Y (1351bp), and also with *Sal*I and *Bam*HI yielding fragment Z (1959bp) (Figure 3.4). Fragments Y and Z were gel purified. pPD96.04 was digested with *Sph*I and *Bam*HI and the product gel purified. Fragments Y and Z were ligated with vector and the ligated products and transformed into Novablue competent cells. Colonies were screened using primers A and C (Table 3.1). Plasmid DNA was prepared from overnight cultures of two positive colonies and DNA examined by restriction digestion. Both clones were found to give the correct pattern and named pCC16 and pCC17.

Figure 3.3

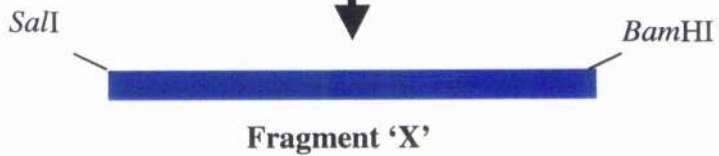
**Strategy for cloning of 1kb PCR-amplified *cpr-5* promoter fragment
into pPD95.67 and pPD96.04**

Figure 3.3

Strategy for cloning of 1kb PCR-amplified *cpr-5* promoter fragment into pPD95.67 and pPD96.04. The amplified *cpr-5* promoter fragment (Fragment X) was subcloned into pGEM-T, digested and ligated into a similarly cut pPD95.67 (pCC5) or pPD96.04 (pCC7/8).



Digest with *SalI/BamHI* to release Fragment 'X'. Gel purify fragment X.



Digest pPD95.67 and pPD96.04 with *BamHI/SalI* and gel purify. Ligate with Fragment X.

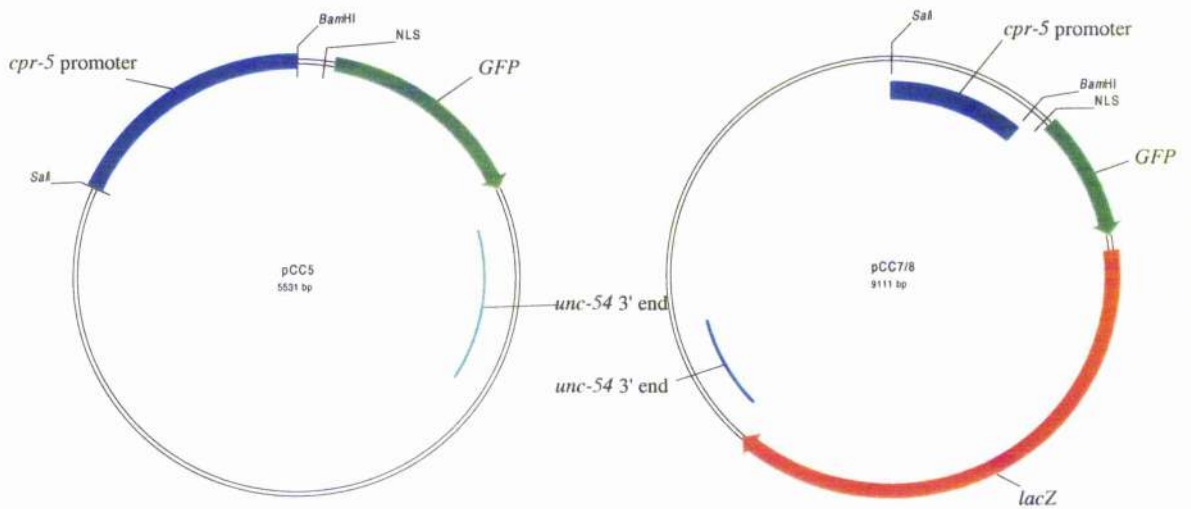


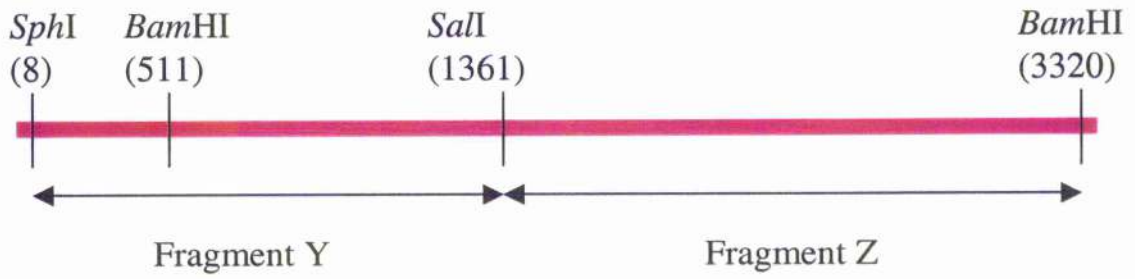
Figure 3.4

**Strategy for cloning of 3kb PCR-amplified *cpr-5* promoter fragment
into pPD96.04**

Figure 3.4.

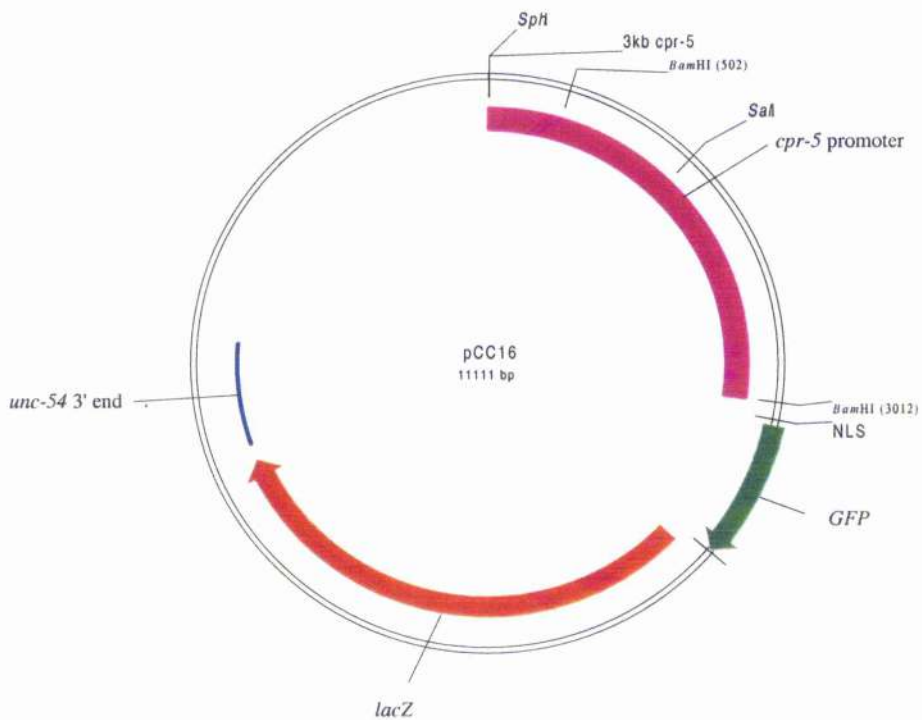
Strategy for cloning of 3kb PCR-amplified *cpr-5* promoter fragment into pPD96.04

The amplified product was first subcloned into pGEM-T. Since an internal *Bam*HI site was present (refer to text), the promoter fragment was digested into 2 fragments (Fragment Y and Z) and both fragments ligated with digested pPD96.04, yielding pCC16.



3028bp *cpr-5* promoter PCR product (Cloned into pGEM)

Digest with (i) *Sph*I and *Sal*I and (ii) *Sal*I and *Bam*HI to release Fragments Y and Z. Ligate into *Sph*I/*Bam*HI digested pPD96.04



3.5. Generation of *C. elegans* lines containing *cpr-5* reporter constructs.

3.5.1. Transgenic lines of pCC5

The syncytial gonads of wild-type N2 young adults were injected with pCC5 at 10ng/ μ l and the marker plasmid pRF4, containing the dominant *rol-6(su1006)* allele, at 100ng/ μ l. Transformed animals can be easily identified because the mutant collagen gene encoded by the *rol-6(su1006)* mutation causes these animals to move in circles (Rol phenotype). Five to ten F1 rollers were transferred onto 5.5cm NGM agar plates. One line was obtained and named IA97. GFP fluorescence was examined under a bench fluorescent microscope. Although it was clearly evident that the GFP expression pattern was restricted to the gut, the fluorescence was not tightly nuclear localised (Figure 3.5). The GFP fluorescence was also variable between animals and mainly restricted to the anterior gut. I also found it difficult to study *cpr-5::GFP* fluorescence using *rol-6* as a marker under the dissecting microscope, because the cuticle and intestine are twisted. I therefore decided to change to *Unc-76* rescue of mutant phenotype as the marker of transgenesis. Worms homozygous for the mutation *unc-76(e911)* have an impaired forward and reverse movement and have a tendency to coil. Injection of these worms with the plasmid p76-16B, containing the wild-type gene of *unc-76*, can rescue the mutant phenotype. Transgenic worms are therefore identified as having wild-type movement. These transgenic worms have the advantage over *rol-6(su1006)* as the cuticle is not twisted.

Transgenic lines containing the cuticular collagen gene *dpy-7* in a translational fusion with *GFPlacZ*, were found to give greater nuclear localisation to hypodermal cells than *dpy-7* fused to *GFP* alone (E. Stuart, pers. comm.). It has been suggested that the incomplete nuclear localisation observed with fusions with *GFP* alone may be due to *GFP* being a small protein, and thus being able to diffuse out of the nucleus (A. Fire, A. Xu, J. Ahn and G. Seydoux, pers. comm.). I therefore chose to concentrate on generating lines with pCC7/pCC8 and pCC16 as these plasmids contained *cpr-5* promoter fused with *GFPlacZ*.

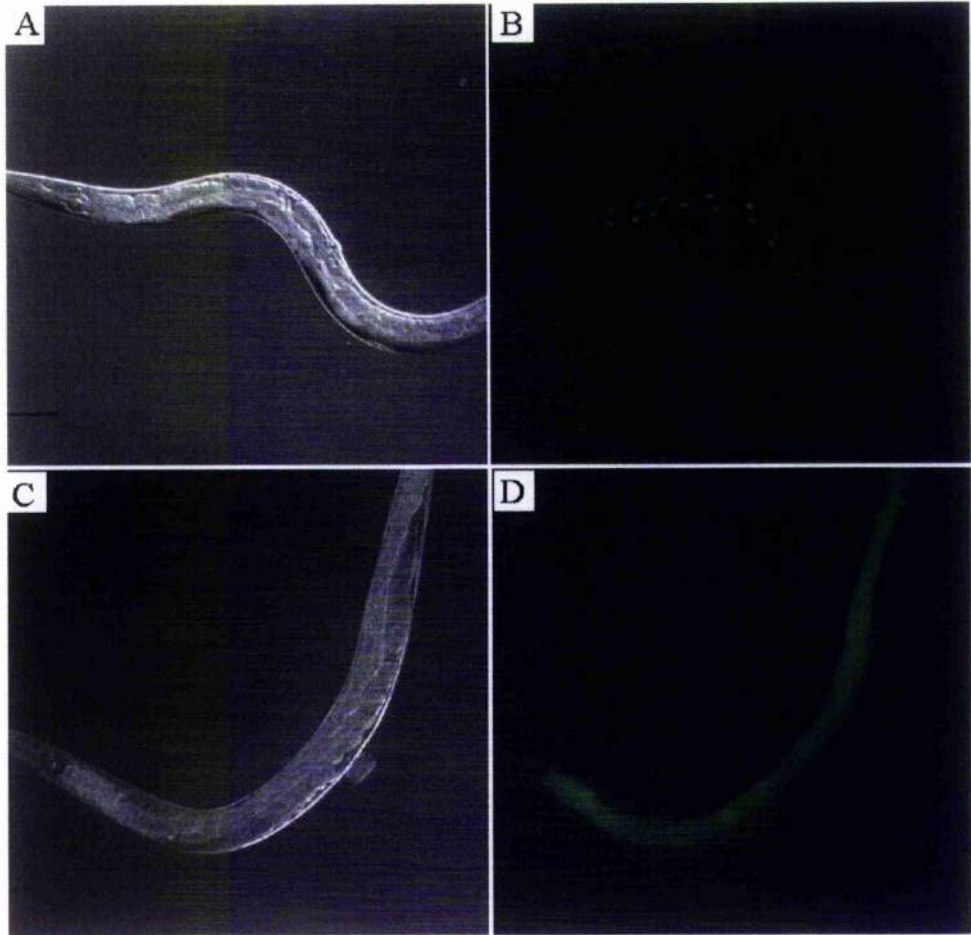


Figure 3.5 Transgenic worms of pCC5 and pCC7. (A) and (C) are Nomarski with respective GFP counterparts (B) and (D). (A) and (B) are transgenic lines containing pCC7 (*cpr-5::GFPlacZ*). (C) and (D) are transgenic lines containing pCC5 (*cpr-5::GFP*). Notice the tight nuclear GFP localisation in (B) whereas GFP appears cytoplasmic in (D). Scalebar in (A) is 100µm

3.5.2. Transgenic lines of pCC7, pCC8 and pCC16

Transgenesis with pCC8 at 10ng/ μ l and p76-16B at 100ng/ μ l yielded 8 lines in F2 generation. These lines varied with respect to penetrance of Unc-rescue and brightness of GFP, as observed under the fluorescent dissecting microscope. Three good lines were obtained. pCC8 was also injected at the higher concentration of 50ng/ μ l. Seven lines were obtained and, as with the lower concentration, variability with respect to penetrance of *unc-76* rescue and brightness of GFP was observed. At both concentrations, excellent GFP nuclear localisation was obtained. However, a mosaic pattern was observed as not all gut nuclei fluoresced in every animal and like pCC5 transformed lines, fluorescence appeared to be more restricted to the anterior gut.

β -galactosidase staining of transgenic worms containing 2.4kb of *cpr-5* upstream sequence in a translational fusion with *lacZ* also showed tight nuclear localisation, but with a mosaic pattern, such that not all intestinal cells were expressing the transgene (Larminie, 1995). One line from injections with pCC7 and three lines from injections with pCC16 had essentially the same staining pattern as described with pCC8. pCC7 and pCC16 were both injected at 10ng/ μ l, with p76-16B at 100ng/ μ l.

3.6. Using excess genomic DNA as a carrier to prevent transgene silencing

Extrachromosomal arrays are transmitted as large repetitive arrays that are composed of many tandem copies of the injected DNA(s) (Mello *et al.*, 1991). These 'simple arrays' have been found to contribute to the silencing of genes in certain tissues in *C. elegans*. Transgenes in non-repetitive arrays, formed by the inclusion of an excess population of carrier DNA consisting of random *C. elegans* DNA fragments, has been shown to increase the expression and improve the uniformity of transgene expression (Kelly *et al.*, 1997; A. Fire, A. Xu, J. Ahn and G. Seydoux, pers. comm.). I decided to try this approach with the *cpr-5::GFPlacZ* transgenes.

Plasmids (pCC7 and pCC16) were digested with *FspI* and purified by passing through a Qiagen Spin Column. *FspI* cuts in the plasmid backbone of pCC7 and pCC16. p76-16B was digested with *SmaI* and similarly purified. *SmaI* has one site in p76-16B, found in the pBluescript backbone. Digested test plasmids and marker plasmids were each injected at a final concentration of 1.5ng/ μ l. *PvuII* cut *C. elegans* genomic DNA (purified as above) was co-injected at a final concentration of 90ng/ μ l.

Three transgenic lines were obtained with the linear pCC7 and one line was obtained with linear pCC16. In both cases, very few F1s were obtained. However, the number of lines obtained was comparable to injections without carrier DNA. Moreover, there was a clear difference in the lines obtained with complex arrays; the previously observed transgene mosaicism with simple arrays was greatly reduced and GFP expression was no longer restricted to the anterior of the gut (although it was still stronger there). Since my aim was to obtain a strain that had a reproducible pattern of GFP expression throughout the whole of the intestine, I decided to integrate lines from injections with complex arrays.

3.7. Isolation of integrated lines

The standard method for generating an integrated transformed line in *C. elegans* is to gamma-irradiate a population carrying an extrachromosomal array. After non-selective growth over two generations, several hundred individuals still expressing the transgene are picked clonally and their progeny examined to test for homozygosity for the transgenes.

Strains IA99 (line derived from injections with linear pCC7) and IA102 (from injections with linear pCC16) were chosen for integration as these lines had the lowest penetrance of Unc-rescue, which facilitated in the ease of screening for integrated lines. F2 progeny were screened for 100% transmittance of the transgene. γ -irradiation of IA99 produced two independent integrated lines (insertional alleles *ijIs10* and *ijIs11*). γ -irradiation of IA102 also produced two integrated lines (insertional allele *ijIs14* and *ijIs15*) (Table 3.2). All integrated lines were outcrossed to N2 three times and the absence of death (indicative of a major chromosomal rearrangements) was checked. The integrated line containing *ijIs15* was later discarded as embryonic lethality was observed during crosses. Strains IA109 and IA122 were chosen for EMS treatment as these were the healthiest out of the integrated lines.

Strain Name	Genotype
IA109	<i>unc-76(e911)</i> , <i>ijIs10[unc-76(+), cpr-5::GFPlacZ]</i> V
IA104	<i>ijIs11[unc-76(⁻), cpr-5::GFPlacZ]</i> ; <i>unc-76(e911)</i> V
IA122	<i>ijIs14[unc-76(+), cpr-5::GFPlacZ]</i> ; <i>unc-76(e911)</i> V

Table3.2 Genotypes of integrated lines.

3.8. Characterisation of *cpr-5::GFP* expression in integrated lines

Strain IA109 was chosen for further characterisation although preliminary analysis with IA104 and IA122 showed that all three integrated lines have identical expression patterns. As with the extrachromosomal arrays, the integrated lines show gut specific expression. Stronger *cpr-5::GFP* expression was observed in those cells at the anterior-most end of the intestine (e.g. Figure 3.7 (C)). *cpr-5::GFP* could be observed from L2 larval stage through to adult under a fluorescent stereomicroscope. High magnification was required however to view GFP in L1 larvae. No *cpr-5::GFP* expression was observed in embryos. This latter result contrasts with the observations made by Larminie (1995), where β -galactosidase expression was observed in late stage embryos containing a *cpr-5::lacZ* transgene.

The nuclear localisation of GFP in these transgenic worms could also be used as a tool for examining nuclear division and endoreduplication. Under the fluorescent stereomicroscope, over 20 gut nuclei could be counted, averaging around 27. The size of intestinal nuclei of larvae and adults could also be differentiated. For example, the ploidy of the intestinal nuclei is 8N during L3, and 32N during adult. I could visualise the increase in size very clearly using the fluorescent stereomicroscope. Following endoreduplication, the change in the size of intestinal nuclei was accentuated under high magnification (Figure 3.6).

L4



Adult



Figure 3.6. L4 and adult gut nuclei. An example of an intestinal cell from L4 (left) and adult (right) The DNA content of gut nuclei is 16C in L4 and 32C in adults. The arrows point to the intestinal cell boundaries. For easier identification of nuclei, GFP and Nomarski images have been merged. Scalebar is 10 μ M

3.9. Background to STS mapping

The STS mapping method, frequently employed in *C. elegans*, is a PCR-based method which relies on Tc1 polymorphisms present in the genome of the Bergerac strain of *C. elegans* (Williams *et al.*, 1992 and Chapter 2), which are not present in wild-type N2 Bristol strain. The Bergerac strain has around 500 or more copies of Tc1 while the Bristol strain has only around 30 copies (Brenner, 1974). The Bergerac strain used most widely for STS mapping is RW7000 (Williams *et al.*, 1992). STS mapping allows rapid determination of positional information of an allele, by carrying out one (or two, if the allele is homozygous lethal) simple cross(es) into the Bergerac background and testing the F2 mutant progeny for the presence or absence of the Tc1 polymorphisms. Large numbers of mutant progeny can also be examined. However, one disadvantage to this system is that RW7000 is in itself a mutator strain with active Tc1 germline transposition. Spontaneous mutations can occur at a relatively high rate (Moerman and Waterston, 1984), thus, confusing results may arise if the test allele displays a similar phenotype to RW7000.

Tc1 polymorphisms behave as dominant genetic markers. To assign a mutation to an autosome, F2 mutant homozygotes are tested with the chromosome assignment reactions (Williams, 1995). Each unlinked Tc1 shall be detected in three-quarters of F2 homozygous mutant progeny. In contrast, linked Tc1 elements will be detected in fewer animals because this requires recombination between the mutation being mapped and the Tc1 element of the homologous Bergerac chromosome. Assignment to the X chromosome is displayed in the F1 generation as all males will display mutant phenotype (males are XO). Following assignment to a chromosome, mutant progeny can be tested with Tc1 polymorphisms spanning that particular chromosome. Recombination events, based on the inheritance of the linked Tc1s, are visualised by the pattern of bands displayed on the gel.

This STS method can be used to map both recessive homozygous viable and lethal mutations. In the latter case, dead embryos are analysed for the presence or absence of the Tc1 polymorphisms. Dominant mutations are managed in a slightly different way. In a chromosomal assignment cross, F2 non-mutant progeny are analysed for the Tc1 polymorphisms. For an unlinked mutation, three-quarters of progeny will show the Tc1 polymorphism whereas almost 100% of progeny will show the linked Tc1. That is, by selecting wild-type progeny, you have selected homozygotic Bergerac for the chromosomal region of the gene being mapped.

3.10. Chromosomal assignment of *ijIs10*

I decided to assign the insertion *ijIs10* to a chromosome as the isolated mutants were only easily scored using GFP expression. This would therefore rule out ambiguous mapping results, if a mutation was linked to *ijIs10*. GFP acts as a dominant marker. Homozygous *ijIs10* males were crossed into RW7000 and the outcrossed F1 hermaphrodites allowed to self. Non-GFP progeny produced in the F2 generation were picked, lysed and tested for the presence or absence of the chromosomal assignment STS markers. Non-GFP progeny were scored and the results for the chromosomal assignment PCR are shown in Table 3.3. From these results it was clear that *ijIs10* was linked to chromosome V.

Chromosome	STS Marker	No. of animals with marker	Total No. of animals tested	Percentage of animals with marker
I	<i>hP4</i>	56	72	77.8
II	<i>maP1</i>	58	72	80.6
III	<i>mgP21</i>	49	72	68.1
IV	<i>sP4</i>	54	72	75.0
V	<i>bP1</i>	71	72	98.6

Table 3.3. STS Chromosome assignment of *ijIs10*.

3.11. Generation of mutants using EMS

EMS was chosen as the mutagen due to its potency and efficiency at generating point mutations. Three screens were carried out, one with IA122 and the others with IA109. Mutants were classified according to their phenotype and designated an allele (Table 3.4). A total of 4000 F1 progeny were screened (8000 mutagenised genomes).

Worms were screened in the F2 generation from L3 to adult stages. Mutants were identified as having an altered pattern of GFP expression. All of the mutants isolated were homozygous viable except *ij51* which was homozygous sterile. A heterozygote was recovered using the method described in Section 2.10.3.

Class	Mutant Phenotype	No. mutants identified	Mutant allele(s)
I	Putative lineage defect	2	<i>ij48, ij52</i>
II	Mono-nucleate cells	1	<i>ij51</i>
III	Multi-nucleate cells	2	<i>ij49, ij50</i>
IV	Abnormal gut morphology	1	<i>ij53</i>

Table 3.4. Classes of mutants identified.

3.12. Characterisation of intestinal mutants

Various classes of mutants covering several aspects of E-cell development were obtained from this genetic screen. These classes are summarised in Table 3.4.

3.12.1. Class I. putative E lineage defect

The typical mutant phenotypes of *ij48* and *ij52* are given in Figures 3.7 and 3.8 respectively. These mutants have extra gut cells, generated during embryogenesis.

Analysis of the genetics of *ij48* suggests that the lesion is both semi-dominant over wild-type and is maternal. *ij48* was mapped to chromosome I using the STS mapping protocol for mapping dominant alleles (Table 3.5). Genetic analysis of *ij52* suggests that this is a recessive zygotic lesion and linked to chromosome IV (Table 3.6.).

Most of my project focussed on the characterisation of the *ij48* and *ij52* mutant alleles. Detailed characterisation of these mutants can be found in Chapters 4 and 5.

Chromosome	STS Marker	No. of animals with marker	Total No. of animals tested	Percentage of animals with marker
I	<i>hP4</i>	42	44	95.5
II	<i>maP1</i>	28	44	63.6
III	<i>mgP21</i>	34	44	77.3
IV	<i>sP4</i>	31	44	70.5
V	<i>bP1</i>	34	44	77.3

Table 3.5. STS chromosome assignment of the dominant allele *ij48*

Chromosome	STS Marker	No. of animals with marker	Total No. of animals tested	Percentage of animals with marker
I	<i>hP4</i>	27	37	73.0
II	<i>maP1</i>	30	37	81.1
III	<i>mgP21</i>	24	37	64.9
IV	<i>sP4</i>	2	37	5.4
V	<i>bP1</i>	22	37	59.5

Table 3.6. STS chromosome assignment of the recessive allele *ij52*

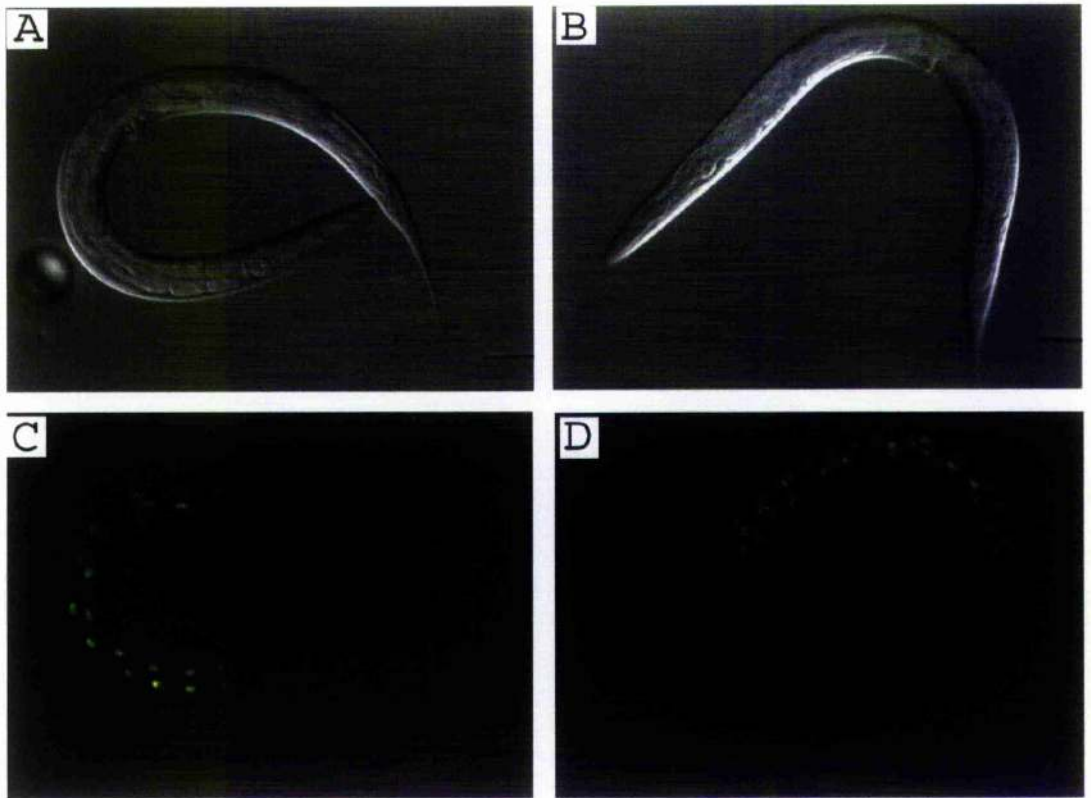


Figure 3.7 Characterisation of *lin-60(ij48)*. (A) and (B) are Nomarski images with respective *cpr-5::GFP* fluorescence counterparts (C) and (D). (A) and (C) are wild-type, (B) and (D) are *lin-60(ij48)*. Scalebar is 100 μ m

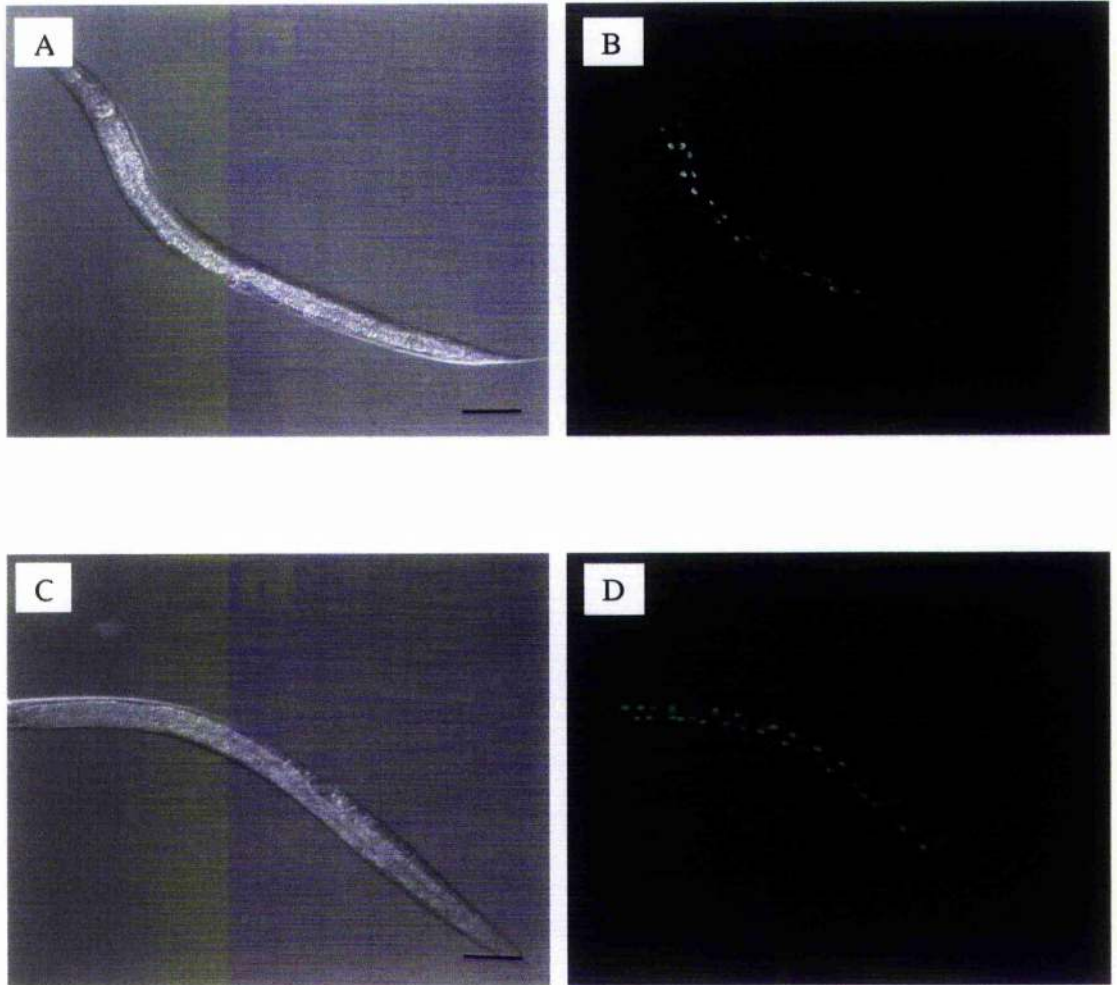


Figure 3.8 Characterisation of *lin-62(ij52)*. (A) and (C) are Nomarski images with respective *cpr-5::GFP* fluorescence counterparts (B) and (D). (A) and (B) are wild type, (C) and (D) are *lin-62(ij52)*. Scalebar in (A) and (C) is 100 μ m.

3.12.2 Class II: mutant with mononucleate intestinal cells.

The phenotype of the *ij51* allele is shown in Figure 3.9. In this mutant, it appears that the nuclear division, which occurs during L1 in wild-type worms, has failed. The nuclei of int-1 and int-2 of *ij51* are identical to wild-type, in that mononucleate cells are present and the nuclei appears to be of the correct size. However, in contrast to wild-type, the cells of int-3 through int-9 appear to be largely mononucleate as opposed to binucleate. It is therefore possible that the nuclear division that occurs during L1 has failed in the intestinal cells of int-3 through int-9. When intestinal nuclei are examined by DAPI staining (Figure 3.9, H), some appear to exhibit an unusual morphology: nuclei were elongated suggestive of a defect in chromosome segregation or completion of nuclear division. The nuclei of these cells in *ij51* are approximately twice as large as each single nucleus of wild-type so it seems likely that equivalent rounds of DNA synthesis have occurred (Figure 3.9, E and F). Homozygous *ij51* hermaphrodites progress through embryogenesis and larval development to reach adulthood without any obvious defects other than in the gut nuclei. They are not Unc, indicating that at least most neuronal post-embryonic cell divisions are likely to be relatively normal. A vulva is also present, although this may be slightly aberrant. This indicates that the defect is not a general failure of post-embryonic nuclear divisions.

Homozygous mutant *ij51* hermaphrodites are sterile. Several causes of sterility of mutants in *C. elegans* include, for example, abnormal germline proliferation (Glp), and abnormal germ line differentiation including feminisation of germline (Fog phenotype), tumorous germline and masculinisation of germ line (Mog phenotype).

To investigate the cause of sterility of *ij51*, the gonads of homozygous mutant hermaphrodites were examined by Nomarski optics (Figure 3.9, I and J). In wild-type *Caenorhabditis elegans* the gonad consists of two arms formed into a U-shaped tube. Germ cells proliferate distally and then enter and progress through meiotic prophase as they move proximally. The first (approximately) forty germ cells mature into (approximately) 160 sperm. The sperm are only capable of fertilisation in the spermatheca. All subsequent germ cells mature as oocytes. Germ cells in the distal region are syncytial but become enclosed in a membrane during diakinesis. As the oocytes move through the loop, they increase in volume. Meiotic maturation, that is the transition from diakinesis of prophase I to metaphase of meiosis I occurs in the most proximal oocyte in the gonad arm. Following maturation, the oocyte is ovulated into the lumen of the spermatheca and when fertilised,

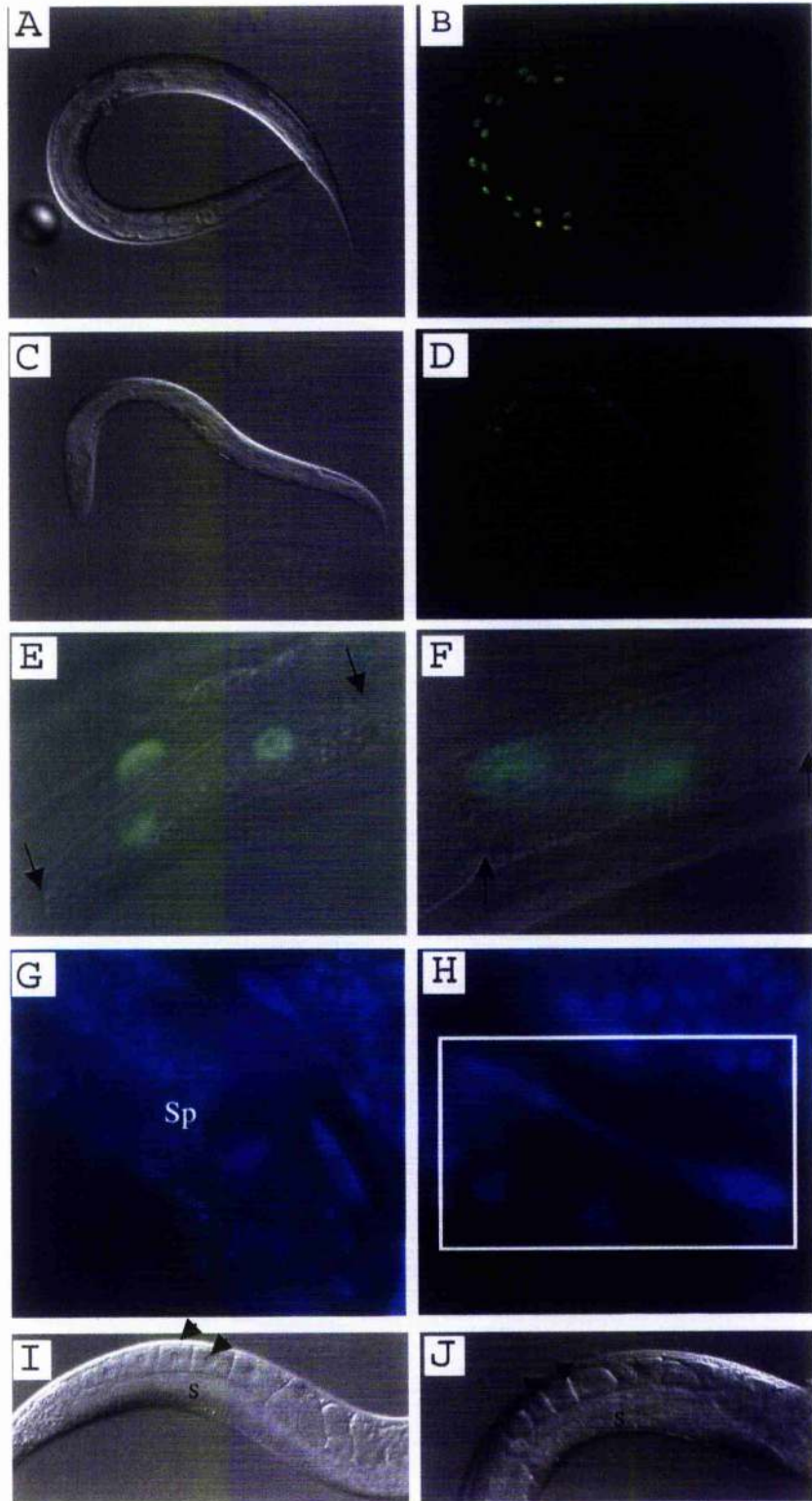
the egg moves proximally into the uterus, where the completion of meiosis I and II occurs (Refer to chapter 1).

In *ij51*, Germline proliferation has clearly taken place, as visualised by Nomarski and DAPI microscopy (Figure 3.9, G and J). Some degree of differentiation of the oocytes occurs, suggesting that the germline is not of a tumorous nature. The oocytes appear to become cellularised and increase in size as they move proximally. Defects appear to occur at around the time of fertilisation and meiotic maturation. I have not examined whether fertilisation occurs but sperm appear to be present, as visualised by DAPI staining (Figure 3.9, G). I also examined homozygous mutant *ij51* hermaphrodites for a sperm defect. Five L4 *ij51* hermaphrodites were mated with 5 N2 males. Three of these crosses were set up. No viable F1 progeny were recovered from any plate, therefore, the sterility of *ij51* cannot be rescued by the provision of sperm from a wild-type male. I conclude that the reason for sterility is not simply a failure to produce viable sperm.

The oocytes appear to move through the spermatheca and into the uterus. However the majority of the oocytes degrade after exiting the spermatheca, thus it is probable that an egg shell is not present. *ij51* hermaphrodites very occasionally lay a few of these defective oocytes, again demonstrating that there are post-embryonic nuclear divisions as a functional vulva is present. These embryos arrest as a ball of around 100 cells. It therefore seems feasible that these worms are sterile due to a cell cycle defect, possibly a defect in completing meiosis.

Figure 3.9
Characterisation of *ij51*

Figure 3.9. Characterisation of *ij51*. (A) and (C) are Nomarski images with GFP fluorescence counterparts (B) and (D). Expression of *cpr-5::gfp* in adults in wild type (A) and (B), and *ij51* (C) and (D). An intestinal cell of wild type (E) and *ij51* (F). For easier identification of intestinal cell nuclei, the GFP and Nomarski images have been merged. Intestinal cell boundaries are indicated by arrows. DAPI staining of *ij51* hermaphrodites (G) and (H). Sperm is present (Sp, G). The white box in H is high magnification of an *ij51* intestinal nuclei. Gonads of wild-type (I) and *ij51*(J) adult hermaphrodites. Some developing oocytes are marked with black arrowheads; the syncytial arm of the gonad is labelled "s".



3.12.2.1. Mapping of *ij51*

ij51 was mapped using the STS method. Homozygous *ij51* worms were picked, lysed and tested with chromosomal assignment markers. This placed *ij51* onto chromosome III. *ij51* homozygotes then were tested with Chromosome III markers *mgP21*, *stP17*, *stP127* and *stP19* (Table 3.7). A representative gel is shown in Figure 3.10 and proposed recombination events shown in Figure 3.11 and Table 3.8. These results place *ij51* very close to *stP17* on the far right arm of chromosome III. However, a recombination event did not occur that would have enabled the placing of *ij51* to the right or left of *stP17*. Most STS markers for chromosome III are found in the left arm and *stP127* and *stP17* are separated by a distance of 19 map units, making it almost impossible to refine the map position of *ij51* by this method.

STS mapping of *ij51*

Figure and Table legends for STS mapping of *ij51*

Table 3.7 STS Chromosome assignment of *ij51*. 68 separate reactions, each reaction performed with DNA from F2 homozygotes, generated by selfing *ij51*/RW7000 hybrid. Approximately 75% of animals should detect each unlinked STS marker. Linkage is detected by a reduced frequency. This table illustrates that *ij51* is linked to chromosome III

Figure 3.10 Representative gel of STS mapping of *ij51* using chromosome III markers.

Lane A contains 50bp ladder.

Lane B is N2 control

Lane C is RW7000 control, showing the positions of bands corresponding to STSs on chromosome III, corresponding to *stP19*, *mgP21*, *stP127* and *stP17*.

All other lanes are PCR reactions, each performed with DNA from an individual F2 *ij51* homozygote produced by self-fertilisation of a Bristol/Bergerac hybrid. A total of 76 *ij51* homozygotes were tested. Lanes D, E and F refer to the recombination events shown in Figure 3.11. The remaining mutants tested negative for all chromosome III STSs.

Figure 3.11 Proposed recombination events between RW7000 and *ij51*. RW7000 chromosome is top line and *ij51* is bottom line. The map is not to scale. Lanes D and E and F refer to the recombination events shown in Figure 3.16. This interpretation places *ij51* to the right of *stP127* and very close to *stP51*.

Table 3.8 Tabulated data of proposed recombination events between *ij51* and RW7000.

Chromosome	STS Marker	No. of animals with marker	Total No. of animals tested	Percentage of animals with marker
I	<i>hP4</i>	48	68	70.6
II	<i>maP1</i>	43	68	63.2
III	<i>mgP21</i>	24	68	35.3
IV	<i>sP4</i>	45	68	66.2
V	<i>bP1</i>	38	68	55.9

Table 3.7



Figure 3.10

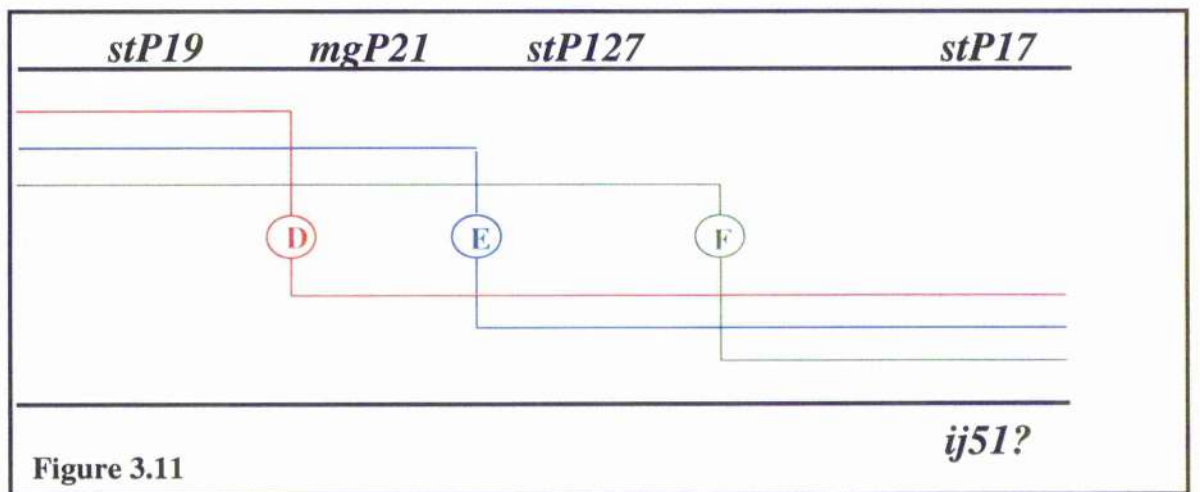


Figure 3.11

Recombinant class	Total Number of Recombinants (/76)
D	2
E	1
F	28

Table 3.8

3.12.3 Class III: Mutants with multinucleate cells

The mutant alleles *ij49* and *ij50* have intestinal cells that are generally trinucleate or tetranucleate, as opposed to the normal binucleate (Figures 3.12 and 3.13 respectively). These mutants are not sterile, although *ij50* has a reduced brood size. The mutant phenotype of both *ij49* and *ij50* is not 100% penetrant. Also, it appears that although there are extra nuclei present, the total DNA content of each cell probably does not increase, as judged by the size of the nuclei. For example, although there are 4 nuclei in the cell in Figure 3.13 (F), two of these are very small.

These *ij49* and *ij50* phenotypes are suppressed by entering the dauer larval stage: dauer larvae picked from starved *ij49* or *ij50* plates to fresh plates do not show the multinucleate phenotype. Since *cpr-5::GFP* expression is not very strong during early larval development, it is difficult to ascertain when the additional nuclei are generated. However, the fact that the mutant phenotype is suppressed following entry into the dauer stage suggests that the defect occurs following the decision to enter the dauer life-cycle.

When attempting to assign these alleles to a chromosome using the STS mapping protocol, it became apparent that the mapping strain RW7000 also had this mutant phenotype. These alleles could therefore not be mapped using this method, and the mapping of *ij49* and *ij50* was terminated.

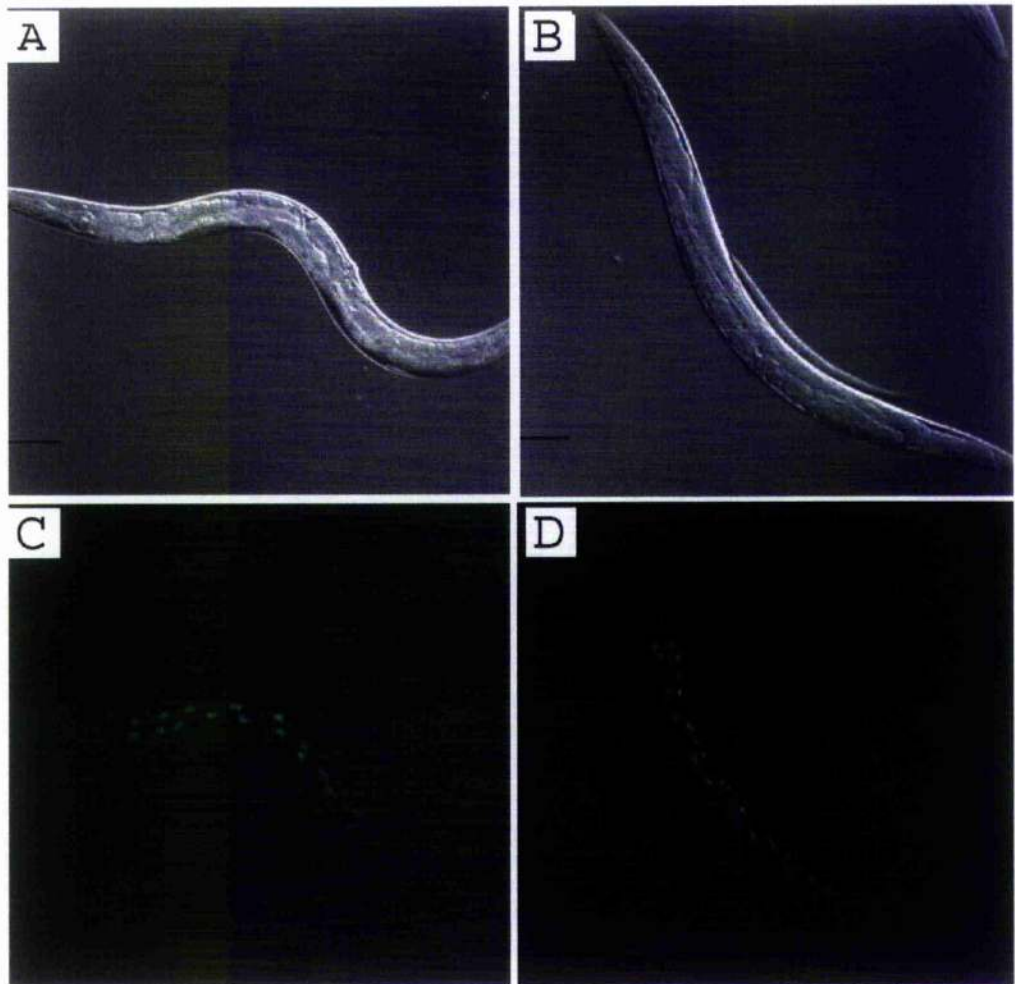


Figure 3.12. Characterisation of *ij49*. (A) and (B) are Nomarski images with respective *cpr-5::GFP* fluorescence counterparts (C) and (D). (A) and (C) are wild-type, (B) and (D) are *ij49*. Scalebar is 100 μ m

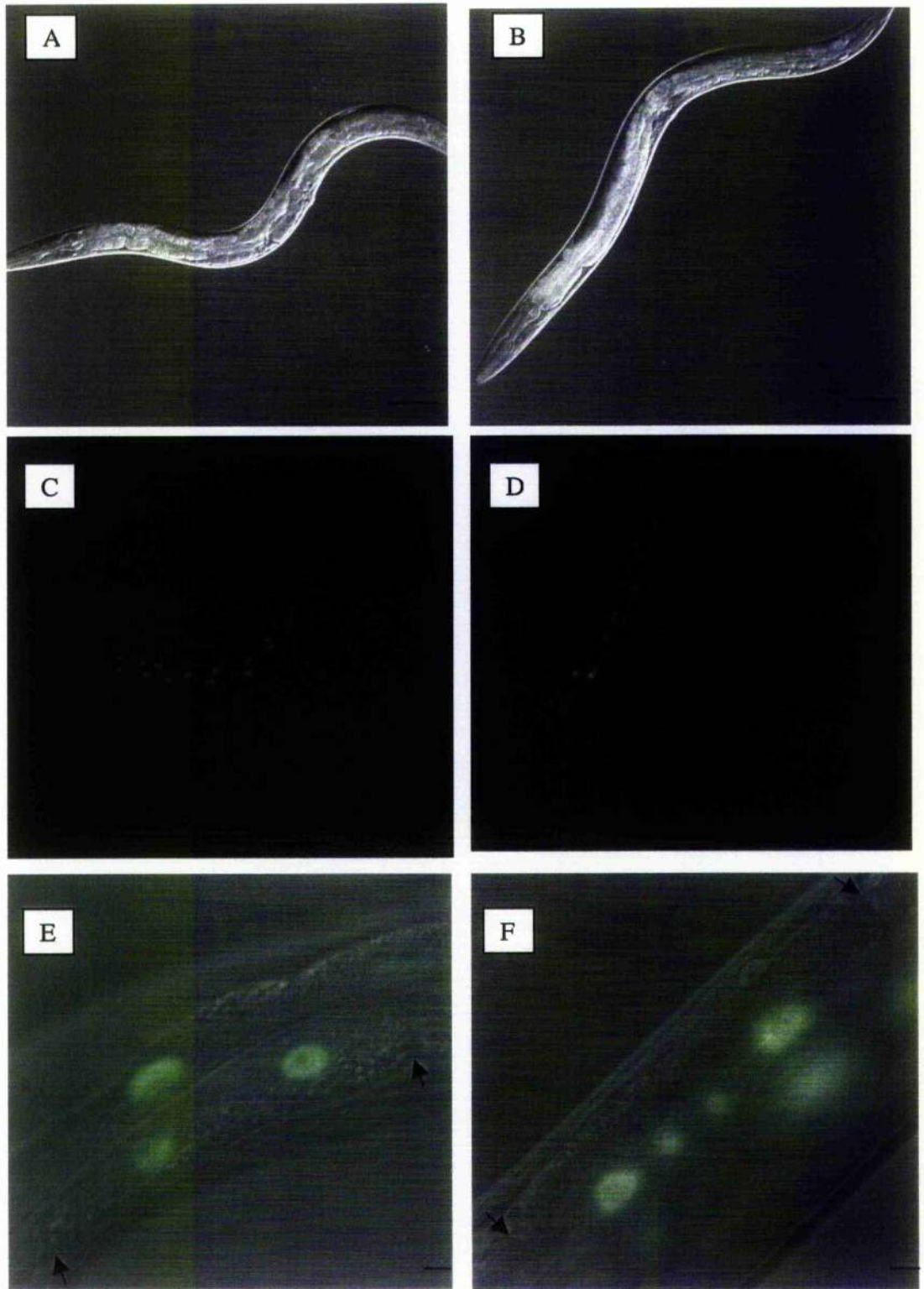


Figure 3.13. Characterisation of *ij50*. (A) and (B) are Nomarski with respective GFP images (C) and (D). (A) and (C) are wild-type, (B) and (D) are *ij50*. Scalebar in (A) and (B) represents 100 μ m. (E) and (F) are individual gut cells of wild-type (E) and *ij50* (F). Arrows point to intestinal cell boundaries. Scalebar represents 10 μ m

3.12.4. Class IV: Mutant with abnormal gut morphology

The phenotype of *ij53* is shown in Figure 3.14. *ij53* homozygotes have a ‘bumpy’ swollen gut appearance. Moreover, there is a huge increase in cytoplasmic fluorescence, as the GFP does not appear to be restricted to the nucleus. I have not examined the *ij53* phenotype in detail so I am therefore unclear as to the cause of this GFP pattern. It may be that the cell biology of the intestine may be significantly aberrant. The brood size of *ij53* is also significantly reduced and many homozygotes are sterile. It was therefore easier to maintain this allele as a heterozygote. STS mapping of *ij53* placed it onto chromosome I, to the left of *stP124* (Figures 3.15 and 3.16, Tables 3.9 and 3.10).

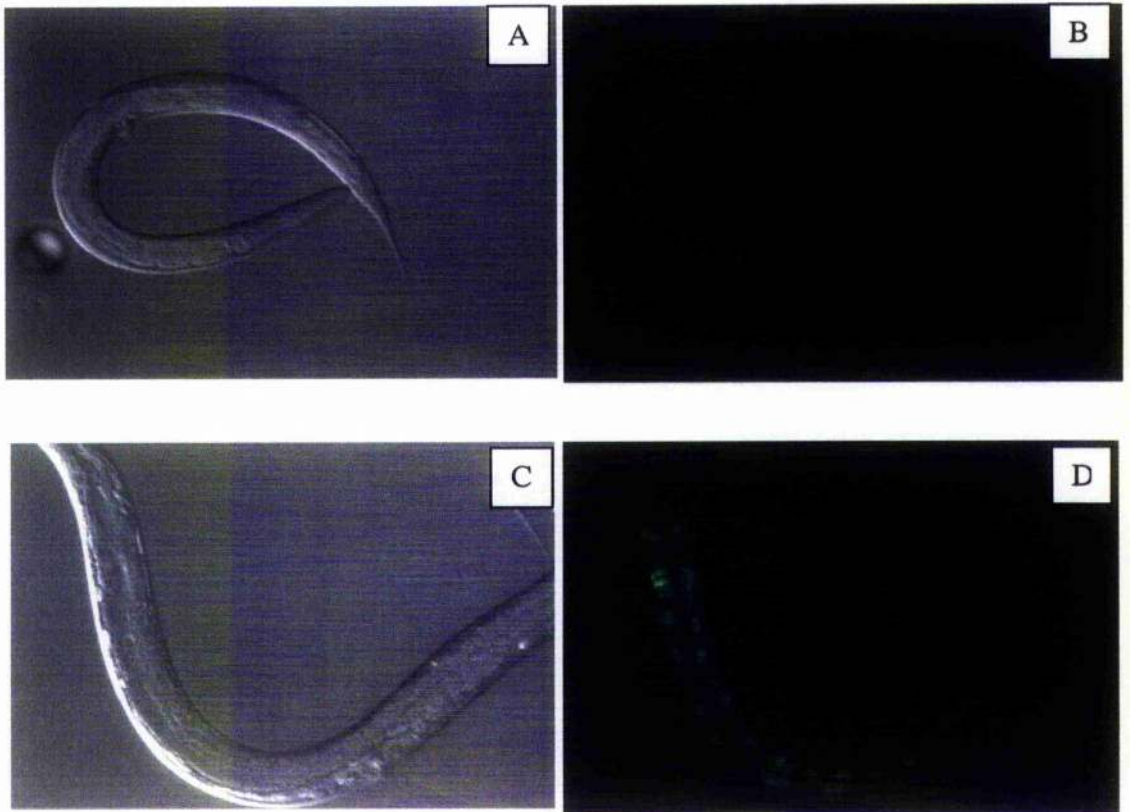


Figure 3.14. Characterisation of *ij53*. (A) and (C) are Nomarski and respective GFP counterparts (B) and (D). (A) and (B) are wild type, (C) and (D) are *ij53*. Note that these images are not taken under same magnification and wild type should only be used as a reference for comparison of GFP expression.

STS mapping of *ij53*

Figure and Table legends for STS mapping of *ij53*

Table 3.9 STS Chromosome assignment of *ij53*. 45 separate reactions, each reaction performed with DNA from F2 mutant homozygotes, generated by selfing *ij53*/RW7000 hybrid. Approximately 75% of animals should detect each unlinked STS marker Linkage is detected by a reduced frequency. This table illustrates that *ij53* is linked to chromosome I.

Figure 3.15 Representative gel of STS mapping of *ij53* using chromosome I markers. 92 separate reactions were performed. Lane A is RW7000 control. Lanes B and C refer to the recombination events shown in Figure 3.16. A total of 45 *ij53* homozygotes were tested. The remaining mutants tested negative for all chromosome I STSs.

Figure 3.16 Proposed recombination events between RW7000 and *ij53*. RW7000 chromosome is top line and *ij53* is bottom line. This interpretation places *ij53* to the left of *stP124*.

Table 3.10. Tabulated data of proposed recombination events

Chromosome	STS Marker	No. of animals with marker	Total No. of animals tested	Percentage of animals with marker
I	<i>hP4</i>	11	45	24.4
II	<i>maP1</i>	37	45	82.2
III	<i>mgP21</i>	30	45	66.6
IV	<i>sP4</i>	29	45	64.4
V	<i>bP1</i>	35	45	77.7

Table 3.9



Figure 3.15

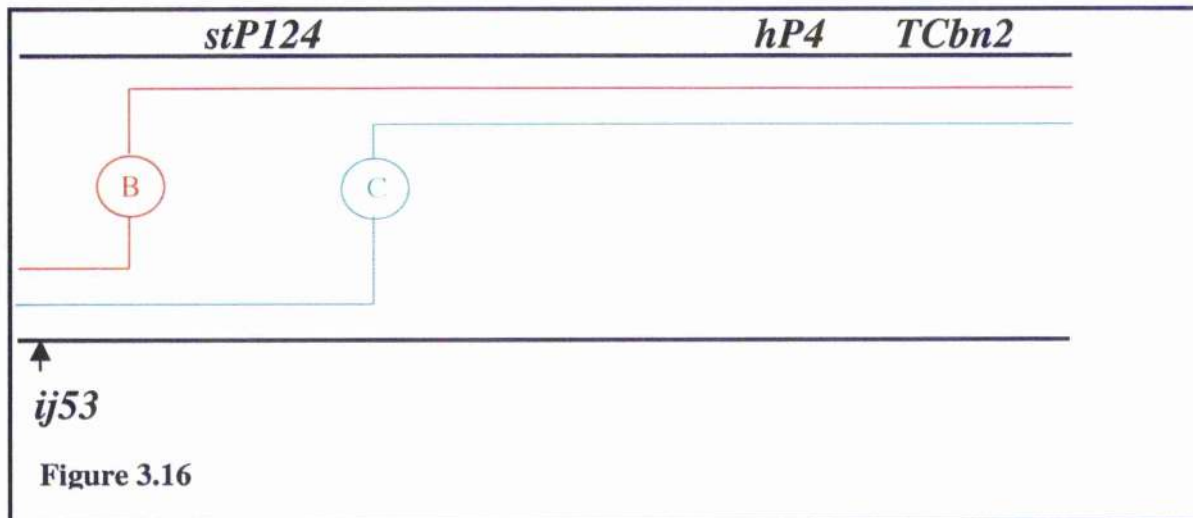


Figure 3.16

Recombinant class	Total Number of Recombinants (/92)
B	3
C	11

Table 3.10

3.13. Discussion

This chapter describes the approaches used to generate stable transgenic lines of *C. elegans*, which showed strong intestinal GFP expression during most of the life cycle. Good intestinal GFP nuclear localisation, which could be viewed easily under a GFP stereomicroscope was a prerequisite, for the identification of desired mutants. This chapter focuses on the problems encountered in constructing such strains and the methods employed to solve them. It also describes the screening and identification of mutants with gut developmental defects. A brief characterisation of the generated mutants was carried out. Further characterisation of two mutants, alleles *ij48* and *ij52* is described in Chapters 4 and 5.

The first issue was the choice of promoter. Previous work in the Johnstone lab with cysteine proteases *cpr-3*, *cpr-4*, *cpr-5* and *cpr-6* showed that these genes were expressed exclusively in the intestine (Larminie, 1995; Larminie and Johnstone, 1996). Semi-quantitative RT-PCR with these genes showed that *cpr-3*, *cpr-4* and *cpr-5* transcript abundance was relatively high during the life cycle. Although any of these genes may have been used, *cpr-5* was chosen.

Constructs containing the *cpr-5* promoter fused to *GFP* or *GFPlacZ* were generated. Although I did not sequence the fusions, transgenic strains containing these promoter fusions showed gut specific expression of the transgene as described by Larminie, (1995). Strains containing the *cpr-5* promoter fused to *GFPlacZ* (as opposed to *GFP* alone) displayed tighter nuclear localisation. Both the *GFP* and *GFPlacZ* vectors contain the SV40 nuclear localisation signal. This difference in the tightness of nuclear localisation observed with the different plasmids has been shown with other genes, including the cuticular collagen gene *dpy-7* (E. Stewart, pers. comm.). It has been suggested that the incomplete nuclear localisation observed with fusions with *GFP* alone may be due to GFP being a small protein, and is thus able to diffuse from the nucleus (A.Fire, A.Xu, J.Ahn and G.Seydoux, personal communication).

The mosaic pattern of expression (i.e. variation with the exact number and position of gut cells staining) observed with transformants of pCC7/8 and pCC16 has also been observed with transformants with the *cpr-1* promoter (Britton *et al.*, 1998). With the *cpr-5* transformations described here, injecting with a higher concentration of DNA and/or injecting a larger promoter fragment (i.e. pCC7/8 vs pCC16) did not reduce the degree of mosaicism. The inclusion of excess genomic DNA as a carrier during DNA transformation has been found to permit stable expression of transgenes in the germline (Kelly *et al.*,

1997). They speculated that transgenes of simple arrays might be silenced because the arrays are recognised as repetitive. Inclusion of carrier DNA increases the complexity, thereby reducing the repetitive nature of the array. The *cpr-5::GFP* expression pattern I observed suggests that that transgene silencing also occurs in the intestine: injecting the *cpr-5* promoter constructs as linear fragments together with *C. elegans* genomic DNA as a carrier permitted robust expression of the transgene in the intestine, with less apparent mosaicism. Although the anterior-most cells still showed stronger transgene expression, most gut nuclei could be easily visualised under a GFP stereomicroscope (average of 28 versus expected 32 in adult). Therefore, the "mosaic" expression pattern I observed with simple arrays may be due to a combination of individual cells losing the array and transgene silencing.

From a screen of 8000 mutagenised genomes, four classes of mutants with gut defects were identified, covering defects in various areas of E cell development. The mutant screen I performed was not saturating as judged by both the number of genomes screened and by the failure of obtaining multiple alleles of each mutant. The number of genes that can be mutated to give these developmental gut defects can therefore not as yet be estimated. More screens should therefore be carried out.

Noticably missing from my screen was a class of mutant where endoreduplication fails. Strong loss-of-function mutants in the cyclin E homologue, *eye-1* in *C. elegans* display this phenotype (Fay and Han, 2000). This mutant contains defects in other tissues and was identified in a screen for mutants with an altered pattern of vulval cell divisions. *eye-1* mutants undergo one round of endoreduplication, such that the average intestinal cell ploidy in *eye-1* mutants is 4C. Endoreduplication has also been shown to be dependent on cyclin E activity in *Drosophila* (Edgar and Orr-Weaver, 2001). Removal of cyclin D1 (*cyd-1*) by RNAi also results in intestinal cells having a terminal ploidy of 4C (Park and Krause, 1999). This however may be simply due to the fact that the RNAi animals arrest during L2 development. Like *eye-1* mutants, removal of *cyd-1* results in abnormalities in multiple post-embryonic cell lineages. In contrast, RNAi of *cyd-1* also results in the failure of the L1 nuclear division, thus most intestinal cells are mononucleate. Since the mutant screen I performed did not reach saturation levels, I may not have "hit" these genes. Moreover, although the *eye-1* mutant arrests as a sterile adult that could theoretically be detected by my screen, removal of *cyd-1* results in L2 larval lethality, which would have proved difficult to detect in my screen.

Class I mutants with a putative lineage defect were characterised further and their phenotypes are described in detail in Chapter 4. These mutants were chosen for further investigation, as they were potentially the most interesting. The other mutants identified were only briefly characterised.

The class II mutant, *ij51*, has two main phenotypes: a post-embryonic gut defect where the post-embryonic nuclear division that normally occurs during L1 fails, and are sterile. Preliminary analysis has shown that these phenotypes cannot be separated recombinationally and thus are probably caused by the same mutation. However, further genetical analysis of this lesion is required. Since endoreduplication appears to occur in intestinal nuclei of *ij51*, it seems likely that the mutant gene is required for M-phase but not S-phase of the cell cycle in the L1 intestine.

Failure of L1 nuclear division has been described by RNAi of *cyd-1* (above), in worms homozygous mutant for the temperature sensitive mutation *abc-1(oj2)* (O'Connell *et al.*, 1998) and for mutants in the *cdc-2*-related kinase, *ncc-1* (Boxem *et al.*, 1999). Like *ij51*, in *abc-1* mutants, the intestinal L1 nuclear division fails. The intestinal nuclei still perform four rounds of endoreduplication and have a ploidy of 64C. Moreover, like *ij51*, *abc-1(oj2)* homozygotes are sterile, lack a normal gonad and show a variably penetrant vulval defect. In contrast to *ij51*, *abc-1(oj2)* is severely uncoordinated and many homozygotes arrest as larvae. These observations with *abc-1* suggest that it may be a gene that is necessary for many or all post-embryonic cell cycles. Since *ij51* maps to chromosome III and *abc-1(oj2)* to chromosome V, these mutants are not allelic.

Although the L1 intestinal nuclear division also fails in *ncc-1* mutants, in contrast with both *ij51* and *abc-1*, the intestinal nuclei of *ncc-1* mutants in adulthood have a ploidy of 32C, suggesting that the intestinal nuclei that are prevented from completing karyokinesis due to lack of *ncc-1* activity are also blocked from entering the first endocycle. Like *abc-1*, many post-embryonic lineages are affected by mutations in *ncc-1*. Although *ncc-1* is on the same chromosome as *ij51*, they are unlikely to be allelic as *ncc-1* maps to around +2 whereas *ij51* maps approximately to position +20.

The reason for sterility of *ij51* is not clear. However, mitotic expansion of the germline seems normal, as viewed with Nomarski and DAPI optics. Oocytes form in the correct place, at the turn of the gonad, cellularise and appear to contain a single nucleus. Sperm is also present. It is possible that the oocytes do not move through the spermatheca normally, or that there is a meiotic defect. The defective oocytes appear to fall apart suggesting that an eggshell is not synthesised. Although I have ruled out several possible

reasons for the sterility in *ij51*, further characterisation is needed to determine the precise reason for sterility.

Preliminary characterisation of the mutant alleles giving rise to the class III defect with multi-nucleate cells, indicates that the mutant phenotype is variably penetrant. In the cells with more than two nuclei present, the nuclei are smaller in size to wild-type and therefore probably have less DNA. It is likely that the total DNA content in multi-nucleate cells is very similar to wild-type, for example, at adult, rather than the 2 nuclei of 32C, they may have 4 nuclei of 16C, as estimated by the nuclear size differences. This suggests that mutations in the genes identified by *ij49* and *ij50* essentially converts an endocycle into a round of karyokinesis. It is possible that this additional nuclear division occurs in *ij49* and *ij50* during L2, that is a reiteration of the L1 nuclear division event during L2, as the mutant phenotypes of both alleles are suppressed by entry into dauer-stage. Many heterochronic genes, including *lin-14*, *lin-28* and *lin-29* are suppressed by entry into dauer (Liu and Ambros, 1989). The relationship of *ij49* and *ij50* to known heterochronic genes should be investigated, in particular *lin-14*. For example it would be desirable to test whether *ij49* and *ij50* are alleles of known heterochronic genes. Mutations in heterochronic genes cause precocious or retarded development of certain cell lineages. Extra intestinal nuclei are observed in mutant backgrounds where *lin-14* activity remains high beyond the first larval molt, presumably by additional nuclear divisions beyond the first larval molt (Chalfie *et al.*, 1981; Ambros and Horvitz, 1984). Although additional nuclei have been observed in these *lin-14* alleles, they have not been characterised. For example, it is unclear whether in addition to extra rounds of karyokinesis, there are additional rounds of endoreduplication. It would be interesting to examine genetic epistasis between *ij51*, *lin-14* and other heterochronic genes.

Other genes, when mutated, also display the multi-nucleate phenotype. In *lin-23* mutants (which are presumed to be deficient in the ubiquitin-mediated proteolysis of positive cell-cycle regulators), all but the four most anterior nuclei undergo two rounds of karyokinesis in the first larval molt (Kipreos *et al.*, 2000). Interestingly, unlike wild-type, the nuclei of *int-2* often undergo a nuclear division in *lin-23* mutants. Although the defects in *ij49* and *ij50* possibly occur at a different larval stage (L2) than *lin-23*, in both cases, the total number of rounds of DNA replication are the same as in wild-type.

Due to the lab stock of the mapping strain RW7000 also having a mutation causing this phenotype, it is still unclear whether *ij49* and *ij50* are allelic. Classical genetic mapping should therefore be used to map these alleles and if appropriate, allelism tests

performed. It would be desirable to determine the precise timing of when the extra nuclear cell divisions occur and any ramifications the extra nuclear divisions have on endoreduplication. Double mutants with the mononucleate/multinucleate mutant classes may identify genetic pathways.

Many genes that have been found to be part of the cell cycle machinery have been shown to affect post-embryonic cell divisions in *C. elegans*. However, many of these mutants have not been examined for an intestinal defect. For example, classes of mutant exist with global failure in post-embryonic divisions. Mutations in *lin-6* have a defect in DNA synthesis (Sulston and Horvitz, 1981) and therefore endoreduplication may fail in this mutant. In contrast, reduction or loss of function for *cul-1* activity results in hyperproliferation of the post-embryonic blast cells (Kipreos *et al.*, 1996).

The phenotype of the mutant with altered gut morphology, *ij53*, should also be examined. The loss of tight GFP nuclear localisation is unlikely to have resulted from a mutation in the GFP construct. It seems likely that there is a structural defect in the intestines of *ij53* homozygotes. The cause of the low brood size and sterility should also be investigated.

In conclusion, this screen identified new classes of E-cell lineage defects relating to both embryonic and post-embryonic development. Two of the new mutants identified, *ij48* and *ij52* are further characterised in Chapters 4 and 5.

Chapter 4.

Characterisation of *lin-60* and *lin-62*

4.1. Introduction

The *Caenorhabditis elegans* intestine consists of twenty cells, all of which are generated from the E blastomere during embryogenesis. Between the specification of the E blastomere itself and the execution of terminal fate in the twenty cells of the developed intestine, there is a precise pattern of cell divisions. The twenty cells cannot be derived from a single progenitor by a symmetrical pattern of cell divisions. At around 300 minutes of development the intestine consists of 16 cells, 12 of which undergo no further cell divisions and 4 of which undergo one further division, thus producing twenty cells. Thus there is asymmetry within the E cell lineage, some cells exiting the cell cycle one division before their sisters. Ultimately, this must involve the differential regulation of common central cell cycle regulators within sister cells, thus the *C. elegans* intestine offers a tractable system for a study of interactions between a developmental programme and central regulators of the cell cycle.

In an attempt to identify genes acting downstream of those necessary to specify E and involved in controlling the highly regulated pattern of cell and nuclear divisions of the E lineage, a standard genetic approach of performing mutant screens to detect animals with altered numbers of intestinal nuclei was used (Chapter 3). *lin-60(ij48)* and *lin-62(ij52)* mutants were chosen for further analysis as these mutants were the most interesting and developmentally significant obtained from the screen. In the study of these mutants, I first aimed to genetically characterise the different alleles and examine their mutant phenotypes. The genetic behaviour of *lin-60(ij48)* and *lin-62(ij52)* alleles were investigated and their map positions refined. The phenotypes generated by these mutant alleles were observed using various terminally differentiated gut markers (GFP and antibody staining), and the E-cell lineages of these mutants were determined.

4.2. Phenotypic characterisation of *lin-60(ij48)*

4.2.1. Gross phenotype of *lin-60(ij48)*

Under a standard bench stereomicroscope, *lin-60(ij48)* mutants are phenotypically wild-type. The intestine is functional, *ij48* animals grow normally and there is no indication of feeding defects. They do not look starved and do not show a tendency to form dauer larvae under standard culture conditions. There is no evidence of additional hypodermal cells as the mutant larvae and adults are normal length. The *ij48* mutant is fertile and has an approximately normal brood size. To investigate the mutant phenotype of *lin-60(ij48)*, I used a variety of terminally differentiated gut markers. When analysing broods from crosses, *lin-60(ij48)* was crossed into the strain IA109, containing the integrated insertion *ijIs10(cpr-5::GFP)* (described in Chapter 3) to facilitate with the visualisation of the intestinal cell nuclei.

4.2.2. Characterisation using terminally differentiated intestinal *GFP* markers

Initial phenotypic characterisation of *lin-60(ij48)* was carried out with *GFP* promoter fusions of *cpr-5* and *elt-2*. *cpr-5* is expressed specifically in the *C. elegans* intestine during larval and adult stages of development and therefore acts as a marker for post-embryonic intestinal cell fate. *elt-2* is a GATA transcription factor that is first expressed when there are two gut cells, and is expressed through all stages of development. *ij48* larvae and adults have additional nuclei expressing the *cpr-5::GFP* transgene compared to wild-type (Figure 4.1 A-D). The spatial distribution of intestinal cell nuclei are different from that observed with the multinucleate class (Section 3.12.3). Their position and appearance suggested there might be extra intestinal cells in these mutants. The possibility that extra E cells were born was investigated.

To determine whether the extra nuclei are born during embryogenesis, a plasmid containing an *elt-2::GFP* transgene was injected into *lin-60(ij48)* worms. I observed that mutant animals generated variably between 30 to 45 nuclei expressing *elt-2* during embryogenesis, by comparison to 20 in the wild-type (Figure 4.1, E-H). Thus in *lin-60(ij48)* mutants, many of the extra nuclei are born during embryogenesis.

In wild-type, no cell divisions occur in E during larval development. A nuclear division however, occurs during L1 in many gut cells, generating binucleate cells. It is unclear whether the intestinal cells of *lin-60(ij48)* are mononucleate (i.e. int-1 and int-2 behaviour) or binucleate. If a nuclear division does occur, it does not apply to all cells;

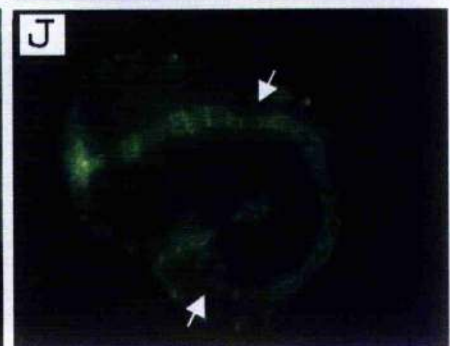
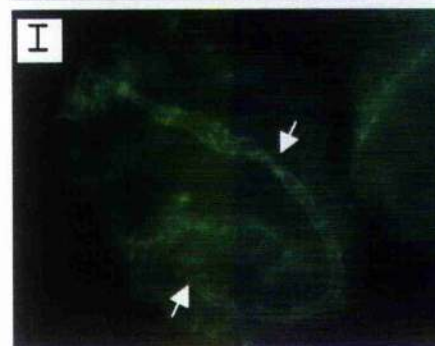
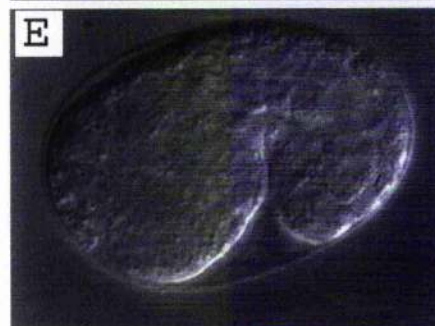
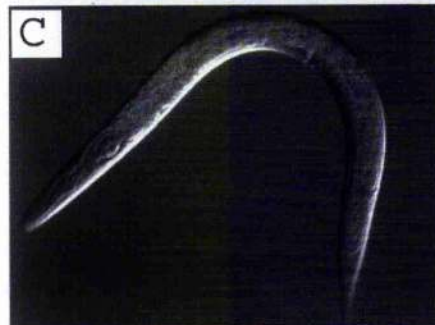
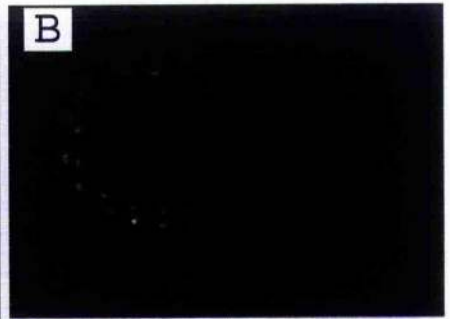
around 40 intestinal nuclei are generated during embryogenesis in *lin-60* mutants (see below) and if they all underwent a nuclear division, there would be at least 60-80 gut nuclei visible with GFP in post L1 larvae, whereas around 50 were observed.

4.2.3. Characterisation of *lin-60(ij48)* with MH27

The monoclonal antibody MH27 recognises a component of adherens junctions, both between adjacent hypodermal cells and within the intestine and pharynx (Francis and Waterston, 1985). In *lin-60(ij48)* mutants, extra intestinal cell boundaries are present (Figure 4.1, I and J). Thus extra gut cells are generated during embryogenesis. Moreover, many or all of these cells participate in forming a functional intestine, as indicated by the more complex pattern of intestinal cell boundaries in the developed intestine, prior to hatch. Although extra cell boundaries are present in the intestine, there does not appear to be extra boundaries in the hypodermis or pharynx, consistent with a specific E-cell lineage defect.

Figure 4.1
Characterisation of *lin-60(ij48)*

Figure 4.1 Characterisation of *lin-60(ij48)*. Examination of intestinal cells in wild type and *lin-60(ij48)* animals. (A), (C), (E) and (G) are Nomarski images with respective GFP fluorescence counterparts (B), (D), (F) and (H). In all cases, GFP is localised to the nuclei of cells by a nuclear localisation signal. Expression of a *cpr-5::GFP* transgene in adults in wild type (A) and (B) and *lin-60(ij48)* (C) and (D) indicates that additional intestinal nuclei are present in the mutant. The expression of an *elt-2::GFP* transgene in wild type (E) and (F) and *lin-60(ij48)* (G) and (H) indicate that the extra nuclei expressing this intestinal marker are born during embryogenesis. The number of nuclei expressing this marker in the *lin-60(ij48)* strain is typically 50-100% greater than wild type. Not all GFP-expressing nuclei can be seen in the given focal plane. Immunofluorescence with the MH27 antibody marking the boundaries between various *C. elegans* epithelial cell types, including intestine (Francis and Waterston, 1985) is shown for embryos at the 1.5-fold stage of development: wild type (I) and *lin-60(ij48)* (J). Both intestinal and pharyngeal cell boundaries can be seen in the given focal plane. White arrows indicate the start and end of the intestine. There are many more intestinal cell boundaries in *lin-60(ij48)* by comparison to wild type, and their organisation appears chaotic.



4.2.4. The E-cell lineage of *lin-60(ij48)* mutant embryos

There are two potential explanations for the generation of extra cells during embryogenesis expressing the intestinal fate. They could either be the result of a variable pattern of extra cell divisions within the E lineage itself, or the result of a transformation to the intestinal fate of cells from another lineage. To distinguish between these two possibilities, cell lineage analysis of the *ij48* mutant was performed. The E-cell lineage of four *lin-60(ij48)* embryos was analysed. Many extra divisions of the cells derived from the E blastomere in *ij48* mutant animals were found (Figures 4.2 and 4.3).

The computer software, "Biocell" was used for E-cell lineage analysis. This software permits a rapid and thorough analysis of the embryonic lineages as well as the reconstruction of various embryonic stages. The analysis is stored in the form of an annotated lineage. Embryonic stages and cell movements can be viewed as 3-D models in which cells can be coloured to better visualize the relative position of cells or groups of cells. The models can be rotated to provide different views of the embryo as well as to allow an easy comparison of different embryos

The E lineage began essentially as wild-type, in all embryos analysed. The first division occurs at approximately the correct developmental time. Presumably this is essential, as the inward movement of Ea and Ep initiate gastrulation. The second round of divisions, that of Fa and Ep occurs slightly earlier in *lin-60(ij48)* embryos, but the divisions appear to be in the correct orientation (left/right). By the third and fourth round of divisions there is an obvious shortening of the E cell cycle (Figure 4.2). For example, the third round of divisions in E in wild-type occurs at approximately the same time as the fourth round in *lin-60* embryos. In addition to the shortening of the cell cycle in E, the precise pattern of the E cell lineage becomes variable (Figure 4.3).

23 intestinal cells were observed to be generated in embryo 1 (Figure 4.3, A, C and E). Of those analysed, this embryo generated the least number of intestinal cells. The first, second and third round of cell divisions divide with a wild-type pattern, with respect to both the timing and pattern of divisions. Seven cells, including the 4 that divide in wild-type, divide again. As with all the lineage analysis performed, the recordings were taken until the embryo wriggles: thereafter, the Biocell software cannot be used reliably.

In embryo 2 (Figure 4.3, B, D and F) 41 cells were derived from E. This is over twice the amount generated in wild-type. In this embryo, the number of cells generated and the timings of cell divisions in the first and second rounds of divisions in E are similar to that of wild-type. Thereafter, the timing of the cell cycle in E is significantly reduced. The

E cell lineage produces 16E cells much faster than wild-type and all cells divide again generating 32 cells (compared to just four dividing in wild-type, generating 20 cells). Eight of these 32 cells undergo a sixth round of divisions. It is possible that more cells were generated later in embryogenesis, but these could not be easily detected with the Biocell software.

Forty cells were generated from the E-blastomere in embryo 3 (Figure 4.3, G, I and K). Like embryo 2, the 16E stage was reached at a faster pace than wild-type. All apart from one of these cells divided again and like embryo 2, some underwent a sixth round of divisions. Thirty-six cells were generated from E in embryo 4 (Figure 4.3, H, J and L). Again, most cells at the sixteen-cell stage divided again and six of these completed a sixth round of divisions.

Thus, many extra cells are generated in *lin-60(ij48)* from the E-blastomere, sufficient to explain the additional intestinal nuclei observed with *elt-2::GFP*. Notably, the E-cell lineage is variable between all the embryos. Unlike that of almost all wild-type *C. elegans* somatic tissue development (Sulston and Horvitz, 1977; Sulston *et al.*, 1983b), the *ij48* mutation causes the *C. elegans* intestine to develop by an indeterminate pattern of divisions. There is a general shortening of the time between cell divisions. Although strict cell cycle control is lost, other aspects of intestinal differentiation are retained, as indicated by the expression of terminal differentiation markers and by the functional nature of the intestine in mutants. Thus the *ij48* defect is proliferative in nature causing a loss of control of the cell cycle in E lineage cells, without significantly altering other aspects of cell determination and terminal differentiation.

Figure 4.2
The E-cell lineage in wild-type and *lin-60(tj48)*

Figure 4.2 The E-cell lineage in wild-type and *lin-60(ij48)*. Data is from lineage of embryo G in Figure 4.3. Timing of cell cleavages in minutes, derived from the E blastomere. The cell marked 'o' could not be followed in the recording. There are no further cell divisions in the wild-type E lineage. Recordings were taken until approximately 400 min of embryonic development; any cleavages beyond this time in the mutant would not be detected. Division rounds (red) are added as an aid to compare wild-type and *lin-60* lineages.

ij48

Division Round

Wild Type

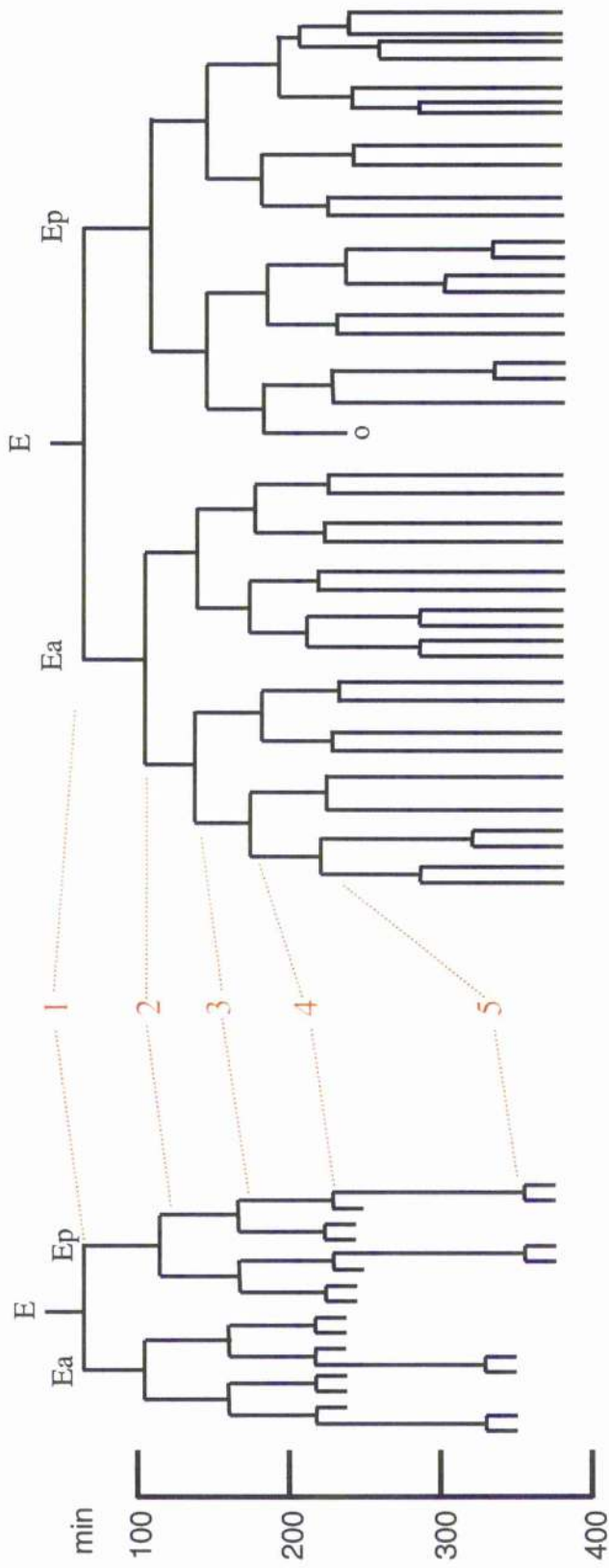
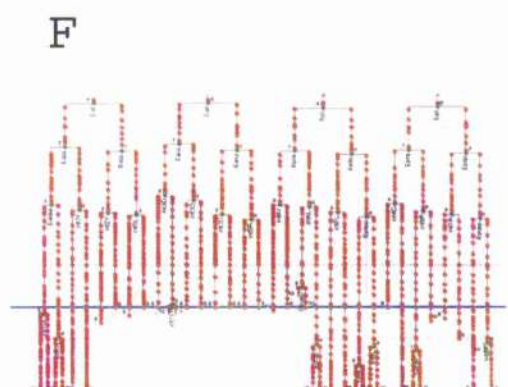
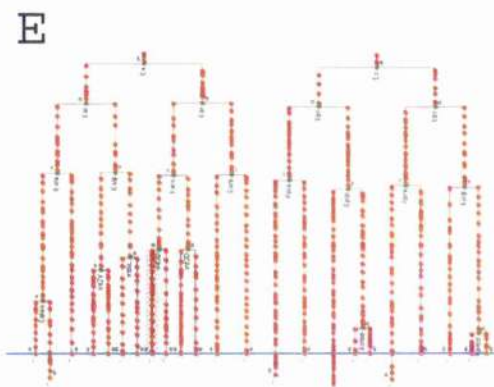
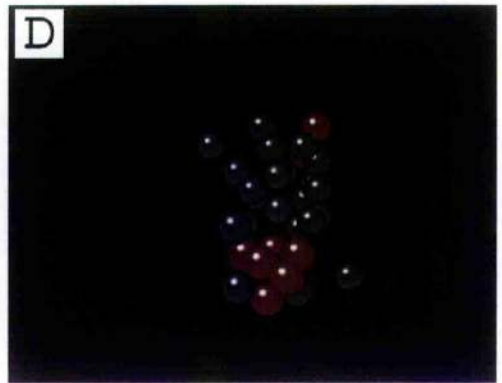
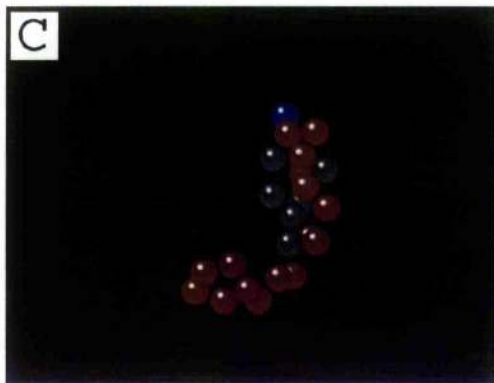
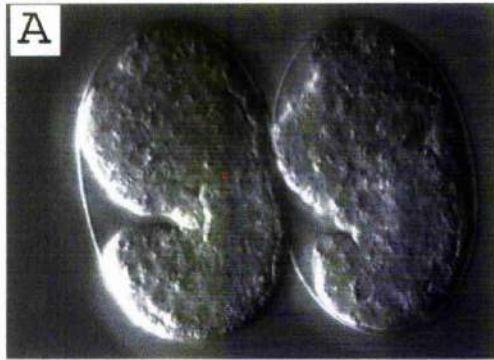


Figure 4.3
The E-cell lineage of *lin-60(ij48)*

Figure 4.3 E-cell lineage of *lin-60(ij48)*. The raw data for 4 lineaged embryos is given. This figure is continued on a second page. (A, left embryo), (B, left embryo), (G, right embryo) and (H, left embryo) are Nomarski images of the lineaged *lin-60(ij48)* embryos. The green dots represent the positions of the intestinal cell nuclei. (C), (D), (I), and (J) are 3-dimensional representations of the intestine. The red "spheres" represent E-cells born and terminating with a wild type lineage; grey "spheres" represent cells derived from a mutant lineage. (E), (F), (K) and (L) are the lineage trees; the red dots were used as an aid to trace the cells in the Biocell programme, the green dots represent a cell division or the end of the recording.

Figure 4.3



As a control, lineage analysis of the D blastomere was determined in the *lin-60(ij48)* mutant and found to be wild type; thus the proliferative defect caused by the *ij48* lesion is not found in all cell types. Evidence that it is restricted to the E lineage is discussed below.

4.2.5. Characterisation of *lin-60(ij48)* using non-intestinal markers

In addition to the D cell lineage, other tissues were tested for evidence of extra cells. At hatch, 10 seam cells run down both lateral surfaces of the worm (Wood, 1988). Seam cells were observed using the GFP marker *wIs84* from *C. elegans* strain JR637 that causes GFP to be expressed specifically in seam cells (a gift from Joel Rothman). Using this marker, the wild-type number of seam cells was observed in *lin-60(ij48)* mutants (Figure 4.4).

The germline of *lin-60(ij48)* hermaphrodites was examined for hyperplasia (Figure 4.5). Germline cells divide throughout the post-embryonic period (Kimble and Hirsh, 1979), however most expansion occurs during the latter stages of larval and early adult development. In *lin-60(ij48)* hermaphrodites, the germline matures as wild-type, the *lin-60(ij48)* hermaphrodites are fertile and have a near wild-type brood size. The mitotic germ cells and their nuclei are the same size as wild-type. The germline cells exit proliferative mitosis appropriately and proceed through meiosis, indicating that they are responsive to the anti-proliferative functions of the *gld* genes (Francis *et al.*, 1995; Kadyk and Kimble, 1998). *lin-60(ij48)* males are also fertile (see below), suggesting that there are no problems with the anatomy of the male tale. I was therefore unable to find any evidence of hyperplasia of the germline in *lin-60(ij48)* mutants.

There is no evidence for hyperplasia in any other tissue. *lin-60(ij48)* mutants are also of wild-type length and are not uncoordinated, suggesting that there is no hyperplasias of the hypodermis and nervous system respectively. The MH27 pattern of the hypodermis and pharynx is wild-type in 3-fold embryos. I am therefore unable to detect evidence that the *ij48* lesion affects any cell type other than intestine, however minor differences cannot be excluded.

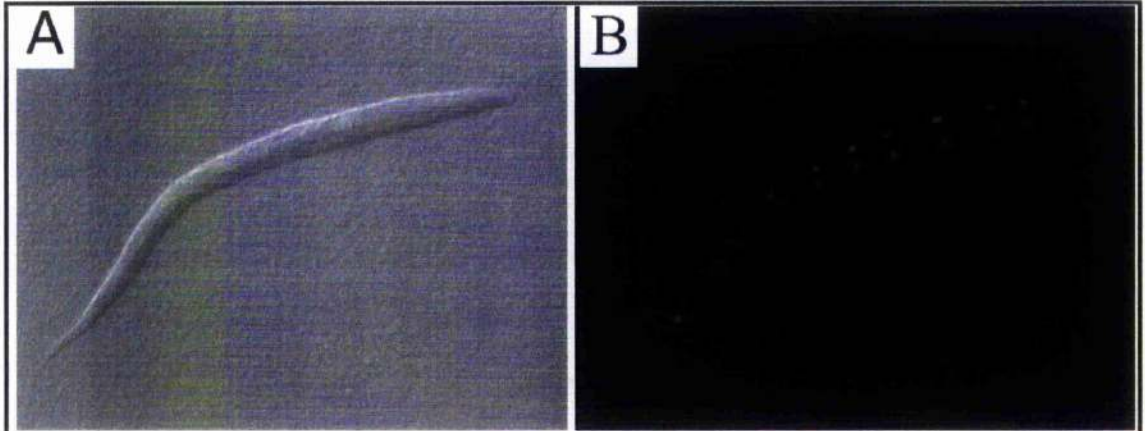


Figure 4.4 Seam cells in *lin-60(ij48)*. (A) is a Nomarski image of an L1 larva with respective GFP counterpart, (B). *lin-60(ij48)* was crossed into strain JR667, containing an integrated *seam-cell-marker::GFP* fusion, *wIs51*. The GFP is localised to the nuclei of the seam cells by a nuclear localisation signal. In *lin-60(ij48)* mutants, there are a wild type number of seam cells in L1 larvae (10 run down each lateral surface), indicating that there are no extra seam cells born.

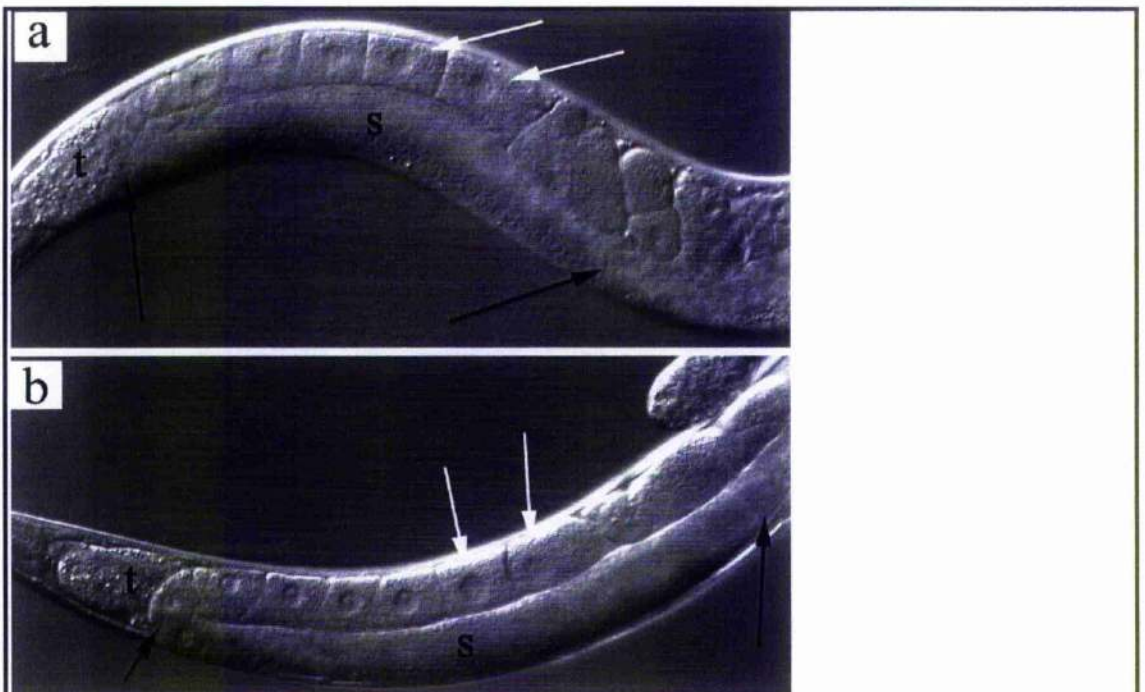


Figure 4.5 The *lin-60(ij48)* gonad. (A) wild type and (B) *lin-60(ij48)*. Some developing oocytes are marked with white arrows; the syncytial arm of the gonad is delineated with black arrows and labelled 's'. This region contains several hundred germline nuclei in both wild type and mutant. The turn of the gonad is marked 't'. This demonstrates that *lin-60(ij48)* mutants do not display excessive germline proliferation.

4.3. Genetic characterisation of the *ij48* allele

4.3.1. The *ij48* allele identifies a maternal gene and is semi-dominant over wild-type

The intestinal hyperplasia displayed by *ij48* is highly penetrant: almost 100% of F₁ progeny of *ij48* homozygotic mothers display mutant phenotype. However, the amount of extra intestinal cells varies from animal to animal (as discussed above). The *ij48* allele displays a maternal pattern of inheritance; when *ij48* homozygotic hermaphrodites are crossed with wild-type males, 100% of F₁ *+ij48* heterozygotes display mutant phenotype. In contrast, if the *ij48* allele is mated from a male, 100% of F₁ *+ij48* heterozygotes are wild-type.

Analysis of 993 F₁ progeny of 22 broods from *+ij48* heterozygotes, gave an average of 73.4% displaying mutant phenotype (Table 4.1). Since the average displaying phenotype for a recessive gene would be 25%, the 73.4% demonstrates the semi-dominance of *ij48*. The proportion of the F₁ progeny displaying the mutant Lin phenotype varied from 21.9% to 96.7% in the 22 broods analysed. To ensure that the correct ratios of genotypes were segregated, the genotypes of 4 broods were analysed (Table 4.2). For standard Mendelian frequencies, progeny of genotypes *++*, *-ij48* and *ij48/ij48* in the ratios 1:2:1 are expected. The F₁ heterozygotic animals were each picked clonally to 3.5cm plates. 22.7% *++* F₁ progeny were observed, demonstrated by generating 100% wild-type F₂ progeny, which is in approximate agreement with Mendelian frequencies.

Brood	Number of progeny Lin	Number of progeny wild-type	Total number of progeny	% Lin	% WT
1	43	13	56	76.8	23.2
2	56	15	71	78.9	21.1
3	41	12	53	77.4	22.6
4	23	4	27	85.2	14.8
5	26	11	37	70.3	29.7
6	30	8	38	79.0	21.0
7	55	23	78	70.5	29.5
8	41	12	53	77.4	22.6
9	56	15	71	78.9	21.1
10	7	25	32	21.9	78.1
11	21	42	63	33.3	66.7
12	26	11	37	70.3	29.7
13	29	1	30	96.7	3.3
14	43	13	56	76.8	23.2
15	55	23	78	70.5	29.5
16	20	4	24	83.3	16.7
17	23	4	27	85.2	14.8
18	30	8	38	79.0	21.0
19	56	15	71	78.9	21.1
20	41	12	53	77.4	22.6
21	47	3	50	94.0	6.0
22	77	17	94	81.9	18.1
Totals/Avc %	722	271	993	73.4	26.6

Table 4.1 Analysis of phenotypes of F1 broods from *+ij48* hermaphrodites

Genotype/ Brood	%	+/+	<i>+ij48</i>	<i>ij48/ij48</i>
A		20	50	30
B		20.9	47.9	31.2
C		21.6	53.4	25
D		28.4	50	21.6
Average		22.7	50.3	27

Table 4.2 Analysis of genotypes of F1 broods from *+ij48* hermaphrodites

To address the question of whether the zygotic genotype was influencing the phenotype, both the genotype and phenotype of each F1 from two broods was determined (Table 4.3). From the sample size analysed, the data suggests that the zygotic genotype may be influencing the outcome of the phenotype. However, if the zygotic genotype does play a role, it is not absolute. This idea is supported with data obtained from deficiency crosses (Section 4.3.3).

Phenotype	No. Lin	No. Lin	No. Lin	Total No. Lin	No. wild-type	No. wild-type	No. wild-type	Total No. wild-type
Genotype	<i>ij48/ij48</i>	<i>+/ij48</i>	<i>+/+</i>		<i>ij48/ij48</i>	<i>+/ij48</i>	<i>+/+</i>	
Brood A	15	24	8	47	0	1	2	3
Brood B	27	41	9	77	3	5	11	19

Table 4.3 Relationship between zygotic genotype and phenotype of progeny from *+/ij48* hermaphrodites

4.3.2. Characterisation of *ij48* over the deficiencies *hDf8* and *qDf16*.

Placing mutant alleles over deficiencies can help with their characterisation. For example, it can be used to distinguish whether an allele is a null or partial loss-of-function. The allele *ij48* was placed over the deficiencies *hDf8* and *qDf16*, both of which map to the region of chromosome I where *lin-60(ij48)* is positioned.

For mothers of genotype *ij48/hDf8*, from 18 broods analysed, an average of 2.2% of the viable F1 progeny displayed mutant phenotype (Table 4.4). For mothers of genotype *ij48/qDf16*, from 12 broods, an average of 22.4% of the viable F1 progeny displayed mutant phenotype (Table 4.5). Both of these figures are drastically different to the average of 73.4% for progeny of *ij48/+* mothers and almost 100% for progeny of homozygous *ij48/ij48* mothers. That the mutant phenotype is modified by the presence of the deficiencies *hDf8* and *qDf16*, is consistent with the gene identified by allele *ij48* being covered by these deficiencies. I therefore concluded that the *ij48/hDf8* and *ij48/qDf16* heterozygotes are hemizygotic for the mutant copy of the gene identified by allele *ij48*.

Brood	% Total progeny dead eggs	% Total progeny Lin	% Total progeny wild-type
1	33	0	67
2	35	6	59
3	29	0	71
4	31	0	69
5	22	0	78
6	26	0	74
7	14	5	81
8	22	3	75
9	18	2	80
10	21	2	77
11	21	0	79
12	24	0	76
13	15	2	83
14	25	6	69
15	29	0	71
16	16	3	81
17	17	2	81
18	20	0	80
Average	23.2	1.7(2.2)	75.1(97.8)

Table 4.4 % Phenotypes of total progeny from *lin-60(ij48)/hDf8*. Values in brackets denote % viable progeny displaying wild-type or Lin phenotype (as opposed to total progeny, where a percentage is lethal).

Plate No	% Total progeny dead eggs	% Total progeny Lin	% Total progeny wild-type
1	22	19	59
2	24	15	61
3	31	15	54
4	21	20	59
5	20	30	51
6	26	27	47
7	27	10	63
8	19	16	65
9	18	8	74
10	23	11	66
11	27	18	55
12	14	18	68
Average	22.6	17.3(22.4)	60.1(77.6)

Table 4.5 % Phenotypes of total progeny from *lin-60(ij48)/qDf16*. Values in brackets denote % viable progeny displaying wild-type or Lin phenotype (as opposed to total progeny, where a percentage is lethal).

I also examined the distribution of phenotypes in relation to their zygotic genotypes when *ij48* was placed over *hDf8* (Tables 4.6 and 4.7) or *qDf16* (Tables 4.8 and 4.9). Two broods from each deficiency were analysed (broods A-D). The probability of displaying the Lin (or wild-type) phenotype is approximately the same, regardless of the genotype. This data suggests that if the zygotic genotype does influence the phenotype, it is not absolute.

		%Phenotype of F1s with genotype	
		Lin	wild-type
Genotype of F1 from <i>lin-60(ij48)/hDf8</i> parent	<i>lin-60(ij48)/hDf8</i>	0	100
	<i>lin-60(ij48)/lin-60(ij48)</i>	0	100

Table 4.6 Relating phenotype to zygotic genotype of F1 progeny from *lin-60(ij48)/hDf8* parent. (Brood A) total viable progeny analysed =25: *lin-60(ij48)/hDf8*=64%, *lin-60(ij48)/lin-60(ij48)*=36%.

		%Phenotype of F1s with genotype	
		Lin	wild-type
Genotype of F1 from <i>lin-60(ij48)/hDf8</i> parent	<i>lin-60(ij48)/hDf8</i>	0	100
	<i>lin-60(ij48)/lin-60(ij48)</i>	0	100

Table 4.7 Relating phenotype to zygotic genotype of F1 progeny from *lin-60(ij48)/hDf8* parent. (Brood B) total viable progeny analysed =26: *lin-60(ij48)/hDf8*=56%, *lin-60(ij48)/lin-60(ij48)*=44%.

		%Phenotype of F1s with genotype	
		Lin	wild-type
Genotype of F1 from <i>lin-60(ij48)/qDf16</i> parent	<i>lin-60(ij48)/qDf16</i>	24.1	75.9
	<i>lin-60(ij48)/lin-60(ij48)</i>	29.4	70.6

Table 4.8 Relating phenotype to zygotic genotype of F1 progeny from *lin-60(ij48)/qDf16* parent. (Brood C) total viable progeny analysed=46: *lin-60(ij48)/qDf16*=63.0%, *lin-60(ij48)/lin-60(ij48)*=37.0%.

		%Phenotype of F1s with genotype	
		Lin	wild-type
Genotype of F1 from <i>lin-60(ij48)/qDf16</i> parent	<i>lin-60(ij48)/qDf16</i>	11.8	88.2
	<i>lin-60(ij48)/lin-60(ij48)</i>	14.3	85.7

Table 4.9 Relating phenotype to zygotic genotype of F1 progeny from *lin-60(ij48)/qDf16* parent. (Brood D) total viable progeny analysed=48: *lin-60(ij48)/qDf16*=70.8%, *lin-60(ij48)/lin-60(ij48)*=29.2%.

This genetic data indicates that *ij48* is a gain-of-function allele and is sensitive to gene dose. Two mutant copies in *ij48* homozygotic mutant mothers result in virtually 100% of the F1 progeny displaying the mutant phenotype. When the mutant gene dose is reduced to one in the mother by placing the mutant allele over a deficiency, only 2.2% of the F1 progeny (in *hDf8* background) display mutant phenotype. That *ij48/+* heterozygotic mothers, that have one mutant and one wild-type copy of the gene, give 73.4% F1 progeny with mutant phenotype, indicates that the wild-type copy of the gene can contribute along with the *ij48* gain-of-function copy to produce extra intestinal cells. It can therefore be concluded that the allele *ij48* is a hypermorph.

Interestingly, when comparing suppression of Lin phenotype when placed over a deficiency, the hyperplasia is suppressed to a greater degree when placed over *hDf8* than *qDf16*. This is strange because the *qDf16* deficiency is predicted to extend further to both the left and right of *hDf8*. The cause of this increased suppression can therefore not be due to an extragenic suppression effect by another gene.

On comparison of the strains containing these deficiencies, although both segregated approximately 25% death, the strain carrying *hDf8* was slow growing and had a lower brood size. Therefore, there may be additional chromosomal rearrangements such as an inversion present. Strains carrying *hDf8* also exhibit a low-penetrant vulval defect, suggestive of extraneous mutations. Thus, the extra suppression may be caused by such additional mutations (see discussion).

4.4. Mapping of *lin-60(ij48)*

The standard route to cloning a gene defined by a mutation in *C. elegans* is to attempt phenotypic rescue with cosmid clones in the genomic region to which the mutation maps. This standard method can only be used for alleles recessive to wild-type and hence was not appropriate here. The data I obtained when characterising the *ij48* allele suggested a method for cloning the gene identified by *ij48*: since the *ij48* mutant phenotype is suppressed over a deficiency, it was proposed that performing RNA-mediated interference (RNAi) to reduce the amount of functional gene product may mimic this. The hypothesis was that the RNAi of the gene identified by *ij48* should suppress the intestinal lineage hyperplasia in the F1 progeny of treated animals. It was therefore imperative to reduce the *lin-60* interval to as small a region as possible.

As a first step towards cloning the gene identified by *ij48*, classical genetics were used to refine its map position. By STS mapping, I showed that *lin-60(ij48)* maps to chromosome I (see chapter 3). This PCR-based method was not used to refine the map position for two reasons. Firstly, the combination of the dominance and maternal genetics of the *ij48* allele causes all classes of genotypes to display the Lin phenotype. Secondly, at the time of mapping, there were only three STS markers available on chromosome I, which were positioned close together on the genetic map.

I first confirmed that *lin-60* was positioned on chromosome I by showing linkage with a gene on the centre of chromosome I (*dpy-5*). Two-factor and multi-factor mapping then placed *lin-60(ij48)* relative to other genes on the genetic map. *lin-60(ij48)* was found to lie in a region of chromosome I which had been targeted previously for lethal screens (McDowall and Rose, 1997a). Moreover, these lethals were placed onto both genetic and physical maps (McDowall and Rose, 1997b), aiding the refinement of the map position of *lin-60(ij48)*. Although this region of chromosome I had many marker genes, *lin-60(ij48)* was positioned within a gene cluster and therefore generated low recombinational frequencies per physical distance (approximately 1cM/1100kb) (Barnes *et al.*, 1995).

4.4.1. Linkage of *lin-60(ij48)* to chromosome I

I tested linkage to *dpy-5*, which maps to position 0 on chromosome I. *lin-60(ij48)* homozygous males were mated with homozygous *dpy-5(e61)* hermaphrodites and outcrossed worms (i.e. those with wild-type length), transferred clonally to 3.5cm plates and allowed to self. F2 Dpys were transferred subsequently to 3.5cm plates, allowed to self, and their brood was examined for the presence or absence of *lin-60(ij48)*. Out of 100

F2 Dpys cloned, only 1 carried *lin-60(ij48)*. This demonstrated that *lin-60(ij48)* mapped approximately 2 map units from *dpy-5* (Figure 4.6). Although two-factor mapping is more important in calculating map distance from a marker allele, whereas multi-factor mapping is used generally to order genes, I decided to concentrate on multi-factor crosses. This decision was made due to the region of Chromosome I to which *lin-60* mapped, which had an abundant number of easily identifiable markers.

4.4.2. Multi-factor mapping of *lin-60(ij48)*

4.4.2.1. *lin-60(ij48)/unc-73(e936) dpy-5(e61)* and *lin-60(ij48)/dpy-5(e61) unc-87(e1216)*

To determine whether *lin-60* was positioned to the left or right of *dpy-5*, crosses were set up with two strains: CB2067 (*unc-73(e936) dpy-5(e61)*) and DR438 (*dpy-5(e61) unc-87(e1216)*) (Tables 4.10 and 4.11 and Figure 4.6). Strains were constructed with genotypes: *lin-60(ij48)/dpy-5(e61) unc-87(e1216)* and *lin-60(ij48)/unc-73(e936) dpy-5(e61)*. From broods carrying *lin-60* (parental genotype *lin-60(ij48)/dpy-5(e61) unc-87(e1216)* or *lin-60(ij48)/unc-73(e936) dpy-5(e61)*), Dpy-non-Unc and Unc-non-Dpy recombinant hermaphrodites were transferred to individual 3.5cm plates and allowed to self. The progeny of these hermaphrodites were scored for the presence or absence of *lin-60(ij48)*. These crosses demonstrated that *lin-60* mapped to the right of *dpy-5* and between *dpy-5* and *unc-87* and was placed approximately at position +0.7 on the genetic map.

Recombinant class	Recombinants carrying <i>lin-60(ij48)</i>	Recombinants not carrying <i>lin-60(ij48)</i>	Total number of recombinants
Dpy-non Unc	4	4	8
Unc-non-Dpy	3	5	8

Table 4.10 Multi-factor data for *dpy-5(e61) unc-87(e1216)/lin-60(ij48)*

Recombinant class	Recombinants carrying <i>lin-60(ij48)</i>	Recombinants not carrying <i>lin-60(ij48)</i>	Total number of recombinants
Dpy-non Unc	0	3	3
Unc-non-Dpy	3	0	3

Table 4.11 Multi-factor data for *unc-73(e936) dpy-5(e61)/lin-60(ij48)*

4.4.2.2. *lin-60(ij48)/dpy-5(e61) air-1(h289) unc-13(e450)*

As stated above, saturated lethal screens had been performed in the region of chromosome I where *lin-60* was positioned. These lethals were placed on both the physical and genetic maps, thus providing a tool for fine mapping of *lin-60*. Strains containing these lethals were obtained from the CGC, balanced by the free duplication *sDp2*. To remove the free duplication, the balanced strain was mated with wild-type males, and the F1 males were crossed back into N2. The outcrossed strains were checked for the correct segregation of phenotypes and removal of *sDp2*. Strains were constructed with the following genotypes: *lin-60/dpy-5(e61) let unc-13(e450)*, where the *let* gene is one of those stated in Table 4.12. The relative positions of these genes are shown in Figure 4.6.

Lethal	Map position
<i>air-1</i>	+0.46
<i>let-602</i>	+0.88
<i>let-607</i>	+1.24
<i>let-604</i>	+1.24
<i>let-382</i>	+1.24
<i>let-608</i>	+1.13

Table 4.12 Map positions of various lethal mutations used for mapping of *lin-60(ij48)*

From broods carrying *lin-60* (parental genotype *lin-60(ij48)/dpy-5(e61) let() unc-13(e1216)*), Dpy-non-Let-non-Unc and Unc-non-Let-non-Dpy recombinant hermaphrodites were picked out clonally and allowed to self. The progeny of these hermaphrodites were then scored for the presence or absence of *lin-60(ij48)*.

The strain *dpy-5(e61) air-1(h289) unc-13(e450)/lin-60(ij48)* was constructed and recombinants obtained (Table 4.13.). This data placed *lin-60* to the right of *air-1* with an approximate position of +0.96 (Figure 4.6).

Recombinant class	Recombinants carrying <i>lin-60(ij48)</i>	Recombinants not carrying <i>lin-60(ij48)</i>	Total number of recombinants
Dpy-non-Let-non-Unc	14	0	14
Unc-non-Let-non-Dpy	11	5	16

Table 4.13 Multifactor data for *dpy-5(e61) air-1(h289) unc-13(e450)/lin-60(ij48)*

4.4.2.3. *dpy-5(e61) let-607(h402) unc-13(e450)/lin-60(ij48)*

lin-60(ij48) had now been mapped to a small genetic interval: to the right of *air-1* and to the left of *unc-87*. The subsequent aim was to reduce this interval and thereby further refine the map position of *lin-60(ij48)*. *let-607* maps to the left of *unc-87*. The strain *lin-60(ij48)/dpy-5(e61) let-607(h402) unc-13(e450)* was constructed and recombinants obtained. The data generated from this cross is shown in Table 4.14. This cross placed *lin-60(ij48)* to the left of *let-607* with an approximate map position of +1.10 (Figure 4.6).

Recombinant class	Recombinants carrying <i>lin-60(ij48)</i>	Recombinants not carrying <i>lin-60(ij48)</i>	Total number of recombinants
Dpy-non-Let-non-Unc	24	3	27
Unc-non-Let-non-Dpy	3	0	3

Table 4.14 Multifactor data for *dpy-5(e61) let-607(h402) unc-13(e450)/(lin-60(ij48))*

4.4.2.4. *dpy-5(e61) let-602(h283) unc-13/lin-60(ij48)*

Multi-factor crosses with lethal mutations positioned from either side of *air-1* and *let-607* were performed. The strain *dpy-5(e61) let-602(h283) unc-13(e450)/lin-60(ij48)* was constructed and the recombinants obtained are tabulated below in Table 4.15. This data placed *lin-60* to the right of *let-602* with an approximate map position of +1.25 (Figure 4.6).

Recombinant class	Recombinants carrying <i>lin-60(ij48)</i>	Recombinants not carrying <i>lin-60(ij48)</i>	Total number of recombinants
Dpy-non-Let-non-Unc	33	0	33
Unc-non-Let-non-Dpy	9	4	13

Table 4.15 Multifactor data for *dpy-5(e61) let-602(h283) unc-13(e450)/lin-60(ij48)*

4.4.2.5. *dpy-5(e61) let-382(h82) unc-13(e450)/lin-60(ij48)*

At the time of mapping, apart from *let-602*, the only other cloned genes in this region were *let-601* and *let-606*. Several independent stocks of these strains were obtained from the CGC, however, when the free duplication was outcrossed, the animals failed to segregate the correct genotypes and therefore these genes were not used as markers. Strains containing the uncloned lethal genes, *let-382*, *let-604* and *let-608* were used for further multi-factor mapping. The genetic map position of these lethal mutants was well ordered. I decided that if I obtained good data with these uncloned mutants, I would position these genes relative to a cosmid on the genetic map. The multi-factor data obtained with *let-382* is shown in Table 4.16 below. This data placed *lin-60* to the left of *let-382* at approximately +1.20 (Figure 4.6).

Recombinant class	Recombinants carrying <i>lin-60(ij48)</i>	Recombinants not carrying <i>lin-60(ij48)</i>	Total number of recombinants
Dpy-non-Let-non-Unc	34	1	35
Unc-non-Let-non-Dpy	8	0	8

Table 4.16 Multifactor data for *dpy-5(e61) let-382(h82) unc-13(e450)/lin-60(ij48)*4.4.2.6. *dpy-5(e61) let-608(h706)unc-13(e450)/lin-60(ij48)*

The recombinants obtained from the strain *dpy-5(e61) let-608(h706) unc-13/lin-60(ij48)* are shown in Table 4.17 below. From this data I was unable to determine whether *lin-60* mapped to the left or right of *let-608*, thus it was concluded that *lin-60(ij48)* mapped very close to *let-608* (Figure 4.6).

Recombinant class	Recombinants carrying <i>lin-60(ij48)</i>	Recombinants not carrying <i>lin-60(ij48)</i>	Total number of recombinants
Dpy-non-Let-non-Unc	45	0	45
Unc-non-Let-non-Dpy	10	0	10

Table 4.17 Multifactor data for *dpy-5(e61) let-608(h706) unc-13(e450)/lin-60(ij48)*

4.4.2.7. *dpy-5(e61) let-604(h293) unc-13(e450)/lin-60(ij48)*

The data obtained from analysis of recombinants from the strain *dpy-5(e61) let-604(h293)unc-13(e450)/lin-60(ij48)* is shown in Table 4.18. From the recombinants obtained, I was unable to ascertain whether *lin-60* was placed to the left or right of *let-604*, thus it was concluded that *lin-60(ij48)* mapped very close to *let-604* (figure 4.6).

Recombinant class	Recombinants carrying <i>lin-60(ij48)</i>	Recombinants not carrying <i>lin-60(ij48)</i>	Total number of recombinants
Dpy-non-Let-non-Unc	36	0	36
Unc-non-Let-non-Dpy	21	0	21

Table 4.18 Multifactor data for *dpy-5(e61) let-604(h293) unc-13/lin-60(ij48)*

4.4.2.8. Conclusion of the genetic mapping of *lin-60(ij48)*

These crosses showed that *lin-60* mapped to the left of *let-607* and *let-382*, and to the right of *air-1* and *let-602*. *lin-60* mapped very close to *let-608* and *let-604*. A summary of the relative positions of *lin-60* using the genetic markers studied is shown in Table 4.19 and Figure 4.6.

During the fine mapping of *lin-60(ij48)*, I obtained recombination events very close to *lin-60*, and at either side. Since these recombinants displayed the Lin phenotype, I was confident that I could rule out anything but a very tightly linked mutation being responsible or acting co-operatively with the lesion in *ij48* to produce the intestinal hyperplasia.

Gene	Calculated genetic map position of <i>lin-60(ij48)</i>
<i>unc-87</i>	+0.7
<i>air-1</i>	+0.96
<i>let-602</i>	+1.25
<i>let-607</i>	+1.10
<i>let-604</i>	very close
<i>let-382</i>	+1.20
<i>let-608</i>	very close

Table 4.19 Approximate map positions of *lin-60(ij48)* calculated from multi-factor data

unc-73 dpy-5 air-1 let-602 let-608 let-604 let-382 let-607 unc-87



lin-60

Figure 4.6. Map position of *lin-60*(*ij48*). Genes in black have been cloned, genes in red have not been cloned. Using multi-factor data, *lin-60* was shown to map to the right of *air-1* and *let-602* and to the left of *let-607* and *let-382*. No recombination was obtained between *lin-60* and *let-608* and *let-604*, suggesting that *lin-60* mapped very close to these genes. Map is not to scale.

4.5. Characterisation of *lin-62(ij52)*

4.5.1. Gross phenotype and genetics of *lin-62(ij52)*

The gross phenotype of *lin-62(ij52)* is similar to that of *lin-60(ij48)* mutants, given that extra intestinal cells are present and the mutant is viable. However, the Lin phenotype of the *lin-62(ij52)* mutant is not 100% penetrant. Also, whereas additional intestinal nuclei were visible along the length *lin-60(ij48)* animals, the extra nuclei were generally confined to the anterior of the intestine in *lin-62(ij52)* animals. When observed with a standard bench stereomicroscope, many *lin-62(ij52)* mutants appear phenotypically wild-type. The intestine of *lin-62(ij52)* mutants appears to be fully functional as there is no indication of feeding defects: *lin-62(ij52)* mutants do not look starved and do not show a tendency to form dauer larvae under standard culture conditions. However they do grow slower than wild-type and in a culture containing homozygous wild-type, heterozygous *lin-62(ij52)* and homozygous *lin-62(ij52)*, it is clear that *lin-62(ij52)* homozygous mutants are out-competed by the other genotypes. There is no evidence of additional hypodermal cells as the *lin-62(ij52)* larvae and adults are of wild-type length. *lin-62(ij52)* mutants are not sterile and have approximately normal brood size.

However, unlike *lin-60(ij48)*, a small proportion of *lin-62(ij52)* embryos fail to hatch (Table 4.20). *lin-62(ij52)* males also display the Lin phenotype. However, homozygous *lin-62(ij52)* mutant males do not mate efficiently and I was unable to establish a male culture, indicating possible lineage defects in the male tail. Approximately 1% of *lin-62(ij52)* mutants have a swollen posterior (Figure 4.7). Additional lineage defects may therefore be present.

Brood	Number of dead embryos	Number of progeny analysed	% death
1	3	42	7.1
2	11	88	12.5
3	4	53	7.5
4	11	76	14.5
5	7	51	13.7
6	4	76	5.3
7	7	83	8.4
8	0	68	0
9	10	75	13.3
10	3	18	16.7
11	5	120	4.2
12	11	90	12.2
13	9	119	7.6
14	16	76	21.1
15	3	44	6.8
16	2	61	3.2
17	9	95	9.5
18	3	130	2.3
Average			9.2

Table 4.20 % death of F1 progeny of homozygotic *lin-62(ij52)* hermaphrodites

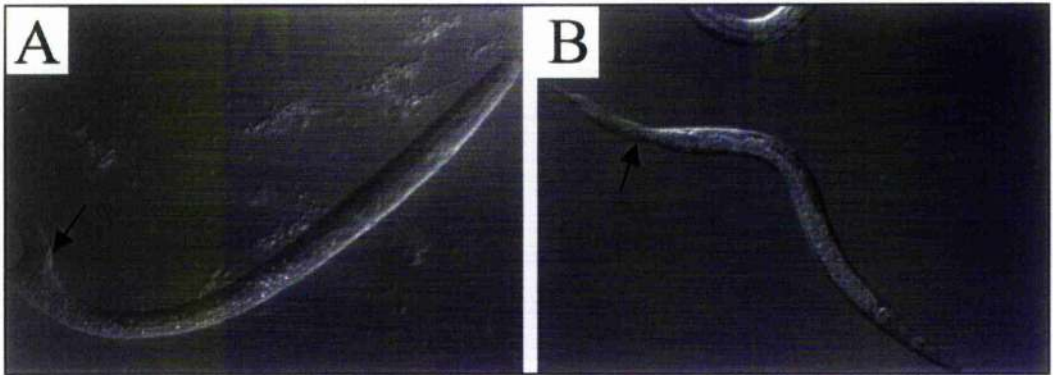


Figure 4.7 Tails of *lin-62(ij52)*. (A) is a young larva with a “stump”(black arrow) at posterior. (B) is an L4 larva whose tail constricts (black arrow) then elongates. This suggests that in addition to E, other lineages may be affected in the *ij52* allele of *lin-62*.

lin-62(ij52) exhibits very different genetics from *lin-60(ij48)*. The *ij52* allele is zygotic and recessive to wild-type based on the following: when *ij52* homozygotes are mated with wild-type males, 100% of the outcrossed progeny are wild-type. When *+/ij52* hermaphrodites are selfed, the F1 progeny are of three potential genotypes, *ij52/ij52* homozygotes, *ij52/+* heterozygotes and *+/+* homozygotes, expected at standard Mendelian frequencies of 1:2:1. From 5 broods analysed, the proportion of F1 progeny displaying mutant phenotype (presumably *ij52/ij52* homozygotes) varied from 7.6 to 23.9% (Table 4.21). The average was 15%. Although this value is lower than the 25% expected, the penetrance of the *lin-62(ij52)* phenotype is less than 100%. When *lin-62(ij52)* is placed over a deficiency, the phenotype of the hemizygote is Lin (or lethal), suggesting that *ij52* is a loss of function allele (see below). When analysing broods from crosses, *lin-62(ij52)* was crossed into the strain IA109(*ijIs10*) to aid visualisation of the nuclei of the intestinal cells.

Brood	Number of F1 progeny Lin	Number of F1 progeny analysed	% progeny Lin
1	7	63	7.6
2	4	25	16
3	5	37	13.5
4	11	46	23.9
5	5	36	13.9
Average			15

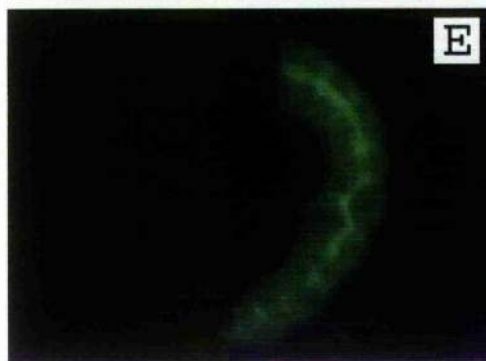
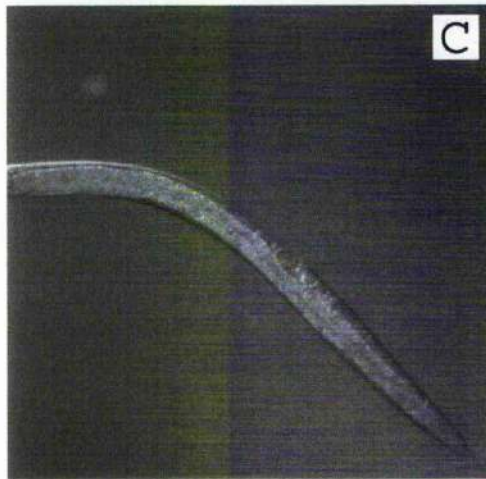
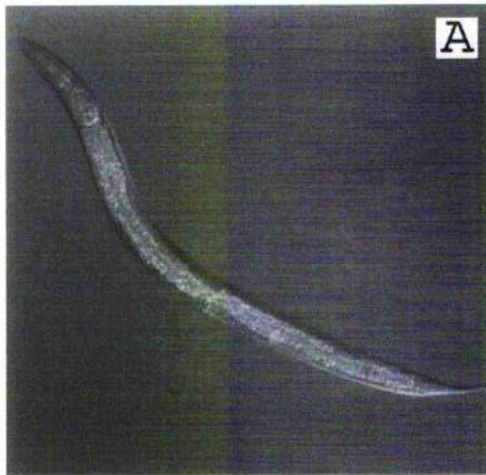
Table 4.21 Analysis of distribution of phenotypes from *+/lin-62(ij52)* heterozygotes

4.5.2. Characterisation of *lin-62(ij52)* using intestinal terminal differentiation markers

Initial phenotypic characterisation of *lin-62(ij52)* was carried out using the strain IA109, containing the *ijIs10* insertional allele (*cpr-5::GFP*). *ij52* larvae and adults have additional nuclei expressing the *cpr-5::GFP* transgene compared to wild-type (Figure 4.8 A-D). As the spatial pattern in intestinal nuclei was similar to *lin-60(ij48)* (and different from that of the multinuclei-cell class), I investigated whether extra intestinal cells were generated in the *lin-62(ij52)* mutant during embryogenesis.

Figure 4.8
Characterisation of *lin-62(ij52)*

Figure 4.8 Characterisation of *lin-62(ij52)*. Intestinal cells in wild type and *lin-62(ij52)*. (A) and (C) are Nomarski images with respective GFP fluorescence counterparts (B) and (D). GFP is localised to the nuclei of cells, in which it is expressed by a nuclear localisation signal. Expression of a *cpr-5::GFP* transgene in adults in wild type (A) and (B) and *lin-62(ij52)* (C) and (D) indicates that additional intestinal nuclei are present in the mutant. The number of nuclei expressing this marker in the *lin-60(ij48)* strain is typically 50% greater than wild type. Immunofluorescence with the ICB4 antibody, which marks the surfaces of the intestine, is shown here for embryos at the 2-fold stage of development: wild type (E) and *lin-62(ij52)* (F). There are many more intestinal cells in *lin-62(ij52)* by comparison to wild type indicating that the extra cells are born during embryogenesis and participate in the formation of an intestine.



4.5.3. Characterisation of *lin-62(ij52)* with ICB4

The ICB4 antibody recognises a mixed variety of cells including the intestine, sperm, IL2 neuron, CEM cells, pharyngeal gland, valve and sensory processes in the male tail (Okamoto and Thomson, 1985; Bowerman *et al.*, 1992). Staining in the intestinal cell surfaces can be observed in mid-stage embryos. ICB4 was used to estimate the number of intestinal cells generated during embryogenesis. *lin-62(ij52)* embryos have upwards of 25 intestinal cells (Figure 4.8, E and F). Moreover, the pattern of ICB4 staining illustrated that these extra cells appear to participate in the formation of an intestine.

4.5.4. E-Cell lineage of *lin-62(ij52)*

To assess whether these extra cells were generated from E or were the result of a transformation of cell fate from another lineage, E-cell lineage analysis was performed on *lin-62(ij52)*. Due to a time limit factor, only one *lin-62(ij52)* embryo was lineaged. However, it was apparent that extra cells were generated from E and 24 E-cells were generated in the studied embryo. The E-lineage appears to be wild-type until the 16E-cell stage (Figure 4.9). Thereafter there are various differences: some cells that do not divide in wild-type, divide in *lin-62(ij52)* and conversely, one cell that would divide in the wild-type, did not divide in *lin-62(ij52)* embryo observed. This pattern of divisions may contribute to the observation that the phenotype of *lin-62(ij52)* is most severe in the anterior of the intestine; many of the extra cells are generated from divisions of cells, which are positioned in the anterior of the intestine. It is clear that *lin-62(ij52)* has additional intestinal cells but it is unknown whether the E-cell lineage varies between different animals. Additional divisions in E may have occurred later, but could not be detected with the Biocell software

4.5.5. Germline of *lin-62(ij52)*

lin-62(ij52) hermaphrodites were examined for evidence of a tumorous germline (Figure 4.10). The germline cells exit proliferative mitosis appropriately and proceed through meiosis, indicating that they are responsive to the anti-proliferative functions of the *gld* genes (Francis *et al.*, 1995; Kadyk and Kimble, 1998). Thus there is no evidence for any proliferative defect in the germline.

Figure 4.9
E-cell lineage of *lin-62(ij52)*

Figure 4.9 E-cell lineage of *lin-62(ij52)*. This is the raw data for one lineaged *lin-62(ij52)* embryo. (A, right) is a Nomarski image of the lineaged *lin-62(ij52)* embryo. The green dots represent the positions of the intestinal cell nuclei. (B) is the 3-dimensional representation of the intestine. The red “spheres” represent E-cells born and terminating with a wild type lineage; grey “spheres” represent cells derived from a mutant lineage. (C) is the lineage tree; the red dots were used as an aid to trace the cells in the Biocell programme, the green dots represent a cell division or the end of the recording. Twenty-four E-derived cells were generated in this embryo, the wild type number is 20. The green crosses represent the cells that would divide in wild type at 16E-stage.

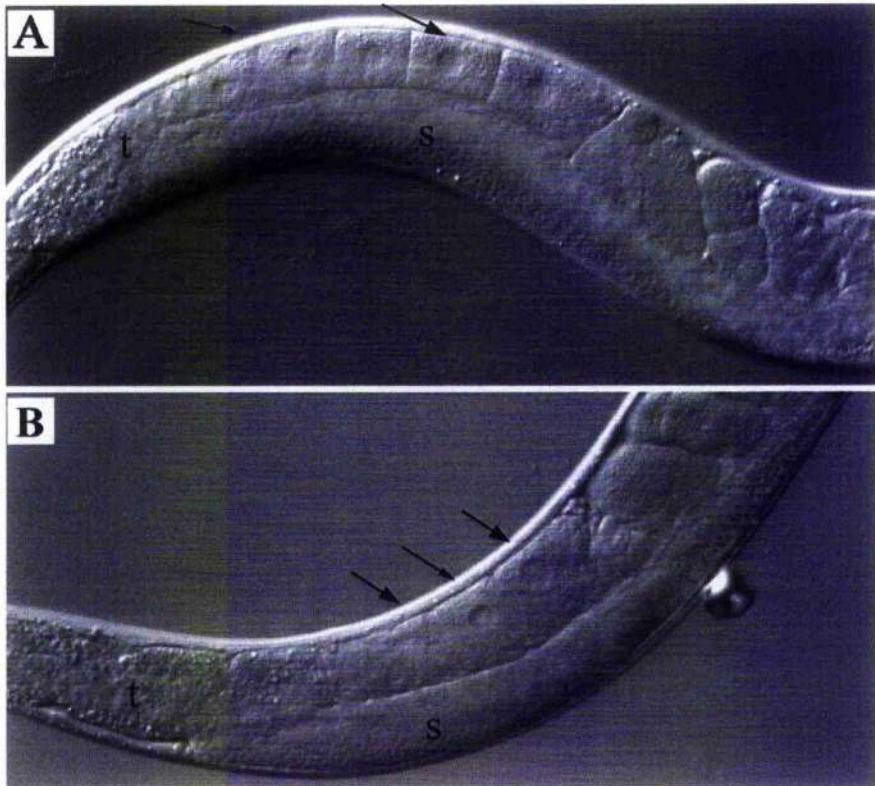


Figure 4.10 *lin-62(ij52)* gonads. (A) is wild type and (B) is *lin-62(ij52)*. Some developing oocytes are marked with black arrows. The syncytial arm of the gonad is labelled 's'; this region contains several hundred germline nuclei in both wild type and mutant. The turn of the gonad is marked 't'. These images demonstrate that *lin-62(ij52)* mutants do not display excessive germline proliferation

4.6. STS mapping of *lin-62(ij52)*

lin-62(ij52) was placed onto chromosome IV by STS mapping (Chapter 3). These initial crosses showed that the *ij52* allele is recessive to wild-type and thus STS mapping was also used for fine mapping of *lin-62(ij52)* (Figure 4.11 and 4.12). From the analysis of 17 recombinants from 81 PCR reactions, *lin-62* was found to be very tightly linked to the polymorphism *stP44*. This data however did not distinguish whether *lin-62* lay to the left or right of *stP44*. To further map *lin-62*, classical genetics and deficiency mapping were used. A genetic map of the region is shown in Figure 4.13 (p130).

4.7. Three-factor mapping of *lin-62(ij52)*

Few cloned genes with easily scored phenotypes were present in this region of chromosome IV. The most useful marker was *bli-6*. Although this gene was not cloned, its map position was well defined at position +3.18. To determine whether *lin-62* lay to the left or right of *bli-6*, two crosses were set up with strains carrying *unc* markers to the left or right of *bli-6*: The strains *lin-62(ij52)/unc-5(e53) bli-6(sc16)* and *lin-62(ij52)/bli-6(sc16) unc-24(e138)* were constructed.

4.7.1. *lin-62(ij52)/unc-5(e53) bli-6(sc16)*

Using the strain *lin-62(ij52)/unc-5(e53) bli-6(sc16)*, Unc-non-Bli and Bli-non-Unc recombinants were selected and scored for the presence or absence of *lin-62(ij52)* (Table 4.23). From this data I concluded that *lin-62* mapped very close, to or to the right of *bli-6*.

Recombinant class	Recombinants carrying <i>lin-62(ij52)</i>	Recombinants not carrying <i>lin-62(ij52)</i>	Total number of recombinants
Bli-non- Unc	0	19	19
Unc-non-Bli	5	0	5

Table 4.23 Three-factor data for *lin-62(ij52)/unc-5(e53) bli-6(sc16)*

4.7.2. *lin-62(ij52)/bli-6(sc16) unc-24(e138)*

Using the strain *lin-62(ij52)/bli-6(sc16) unc-24(e138)*, Unc-non-Bli and Bli-non-Unc recombinants were selected and scored for the presence or absence of *lin-62(ij52)* (Table 4.24). From this data it was concluded that *lin-62* mapped between *bli-6* and *unc-24*, approximately in the middle. *bli-6* maps to position +3.18 and *unc-24* maps to position +3.55. I did not focus on obtaining many recombinants as such a small map distance

STS mapping of *lin-62(ij52)*

Figure 4.11 Representative gel of STS mapping of *lin-62(ij52)*. Lane (1) is 50bp ladder (arrow points to 350bp), lane (2) is N2 negative control and lane (3) is RW7000 control, showing the bands corresponding to STS markers *stP51*, *stP5*, *stP13*, *stP44*, *sP4* and *stP35*, positioned along chromosome IV. All other lanes are PCR reactions, each performed with DNA from an individual F2 *lin-62(ij52)* homozygotes produced by self-fertilisation of a Bristol/Bergerac hybrid. A total of 81 *lin-62(ij52)* homozygotes were tested. (A), (B), (C), (D) and (E) represent recombination events illustrated in Figure 4.12. The remaining mutants tested negative for all chromosome IV STSs.

Figure 4.12 Proposed recombination events between *lin-62(ij52)* and RW7000. Top line is the Bergerac chromosome and the bottom line is the Bristol chromosome. (A), (B), (C), (D) and (E) represent the recombination events between the Bristol and Bergerac chromosomes of the F1 hybrids. The total number of recombinants from each class is shown in Table 4.21. This data places *lin-62(ij52)* to the right of *stP51* and to the left of *stP5*, and very close to *stP44*.

Table 4.22 Tabulated data of recombination events between *lin-62(ij52)* and RW7000.

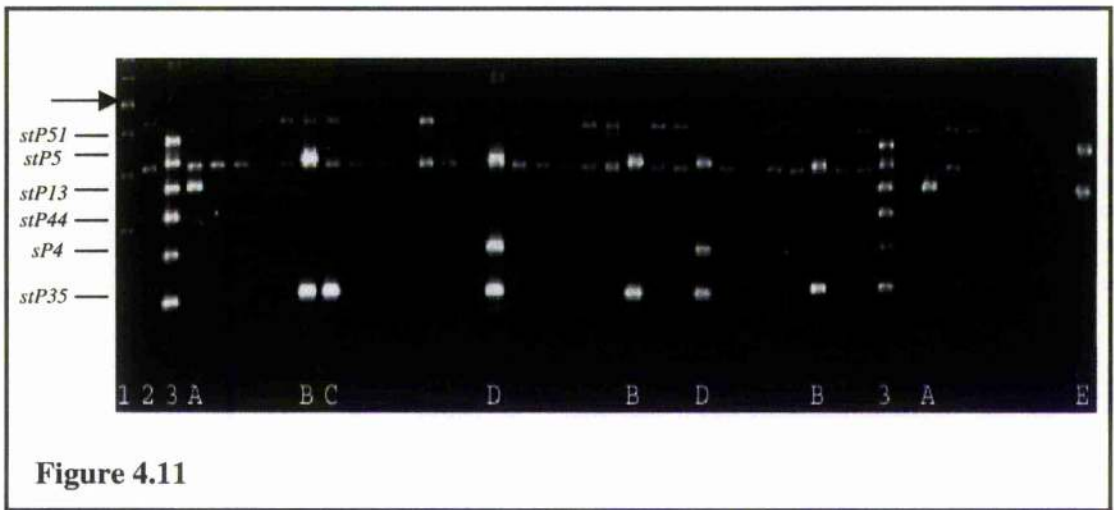


Figure 4.11

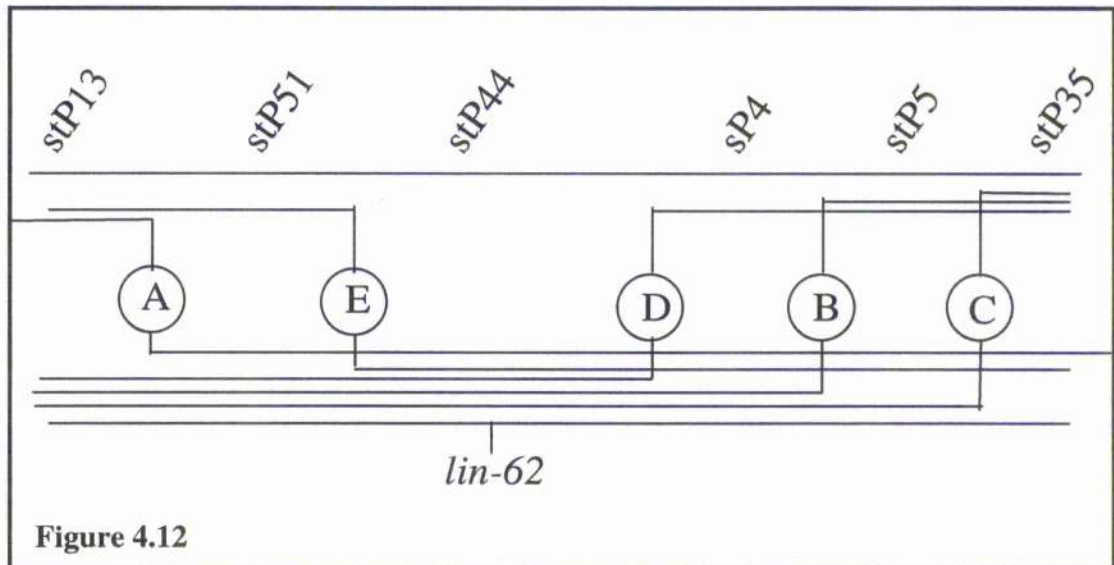


Figure 4.12

Recombinant class	Total Number of Recombinants (/81)
A	5
E	2
D	3
B	6
C	1

Table 4.22

separated *bli-6* and *unc-24*. My data, however, placed *lin-62* to approximately position +3.37. This was in agreement with the STS mapping data, which placed *lin-62* at position +3.29. Since recombination was achieved from both sides of *lin-62*, it seemed likely that only one mutant gene was responsible for the Lin phenotype observed, or if a second mutation was involved, it must be very tightly linked to the *ij52* lesion.

Recombinant class	Recombinants carrying <i>lin-62(ij52)</i>	Recombinants not carrying <i>lin-62(ij52)</i>	Total number of recombinants
Bli-non- Unc	2	2	4
Unc-non-Bli	1	2	3

Table 4.24 Three-factor data for *lin-62(ij52)/bli-6(sc16) unc-24(e138)*

4.8. Characterisation of *lin-62(ij52)/Df*

To further characterise and map the *ij52* allele, it was placed over deficiencies predicted to cover this region of the genetic map. These crosses were set up in such a way as to enable identification of outcrossed F1 animals and determine whether they were covered by the test deficiency without the requirement of the analysis of the outcrossed F1 broods. To do this, hermaphrodites bearing the deficiency, and cultured until exhausted for sperm, were mated with *lin-62* /+ males.

To set up the cross, *lin-62(ij52)* in an *ijIs10(cpr-5::GFP)* background, was crossed with wild-type N2 males. The F1 males, genotype *lin-62(ij52)/+ ijIs10/+*, were crossed with hermaphrodites carrying the deficiencies *stDf7*, *stDf8*, *eDf18* or *eDf19*. Only outcrossed worms can carry *ijIs10*, thus it was possible to differentiate between selfed and outcrossed progeny. If *ij52* was a loss-of-function allele and covered by a deficiency, approximately 25% of the outcrossed F1 brood, genotype *lin-62(ij52)/Df*, would display the mutant phenotype. If *ij52* was a partial-loss-of-function allele, it was possible that this class of progeny would display a more severe phenotype than *lin-62(ij52)*. If *lin-62(ij52)* was not covered by the test deficiency, all F1 progeny would be wild-type. The genotype of each F1 was determined by examining its progeny.

The only problem with these crosses was that only 50% of F1 progeny contained the GFP transgene (as the mating males were heterozygous for GFP). Moreover, although GFP is dominant, it was often difficult to determine the phenotype of the heterozygotes, as the GFP fluorescence is substantially lower than in homozygotes. In addition, 50% of the outcrossed progeny contained the wild-type allele from the *lin-62(ij52)/+* males.

Therefore, only one-quarter of F1 progeny from a mated hermaphrodite were suitable for scoring.

4.8.1. *lin-62(ij52)/stDf7*

stDf7 is a small deficiency covering the region +2.48 to +3.40 in chromosome IV. *lin-62(ij52)/+* males were mated into the strain RW1324, genotype *fem-1(e1991) unc-24(e138) unc-22(s12)/stDf7*. Outcrossed GFP positive progeny were expected to have genotypes *+/fem-1(e1991) unc-24(e138) unc-22(s12)*, *lin-62(ij52)/fem-1(e1991) unc-24(e138) unc-22(s12)*, *+/stDf7* or *lin-62(ij52)/stDf7* in the ratios 1:1:1:1. On analysis of F1 progeny of the cross described above, one outcrossed worm displayed the *lin-62(ij52)* mutant phenotype, suggesting that its genotype was *lin-62(ij52)/stDf7* and that *lin-62(ij52)* was covered by this deficiency. The outcome of the cross is tabulated in Table 4.25. In addition to the Lin F1, a small proportion of larvae arrested during development. It was not possible to ascertain whether these larvae were Lin or wild-type. However the gut did not appear normal in these larvae. This suggests that *ij52* may not be a true null allele.

The phenotypes generated in the F2 generation were examined to determine the genotype of each F1. From the *lin-62(ij52)/stDf7* strain obtained, greater than 25% F2s arrest as embryos or larvae, indicating heterozygotic death. All heterozygotes displayed the Lin phenotype.

Genotype of outcrossed F1	Number of outcrossed F1s	Phenotype of outcrossed F1
<i>lin-62(ij52)/fem-1(e1991) unc-24(e138) unc-22(s12)</i>	3	wild-type
<i>lin-62(ij52)/stDf7</i>	1	Lin
<i>+/fem-1(e1991) unc-24(e138) unc-22(s12)</i>	6	wild-type
<i>+/stDf7</i>	0	-

Table 4.25 Analysis of progeny from *lin-62(ij52)* X RW1324

4.8.2. *lin-62(ij52)/stDf8*

The deficiency *stDf8* overlaps with *stDf7* and has been assigned to cover the region +2.48 to +3.39. Like *stDf7*, the physical breakpoints of this deficiency have not been determined. The following cross was set up: *lin-62* ⁺ males were mated into the strain RW1333, genotype *fem-1(e1991) unc-24(e138) unc-22(s12)/stDf8*. Similar to the results obtained with *stDf7*, 4 F1 progeny with Lin phenotype were obtained, suggesting that *lin-62* is covered by the deficiency *stDf8* (Table 4.26). As with *stDf7*, in addition to Lin F1s, a small proportion of larvae arrested during development. Again, it was not possible to ascertain whether these larvae were Lin or wild-type. However, the gut did not appear normal in these larvae. This again suggested that *ij52* may not be a null allele.

The phenotypes generated in the F2 generation were examined to determine the genotype of each F1. From each F1 of genotype *lin-62(ij52)/stDf8*, greater than 25% F2s arrested as embryos or larvae indicating heterozygotic death. All heterozygotes displayed the Lin phenotype.

Genotype of outcrossed F1	Number of outcrossed F1s	Phenotype of outcrossed F1
<i>lin-62/fem-1(e1991)unc-24(e138)unc-22(s12)</i>	9	wild-type
<i>lin-62/stDf8</i>	4	Lin
<i>+fem-1(e1991)unc-24(e138)unc-22(s12)</i>	11	wild-type
<i>+/stDf8</i>	7	wild-type

Table 4.26 Analysis of progeny from *lin-62(ij52)* X RW1333

4.8.3. *lin-62(ij52)/eDf18*

The deficiency *eDf18* deletes the region from +3.63 to +4.25. *lin-62(ij52)/+* males were mated with deficiency-bearing hermaphrodites from the strain CB3823, genotype *unc24(e138) dpy20(e1282)/eDf18*. The progeny from each F1 was examined to determine its genotype. *lin-62(ij52)/eDf18* animals were phenotypically wild-type (Table 4.27) suggesting that *lin-62(ij52)* is not covered by *eDf18*.

Genotype of outcrossed F1	Number of outcrossed F1s	Phenotype of outcrossed F1
<i>lin-62 /unc-24(e138)dpy-20(e1282)</i>	3	wild-type
<i>lin-62 /eDf18</i>	2	wild-type
<i>+ /unc-24(e138)dpy-20(e1282)</i>	3	wild-type
<i>+ /eDf18</i>	1	wild-type

Table 4.27 Analysis of progeny from *lin-62(ij52)* X CB38234.8.4. *lin-62(ij52)/eDf19*

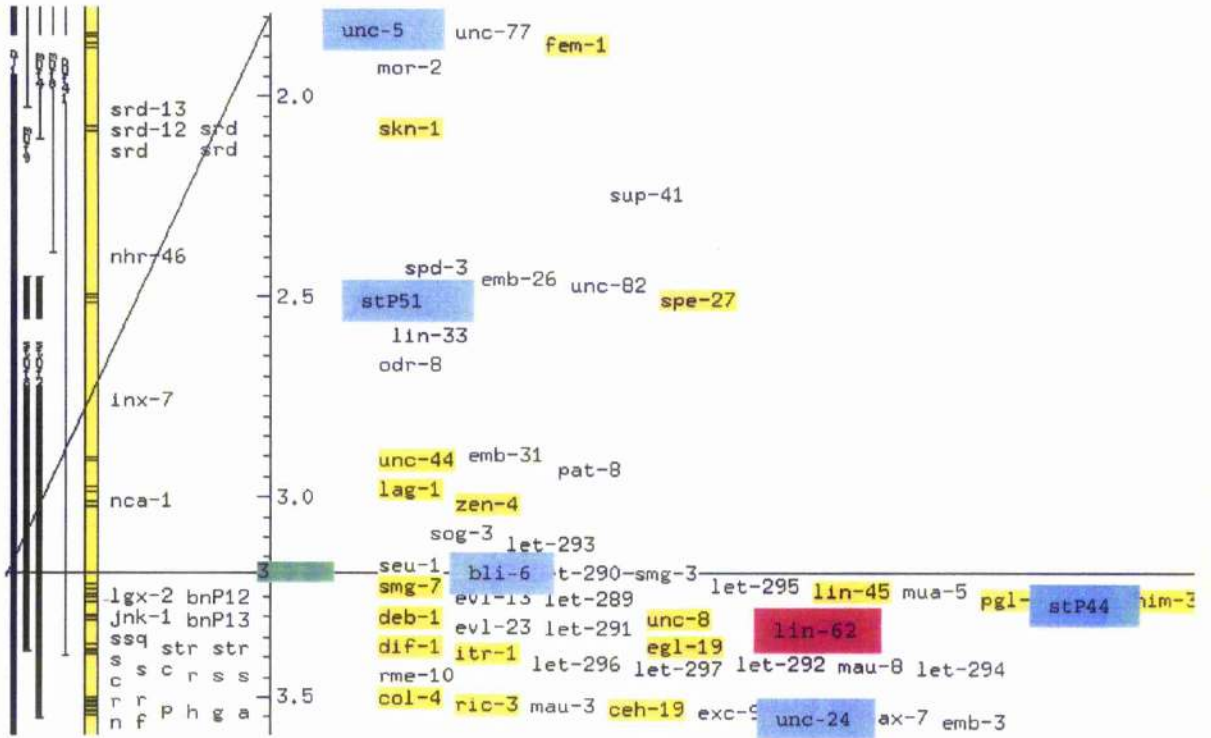
The deficiency *eDf19* overlaps with *eDf18* and deletes the region +3.6 to +4.6. Males of genotype *lin-62/+* were mated with deficiency-bearing hermaphrodites of the strain CB3824, genotype *unc-24(e138)dpy-20(e1282)/eDf19*. The progeny from each F1 was examined to determine its genotype. As with the deficiency *eDf18*, *lin-62(ij52)/eDf19* is phenotypically wild type, suggesting that *lin-62(ij52)* is not covered by *eDf19* (Table 4.28).

Genotype of outcrossed F1	Number of outcrossed F1s	Phenotype of outcrossed F1
<i>lin-62 /unc-24(e138)dpy-20(e1282)</i>	0	-
<i>lin-62 /eDf19</i>	2	wild-type
<i>+ /unc-24(e138)dpy-20(e1282)</i>	3	wild-type
<i>+ /eDf19</i>	2	wild-type

Table 4.28 Analysis of progeny from *lin-62(ij52)* X CB38244.8.5. Conclusion on the genetics of *lin-62(ij52)*

In contrast with *lin-60(ij48)*, the genetic data for *lin-62(ij52)* suggests that the *ij52* allele is recessive to wild-type and *lin-62* is a zygotic gene. It maps to position +3.3 on chromosome IV, between *bli-6* and *unc-24* (Figure 4.13). It is covered by the deficiencies

stDf7 and *stDf8*, but not *eDf18* and *eDf19*. Animals of genotype *lin-62(ij52)/stDf7* and *lin-62(ij52)/stDf8* genotype display the Lin-62 phenotype or arrest as embryos or larvae. This suggests that *ij52* is not a null allele.



4.9. Discussion

In this chapter I have characterised two mutants, *lin-60(ij48)* and *lin-62(ij52)* which both have an increased number of intestinal cells. Certainly with the case of *lin-60(ij48)*, the defect appears to be specific to the E-cell lineage whereas the mutation in *lin-62* identified by *ij52*, may also disrupt other lineages.

The map positions of *lin-60(ij48)* and *lin-62(ij52)* have been refined. *lin-60(ij48)* maps to chromosome I, between *let-602* and *let-607*. This interval spans approximately 17 cosmids. *lin-62(ij52)* maps to chromosome IV, between *bli-6* and *unc-24*, which is a region spanning approximately 40 cosmids. Therefore, *ij48* and *ij52* identify two independent genes. However, what is interesting is that in E-cell development, loss of one gene appears to give the same phenotype as gain of the other. Moreover, *lin-60* identifies a maternal gene whereas *lin-62* identifies a zygotic gene. An area of future interest will therefore be to ascertain whether both these genes function in the same developmental pathway, and analyse the phenotype of the double mutant. The cloning of *lin-60(ij48)* is described in Chapter 5. Since *lin-62(ij52)* is a zygotic loss-of-function allele, the cloning of this gene should be relatively straightforward and is an area of future interest.

The cell lineage pattern of *lin-60(ij48)* is consistent with a hyperplasia of the intestine. Mutants have been identified that cause hyperplasia of all post-embryonic blast cells, for example *cul-1* (Kipreos *et al.*, 1996). Loss of another gene, *cki-1*, results in extra cell divisions in numerous lineages causing abnormalities in the organogenesis of the vulva, the somatic gonad and the hypodermis (Hlong *et al.*, 1998). However, these other mutations are not tissue specific and to date, the mutation identified by *ij48* is the only hyperplasia associated exclusively with the intestine.

The process of morphogenesis of the *C. elegans* intestine has previously been well described (Leung *et al.*, 1999). I have not determined how similar the actual process of morphogenesis of the intestines in *lin-60(ij48)* or *lin-62(ij52)* mutants are to wild-type, although clearly, this may be an area of future interest. The apparent healthy nature of these animals indicates that their intestines are functional. Many of the extra cells generated are incorporated into the intestine, as judged by the complex boundaries shown with immunofluorescence studies with MH27 [*lin-60(ij48)*] and ICB4 [*lin-62(ij52)*]. This is significant with respect to tissue morphogenesis in *C. elegans*. Although the morphogenesis process has evolved in the nematode to assemble tissues and organs from an effectively invariant cell lineage, and hence invariant number of cells, I have shown that it has the flexibility to deal successfully with many extra cells, at least as far as

morphogenesis of the intestine is concerned. In wild-type *C. elegans*, some embryos hatch with 21E-derived cells (Sulston *et al.*, 1983). The intestine may therefore be a tissue that can accommodate a varying number of cells: using *elt-2::GFP* and by lineage analysis, between 23 and 45 intestinal cells were counted as being produced during embryogenesis in the *lin-60(ij48)* mutant.

One interesting observation is that in all *lin-60(ij48)* and *lin-62(ij52)* embryos lineage, they all proceeded to the 16E stage with the correct pattern of divisions (although 16E cells were born in *lin-60* more rapidly than in wild-type). In wild-type at 16E, certain morphogenic movements occur in the intestine: the intestinal cells intercalate and the intestinal twist is initiated (Leung *et al.*, 1999). Therefore, it may be that a class of mutant where 16E-cells are not generated at approximately the same time would not be viable.

The mutant screen performed (Chapter 3) uncovered mutants that generated extra cells derived from the F blastomere. The screen however failed to identify a mutant with a polarity defect in E, such as equivalence of all E-derived cells at the 8E stage (and thus all cells at the 16E-cell stage would divide generating precisely 32 intestinal cells). The basis for the difference in lineage behaviour among the intestinal cells has not been elucidated. It is not known whether the characteristic division patterns of each intestinal cell are due to intrinsic differences between the gut cells or whether it results from intercellular signalling. This lack of data contrasts with the specification of E where the early embryo is known to contain asymmetrically localised, maternally provided factors that promote or, prevent the intestinal cell fate (Wood W.B., 1988; Bowerman, 1998; Labouesse and Mango, 1999). Further cell specification occurs through the Wnt-signalling pathway (Lin *et al.*, 1995; Thorpe *et al.*, 1997; Rocheleau *et al.*, 1997) and MAPK-kinase cascade (Rocheleau *et al.*, 1999). In response to these early events, the E blastomere expresses zygotic genes such as the GATA-like transcription factors *end-1* and *elt-2* that promote intestinal differentiation (Zhu *et al.*, 1997; Fukushige *et al.*, 1998; Newman-Smith and Rothman, 1998). In *lin-60 (ij48)* and *lin-62(ij52)* mutants, the extra cells generated behave as terminally differentiated intestinal cells.

The questions whether the *lin-60(ij48)* or *lin-62(ij52)* defects of the E-cell lineage act in a cell autonomous manner, or whether signals from surrounding blastomeres are required, have not been addressed. Laser ablating all blastomeres apart from F following the division of EMS, and allowing E to develop would investigate this. If signalling from other blastomeres is required, the wild-type number of cells might be generated. If signalling from other blastomeres is not required, the number of E-derived cells in the

cultured E blastomeres may be the same as the amount of E-derived cells from *lin-60(ij48)* and *lin-62(ij52)* animals, or at least greater than wild-type cultured E. Conversely, it would be interesting to investigate whether any gut cells are derived from other lineages. Although lineage analysis of *lin-60(ij48)* and *lin-62(ij52)* has demonstrated that the number of cells that are generated from E are sufficient to explain the number of intestinal cells counted using terminally differentiated markers, it does not rule out the possibility that some intestinal cells are derived from other lineages. This would be an important experiment to perform with *lin-60(ij48)*, where E divides at a faster pace than wild-type, as it has been postulated that abnormal cell division timing can cause cell fate transformations during vulval development (Ambros 1999).

Although the results reported here indicate that extra cells are generated from the E blastomere, I have not tested whether once a cell is specified as E, it would be susceptible to the *ij48* and *ij52* mutations and conversely, if E was specified as another blastomere, whether it would no longer be susceptible to *ij48* and *ij52*. Crossing *ij48* and *ij52* alleles, into *mom-2* (E transformed to MS) or *pop-1* (MS transformed to E) mutant backgrounds would investigate these possibilities.

One candidate for a factor that may be involved in generating the asymmetric patterns of divisions in the E-cell lineage is POP-1. Immunostaining with POP-1 antibody revealed that it is present in many cells throughout development (Lin *et al.*, 1995; Lin *et al.*, 1998b). In many sister cells arising from cell division along the anterior-posterior axis, POP-1 immunostaining is detectable at higher levels in the anterior compared with posterior nuclei (Lin *et al.*, 1998a). Immunostaining of POP-1 is asymmetrically distributed between the anterior posterior sisters at the 8E and 16E cell stage (Lin *et al.*, 1998b). It may therefore be postulated that a class of mutation in POP-1 could be obtained that would render the daughters of the cells at 8E to divide symmetrically, generating 32 cells. Most work to date studying POP-1 function has been concerned with the role of POP-1 in EMS polarity. However, roles for zygotic POP-1 have recently been discovered. For example, POP-1 is distributed asymmetrically to the descendants of the precursors of the somatic gonad, Z1 and Z4 and mutations in *pop-1* have been identified that render the Z1/Z4 divisions symmetrical (Siegfried and Kimble, 2002).

POP-1 belongs to the TCF/LEF-1 family of transcription factors, which are controlled by Wnt signalling (Wodarz and Nusse, 1998). Components of the Wnt-signalling pathway, when mutated, have been shown to reverse or obliterate the polarities of asymmetric cell divisions in both embryonic and post-embryonic development in many

tissues. This pathway may therefore be involved in generating the asymmetry in the E-lineage. Different constituents of Wnt signalling may function in different tissues to either facilitate or antagonise POP-1 activity. During embryonic development, Wnt signalling has been implicated in establishing the polarity of EMS (refer to introduction). During post-embryonic development, Wnt signalling has been implicated in controlling polarity in many cell types including T-blast cells (Herman, 2001) and Pn.p cells (Sawa *et al.*, 1996; Sternberg and Horvitz, 1988). Wnt signalling also controls the cell polarities in the tail of developing *C. elegans* larvae. Mutations in the Wnt gene *lin-44* cause the polarities of certain cells that divide asymmetrically in the tail of the animal, the B, TL and TR cells, to be reversed. Mutations in the putative receptor for *lin-44*, *lin-17* also displays a phenotype reminiscent of a polarity defect; the affected cell divisions are asymmetric in wild-type but symmetric in *lin-17* animals, producing sister cells with similar fates.

In characterising *ij48*, an interesting phenomenon was discovered; *lin-60(ij48)* behaves differently when hemizygous over two separate deficiencies. The basis for this difference is not simple: the Lin phenotype produced by the *ij48* lesion is suppressed to a greater extent over the small deficiency *hDf8*, than over the large deficiency, *qDf16*. This rules out the possibility of other genes removed by the large deficiency acting in cooperation to give rise to increased suppression. As stated in Section 4.3.3, strains carrying the *hDf8* are sicker than those bearing the *qDf16* deficiency, possibly indicative of extraneous rearrangements. This may be the cause of the heightened suppression. However, the left breakpoint of *hDf8* was mapped and the gene identified by *ij48* cloned (Chapter 5). These were found to be separated by only 3 cosmids. The effect of the chromosome structure when the end points of deficiencies are fused is not known; it may generate regions of heterochromatic DNA, which exists as euchromatic DNA in wild-type chromosomes. This is a possible explanation for the exaggerated suppression over *hDf8*, as the levels of gene expression from the *ij48* chromosome may be reduced. This phenomenon of position-effect variegation (PEV) is an epigenetic phenomenon associated with heterochromatic regions of the genome. It is generally used to describe transcriptional silencing in *cis*, following chromosomal rearrangements, with one breakpoint within heterochromatin (Grewal and Elgin, 2002). However, there is an example in *Drosophila* where variegated inactivation of the wild-type copy of the gene occurs in the homologous chromosome. This 'trans-inactivation' is induced by a dominant mutation of the brown allele (*bw^D*), which is a null mutation caused by an insertion of a large block of heterochromatin into the coding sequence of the gene (Slatis, 1955). The dominance of this

allele is dependent on the pairing between the bw^D chromosome and the wild-type homologue, where the inserted heterochromatin in mutant bw , drags the wild-type copy to an abnormal nuclear position, where transcription is repressed (Henikoff, 1996). However, the strength of trans-repression by the bw^D allele is strongly influenced by its chromosomal position; its effect can be suppressed by chromosomal rearrangements that move the region containing bw^D to a position more distant from centric heterochromatin (Talbert *et al.*, 1994) whereas translocation to a more centromere-proximal position strengthens its silencing ability (Henikoff *et al.*, 1995).

To summarise, two mutant alleles generating an intestinal lineage defect have been characterised. The remainder of this thesis concentrates on the efforts to clone the gene identified by the allele *ij48*.

Chapter 5.

The cloning of *lin-60(ij48)*

5.1. Introduction

The *C. elegans* physical map consists of overlapping bacterial cosmid clones and yeast artificial chromosomes (YACs). The classical method of cloning loss-of-function alleles is to inject cosmids or YACs surrounding the area to which a mutant allele maps, and in effect rescue the mutant phenotype. Once a cosmid capable of rescue is identified, using information available from ACeDB, each predicted gene can be subcloned from the cosmid/YAC and tested for rescue. Due to the completion of the genome project, the sequence of the wild-type copy of the gene is available. Sequencing the putative mutant allele and identifying a mutation provides confirmation that the fragment generating rescue is the wild-type copy of the mutant allele.

lin-60 is a maternal gene and *ij48* is a dominant lesion (refer to Chapter 4). There are two complications when considering cloning a gene of this nature. Firstly, a gene identified by an allele that is dominant over wild-type cannot be cloned by rescue of mutant phenotype with the wild type copy. Genes are rarely cloned from dominant alleles. The cloning of genes identified by dominant alleles generally involves complex approaches that are very specific to the particular gene. For example, to clone the gene *rol-6* from the dominant allele *su1006*, the genetics of *rol-6* were studied and from its behaviour, it was postulated that it might be a collagen gene (Kramer *et al.*, 1990). Cosmids spanning the area to which *rol-6* mapped were probed with the collagen gene *col-2* and *rol-6* was identified. Clearly this was a highly specific approach that could not be generally applied. Secondly, transgenic arrays of maternal genes may be poorly expressed in the germline. For example, it is often difficult to rescue maternal-effect lethal mutations with cosmids. The use of genomic DNA as a carrier to promote the promotion of complex arrays can assist with the expression of maternal genes (refer to Chapter 3), but it is not always effective.

lin-60 maps to position +1.1 in the centre of chromosome I (Chapter 4). This area has been the subject of saturation screens of lethal mutations (McDowall and Rose, 1997a). Many of these lethal mutations have been rescued with cosmids, resulting in a very good alignment of the physical and genetic maps in this area. Moreover, with such screens, there are many genetic markers with lethal or sterile phenotypes. This allowed detailed

positional mapping to be carried out for *lin-60(ij48)* (Chapter 4). Recombination frequencies vary between chromosomes and arms ranging from, for example 1cM/50kb on the right arm of chromosome IV to 1cM/300kb on the left arm of chromosome V. *lin-60* maps to an area of chromosome I where the recombination frequency is approximately 1cM/1100kb (Barnes *et al.*, 1995).

My first aim was to reduce the size of this area to a small number of cosmids, and thus predicted genes. *lin-60(ij48)* lies between two cloned genes, *let-602* and *let-607*. This area is covered by around 17 cosmids (Figure 5.1). To reduce this number of cosmids, the left breakpoint of *hDf8*, a deficiency that contains *lin-60(ij48)* (Chapter 4), was mapped. *lin-60(ij48)* also maps very close to *let-604*. Although good positional information was available for *let-604* (J.S. McDowall, ACeDB), this gene had not been cloned. I therefore decided to place this gene onto the physical map by cloning it. Together, these approaches dramatically reduced the number of cosmids within the *lin-60(ij48)* interval. The penetrance of the *lin-60(ij48)* phenotype is greatly reduced when *lin-60(ij48)* is placed over a deficiency. I therefore decided to use an RNAi based approach to clone *lin-60(ij48)*. My aim was to mimic the deficiency effect by injecting dsRNA corresponding to genes in the *lin-60(ij48)* interval, and identify a gene that, when subject to RNAi, partially reduces the amount of maternal *lin-60(ij48)*, causing suppression of the Lin phenotype in the F1 progeny of treated mothers.

I found that the intestinal hyperplasia displayed by *lin-60(ij48)* mutants is caused by a mutation in the general cell cycle gene *cdc25*. I found that RNAi can reduce the oncogenic nature of this mutant whereas introduction of a mutant copy of this gene by transgenesis can create the intestinal hyperplasia.

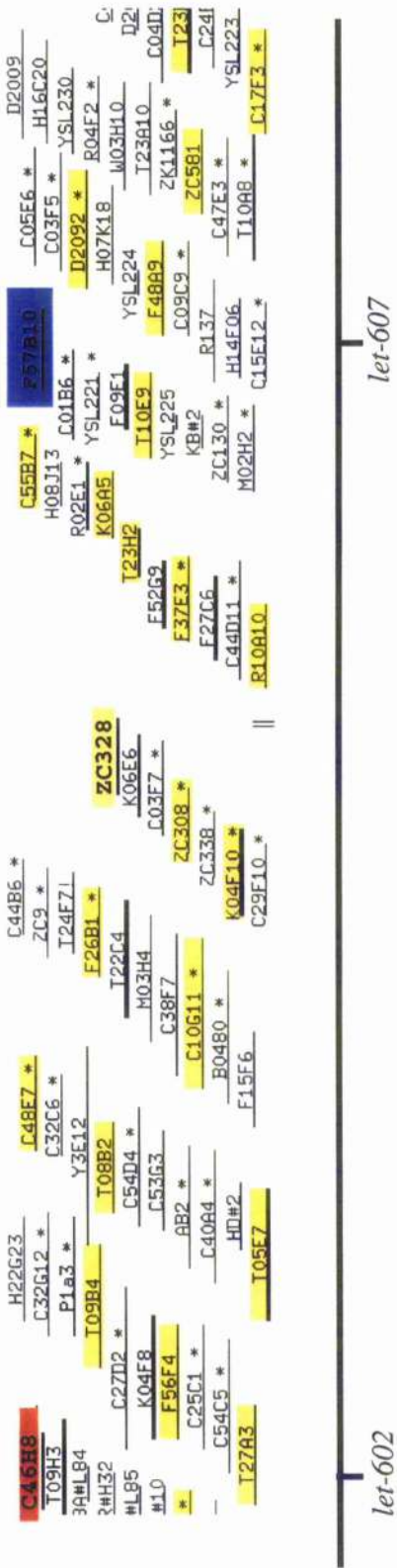


Figure 5.1 Cosmid map of the *let-602/let-607* interval. Cosmids highlighted in yellow have been sequenced. *let-602* is rescued by C46H8 (red) and *let-607* is rescued by F57B10 (blue). Figure extrapolated from ACeDB.

5.2. Mapping the left breakpoint of *hDf8*

The left breakpoint of *hDf8* was previously assigned to the cosmid C44D11 by restriction analysis (Thacker *et al.*, 1995). This cosmid has not been sequenced. *lin-60(ij48)* is covered by the deficiency *hDf8* (Chapter 4). To reduce the number of predicted genes in the *lin-60* interval and to confirm that the breakpoint of *hDf8* was in the area suggested by Thacker *et al.*, (1995), I decided to assign the physical breakpoint of *hDf8* to a sequenced cosmid. To do this, I used a PCR-based approach where homozygous mutant deficiency embryos were tested with primers specific to a predicted gene present in cosmids surrounding C44D11 (Cosmid Sequence Markers, CSMs) (Figure 5.2 and Section 2.13). Each homozygous deficiency embryo was tested with a positive control, a negative control and two test primer sets. The mutant *let-381* is rescued with F26B1. Since *let-381* is not deleted by *hDf8*, I used this as a positive control for PCR. The mutant *let-607* is deleted by *hDf8* and is rescued with the cosmid F48A9 and hence F48A9 should be covered by this deficiency. I therefore used the cosmid F48A9 as a negative control. A negative control was essential to allow the identification of any heterozygotic death. By detecting for the presence or absence of amplified products, I was able to determine that the left breakpoint of *hDf8* was present in the cosmid R10A10 and lies in or between the predicted genes R10A10.1 and R10A10.2 (Figure 5.2). Since R10A10.1 is the first gene not covered by *hDf8*, *lin-60(ij48)* (which is deleted by *hDf8*) must lie to the right of R10A10.1. This reduced the number of candidate genes in the *lin-60(ij48)* interval to 50 (Table 5.1). This figure includes genes present in cosmids F57B10 and F48A9. However, since recombination occurs between *lin-60(ij48)* and *let-607(h402)* (Section 4.4.2.3), with *let-607* being rescued with F48A9, the number of candidate genes could be reduced to around 36.

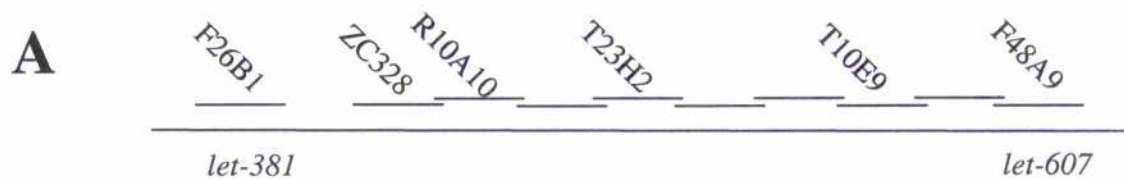
Name of Cosmid	Number of predicted genes
R10A10	2(*)
F37E3	3
T23H2	5
K06A5	6
C55B7	12
T10E9	9
F57B10	11
F48A9	3
Total	51

Table 5.1. Number of predicted genes in *lin-60* interval. (*) One of these genes (R10A10.2) is deleted by *hDf8*.

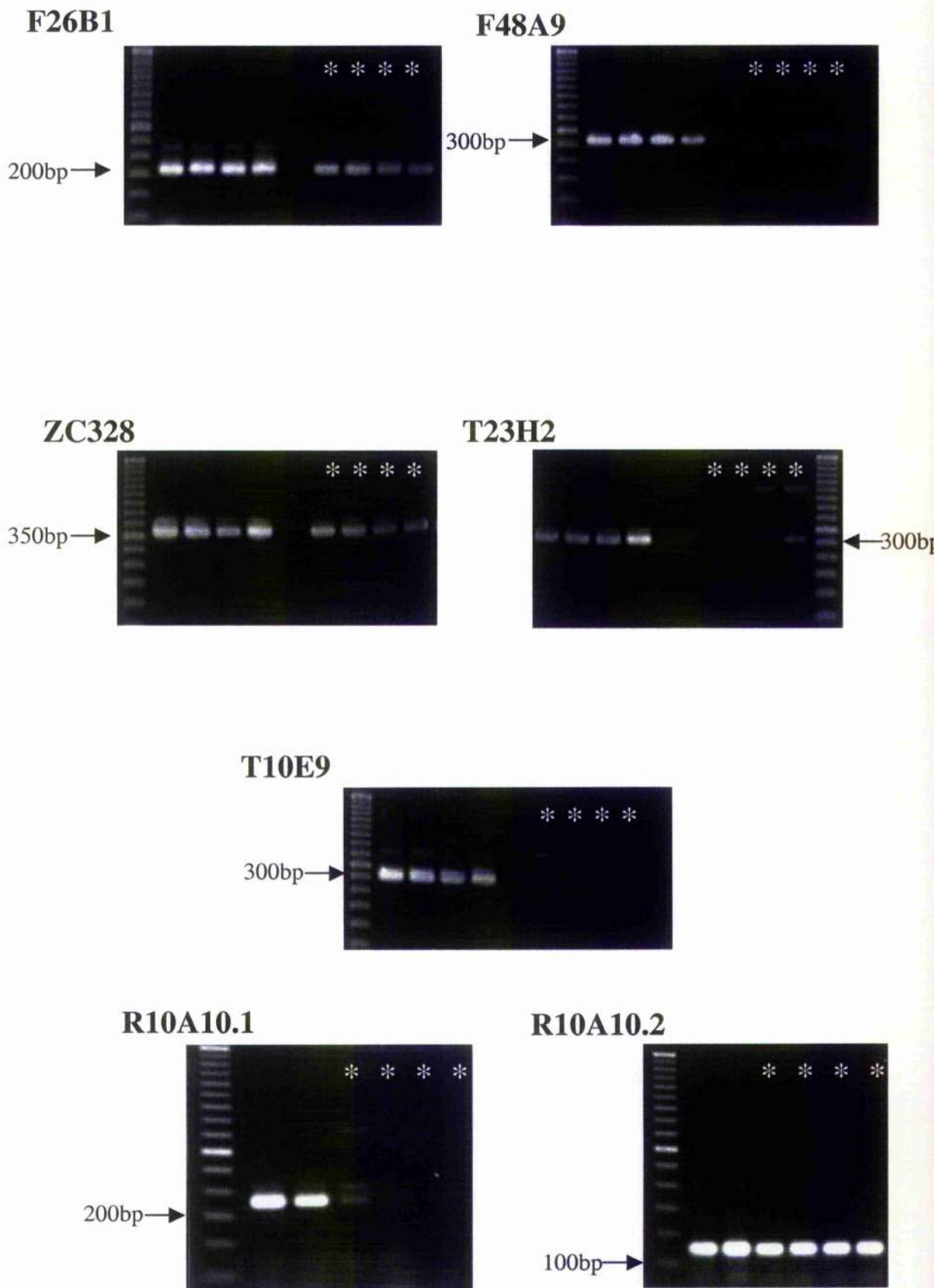
Figure 5.2
Mapping left-hand breakpoint of *hDf8*

Figure 5.2 Mapping left-hand breakpoint of *hDf8*

- A. Positions of cosmids tested with CSMs. *let-381* is not deleted by *hDf8* and was used as positive control for the PCR reactions. *let-607* is deleted by *hDf8* and is rescued by the cosmid F48A9. F48A9 was therefore used as a negative control for the PCR reactions.
- B. Agarose gels of PCR products. Wild type N2 embryos or homozygous *hDf8* dead embryos were used as DNA template, and tested with appropriate CSM primers. In each gel, the ladder is 50bp (Gibco). The first four lanes from the left in gels for F26B1, F48A9, ZC328, T23H2, and T10E9 are N2 embryos. The first two lanes from the left in R10A10.1 and R10A10.2 are N2 embryos. In all gels, the first four lanes from the right (denoted by white asterix) are *hDf8* embryos. Since R10A10.1 is deleted by *hDf8* whereas R10A10.2 is not deleted by *hDf8*, the left breakpoint must lie either between, or in R10A10.1 and R10A10.2.



B



5.3. Positioning of *let-604(h293)* onto the *C. elegans* physical map

lin-60(ij48) was found to map very close to the sterile mutant *let-604(h293)* (Chapter 4). Using genetic data regarding the free duplications *hDp56*, *hDp39* and *hDp54* (ACeDB), I was able to place *let-604* between other uncloned mutants, *let-608* and *let-382* (Figure 5.3). The right breakpoint of the free duplication *hDp39* has been deduced to lie in K06A5 (S. Clark-Maguire, ACeDB). Since *let-604(h293)* is covered by the deficiency *hDf8*, where the left breakpoint is in R10A10 (see above), *let-604(h293)* must lie in the cosmids R10A10, F37E3, T23H2 or K06A5. DNA from cosmids R10A10, F37E3, T23H2, K06A5 and C55B7 was isolated and examined by restriction digest for the presence of deletions. Clones that appeared, as judged by the expected sizes of digested products intact were included in the injection mix (Figure 5.4). As a marker of transgenesis, I used a plasmid (pMW002) containing the cuticular collagen gene promoter of *dpy-7* (Johnstone *et al.*, 1994) fused with *GFP*. Transformed progeny could therefore be screened using a UV-stereomicroscope. The plasmid pTag was also present in the injection mix. pTag contains both the ampicillin and kanamycin resistance genes, thus providing DNA homology for array formation with the ampicillin (R10A10, C55B7) and kanamycin (F37E3, K06A5 and T23H2) resistant cosmids.

The strain containing *let-604*, KR637, was available as homozygous *dpy-5(e61) let-604(h293) unc-13(e450)*, balanced with the free duplication *sDp2*. To remove any complications from the free duplication, KR637 was outcrossed by mating with wild-type males, and crossing the generated F1 males with N2 hermaphrodites. Progeny containing the genotype *dpy-5(e61) let-604(h293) unc-13(e450)/+/-* were isolated and maintained from the second cross. Phenotypically wild-type progeny from this strain were injected with the cosmid mixture.

Previous studies had indicated that *let-604(h293)* was not rescued with an extrachromosomal array (*hEx35*) containing the cosmid T23H2 and marker plasmid pRF4 (McDowall and Rose, 1997b). This array did not contain the left- or right- hand neighbour of T23H2 and it has been documented previously that loci that are split over two cosmids can often reform a wild-type locus during array formation. T23H2 was therefore included in the injection mix.

Rescue was observed in one line by the appearance of fertile DpyUnc progeny, which also showed *dpy-7::GFP* expression under the UV stereomicroscope. In this line, worms that were GFP negative, and hence had lost the free arrays, were sterile. Thus, the mapping information available in ACeDB for *let-604* was correct, and *let-604(h293)* is

rescued with a cosmid mixture containing R10A10, F37E3, K06A5, T23H2 and C55B7. Since no recombination was achieved between *let-604(h293)* and *lin-60(ij48)* (Section 4.4.2.7.), it seemed likely that the gene identified by *lin-60(ij48)* was present in this group of cosmids.

Figure 5.3
Positional information for *let-604(h293)*

Figure 5.3 Positional information for *let-604(h293)*

Using genetic data regarding the free duplications *hDp56*, *hDp39* and *hDp54* (ACeDB), I was able to place *let-604* between two uncloned mutants, *let-608* and *let-382*. *let-608* is covered by the free duplication *hDp56* but not *hDp39*, or *hDp54*. *let-604* is not covered by *hDp56* but is present in *hDp39* and *hDp54*, so must lie to the right of *let-608*. *let-382* is not covered by *hDp56* or *hDp39*, but is covered by *hDp54*, so must lie to the right of *let-604*. *let-607* is not present in *hDp56*, *hDp39* or *hDp54*, so must lie to the right of *let-382*. All four genes are deleted by the deficiency *hDf8*. The right breakpoint of the free duplication *hDp39* has been deduced to lie in K06A5 (S. Clark-Maguire, ACcDB). Since *let-604* is covered by the deficiency *hDf8*, where the left breakpoint is in R10A10 (see Figure 5.2), *let-604* must lie in the cosmids R10A10, F37E3, T23H2 or K06A5.

Cosmid	Enzyme	Expected sizes of fragments
R10A10	<i>Xba</i> I	At time of experimentation, only draft sequence was available and start and end points were not defined
F37E3	<i>Xba</i> I	14466, 6078, 5098, 4520, 3577, 2908, 2640, 1356, 1287, 471, 64, 12.
T23H2	<i>Xba</i> I	12808, 6078, 4520, 3577, 2909, 2633, 1977, 1818, 1543, 1356, 1287, 471.
K06A5	<i>Xba</i> I	8670, 7623, 6811, 6664, 3130, 3001, 2633, 1543, 839, 704, 354, 168, 88, 57, 32
C55B7	<i>Pst</i> I	9433, 9181, 7992, 6474, 2702, 1586, 1117, 923, 437, 86.

Table 5.2. Restriction enzymes and predicted sizes of digested products of cosmids used to rescue *let-604*

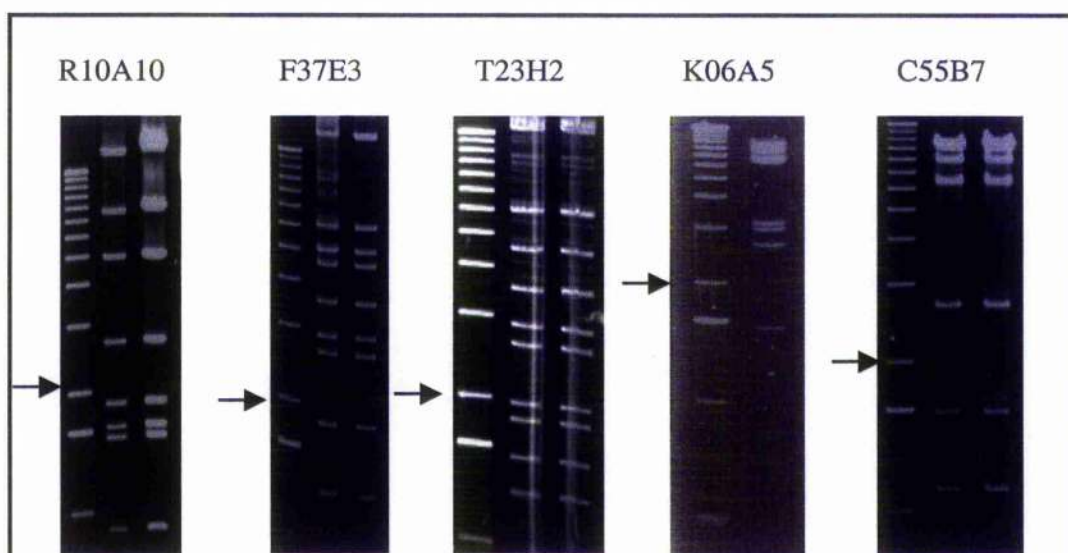


Figure 5.4 Restriction digests of cosmids used in positioning *let-604* onto physical map.

The cosmids R10A10, K06A5, F37E3, T23H2 and C55B7 were digested with the restriction enzymes stated in Table 5.2. The expected sizes of fragments are also shown in Table 5.2. In all gels, the 1st lane from left is 1kb DNA ladder, the black arrow points to the 2kb band. Two digested cosmid DNA samples are shown for all except K06A5, where one digest is shown. These gels show that the expected sizes of digested cosmids were obtained, thus these cosmids were not deleted.

5.4. RNA interference of genes in the *lin-60(ij48)* interval to suppress the *lin-60(ij48)* phenotype

5.4.1. Background to RNA interference

RNA interference (RNAi) is a relatively new reverse genetics tool that can specifically inhibit the function of a gene under study. It is therefore a very powerful tool in understanding the function of a particular gene. Fire *et al.* (1991) reported that antisense RNA expressed from a transgene could mimic a null mutation. Sense transcripts were also found to be effective. This interference effect was further demonstrated by Guo and Kemphues (1995), who showed that both sense and antisense RNA could be used to block gene expression in the maternal germline. Since then, it has been established that double-stranded RNA (dsRNA) is substantially more effective at inducing interference than either single strand (Fire *et al.*, 1998). These authors also suggested that it was the tiny amounts of dsRNA present in the single strand preparations that attributed to the interference observed.

Following dsRNA treatment, the corresponding gene products are reduced from the somatic cells of the organism as well as the F1 progeny (Fire *et al.*, 1998). RNAi has been shown to be very specific with a variety of genes, when comparisons are made between the genetic null and corresponding RNAi-induced phenotype. Moreover, both maternal and zygotic genes can be targeted. dsRNA can be administered by injection into the intestine or gonad, or by soaking the worms in the dsRNA preparation (Tabara *et al.*, 1998; Fire *et al.*, 1998). dsRNA can also be introduced into the worms by feeding the worms with bacteria that express dsRNA (Timmons and Fire, 1998). It is therefore clear that dsRNA can cross from the lumen into the intestinal cells and that the RNAi effect can be transmitted between cells. These observations with RNAi suggest the existence of transport and perhaps amplification of the interfering agent. The notion that an amplifying agent may be involved also stems from mutants in a gene required for germline development in *C. elegans*, *ego-1* (enhancer of *glp-1*). The EGO-1 protein is a member of the RNA-directed RNA polymerase family. Interestingly, *ego-1* mutants are defective for RNAi of maternal genes but not zygotic genes (Smardon *et al.*, 2000).

The mechanism by which RNAi produces its effect is currently under investigation. This work has focussed on four areas of gene expression in order to find the exact nature of the RNAi target: whether the gene itself is a target for mutagenesis, if initiation or elongation of transcription of the target gene is prevented, if the transcript of the target

gene is targeted for degradation or whether translation of the target gene is inhibited. Initial investigations indicated the gene itself is not mutated (Montgomery *et al.*, 1998) and that the prevention of initiation of transcription is not the mechanism for RNAi (Fire *et al.*, 1998; Montgomery *et al.*, 1998). The observation that the steady-state level of transcripts from reporter constructs is reduced in the nucleus whereas in the cytoplasm, these transcripts are virtually eliminated has led to the hypothesis that the endogenous mRNA is the target for RNAi (Montgomery *et al.*, 1998). Studies of dsRNA-induced interference in plants and trypanosomes have led to similar conclusions (Ngo *et al.*, 1998; Waterhouse *et al.*, 1998)

Interestingly, investigations with transcriptional operons have also provided evidence that RNA is the target for RNAi. The genes *lin-15a* and *lin-15b* together form a standard operon. Deletions in the 5' end of the upstream gene, *lin-15b*, lead to a loss of function of both genes, producing a multi-vulval (Muv) phenotype (Clark *et al.*, 1994; Huang *et al.*, 1994). However, RNAi of the upstream gene does not produce the Muv phenotype: this phenotype was only evident when both *lin-15a* and *lin-15b* were targeted by RNAi. This observation argues against an effect on initiation or elongation of transcription. Moreover, Boshier *et al.* (1999) demonstrated that pre-mRNA can be the target for RNAi. In contrast with the results generated by RNAi of the *lin-15* operon, with the *lir-1/lin-26* operon, inactivation of the upstream gene produces a phenotype identical to the genetic null of the downstream gene. A genetic null of the upstream gene was phenotypically wild-type. These results by Boshier *et al.*, (1999), also enhance the idea that although RNAi can be a very effective tool for analysing gene function, care must be taken when analysing the phenotype produced. The structure of a gene must therefore also be considered.

Classical genetic screens have identified mutants that are resistant to the effects of RNAi (Tabara *et al.*, 1999; Ketting *et al.*, 1999). One gene (*rde-1*) was found to encode a member of the *piwi/sting/argonaute/zwille/IF2C* gene family (Tabara *et al.*, 1999). Interestingly, a subset of these genes, including mutants of *rde-2*, *rde-3* and *mut-7*, have been found to permit the mobilisation of transposons in the germline and it has been speculated that one natural function of RNAi is transposon silencing. Two other mutants for RNAi, *rde-1* and *rde-4* do not show transposon silencing. These genes are however required for inheritable RNAi (Grishok *et al.*, 2000). It has been proposed that *rde-1* and *rde-4* act as initiators of RNAi, producing a secondary extragenic agent, which acts on the downstream effector genes, *rde-2* and *mut-7*, to target specific mRNA for post-transcriptional gene silencing. These authors also speculate that other reported situations

that can lead to gene silencing, such as repetitive DNA on some transgenes, act as initiators that may produce the same secondary extragenic agent as *rde-1* and *rde-4*.

Using a *Drosophila in vitro* system, it has been shown that RNAi is an ATP-dependent mechanism which does not require the recognition of the 7-methyl-guanosine cap of the targeted mRNA or mRNA translation (Zamore *et al.*, 2000). Rather, both the dsRNA and mRNA are cleaved at identical 21-23 nucleotide intervals, suggesting that the fragments from the dsRNA are targeting the cleavage of the mRNA.

When *lin-60(ij48)* is hemizygous over a deficiency, most animals are phenotypically wild-type. From this observation I decided to use an RNAi based approach with the intention of partially reducing the penetrance of the *lin-60(ij48)* phenotype. As stated above, mapping of *lin-60* positioned it to within approximately 36 predicted genes. Some of these genes could reasonably be excluded as they encoded, for example, tRNAs and general metabolism genes. Given the specific developmental phenotype of the *lin-60(ij48)* mutant, I focussed on genes that I thought were more likely to be developmental control genes.

5.4.2 RNA interference of genes in the *lin-60(ij48)* region

Primers were designed to amplify a specific region within each predicted gene. As a general rule, a fragment containing at least 500bp of exonic sequence was chosen for amplification. Where possible, cosmid DNA was used as a template for PCR. Since the sense and antisense primers had the promoters of T3 or T7 engineered onto their 5' ends, the amplified DNA was purified and used directly as a template for *in vitro* transcription. An example of a gel showing the single-stranded RNA products produced by *in vitro* transcription and annealed dsRNA is shown in Figure 5.5.

dsRNA was injected into young adult hermaphrodites using the method described in Section 2.14. Following injection, the worms were left to recover for at least five hours before being picked clonally onto 3.5cm plates. 24 hours post-injection, each worm was transferred onto a fresh plate. Over the following days, in addition to suppression of *lin-60(ij48)* phenotype, each plate was scored for other visible effects such as death, sterility, uncoordination and changes to body shape morphology. The results for RNAi are shown in Tables 5.3, 5.4 and 5.5.

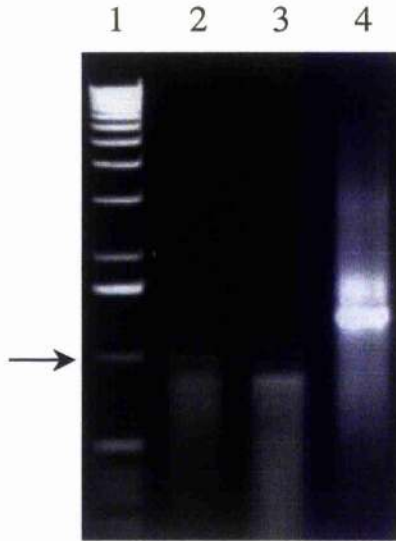


Figure 5.5 Agarose gel of RNA products from *in vitro* transcription. Example of an ethidium bromide stained gel showing RNA that was produced by *in-vitro* transcription. The promoter for T3 polymerase was added to the 5' end of the sense primer and the promoter of T7 polymerase was added to the 5' end of the antisense primer. (Lane 2) 1 μ l of single-stranded T3 product. (Lane 3), 1 μ l of single-stranded T7 product. (Lane 4) 500ng double stranded RNA produced by annealing the T3 and T7 single strands. Lane 1 is 1kb DNA ladder. Arrow points to 1kb.

The percentage suppression of the *lin-60(ij48)* phenotype following RNAi with 14 genes varied from 0.3% to 34.8% (Table 5.3). The suppression obtained for most genes was from 0.3 to 7.5%. One exception however was with RNAi of K06A5.7a, where 34.8% suppression was achieved (see below). Out of the 12 genes tested for suppression, only 2 genes gave a visible phenotype (Tables 5.4 and 5.5): RNAi of F57B10.1 and K06A5.7a.

Name	Similarity	Total no. F1s analyzed	Total no. wild-types	% Suppression
Injection buffer control	-	1394	12	0.8
R10A10.2	Zinc finger protein	1935	16	0.83
F37E3.2	Leucine rich proteins	1041	78	7.49
F37E3.3	-	2201	129	5.86
T23H2.1	Integral membrane protein	561	21	3.74
T23H2.2	C2 domain protein			
T23H2.4	-	2091	11	0.53
T23H2.5	RAS	1598	5	0.31
K06A5.7A	CDC25 phosphatase	184	64	34.78
K06A5.8	-	1547	27	1.75
C55B7.2	Alpha-1,3(6)-mannosylglycoprotein beta-1,6-N-acetylglucosaminyltransferase	1941	6	0.31
C55B7.3	Protein-tyrosine phosphatase	1696	89	5.25
C55B7.10	Casckin kinase	1490	9	0.60
C55B7.12	Zinc finger protein	1049	27	2.57
F57B10.1	contains similarity to bZip proteins	919	19	2.07

Table 5.3. Suppression of the *lin-60(ij48)* phenotype following injection with dsRNA corresponding to genes in the *lin-60(ij48)* area. Bold denotes genes that gave a visible phenotype with RNAi. In these cases, it is the total number of viable progeny that were analysed for suppression.

F57B10.1 is predicted to encode a transcription factor containing basic-leucine zipper (bZIP) and tyrosinase domains. RNAi with F57B10.1 gave an embryonic lethal or Dpy phenotype. (Table 5.4, Figure 5.6). The dead embryos appear to elongate to around three-fold then retract, suggesting a possible defect in cuticle synthesis or secretion. This idea is enhanced with the observation of Dpy survivors. To show that this was not a synthetic phenotype in the *lin-60(ij48)* background, RNAi of F57B10.1 was also performed in the wild-type N2 and in the *ijIs10(cpr-5::GFPlacZ)* (strain IA109, see Chapter 3) backgrounds. Since the phenotype produced by RNAi of F57B10.1 was suggestive of a cuticle defect, I also performed RNAi of F57B10.1 in the strain IA105. This strain is an integrated line containing the collagen gene promoter *dpy-7* fused with *GFPlacZ*. The dead embryos and Dpys produced had the wild-type expression profile of *dpy-7* (data not shown).

The percentage of embryonic lethal and Dpy phenotypes varied between the progeny of each injected hermaphrodite and strain. For example, RNAi of F57B10.1 in the strain IA105 produced a low amount of embryonic lethality, whereas a high level of embryonic lethality was observed in the IA109 background. I also observed a variation with regards to the level of Dpy phenotype between each F1 animal. In some cases, the F1 was severely shorter than wild-type length and looked very unhealthy whereas in other examples, the F1 was only slightly smaller than wild-type length. Due to these notable variations, RNAi of F57B10.1 needs to be repeated in all backgrounds. One cause of the observed differences may be that the RNA was degraded in some preparations.

Strain injected with F57B10.1 dsRNA	Total F1 Progeny analyzed	% Total Progeny		
		Dead embryos	Dpy	wild-type
IA123 (<i>lin-60(ij48); ijIs10</i>)	1138	19.24	26.80	53.95
N2	504	35.91	63.29	0.79
IA105	1187	2.52	57.79	39.68
IA109	943	79.22	19.94	0.85

Table 5.4 % of Dpy and Let phenotype following injection with F57B10.1 dsRNA.

K06A5.7a encodes a CDC25 protein phosphatase (CDC-25.1) (Ashcroft *et al.*, 1998). This gene is an essential regulator of the cell cycle. One of its best-known roles of this gene is the dephosphorylation and activation of CDC2, required for the progression into M-phase of the cell cycle.

RNAi of *cdc-25.1* in a wild-type background produces an embryonic lethal phenotype (95%) or sterile phenotype (5%) (Ashcroft *et al.*, 1999) in the F1 progeny. RNAi with *cdc-25.1* in the *lin-60(ij48)* background also resulted in an embryonic lethal (93%) or sterile phenotype (6%). I examined the relationship between the sterile and Lin phenotypes (Table 5.5). Interestingly, a proportion of the sterile worms (36/86, 42%) were suppressed for the *lin-60(ij48)* phenotype (Table 5.5). I assumed that RNAi did not have an observable effect on the F1 survivors that were not sterile. However, since substantial suppression of the Lin phenotype was obtained, the possibility that *ij48* was an allele of *cdc-25.1* was investigated.

% Total Progeny			% Viable progeny			
Total F1 Progeny analyzed	Dead eggs	Viable Progeny	Lin Fertile	Lin Sterile	WT fertile	WT sterile
743	93.3	6.7	14	50	0	36

Table 5.5 Analysis of dead embryos and survivors following injection with *cdc-25.1* dsRNA. This sample was taken from the progeny of 6 injected hermaphrodites and is part of the sample included in Table 5.3.



Figure 5.6 Dead embryo from F57B10.1 RNAi injections in *lin-60(ij48)* background. Black arrow points to grinder structure. White arrowhead points to pharynx. White arrow points to buccal cavity.



Figure 5.7 Dead embryo from K06A5.7a (*cde-25.1*) RNAi injections in *lin-60(ij48)* background.

5.5. Sequencing of *cdc-25.1* from the *lin-60(ij48)*, wild-type and IA109 backgrounds

5.5.1. Sequencing of *cdc-25.1* from the *lin-60(ij48)* background

Genomic DNA was prepared from *lin-60(ij48)* worms. Primers were designed for sequencing the genomic copy of *cdc-25.1*. The positions of these oligos are shown in Table 2.8 and Figure 5.8. Primers were designed such that around 400 bases could be sequenced from a given sequencing primer (Table 5.6). I attempted to sequence PCR fragments directly. This was successful for most of the gene; however, the first 800 bases gave very poor sequence. A fragment containing this sequence was cloned into the vectors pGEM (Promega) and PCRscript (Stratagene). Sequencing reactions were repeated with an independent PCR product if an ambiguous peak was observed in the sequencing trace. For region 450 to 800bp, two independent cloned PCR-fragments were sequenced. For region +1 to +450bp, a total of four independently cloned PCR fragments were sequenced. Sequencing more than one clone, with each cloned fragment derived from a separate PCR reaction, allowed confirmation that any detected mutations were indeed present in genomic DNA, and not mutations caused by misincorporation of a base during PCR reactions. In all four sequencing runs from bases +1 to +450, a C→T point mutation was detected at base +137, relative to the ATG of *cdc-25.1*. This mutation appeared as an unambiguous peak on the sequencing trace (Figure 5.9). In all cases, the sequence data was compared with the wild-type copy of *cdc-25.1* (Accession No. AF039038).

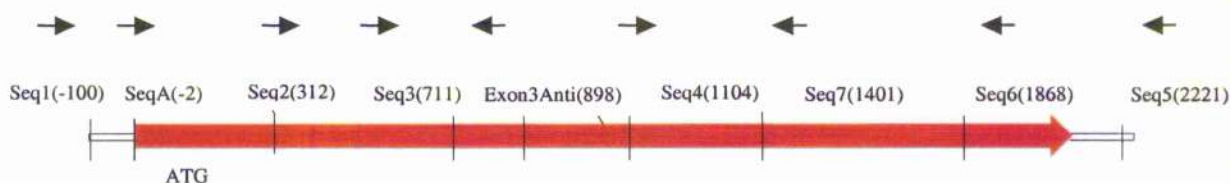


Figure 5.8 Schematic diagram of *cdc-25.1* coding sequence showing positions and directions of sequencing primers. The red arrow denotes the *cdc-25.1* coding sequence and the black arrows show the position and direction of sequencing primers. The position of the sequencing primers (in brackets) are relative to the ATG of *cdc-25.1*.

Readable sequence (relative to ATG)	Primer combination for PCR product	Primer used for sequencing	PCR fragment or clone sequenced	Change in sequence
-100 to +598	seq1 & seq7	T3, T7 or SP6	Clone	C→T (Base +137)
462 to 993	seq1 & seq7	seq2	Clone	None
781 to 1121	seq1 & seq6	seq3	PCR	None
1104 to 1374	seq4 & seq5	seq7	PCR	None
1350 to 1826	seq4 & seq5	seq6	PCR	None
1800 to 2200	seq4 & seq5	seq5	PCR	None

Table 5.6 Combinations of DNA fragments and primers used for sequencing *cdc-25.1*. The relative positions of these primers on the coding sequence are shown in Figure 5.8. 'Readable sequence' denotes good sequences obtained from the trace from sequencing gels.

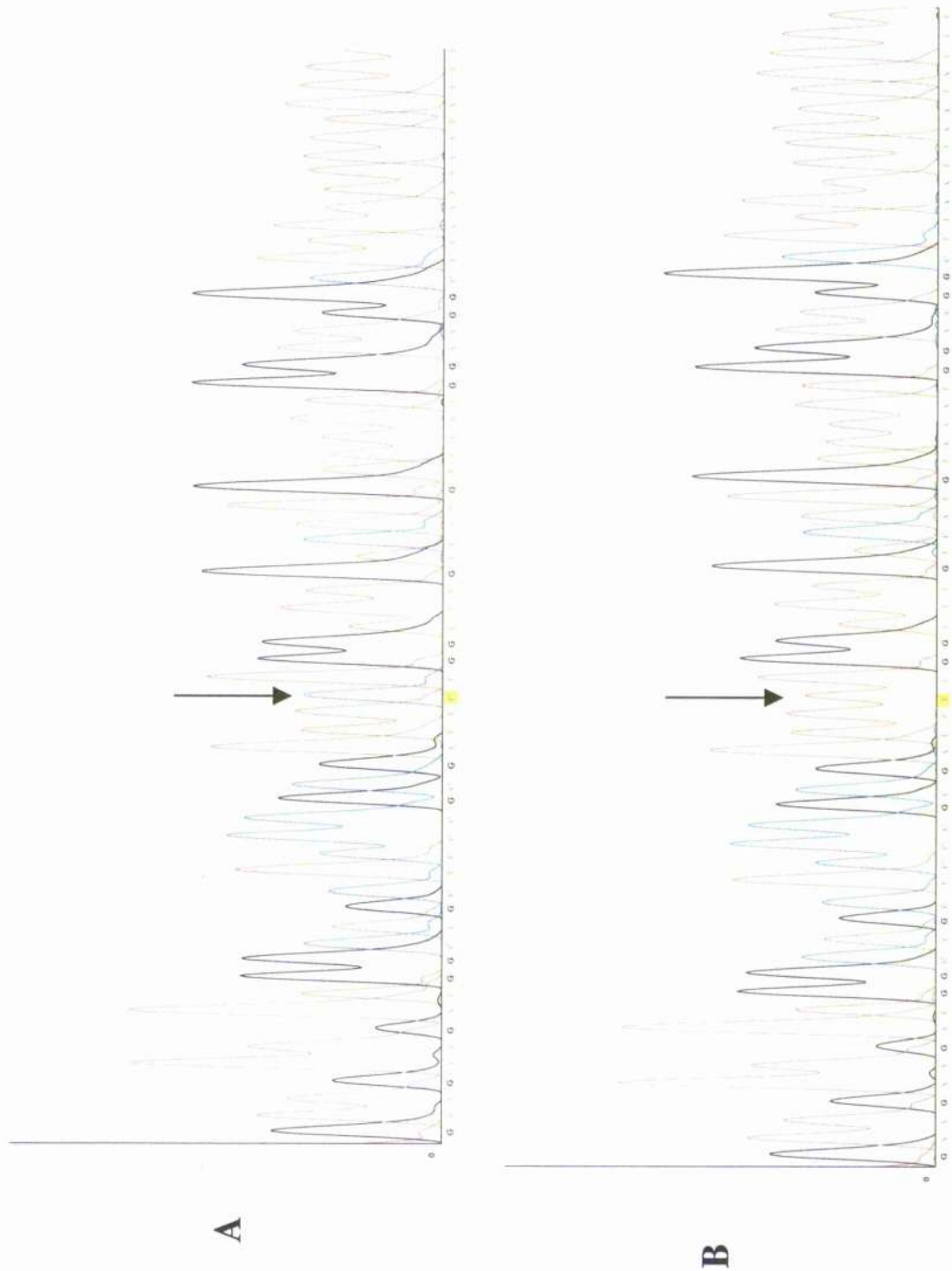


Figure 5.9 Sequencing trace from wild-type and *lin-60(ij48)*. The coding sequence of *cdc-25.1* was sequenced in both backgrounds. (A) is wild type, (B) is *lin-60(ij48)*. The black arrow points to base +137 of *cdc-25.1*, where a C→T point mutation is present in *lin-60(ij48)*.

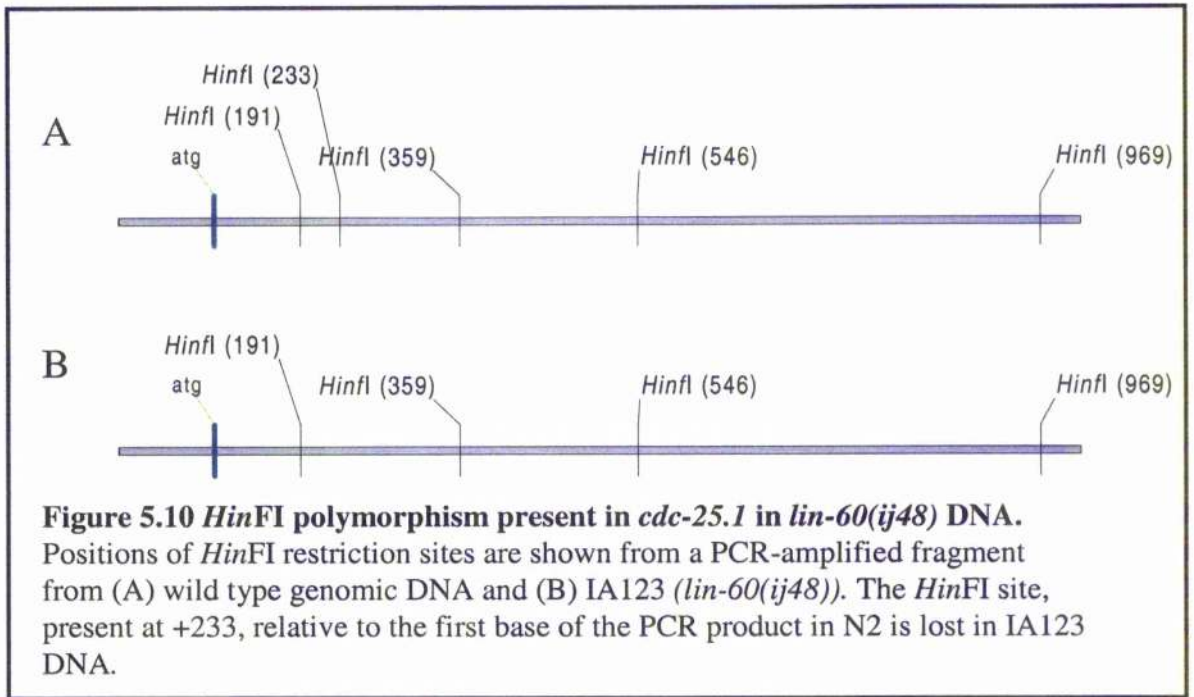
5.5.2. Sequencing of *cdc-25.1* in wild type and IA109 backgrounds

To confirm the published sequence, *cdc-25.1* was sequenced in the wild type N2 background, over the area of the mutation detected in *lin-60(ij48)*. Wild-type sequence was obtained by cloning a PCR-generated fragment, as described above, into pGEM and sequencing using the primer SP6. The cosmid K06A5 was used as a template for amplification. The sequence obtained agreed with the published sequence (Figure 5.9).

The strain IA109 contains 1kb of the *cpr-5* promoter fused with *GFP_{lacZ}*, and is integrated into the genome (Chapter 3). This was the strain used for screening intestinal mutants (Chapter 3). To check that the C→T point mutation was not present prior to mutagenesis, strain IA109 was also sequenced across the region where the mutation was present. Genomic DNA prepared from single worms was used for PCR amplification. Two independent clones containing DNA from two separate PCR reactions were sequenced across this region and no sequencing errors were identified. This demonstrated that this mutation was not present in IA109 prior to mutagenesis.

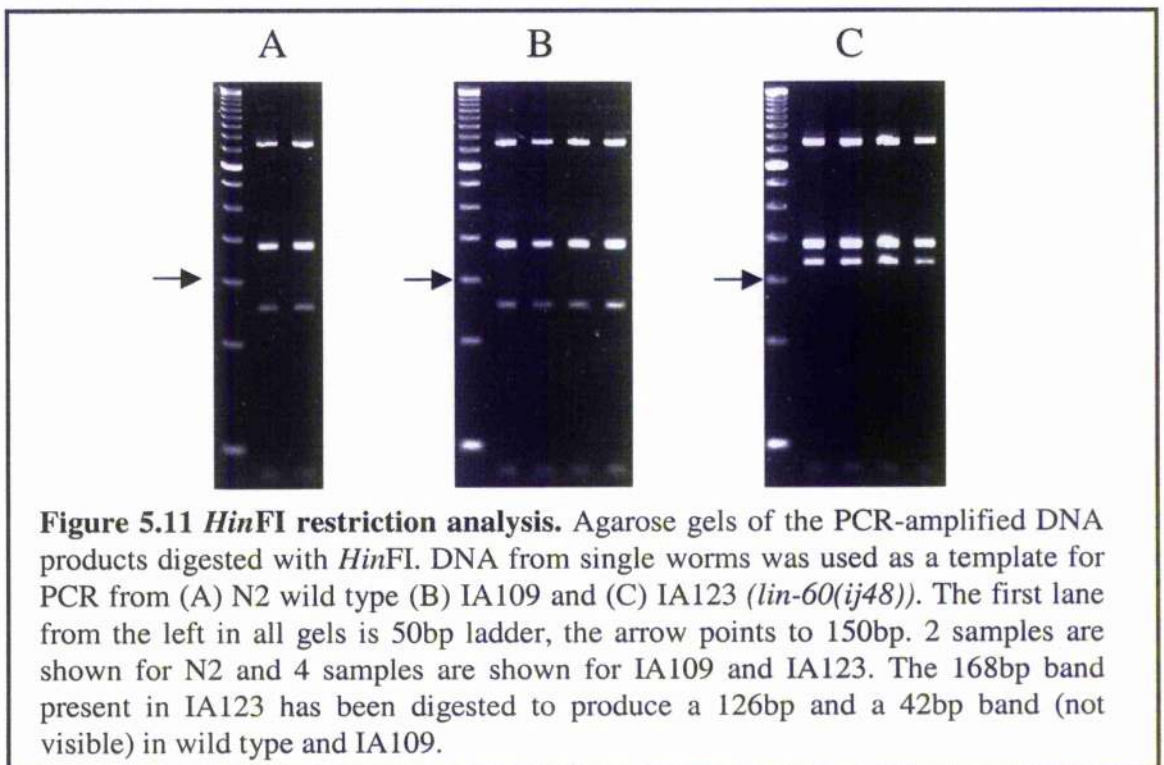
5.6. A *HinFI* polymorphism is present in *lin-60(ij48)*

The base change present in *cdc-25.1* in *lin-60(ij48)* animals creates a *HinFI* polymorphism. *HinFI* cuts the sequence 5'...G[▼]ANTC...3'. Thus, the mutation present at base 137 would remove a *HinFI* site. PCR amplified fragments, using single worms as template and primers seq1 and Exon3Anti (Figure 5.8), were generated using strains N2, IA109 and IA123[*lin-60(ij48); ijIs10*] and digested with *HinFI* (Figures 5.10 and 5.11). The expected sizes of the PCR-generated fragments following digestion with *HinFI* of wild-type, IA109 and IA123 are shown in Table 5.7. A total of 8 separate reactions from each strain were set up. Agarose gels showing the digested products from 2 samples from N2 and 4 samples from IA109 and IA123 are shown in Figure 5.11. This confirms the sequencing data, that the C→T point mutation is present in the coding sequence of *cdc-25.1* in IA123 and not IA109 or N2.



Expected sizes of fragments (bp)	
N2 wild-type, IA109	423, 190, 187, 126, 43, 42
IA123 (<i>lin-60(ij48)</i>)	423, 190, 187, 168, 43

Table 5.7 Predicted sizes of fragments from a PCR-amplified fragment containing *cdc-25.1* genomic sequence from N2, IA109 and IA123 DNA, following digestion with *HinFI*



5.7. Substitution of C→T at base 137 creates a predicted Ser→Phe amino acid change

The full length cDNA of *cdc-25.1* has been cloned and sequenced (Ashcroft *et al.*, 1998). Thus, the intron/exon structures have been determined experimentally. *cdc-25.1* consists of seven exons and is *trans*-spliced to SL1. Based on the predicted amino acid sequences from the *cdc-25.1* cDNA, substitution of C→T at base 137 (relative to ATG) creates a predicted Ser→Phe change at amino acid position 46 (Figure 5.12).

The mutation is therefore present in the first exon of *cdc-25.1*. The N-terminus of CDC25 has been shown to be involved in the regulation of CDC25 phosphatases in *Xenopus* (Kumagai and Dunphy, 1992).

5.8. Ser₄₆ is contained within a conserved domain

There are four CDC25 homologues in *C. elegans* (Ashcroft *et al.*, 1998). Only one CDC25 from *C. briggsae* (CBCDC25.1) was obtained from a blast search of the *C. briggsae* genomic sequence. However, the sequencing project of *C. briggsae* is not complete and it is likely that there are more CDC25s in *C. briggsae*. Alignments were made with the CDC25s of *C. elegans* and *C. briggsae*. From the alignments it is clear that there is a large amount of conservation in one domain (the phosphatase domain) towards the C-terminal region. This domain is conserved when aligning CDC25s from other species (Ashcroft *et al.*, 1998).

In contrast with the phosphatase domain, the N-terminal region is not highly conserved between the CDC25 homologues. Interestingly, the N-terminal region of CBCDC-25 and CECDC-25.1 are conserved whereas the N-terminal region between the CDC25s of *C. elegans* are not highly conserved. However, one obvious region of conservation that exists between CECDC-25.1, CECDC-25.2 and CBCDC-25 is an SRDSG domain (Figure 5.12). Furthermore, the Ser₄₆→Phe₄₆ is at position +4 within this domain. The N-terminus has been shown to be involved in the negative regulation of CDC25 in *Xenopus* (Kumagai and Dunphy, 1992). Negative regulation of CDC25 is essential as CDC25 (and thus Cdk1-CyclinB) must only be active for a brief period during the cell cycle, since it plays a crucial role as a mitotic inducer. The *Xenopus* Cdc25 is virtually inactive during interphase but undergoes a strong activation at mitosis due to phosphorylation of its N-terminal regulatory domain (Izumi *et al.*, 1992; Kumangi and Dunphy, 1992). This SRDSG domain found in the N-terminus of CBCDC-25, CECDC-25.1 and CECDC-25.2 may therefore be involved in the regulation of these molecules.

phenotype. Both of these lines originated from F1s which did not display the Lin phenotype.

As an alternative test, I attempted rescue of a deletion mutant of *cdc-25.1*, *cdc-25.1(nr2036)*, with the *cdc-25.1(ij48)* fragment. *cdc-25.1(nr2036)* homozygotes are sterile (a gift from Neville Ashcroft). The hypothesis was that if *lin-60(ij48)* is *cdc-25.1* and rescue was achieved, the rescued worm should be Lin. With these injections, I used linearised pCC7 (containing *cpr-5::GFPlacZ*), or pJM67 (containing *elt-2::GFPlacZ*) as a marker of transgenesis. Heterozygotes of the balanced strain AG82 [*unc-40(e271) cdc-25.1(nr2036)/dpy-5(e61) unc-13(e450)*] were injected. Transformed F1 progeny (GFP positive seen under stereomicroscope) were examined for the *lin-60(ij48)* phenotype. If lines with strong GFP fluorescence were identified, the Uncs were subsequently picked to a separate plate and examined for rescue of sterility and if achieved, their progeny were examined for the *lin-60(ij48)* phenotype (Tables 5.8).

The *cdc-25.1(ij48)* fragment was injected into AG82 at 2, 5 or 10ng/ μ l (Table 5.8). A proportion of the transgenic F1s were Lin and lines were obtained. However, out of a total of 6 lines, only one transmitted the Lin phenotype (injection round 7, line C) (Figure 5.13). In this line, transgenic *cdc-25.1(nr2036)* heterozygotes and homozygotes both show the *lin-60(ij48)* phenotype. GFP-positive Uncs (*cdc-25.1* homozygotes) from this line are fertile whereas GFP negative worms are sterile, thus the *cdc-25.1(ij48)* fragment is functional. However, the fertile GFP-positive Uncs, had a low brood size, indicative of partial rescue.

Nevertheless, it has been shown that transformations with a *cdc-25.1* PCR-fragment, amplified from *lin-60(ij48)* genomic DNA, containing *cdc-25.1* coding sequence and necessary upstream and downstream sequences is functional (due to observation of partial rescue) and can synthesise the *lin-60(ij48)* phenotype. This evidence together with the mapping, RNAi and sequencing data suggests that the Ser₄₆→Phe₄₆ substitution in CDC-25.1, present in *ij48*, is sufficient to produce extra gut cells.

Injection set	Strain injected	Concentration of <i>cdc25.1(j48)</i> fragment (ng/ μ l)	Marker and concentration (ng/ μ l)	Transgenic F1s with <i>lin-60(j48)</i> phenotype	Transgenic F1s without <i>lin-60(j48)</i> phenotype	No. lines with <i>lin-60(j48)</i> phenotype	No. lines without <i>lin-60(j48)</i> phenotype
1	IA109	10	pRF4@5	1	5	0	0
2	IA109	10	pRF4@5	2 ^a	4	0	2 ^b
3	AG82	10	pCC7@2	1	3	0	0
4	AG82	5	pCC7@2	0	0	0	0
5	AG82	10	pJM67@2	1 ^c	4	0	0
6	AG82	10	pJM67@0.2	1 ^c	4	0	0
7	AG82	5	pJM67@0.2	7 ^c	4	1 ^d	3 ^b
8	AG82	2	pJM67@0.2	2 ^c	2	0	2

Table 5.8 Transgenesis with *cdc25.1(j48)* fragment. The *cdc25.1(j48)* fragment was injected into the strains IA109 or AG82 at concentrations ranging from 2ng/ μ l to 10ng/ μ l. pRF4, pCC7 or pJM67 were used as a markers of transgenesis. One line was generated that displayed the Lin phenotype. This line was formed in the strain AG82 [*unc-40(e911); cdc25.1(m-2036)/dpy-5(e61) unc-13(e450)*]. The presence of Lin animals demonstrated that the *cdc25.1(j48)* fragment is sufficient to generate intestinal cell hyperplasia. The presence of fertile GFP positive Unc adults, (which are GFP negative and sterile when the array is lost) demonstrates that the *cdc25.1(j48)* molecule is functional.

^a One of these F1s displayed Lin phenotype but did not Rol

^b Lines obtained from F1s that did not display the Lin phenotype

^c Transgenic (observed by GFP) dead eggs and larvae obtained, suggesting that a component in the injection mix is toxic. Since lethality has previously been observed with pJM67 (C. Clucas and I. Johnstone, unpublished results), it is probable that this plasmid is causing the lethality.

^d Line obtained from F1 that displayed the Lin phenotype

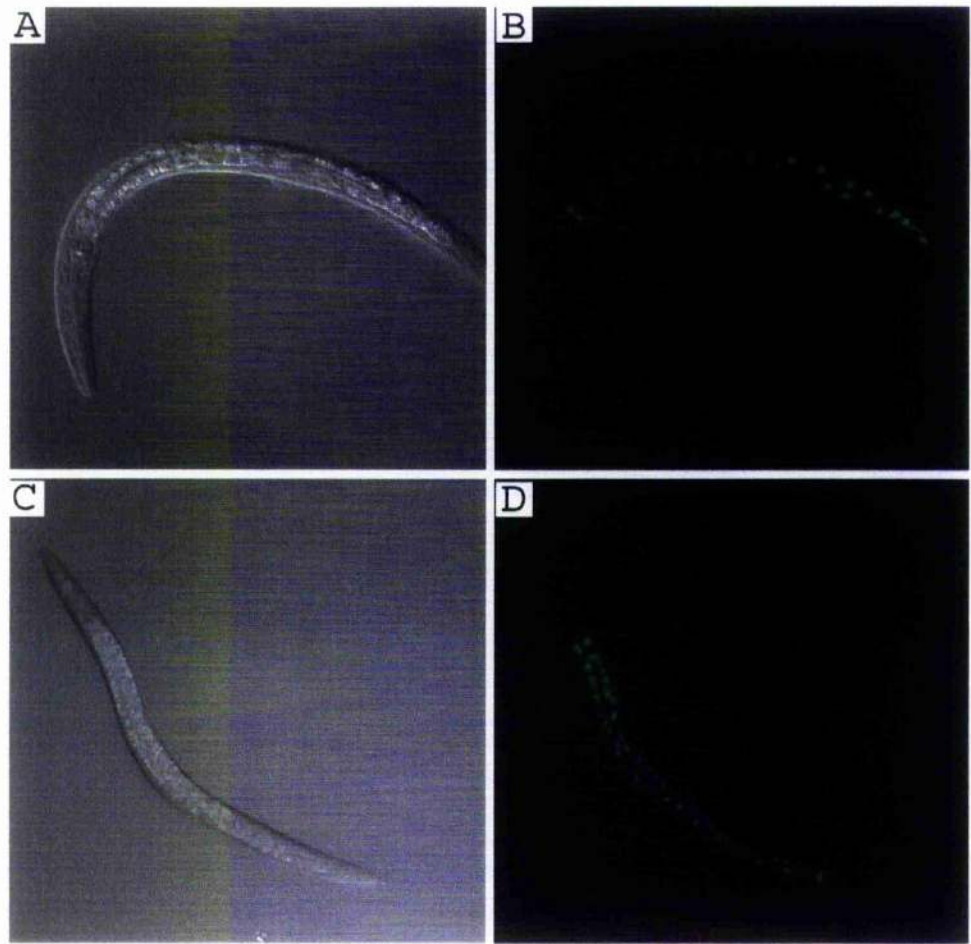


Figure 5.13 Microscopy of rescued lines. Intestinal cells in wild-type (A) and (B) and in a *cdc-25.1(nr2036)* rescued line (C) and (D). (A) and (C) are Nomarski images with respective *elt-2::GFP* fluorescence counterparts (B) and (D). Rescue was obtained from injections with a PCR-amplified fragment from *lin-60(ij48)* genomic DNA, containing the *cdc-25.1* coding sequence and untranslated regions. Although rescue was achieved, the rescued animals also displayed the *lin-60(ij48)* phenotype.

5.10. Characterisation of RNAi of *cdc-25.1*

The RNAi phenotype of *cdc-25.1* in wild-type *C. elegans* has recently been studied (Ashcroft *et al.*, 1999). It was shown that CECDC-25.1 was an essential maternal gene and disruption with RNAi resulted in an embryonic lethal phenotype. The embryos suffered from anuploidy, resulting from a defect in meiosis. This was due to an aberrant cortical membrane, whereby excessive cortical membrane contractions resulted in defects with meiotic spindle attachment, and polar body extrusion. The cleavage furrow of the first mitosis was mispositioned, resulting in a Par phenotype. However, disruption of *cdc-25.1* by RNAi did not alter the anterior-posterior polarity of the mitotic spindle at the first mitotic division, which occurs as wild-type, along the anterior/posterior axis. This was not true for subsequent divisions where cleavage planes were aberrant. The timing of all mitotic divisions was abnormal and incomplete furrow formation was observed in these lethal embryos.

To investigate whether reduction of wild-type *cdc-25.1* had the opposite effect from the *ij48* gain-of-function allele with respect to cellular proliferation, RNAi was performed on transgenic strains containing *GFP* fused to promoters of gut or hypodermal terminal differentiation markers. This allowed me to count the number of intestinal or hypodermal cells generated in the F1 lethal embryos.

Instead of administering RNAi by microinjection, I used the bacterial feeding method (Timmons *et al.*, 2001). A genomic fragment of *cdc-25.1*, amplified using Taq DNA polymerase and primers Seq1 and Seq5, (Table 2.17) was cloned into pGEM (Promega Corporation), digested with *SpeI* and *NcoI* and ligated with a similarly digested L4440 vector (Timmons and Fire, 1998). The L4440 vector is the vector used to clone inserts for RNAi feeding and contains two T7 polymerase promoters oriented in opposing directions. The *cdc-25.1/L4440* ligated product (pCC54) was transformed into the HT115(DE3) bacterial strain using standard procedures. This *E. coli* strain is RNAse III deficient and thus will not degrade any foreign RNAs. T7 polymerase expression can be induced by the addition of IPTG.

For some genes it has been found that RNAi administered by bacterial feeding can be used to generate a spectrum of severity of RNAi effects that probably represents varying degrees of reduction of gene products in the treated animal (I. Johnstone, personal communication). When L4 animals were placed on the bacterial RNAi lawns, most of the F1 progeny failed to hatch. The embryonic lethal class displayed a broad spectrum of effects generating variable numbers of cells before death, probably the result of varying

degrees of reduction of *cdc-25.1* activity by incomplete RNAi. However, if embryos or L1s were placed on the *cdc-25.1* RNAi lawn and permitted to grow, they developed into sterile adults. The embryonic lethal class presumably resulted from perturbation of maternal CDC-25.1 protein whereas the sterile adults resulted from loss of zygotic CDC-25.1.

5.10.1. Analysis of intestinal and hypodermal cell number from *cdc-25.1* RNAi lethal embryos

L4 hermaphrodites from integrated lines, marking gut (JR1838) or hypodermal nuclei (IA105) were transferred to plates expressing *cdc-25.1* dsRNA. These hermaphrodites were allowed to egg-lay and after 24 hours transferred onto fresh plates. The original plates were scored for embryonic lethality and sterile phenotypes. Like the RNAi effect observed with the injection method, the first 5% of embryos that were laid hatched and developed as sterile adults whereas the remainder arrested as eggs.

JR1838 contains an integrated *elt-2::GFPlacZ* plasmid. GFP can be visualised when the gut has only two cells (Fukushige *et al.*, 1998). RNAi with this strain also produced sterile adults and dead eggs. I observed a spectrum of timing of arrest as some embryos arrested early with no morphogenesis whereas others arrested later in development during the process of elongation. A range of counts of intestinal cell nuclei was also observed. Some embryos arrested with the normal complement of 20 gut nuclei whereas others arrested with no gut nuclei being born (Table 5.9 and Figure 5.14). The average from 17 embryos was 11 intestinal nuclei. As described above, the probable reason for such a spectrum of effects is varying degrees of knockdown by the RNAi process.

Embryo	Number of intestinal cells	Embryo	Number of intestinal cells
1	13	10	0
2	0	11	0
3	18	12	16
4	10	13	20
5	0	14	16
6	18	15	16
7	4	16	18
8	10	17	20
9	13	Average	11

Table 5.9. Number of intestinal cells following *cdc-25.1* RNAi

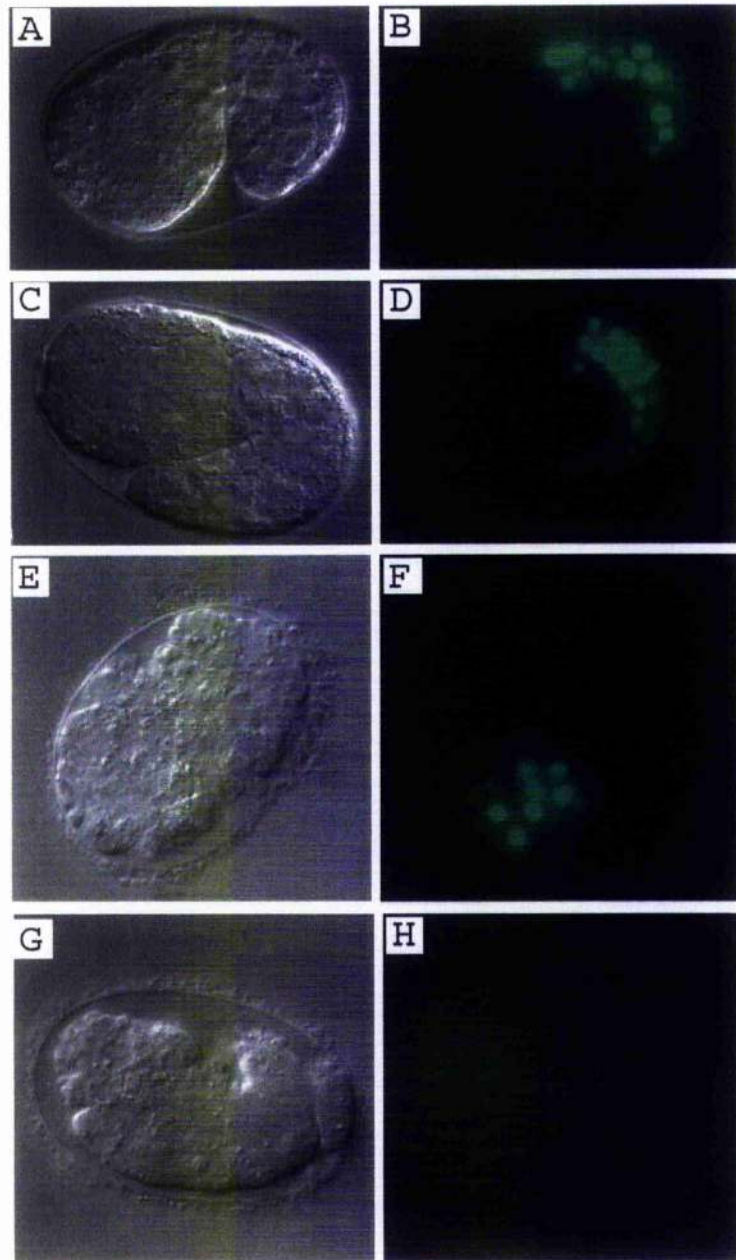


Figure 5.14 Intestinal cells in embryos of wild-type, *lin-60(ij48)* and *cdc-25.1* RNAi. (A), (C), (E) and (G) are Nomarski images with respective *elt-2::GFP* counterparts (B), (D), (F) and (H). (A) and (B) are wild type, (C) and (D) are *lin-60(ij48)*, showing that additional intestinal nuclei expressing this marker are present in this mutant (Chapter 4). (E), (F), (G) and (H) are F1 embryos derived from a mother treated as an adult with *cdc-25.1* RNAi by bacterial feeding. In embryo (E), 7 cells are expressing *elt-2::GFP* whereas no expression of *elt-2::GFP* is observed in (G).

RNAi with the integrated *dpy-7::GFP* line, IA105, produced a similar effect. In wild-type, 85 hypodermal cells are born during embryogenesis and many of these are visible with the IA105 strain (I. Johnstone personal communication). RNAi of *cdc-25.1* in this *dpy-7::GFP* background strain reduced the number of hypodermal cells born (Table 5.10 and Figure 5.15). From 20 embryos analysed, the average count was 25 hypodermal cells.

Thus, reduction of *cdc-25.1* activity by RNAi can cause a reduction in the number of cells expressing intestinal fate in the developing embryo. However, this effect is not restricted to intestinal cells, as indicated by the effect seen on hypodermal cells.

Embryo	Number of hypodermal cells	Embryo	Number of hypodermal cells
1	25	12	24
2	23	13	26
3	13	14	8
4	32	15	30
5	18	16	36
6	23	17	32
7	29	18	27
8	33	19	30
9	34	20	7
10	17	Average	25
11	30		

Table 5.10. Number of hypodermal cells following *cdc-25.1* RNAi

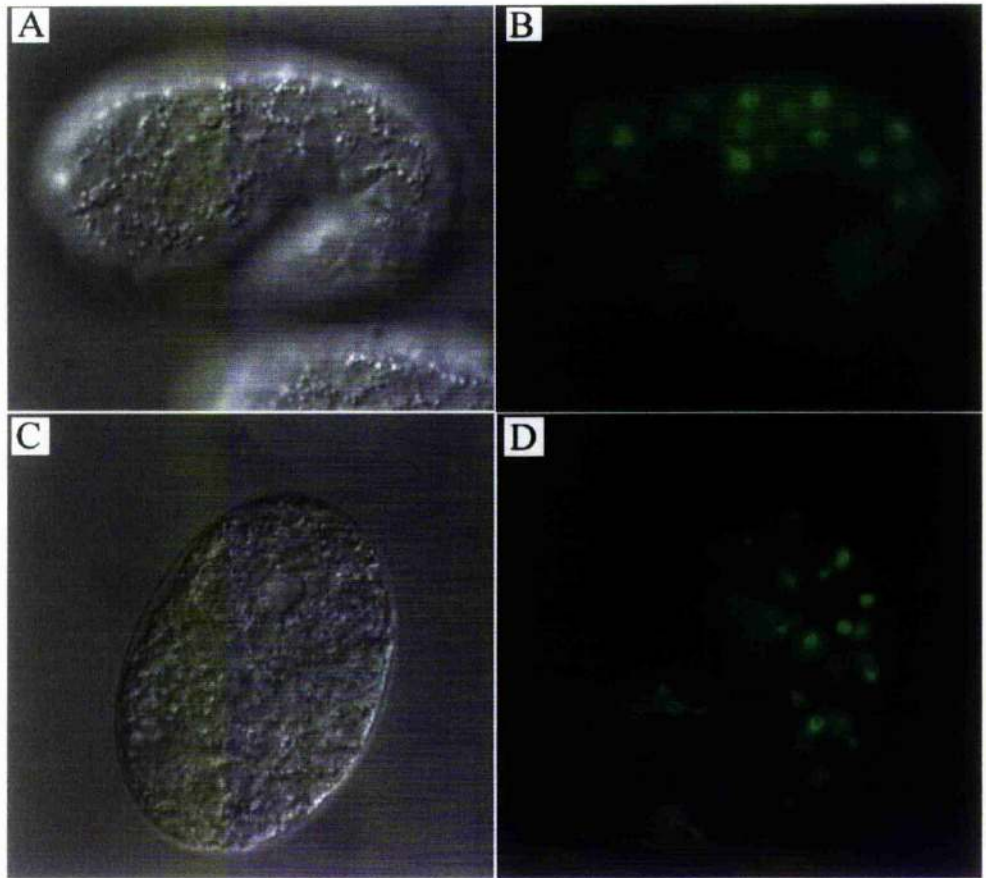


Figure 5.15 Hypodermal cells in embryos of wild-type and *cdc-25.1* RNAi. (A) and (C) are Nomarski images with respective *dpy-7::GFP* counterparts (B) and (D). (A) and (B) are wild type, (C) and (D) are F1 embryos derived from a mother treated as an adult with *cdc-25.1* RNAi by bacterial feeding. In embryo (D), around 30 cells are expressing *dpy-7::GFP* whereas around 85 are observed in wild type. Not all GFP-positive nuclei can be seen in any given focal plane.

5.10.2. Analysis of germline development in *cdc-25.1* RNAi

Germline development in *lin-60(ij48)* was characterised in Chapter 4 and found to be wild type. As stated above, *cdc-25.1* RNAi results in sterility in some of the F1 progeny. To test whether the germline proliferation defect was the result of interference of zygotic *cdc-25.1* activity, wild-type embryos were allowed to develop normally and after hatch, placed onto *cdc-25.1* bacterial RNAi lawns and permitted to develop to adults, thus restricting the RNAi effect on these animals to post-embryonic development. More than 90% of these animals developed into sterile adults, indicating that *cdc-25.1* has zygotic as well as maternal functions. Removal of zygotic *cdc-25.1* by RNAi severely compromises germline proliferation (Figure 5.16). There is a severe reduction in the number of germline nuclei. This reduction in the number of is varied between different animals, but the example shown in Figure 5.16 is typical. Compared to wild-type, the germ line nuclei are also enlarged, and have a rounded appearance. No oocytes were ever observed and cellularisation did not occur. I did not examine for the presence of sperm.

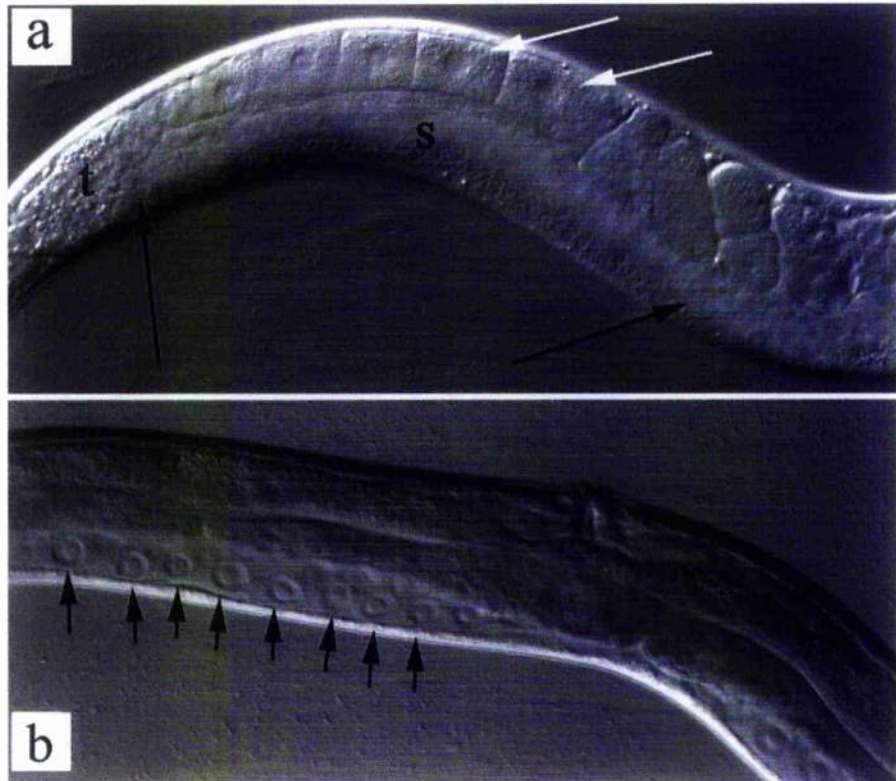


Figure 5.16 Gonads of adult hermaphrodites treated with *cdc-25.1* RNAi. Wild-type (a) Some developing oocytes are marked with white arrows, the syncytial arm of the gonad is delineated with black arrows and labelled "s". This region contains several hundred germline nuclei. The turn of the gonad arm is labelled "t". A similar region of the anatomy of a sterile adult generated by post embryonic *cdc-25.1* RNAi by bacterial feeding is shown in (b). Individual germline nuclei are marked with black arrows. The reduction in number of germline nuclei by this RNAi is varied in different animals, but the example shown is typical.

5.11. Analysis of CDC-25.1 protein distribution on wild-type and *lin-60(ij48)*

To investigate whether the tissue specific nature of the *ij48* lesion could be explained by differential protein distribution in mutants, I stained *lin-60(ij48)* mutants with an anti-*CDC-25.1* antibody (Clucas *et al.*, 2002). To generate this antibody, two peptide sequences, peptide A (CRYNGLNPNRDDPFG) and B (NILYGLDDERRPKWV), were coupled to keyhole limpet haemocyanin and used to generate rabbit antibodies reactive to CDC-25.1. Peptide sequences A and B are present at the N-terminus of the protein. The antibody generated detected a protein on a western blot of the correct size and staining was depleted when the antibody was preincubated with the synthetic peptide B, and in lysates of worms treated by *cdc-25.1* RNAi (Clucas *et al.*, 2002). Thus this antibody appears to be specific to CDC-25.1.

The staining pattern for CDC-25.1 had been described previously (Ashcroft *et al.*, 1999). However, these authors used a different region of the molecule, where a synthetic peptide was raised against the C-terminus of *cdc-25.1*. Staining of the antibody generated by Ashcroft *et al.*(1999) was observed in the hermaphrodite germline, the labelling being strongest in the proximal gonad. Prior to fertilisation, staining was observed in the cytoplasm of oocytes. However following fertilisation and completion of meiosis, staining was observed in both oocyte and sperm pronuclei. Following cleavage, staining was observed in a cell cycle dependent manner, with staining of all nuclei during interphase and prophase, and cytoplasmic staining evident following breakdown and entry into M phase. This staining pattern persisted until around the initiation of gastrulation (24-28 cells). Labelling was also observed in the cortical membrane at all stages of the cell cycle.

My aim however was not to characterise CDC-25.1 distribution in wild-type, but to determine whether there was any difference in the protein distribution between wild-type and mutant. I first compared the staining of our CDC-25.1 antibody with of Ashcroft *et al.*, (1999). Staining was present in the germline of adults and in oocytes. The protein was also detected in the nucleus and cortical membranes in embryos until approximately the 100-cell stage (Figure 5.17). As with the western data (Clucas *et al.*, 2002), the staining could be competed with one of the peptides ("peptide B"). This immunolocalisation data is consistent with that observed by Ashcroft *et al.*, (1999) with the exception that with our CDC-25.1 antibody, staining persisted in most or all nuclei until around the 100-cell stage, whereas Ashcroft *et al.*, (1999) observed staining until only the 28 cell stage. The intensity of staining observed with our CDC-25.1 antibody clearly declines as the number of embryonic cells increase, consistent with its provision as a maternal product. Staining was

also observed in the developing germline. The detectible presence of the protein in the embryo is consistent with the timing of the generation of extra intestinal cells in the mutant and the abundance of the protein in the developing germline is consistent with its essential role in germline proliferation

Anti-CDC-25.1 staining on *lin-60(ij48)* embryos gave an identical pattern to wild-type. There was no difference in the pattern or intensity of immunofluorescent detection of the CDC-25.1 protein in the cells of the E lineage that could readily explain the tissue-specific nature of the *lin-60(ij48)* phenotype (Figure 5.17). For example, there was no difference in the intensity of the staining between E and its sister lineage blastome,MS, at the level of detection which I could observe. Also, staining did not persist for longer in the descendants of E. I therefore concluded that the *lin-60 (ij48)* phenotype is not explained by the gross distribution of CDC-25.1 protein.

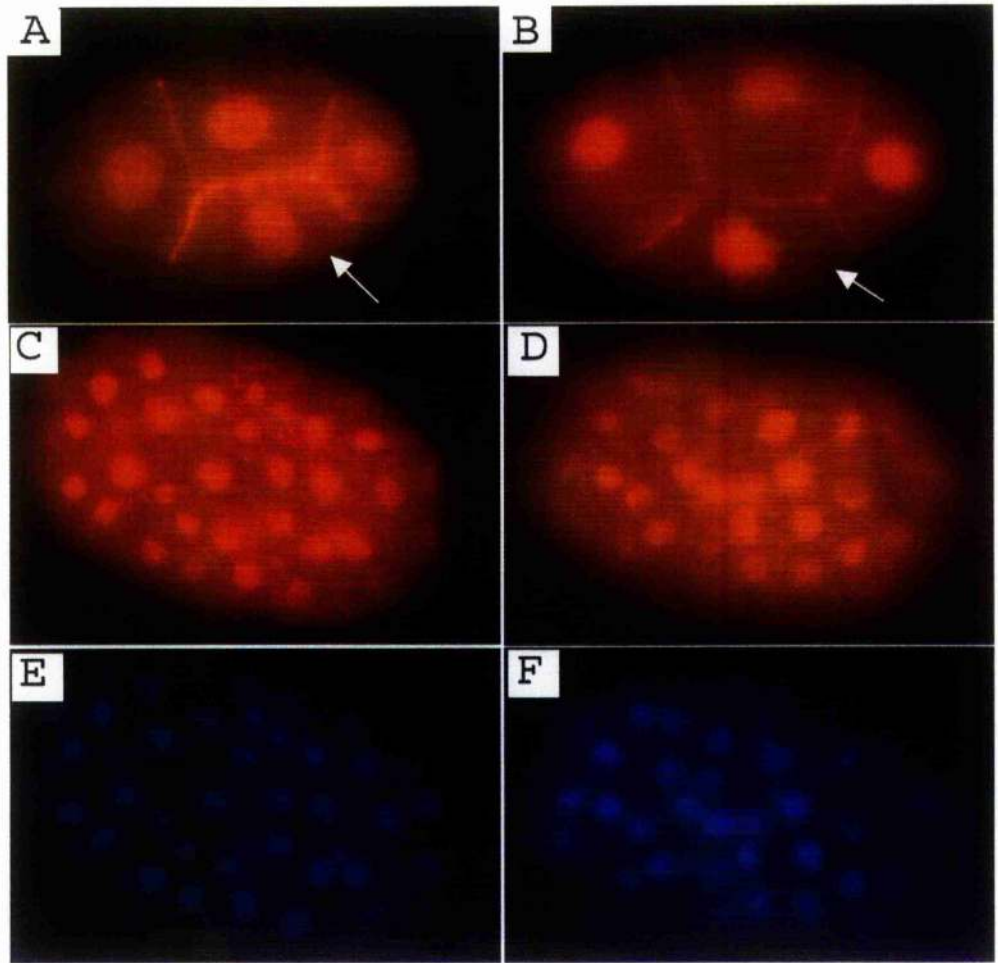


Figure 5.17 Detection of the CDC-25.1 protein. (A-D) Immunofluorescent detection of CDC-25.1 is shown in *C.elegans* embryos with anti-CDC-25.1 antibody. The embryos in (C) and (D) were co-stained with DAPI to detect all nuclei, shown in (E) and (F) respectively. (A) is wild type, (B) is *lin-60(ij48)*, both at 4 cell stage, the embryonic blastomere EMS is marked with a white arrow (this cell is the parent of the E and MS blastomeres). CDC-25.1 is detected in the nuclei of all four blastomeres at this stage in wild type and *lin-60(ij48)*. Staining of the boundaries of the cells is also seen. Both patterns of staining are competed by peptide B. (C-F) are approximately 40-50 cell stage embryos, (C) and (E) are wild type, (D) and (F) are *lin-60(ij48)*. The CDC-25.1 protein is detected in most or all nuclei of both as seen by comparing anti-CDC-25.1 staining in (C) and (D) with the DAPI co-stained images (E) and (F).

5.12. RNAi with *wee-1.1* and *wee-1.3*

CDC25 is a phosphatase that removes inhibitory phosphates, thus activating CDC2. The inhibitory kinases of CDC2 are members of the Wee-1/Mik-1 family of kinases. Phosphorylation by these kinases prevent progression of the cell cycle from G2 to M phase.

There are three *wee-1* like kinases in *C. elegans* (*wee-1.1*, *wee-1.2* and *wee-1.3*), although *wee-1.2* is thought to be a pseudogene as no cDNAs have been identified (Wilson *et al.*, 1999). *in situ* analysis with *wee-1.1* gives a staining pattern which is both temporally and spatially restricted (Wilson *et al.*, 1999). Expression of *wee-1.1* was first observed in the nucleus of the E blastomere in the 12-cell stage embryo and later in 8 descendents of the AB blastomere at the 16-cell stage. Staining was not observed before or after these stages. Since staining was observed in the F blastomere, I decided to perform RNAi with *wee-1.1* to examine whether it phenocopied the *lin-60(ij48)* phenotype. dsRNA corresponding to *wee-1.1* was injected into IA109 hermaphrodites and the phenotype of the F1 progeny examined. No F1 progeny displayed the *lin-60(ij48)* phenotype.

RNAi of *wee-1.3* had previously been shown to cause sterility in the P₀, due to premature exit of the most proximal oocytes from diakinesis (A. Golden, personal communication). I also performed RNAi with *wee-1.3*, and *wee-1.3* in combination with *wee-1.1*. In both cases, the injected worms became sterile and thus progeny could not be examined for the *lin-60(ij48)* phenotype.

5.13. Discussion

This chapter has described my attempts to clone *lin-60(ij48)*. It has dealt with the problems encountered, the most significant being that *lin-60* is a maternal gene and the *ij48* allele is dominant. By multiple crossovers on both chromosomes, it seemed probable that only one mutant gene was responsible for the phenotype observed in *lin-60(ij48)* hermaphrodites. However, the possibility that closely linked extraneous mutations may also be present could not be ignored. I mapped the left breakpoint of the deficiency *hDf8* to the cosmid R10A10, in or between the genes R10A10.1 and R10A10.2. This data will also help other researchers whilst attempting to clone other genes in this region. Since mapping data (Chapter 4) suggested that *lin-60(ij48)* maps very close to *let-604(h293)*, I also decided to place this gene on the physical map. This data suggested that *let-604(h293)* should lie within the cosmids R10A10, F37E3, T23H2, K06A5 or C55B7. My RNAi data, together with data from Fraser *et al.*, 2000, suggests that apart from *cdc-25.1*, the only other genes from these cosmids, which give a positive RNAi assay, are K06A5.4, F37E3.1, C55B7.2 and C55B7.5. All of these genes give embryonic lethality when subject to RNAi. Given the position of *let-604(h293)* and its sterile phenotype similar to the *cdc-25.1* null allele, *nr2036*, it is possible that *let-604(h293)* is another allele of *cdc-25.1*. Further investigation such as complementation tests, and if appropriate, sequencing of *cdc-25.1* in *let-604(h293)* background should be carried out. If this is an allele of *cdc-25.1*, it would be interesting to determine if *let-604(h293)* it is a true null (as is the case with the deletion mutant). A series of alleles ranging from complete loss of function to gain of function would help both with the characterisation of the gene and the significance of each mutation present in each allele. However when mapping with *let-604(h293)*, I did not observe suppression of the *lin-60(ij48)* mutant phenotype when placed over *let-604(h293)*.

As stated in Section 5.1, genes where only a dominant allele exists are rarely cloned. If an attempt is made at cloning these genes, it is usually by a more molecular approach. However, I have demonstrated that RNAi can be used as a tool to clone genes identified by dominant alleles. Moreover, it can be used to modulate the intestinal hyperplasia of *lin-60(ij48)*.

In chapter 4 and this chapter, I have provided evidence that *lin-60(ij48)* is a gain-of-function allele of the cell cycle phosphatase CDC25 (CDC-25.1). Since *cdc-25.1* was a previously identified gene, I may now refer *lin-60(ij48)* as *cdc-25.1(ij48)*. I have shown that the gain-of-function allele *cdc-25.1(ij48)* causes excessive proliferation of intestinal cells and its reduction by RNAi causes a failure of proliferation of a variety of cell types

including intestinal cells. The opposite effects associated with loss and gain demonstrates that *cdc-25.1* plays a critical role in the correct control of cell proliferation during *C. elegans* development.

Cdc25 phosphatase was initially discovered in yeast as a mitosis promoting factor (Russell and Nurse, 1986). This gene is an essential regulator of the cell cycle (Figure 5.18). Three isoforms have been discovered in mammalian cells, Cdc25A, B and C. One of the best documented functions of CDC25 is the dephosphorylation of Cdk1(Cdc2)/cyclin B on tyrosine-15 in the fission yeast *Schizosaccharomyces pombe*, and both threonine-14 and tyrosine-15 in higher eukaryotic cells which ultimately drives the cells into mitosis. Activated Cdk1/cyclinB phosphorylates target molecules, leading to nuclear envelope breakdown and spindle assembly (Heald and McKeon, 1990; Peter *et al.*, 1990).

In *C. elegans*, *cdc-25.1* is one of four *cdc25* homologues (Ashcroft *et al.*, 1998). The phenotype of hyperplasia associated with a hypermorphic gain-of-function allele in *cdc-25.1* is consistent with the known function of the CDC25 phosphatase family members as positive regulators of the eukaryotic cell cycle (Russell and Nurse, 1986; Kumagai and Dunphy, 1991; Draetta and Eckstein, 1997). The human *cdc25A* and *cdc25B* genes have been shown to be capable of co-operating with activated RAS to cause oncogenesis (Galaktionov *et al.*, 1995) and their over-expression has been found in some tumours (Hernandez *et al.*, 1998).

The mutation identified by *cdc-25.1(ij48)*, present at base 137 relative to ATG causes a predicted serine to phenylalanine substitution at residue 46 of the encoded protein CDC-25.1. By injection of *cdc-25.1(ij48)* fragment, I confirmed that the *cdc-25.1(ij48)* mutant gene was sufficient to generate the mutant phenotype, and hence directly responsible for the intestinal hyperplasia. The mutation is present in the N-terminal region of CDC25, a region which has been shown to be critical for CDC25 regulation and interaction with other proteins. The regulation of CDC25s is achieved by extensive phosphorylation in the N-terminal region (Kumagai and Dunphy, 1996; Kumagai *et al.*, 1998; Kumagai and Dunphy, 1999; Patra *et al.*, 1999). When aligning CE CDC-25.1, CE CDC25.2 and CB CDC-25.1, I found the short motif, SRDSG, to be perfectly conserved. It is the second serine of this motif that is affected by the S46F substitution. It is plausible that this serine may identify a site of interaction with protein(s) which negatively regulate CDC25. The large phenylalanine residue, present in *cdc-25.1(ij48)* may impede binding of molecules, which may be involved in the regulation of CDC25. Given the tissue specific

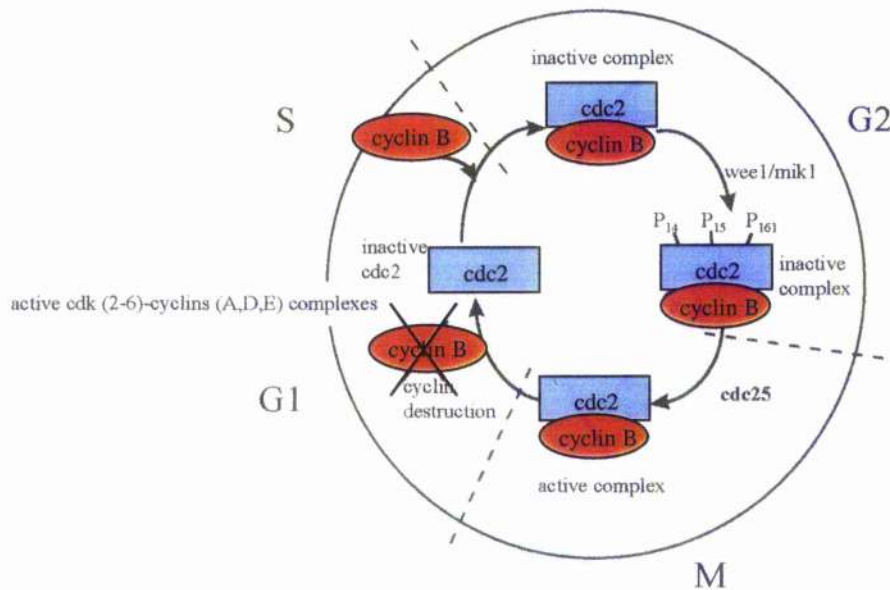


Figure 5.18 The vertebrate cell cycle.

The central components of the cell cycle are the Cdc2-like cyclin-dependent kinases and their associated cyclins (Cdc2/cdks). This figure illustrates the association between cyclin B (red) and cdc 2 (lilac) during the vertebrate cell cycle. Regulators of the Cdc2/cdks include the negative acting WEE1/MIK1 kinase that provides inhibitory phosphorylation of Cdc2/cdks and Cdc25 phosphatase that removes negative acting phosphates on Thr₁₄ and Tyr₁₅ from the Cdc2/cdks, which drives the cells into mitosis. To gain full activity, the cdk/cyclin complex undergoes phosphorylation on a conserved residue (Thr₁₆₁ in cdc2), catalysed by the Cdk-activating kinases, Cak. Figure adapted from Jessus and Ozon, 1995.

nature of the phenotype present in *cdc-25.1(ij48)* mutants, this may identify a site for intestinal specific regulation of CDC25.

The hyperplasia caused by the *cdc-25.1(ij48)* lesion is not dependent on mutation of any other genes as indicated by the ability of the mutant transgene to efficiently produce the intestinal hyperplasia when transformed into a wild-type strain of *C. elegans*. This demonstrates the direct oncogenic potential of this CDC25 family member in *C. elegans*. The suppression of the hyperplasia in a *cdc-25.1(ij48)* homozygote by partial *cdc-25.1* RNAi, demonstrates modulation of the oncogenic properties of this allele by administered RNAi.

The tissue specific nature of the *cdc-25.1(ij48)* hyperplasia cannot be explained by the spatial localisation of the protein in the early embryo. It is present in all early blastomeres and the *ij48* lesion does not alter this localisation. That the extra cell divisions resulting in hyperplasia are temporally restricted to embryonic development is consistent with the demonstrated temporal abundance of the protein, being present during early embryogenesis but rapidly depleting during subsequent embryonic cell divisions. As discussed in Section 5.11, the protein is also abundant in the developing germline and continues to be abundant as germline nuclei mature into oocytes and proceed through fertilisation. The *cdc-25.1(ij48)* allele shows a strict maternal pattern of inheritance consistent with its maternal supply to the developing oocyte and zygote. It therefore is probable that all of the CDC-25.1 protein present in the embryo is maternally supplied either as protein or mRNA. Thus the timing of extra cell divisions resulting in hyperplasia in the mutant is consistent with the temporal presence of the protein in the embryo.

The counteracting kinases of CDC2 are members of the WEE1 family of protein kinases. The mechanism controlling the interplay between CDC25 and WEE1, and how it is reversed at entry into M-phase is not known. Okumura *et al* (2002) speculated that the switch might be through a pathway involving the kinase Akt (or protein kinase B, PKB), where PKB was found to phosphorylate and downregulate a member of the Wee1 family, Myt1, in oocytes from the starfish *Asterina pectinifera*. In *C. elegans*, PKB has been shown to be involved in the regulation of dauer formation (Paradis and Ruvkin, 1998). In *cdc-25.1(ij48)* mutants, the balance of WEE1 and CDC25 may be in favour of CDC25 in the intestine. Interestingly, the transcript of *wee-1.1* is induced at the 12 cell stage in the E blastomere, disappearing when E divides for the first time (Wilson *et al.*, 1999). Although I observed no phenotype with RNAi of *wee-1.1*, it is conceivable that it may be acting in a redundant pathway with another Cdk inhibitor. In *S. pombe*, mutations in *wee1* gene are

not lethal, due to the presence of the redundant family member *mik1*. Double mutants *wee1 mik1* undergo mitotic catastrophe, as these cells attempt mitosis before the completion of S phase (Lundgren *et al.*, 1991). A single *wee1* gene has been found in *Drosophila* and mutations in this have no zygotic defects but *wee1* is required maternally for completing the embryonic cell cycles (Campbell *et al.*, 1995). An interesting experiment would be to perform *wee1.1* RNAi in the *cdc-25.1(ij48)* background. In fission yeast, *wee1+* activity is required to prevent lethal premature mitosis in cells that overproduce *cdc25+* (Russell and Nurse, 1986).

To conclude, I have identified a mutation in *cdc-25.1* present in *lin-60(ij48)* mutants. I have shown that a PCR-amplified DNA fragment containing the *ij48* mutant copy of *cdc-25.1* is sufficient to generate the intestinal cell hyperplasia. In contrast, removal of *cdc-25.1* in the *cdc-25.1(ij48)* background suppresses the intestinal cell hyperplasia. The distribution of the CDC-25.1 protein in the *cdc-25.1(ij48)* mutant does not explain the intestinal specific hyperplasia.

Chapter 6.

Final discussion

6.1. Summary of Results

The work presented in this thesis has been concerned with the identification and characterisation of mutants involved in the execution of the E-lineage in the nematode *Caenorhabditis elegans*. I have used a novel genetic screen and identified 4 classes of viable mutants with an altered E-cell development, reflecting both embryonic and post-embryonic development of E. I identified two mutants with extra intestinal cells, which were born during embryogenesis. I have characterised these two independent loci, *lin-60(ij48)* and *lin-62(ij52)*, in detail. The characterisation of *lin-60(ij48)* and *lin-62(ij52)* suggests although *C. elegans* has evolved to assemble tissues and organs with an effectively invariant cell lineage (Sulston and Horvitz, 1977; Sulston *et al.*, 1983), it has the flexibility to deal successfully with many extra cells, at least as far as the morphogenesis of the intestine is concerned. I cloned *lin-60(ij48)* using a novel RNAi-based approach and found that it identifies a *C. elegans* homologue of the cell cycle control gene Cdc25. This gene had been previously named *cdc-25.1* (Ashcroft *et al.*, 1998).

Two other classes of mutant having phenotypic defects in intestinal post-embryonic nuclear divisions were identified; one class causes a failure of post-embryonic nuclear division in the intestine whereas the other class generates additional post-embryonic nuclear divisions in the intestine. The final class, identified as having abnormal gut morphology, may cause a structural defect in the intestine.

6.2. Lineage mutations causing defective E-cell lineage

6.2.1. *lin-60(ij48)* is a maternal gene and identifies the cell cycle gene CDC-25.1

lin-60(ij48) was identified as a maternal gene and *ij48* was identified as being a partial gain-of-function allele of *cdc-25.1*. E-cell lineage analysis was performed on four embryos. Although all four reached 16E cell stage by the same cleavage pattern as wild type, it was reached at a faster pace. Moreover, the lineage following 16E differed between each embryo and thus the mutation identified by *ij48* generates a true hyperplasia of the intestine. In contrast, reduction of *cdc-25.1* causes a failure of proliferation in a variety of cell types including intestinal cells. The opposite effects associated with loss and gain demonstrates that *cdc-25.1* plays a critical role in the correct control of cell proliferation

during *C. elegans* development. The phenotype of hyperplasia associated with a hypermorphic gain-of-function allele in *cdc-25.1* is consistent with the known function of the CDC25 phosphatase family members as positive regulators of the eukaryotic cell cycle (Russell and Nurse, 1986; Kumagai and Dunphy, 1991; Draetta and Eckstein, 1997). The human *cdc25A* and *cdc25B* genes have been shown to be capable of co-operating with activated RAS to cause oncogenesis (Galaktionov *et al.*, 1995), and their overexpression has been found in some tumours (Hernandez *et al.*, 1998). Interestingly, mammalian Cdc25A expression has been shown to be upregulated by c-Myc and has been found to exhibit oncogenic properties (Galaktionov *et al.*, 1996). However, to date, this is the first description of the direct oncogenic capability of Cdc25.

The hyperplasia caused by the *cdc-25.1(ij48)* lesion is not dependent on mutation of any other genes, as indicated by the ability of the mutant transgene to produce the intestinal hyperplasia efficiently when transformed into a strain of *C. elegans* that was either wild-type for *cdc-25.1*, or was a null mutant of *cdc-25.1*. This demonstrates the direct oncogenic potential of this CDC25 family member in *C. elegans*. The suppression of the hyperplasia in a *cdc-25.1(ij48)* homozygote by partial CDC-25.1 RNAi demonstrates modulation of the oncogenic properties of this allele by administered RNAi. The *cdc-25.1(ij48)* phenotype could not be explained by the distribution of CDC-25.1 protein as identical staining patterns were observed between *cdc-25.1(ij48)* and wild-type animals. However the detectable presence of the protein in the embryo is consistent with the timing of the generation of extra intestinal cells in the mutant.

CDC25s are essential regulators of the cell cycle and their classic role is in the dephosphorylation of CDC2 that promotes entry into M-phase. To avoid execution of mitosis at inappropriate points of the cell cycle, the activity of Cdc2/Cyclin B is tightly regulated. As Cyclin B is synthesised, it binds to Cdc2, which is inactive in its monomeric form. Although the Cdc2/Cyclin B complex is potentially active at the time of formation, it is held in check during interphase by phosphorylation on two sites on Cdc2, Tyr₁₅ and Thr₁₄ (Norbury *et al.*, 1991; Krek *et al.*, 1992; Solomon *et al.*, 1992). Wee1, a nuclear enzyme is capable of phosphorylation of both these residues. Myt1, a membrane bound enzyme, can catalyse only the phosphorylation of Thr₁₄ (Atherton-Fessler *et al.*, 1994; Kornbluth *et al.*, 1994; Watanabe *et al.*, 1995; McGowan and Russell, 1995; Mueller *et al.*, 1995a; Mueller *et al.*, 1995b; Liu *et al.*, 1997). At G2/M, Tyr₁₅ and Thr₁₄ are rapidly dephosphorylated by the dual-specific Cdc25 phosphatase (Dunphy and Kumagai, 1991; Millar and Russell, 1992).

Four *cdc25s* have been identified in *C. elegans* (Ashcroft *et al.*, 1998) and the mutation identified by *ij48* is present in the N-terminal region of *cdc-25.1* and generates a predicted Ser-Phe substitution. The fact that cell types other than those of the E lineage in *cdc-25.1(ij48)* homozygotes are unaffected indicates that the mutant CDC-25.1(S46F) protein is performing its role in a manner similar to wild type in other tissues, as far as I could determine. There is certainly no similar shortening of the cell cycle in cells derived from blastomeres other than E.

6.2.2. The site of the *cdc-25.1(ij48)* lesion identifies a conserved motif which may be involved in its regulation.

The serine affected by the *ij48* lesion lies in a conserved domain, SRDSG, which is shared by CECDC-25.1, CECDC-25.2 and the *C. Briggsae* orthologue of CECDC-25.1, CBCDC-25.1. Moreover, the N-terminal region of CDC25s has been found to be the regulatory domain of the molecule, whereas the C-terminus is the catalytic domain. It is known that CDC25 becomes highly phosphorylated and activated at mitosis. Since serines can be subject to phosphorylation, the serine that is mutated in *cdc-25.1(ij48)* may be subject to phosphorylation and may control protein-protein interactions. Given the tissue specific nature of the *cdc-25.1(ij48)* defect, the conserved domain may be a site of binding of regulatory molecules that gives rise to lineage specific regulation of CDC-25.1. It is probable that this domain identifies a site of negative regulation of the molecule where E tissue specific regulators interact and that other regions of CDC-25.1 will be necessary for its correct regulation in other cell types. Alternatively, the introduction of a phenylalanine residue may impede the binding of regulatory molecules at another site. A set of asymmetric cell divisions during early embryogenesis generates five somatic founder cells from the zygote, AB, MS, E, C and D plus the germline founder P4. These blastomeres then undergo sets of cell divisions to produce the various tissues of the organism. The periodicity of the cell division cycles is distinct for the cell lineages derived from each somatic founder cell (Sulston and Horvitz, 1977; Sulston *et al.*, 1983) and are achieved at least in part through tissue-specific regulation of a *C. elegans* CDC25. Lineage specific control of CDC25 has been shown in other systems. In leech embryos, there is lineage specific regulation of *cdc25* where the levels of *cdc25* RNA remain constant throughout the cell cycle of some cells, but fluctuate throughout the cell cycles of other cells (Bissen, 1995). Cdc25 also regulates the timing of the asynchronous cell divisions of postblastoderm *Drosophila* embryos (Edgar and O'Farrell, 1990).

The identification of molecules that are involved in the regulation of Cdc25 is an active area of research. It has been shown that activated Cdk1/cyclinB can phosphorylate Cdc25, creating a positive feedback loop, leading to full activation of Cdk1 and entry into mitosis (Kumagai and Dunphy, 1992; Hoffmann *et al.*, 1993).

Other molecules may also be involved in the initiation of this autocatalytic loop. One such molecule is the peptidyl-prolyl-isomerase Pin1. Overexpression of Pin1 in HeLa cells causes G2 arrest, implicating Pin1 as a negative regulator of mitosis (Lu *et al.*, 1996). In *Xenopus*, it has been demonstrated that Pin1 interacts with Cdc25 (Crenshaw *et al.*, 1998; Shen *et al.*, 1998). Pin1 catalyses rotation around the peptide bond preceding proline residues and binding of Pin1 to Cdc25 is dependent upon M-phase specific phosphorylations on Ser/Thr-Pro residues of Cdc25 (Crenshaw *et al.*, 1998; Shen *et al.*, 1998). It has been postulated that Pin1 plays a part in mitosis progression via sequence specific and phosphorylation-dependent proline isomerisation. Pin-1 binds peptides containing phosphorylated Ser-Pro flanked by hydrophobic residues or Arg (Yaffe *et al.*, 1997a). The SRDSG motif is therefore unlikely to confer a Pin1 binding domain.

14-3-3 proteins are involved in numerous signal transduction pathways. They have been shown to bind to a critical phosphoserine of human Cdc25C (Ser₂₁₆) and *Xenopus* Cdc25C (Ser₂₈₇), and thereby negatively regulate its function (Peng *et al.*, 1997; Sanchez *et al.*, 1997). In *Xenopus*, two 14-3-3 proteins have been shown to bind to the inactive form of Cdc25 and serve to suppress the activation of Cdc25 throughout interphase (Kumagai *et al.*, 1998). There are two 14-3-3 genes in *C. elegans*, *fit-1* and *fit-2* (Wang and Shakes, 1997). FTT-1 has recently been shown to have a role in determining anterior-posterior cell polarity (Morton *et al.*, 2002). Interestingly, *in-situ* studies have shown that *fit-2* transcripts are found in the intestine and gonad in comma stage embryos, although the function of *fit-2* is not known and no mutants have been identified. Two 14-3-3 motifs have been reported: RSXpSXP and RX[Y/F]XpSXP (Yaffe *et al.*, 1997b), the middle serine residues being phosphorylated. These motifs are conserved in many proteins such as Raf, *Xenopus* Cdc25 and human Cdc25. In *C. elegans* CDC-25.1, there is a possible FTT binding site at around residue 290 (Neville Ashcroft, personal communication), however this does not follow the exact motif reported in the literature. Although 14-3-3 can tolerate a few minor changes to this motif and still bind, a FTT motif is not found at the extreme amino terminal of CDC-25.1. It is therefore unlikely that the SRDSG domain is a 14-3-3 binding site.

The Polo-like kinases have multiple roles during the cell cycle and have also been implicated to be involved in the activation of Cdc25. A *Xenopus* homologue, Plx1, was

isolated by virtue of its association with Cdc25 *in vitro*, where Plx1 was found to bind, phosphorylate and stimulate the phosphatase activity of *Xenopus* Cdc25C (Kumagai and Dunphy, 1996). Recently, human Plk1 has been shown to promote nuclear translocation of human Cdc25C during prophase, which in turn activates the M-phase promoting factor (Toyoshima-Morimoto *et al.*, 2002). Polo-like kinases have also been shown to be required for the functional maturation of mitotic centrosomes (Sunkel and Glover, 1988), and regulation of the activity of the Anaphase-Promoting Complex (APC), whose activation is required for entry into anaphase (Kotani *et al.*, 1998; Shirayama *et al.*, 1998). The APC is responsible for the targeted destruction of several cell cycle regulatory proteins including Cyclin B and proteins involved in sister chromatid cohesion (Cohen-Fix *et al.*, 1996). Members of the Polo-like kinase family have also been shown to play a role in cytokinesis (Nigg, 1998; Carmena *et al.*, 1998). Using RNAi, a *C. elegans* Polo-like kinase homologue, *plk-1*, was found to be required for nuclear envelope breakdown and completion of meiosis (Chase *et al.*, 2000). *plk-1* dsRNA treated hermaphrodites give rise to a brood of single-celled embryos and although fertilisation occurs, there is a delay in nuclear envelope breakdown, a defect in polar body formation, extrusion, and defects in chromosome segregation.

Although the tissue specific nature of the *cdc-25.1(ij48)* hyperplasia could not be explained by the spatial or temporal localisation of the protein in the early embryo, I examined whether the SRDSG motif identifies a domain essential for protein turnover. A human homologue of *C. elegans* CDC-25.1, Cdc25A is activated by phosphorylation (Hoffmann *et al.*, 1994) and its abundance is regulated by the ubiquitin-proteasome pathway (Mailand *et al.*, 2000). Ubiquitylation and subsequent degradation via the proteasome represent a fundamental mechanism for regulating protein abundance through an irreversible mechanism (Pickart, 2001). The system operates by transferring ubiquitin moieties to protein substrates via a series of enzymatic reactions catalysed by E1, E2 and E3 enzymes, the latter being the determinant for target selectivity and timing of degradation (Hochstrasser, 1996; Hershko, 1997). Mutagenesis experiments have demonstrated that substitution of the serine residues in the glycogen synthase kinase 3 β (GSK3 β) phosphorylation consensus motif in β -catenin inhibits ubiquitination, and results in stabilisation of the protein (Aberle *et al.*, 1997). This motif, DSGfXS, where f is a hydrophobic residue, is similar to the sequence flanking the mutation in *cdc-25.1(ij48)*. The sequence SRDSDVSM is mutated to the sequence SRDPGVSM in *cdc-25.1(ij48)*.

There is therefore clear similarity between the DSGVS sequence and the GSK3 β consensus. A similar motif (DpSGLDpS), where pS represents a phosphoserine is present in I κ B (inhibitor of NF κ B), is required for the phosphorylation dependent degradation of I κ B via the ubiquitin-proteasome pathway. Therefore, although I did not detect a difference in the abundance of CDC-25.1 in *cdc-25.1(ij48)*, if the mutated domain identifies a site that results in inhibition of ubiquitination and stabilisation of the protein, it is possible that CDC-25.1 may persist for longer in the mutant. A *C. elegans* GSK-3 homologue, SGG-1, has been found to act positively in the *C. elegans* Wnt pathway and may identify a branch point in the transduction of the Wnt signal that both reorients the EMS mitotic spindle and induces endoderm from EMS (Schlessinger *et al.*, 1999).

To conclude, an SRDSG motif, found in CECDC-25.1, CECDC-25.2 and CBCDC-25.1 is mutated to SRDFG in the *cdc-25.1(ij48)*. No conservation of this domain was found in the sequence of any other Cdc25s present in the current databases, although it does have a similarity to a GSK3 β and I κ B binding domain. The SRDSG motif is in the N-terminal end of the protein, a region that is involved in the regulation of CDC25 but is divergent between CDC25s of different organisms.

6.2.3 Other roles and functions of CDC25

In addition to a positive regulatory role in promoting mitosis, Cdc25 phosphatases are the target of negative regulation of the cell cycle. In yeast and vertebrate cells, inactivation of Cdc25 phosphatases are required for checkpoint controls that mediate cell cycle arrest in G₂ following irradiation (Furnari *et al.*, 1997; Peng *et al.*, 1997; Sanchez *et al.*, 1997).

It has also been shown that Cdc25 can also play a part in orchestrating other phases of the cell cycle, other than G₂-M phase. Human Cdc25A is necessary for the regulation of G₀ to S-phase where Cdc25A can act as a target of the Cdk2/Cyclin E complex at the G₁/S transition, creating a positive autoregulatory feedback loop (Hoffmann *et al.*, 1994, Blomberg and Hoffmann, 1999). Questions that need to be addressed are therefore, at which point of the cell cycle does CDC-25.1 play its role and whether Cyclin E has a role in the hyperplasia displayed by the *ij48* allele.

Other substrates of Cdc25 have also been identified. Interestingly, in mammalian proliferating cells, Cdc25A has also been shown to interact, dephosphorylate (serine residues) and increase the binding activity of the homeodomain transcription factor Cut

(Coqueret *et al.*, 1998). These authors showed that Cut acts as a transcriptional repressor which downregulates transcription of the CDK inhibitor, p21^{WAF1/CIP1/SDI1} in S phase controlling the G1 to S transition. In *Drosophila*, Cut has been shown to be involved in the determination and maintenance of the cell-type specificity of a variety of tissues (Bodmer *et al.*, 1987; Blochlinger *et al.*, 1990; Jack *et al.*, 1991; Liu *et al.*, 1991; Liu and Jack, 1992).

6.2.4. E-cell development of *cdc-25.1(ij48)* and *lin-62(ij52)* must be correctly coordinated with developmental cues.

There must be a molecular basis to the lineage dependent temporal regulation of the cell cycle such that the central regulators of the cell cycle function at different periodicities. This aspect of cell cycle control is clearly defective in the cells generated from the E blastomere in *cdc-25.1(ij48)* mutants. When the E-cell lineage is compared between the wild-type and *cdc-25.1(ij48)* mutant, it is evident that the cell cycle is shortened in the mutant. This shortening of the cell cycle periodicity is specific to E and as discussed above, it is probable that the *ij48* lesion identifies a site on CDC-25.1 necessary for E-specific control of the cell cycle in *C. elegans*. However, the shortening of the cell cycle in E in *cdc-25.1(ij48)* is not evident until after gastrulation has commenced. In *lin-62(ij52)*, extra cells are generated after the 16E stage, at least in the embryo that was lineaged. Thus all negative regulators of the cell cycle must function in E at least until after the initiation of gastrulation in *cdc-25.1(ij48)* and until 16E in *lin-62(ij52)*.

Gastrulation and morphogenesis in *C. elegans* is initiated by the descendants of the E blastomere, Ea and Ep migrating to the centre of the embryo. This creates a fissure, known as the ventral cleft, through which other cells subsequently migrate. Maternal effect mutations in any of the genes *gad-1*, *emb-5*, *emb-13*, *emb-16*, *emb-23* or *emb-31* cause failure of either the initiation or the later stages of gastrulation (Knight and Wood, 1998; Denich *et al.*, 1984; Nishiwaki *et al.*, 1993). In all of these mutants, the Ea and Ep divisions occur prematurely and often in an anterior/posterior rather than the normal left-right orientation. It has also been shown that blocking zygotic transcription by RNAi of RNA polymerase II, results in premature Ea and Ep divisions (Powell-Coffman *et al.*, 1996). These embryos arrest with approximately 100 cells but divide with a normal pattern of cell divisions until the 26-cell stage. This would suggest that zygotic genes are essential for the initiation of gastrulation, that these are regulated by maternal effect genes and zygotic transcription is not required for cycling until the 100 cell stage (Powell-Coffman *et*

al., 1996; Edgar *et al.*, 1994). The CDC-25.1 protein is detectable prior to gastrulation (Ashcroft *et al.*, 1999; Clucas *et al.*, 2002). Thus in *cdc-25.1(ij48)* mutants, cell cycle regulators must be able to suppress extra divisions in E prior to the onset of gastrulation, up to the second round of cell divisions. *in-situ* studies have shown that *wee-1.1* is transcribed at this time, suggesting that *wee-1.1* may play a role in preventing mitotic chaos in *cdc-25.1(ij48)* mutants.

The morphogenesis of the intestines of *cdc-25.1(ij48)* and *lin-62(ij52)* have not been studied although antibody staining revealed that the extra intestinal cells are incorporated into the intestine. The intestine of *C. elegans* is asymmetrical, a phenomenon which becomes evident during cell intercalation at 16E, where three of the anterior cells in the right row of the primordium move counterclockwise to the left, as the contralateral three left cells move simultaneously towards the right (Sulston *et al.*, 1983; Leung *et al.*, 1999). This morphogenic movement generates a left-handed twist of around 90°, which increases to 180° following attachment of the intestine to the pharyngeal-intestinal valve, by the time the larva hatches (Sulston *et al.*, 1977). It has been suggested that this asymmetry may influence subsequent morphogenesis of the gonad. Formation of the intestinal twist involves cell-cell interactions between E and cells from other lineages, and asymmetric expression of genes in the E lineage, including molecules that are involved in the Notch-like signalling pathway (Hermann *et al.*, 2000). The intestinal twist in *cdc-25.1(ij48)* and *lin-62(ij52)* mutants has not been examined. However, if a twist forms in the intestine of these mutants, the E-derived cells must be able to orient themselves to receive external cues and differentially express genes in a manner similar to wild type. Regardless of whether a twist forms, the intestine is functional in *cdc-25.1(ij48)* and *lin-62(ij52)* mutants.

6.3. Future Work

6.3.1. Further genetic screens to identify mutants with an altered E-lineage

As discussed in Chapter 3, the genetic screen I performed did not reach saturation. Additional genetic screens should therefore be performed. It would also be useful to obtain additional alleles of the mutants generated.

6.3.2. Characterisation and cloning of mutants with mononucleate and binucleate cells

Cloning the wild-type copy of the genes identified by *ij49*, *ij50* and *ij51* would also be an area of interest. Since these mutants are altering nuclear number, they probably define genes that are involved in the cell-cycle. These mutants do not display general loss of/excessive post-embryonic cell divisions and therefore may identify molecules and/or motifs in molecules that are necessary for post-embryonic E cell cycle control. The mutant alleles identified as having additional nuclear divisions in the intestine may identify intestinal-specific heterochronic genes, such that the L1 nuclear division is repeated during L2.

The genetics of these mutants should also be studied. These alleles are recessive to wild-type, however each allele should be placed over a deficiency to determine whether it is a null. Genetic crosses should be performed to determine whether these genes function in the same genetic pathway. If these genes function in a common pathway, one would expect a degree of epistasis. If however they act in parallel pathways, some enhancement would be apparent.

6.3.3. Identification of molecules that bind to the SRDSG motif in CDC25

It would clearly be of interest to identify molecules that may interact with the SRDSG motif and examine differences between wild type and *cdc-25.1(ij48)*. Since an antibody reacting to CDC-25.1 is available, it should be possible to co-precipitate proteins that bind to CDC-25.1. Comparisons could be made between wild type and *cdc-25.1(ij48)* cell extracts to test for differential binding of proteins between wild-type and mutant.

Alternatively, a suppressor screen may be performed. If *ij48* prevents binding of a regulator to CDC-25.1, it may be possible to generate a compensating mutation in that regulator, thus suppressing *ij48*.

6.3.4. The role of POP-1 in the E-cell lineage

One mutant I would have expected to isolate from the screens was a mutant where all intestinal cells are equivalent at 8E cell stage, which would generate 32 intestinal cells. As discussed in Chapter 4, I did not obtain such a mutant; *cdc-25.1(ij48)* homozygotes generated worms with varying numbers of intestinal cells and *lin-62(ij52)* did not display this pattern of divisions. One molecule that may be involved in generating diversity in the progenitors of E is POP-1.

POP-1 is present in multiple cells during embryogenesis (Lin *et al.*, 1998). It has been postulated that POP-1 may be part of a general mechanism that couples cell division sequence to different patterns of gene expression in sister cells born from anterior-posterior cell lineages. Moreover, POP-1 is distributed asymmetrically between E_{xxxxa} and E_{xxxxp} (i.e. anterior-posterior daughters of the fourth round of E-cell lineage). In the E-cell lineage, the divisions that occur in the anterior at the 16E-cell stage (E_{alaa} and E_{araa}) are dorsal-ventral whereas the divisions that occur in the posterior (E_{plpp} and E_{prpp}) are anterior-posterior. The role for zygotic POP-1 has recently been investigated using a novel technique (Herman, 2001). This author performed POP-1 RNAi in an RNAi-resistant mutant background, *rde-1*. The *rde-1(ne219)* mutant (Tabara *et al.*, 1999) is a recessive loss-of-function mutation that confers maternal and zygotic resistance to RNAi. However, if RNAi-treated hermaphrodites are crossed with wild type males, the progeny are sensitive to RNAi of zygotic genes (Herman, 2001). A similar method could therefore be used to elucidate the role of zygotic POP-1 in the E-cell lineage. Previous studies have shown that POP-1 has roles in establishing anterior-posterior patterning in the intestine: it has a role in anterior-posterior patterning in differentiating which cells undergo the intestinal twist and the patterning of a terminally differentiated intestinal gene, *ges-1* (Schroeder and McGhee, 1997). Loss of maternal POP-1 results in the MS blastomere adopting an E-like fate. By using this genetic trick developed by Herman, 2001, it might be possible to examine whether zygotic POP-1 has a role in determining the polarity of the E-lineage.

6.3.5. Cloning the gene identified by *lin-62(ij52)*

In Chapter 4, I mapped *lin-62(ij52)* to a defined region on chromosome IV. This region spans around 50 cosmids. Since *lin-62* identifies a zygotic gene and *ij52* is recessive to wild type, cloning of this gene by transgenesis should be relatively straightforward. Further screens should also be performed (e.g. non-complementation screens) to identify additional alleles of this gene.

Reference List

- Aberle, H., Bauer, A., Stappert, J., Kispert, A., and Kemler, R. (1997). Beta-catenin is a target for the ubiquitin-proteasome pathway. *EMBO Journal* **16**, 3797-3804.
- Ambros, V. and Horvitz, H.R. (1984). Heterochronic mutants of the nematode *Caenorhabditis elegans*. *Science* **226**, 409-416.
- Ambros, V. (1999). Cell cycle-dependent sequencing of cell fate decisions in *Caenorhabditis elegans* vulva precursor cells. *Development* **126**, 1947-1956.
- Anderson (1995) Mutagenesis. In *Caenorhabditis elegans: Modern Biological Analysis of an Organism* (eds. Epstein, H.F. and Shakes, D.C.), pp. 31-58. Academic Press. San Diego.
- Ashcroft, N.R., Kosinski, M.E., Wickramasinghe, D., Donovan, P.J., and Golden, A. (1998). The four *cdc25* genes from the nematode *Caenorhabditis elegans*. *Gene* **214**, 59-66.
- Ashcroft, N.R., Srayko, M., Kosinski, M.E., Mains, P.E., and Golden, A. (1999). RNA-mediated interference of a *cdc25* homolog in *Caenorhabditis elegans* results in defects in the embryonic cortical membrane, meiosis, and mitosis. *Developmental Biology* **206**, 15-32.
- Atherton-Fessler, S., Liu, F., Gabrielli, B., Lee, M.S., Peng, C.Y., and Piwnica-Worms, H. (1994). Cell cycle regulation of the p34(Cdc2) inhibitory kinases. *Molecular Biology of the Cell* **5**, 989-1001.
- Barnes, T.M., Kohara, Y., Coulson, A., and Hekimi, S. (1995). Meiotic recombination, noncoding DNA and genomic organization in *Caenorhabditis elegans*. *Genetics* **141**, 159-179.
- Batchelder, C., Dunn, M.A., Choy, B., Suh, Y., Cassie, C., Shim, E.Y., Shin, T.H., Mello, C., Seydoux, G., and Blackwell, T. K. (1999). Transcriptional repression by the *Caenorhabditis elegans* germ-line protein PIE-1. *Genes & Development* **13**, 202-212.
- Bissen, S.T. (1995). Expression of the cell-cycle control gene, *cdc25*, is constitutive in the segmental founder cells but is cell-cycle regulated in the micromeres of leech embryos. *Development* **121**, 3035-3043.
- Blochlinger, K., Bodmer, R., Jan, L.Y., and Jan, Y.N. (1990). Patterns of expression of Cut, a protein required for external sensory organ development in wild-type and *cut* mutant *Drosophila* embryos. *Genes & Development* **4**, 1322-1331.
- Blomberg, I. and Hoffmann, I. (1999). Ectopic expression of Cdc25A accelerates the G(1)/S transition and leads to premature activation of cyclin E- and cyclin A- dependent kinases. *Molecular and Cellular Biology* **19**, 6183-6194.

- Blumenthal, T., Squire, M., Kirtland, S., Cane, J., Donegan, M., Spieth, J., and Sharrock, W. (1984). Cloning of a yolk protein gene family from *Caenorhabditis elegans*. *Journal of Molecular Biology* **174**, 1-18.
- Bodmer, R., Barbel, S., Sheperd, S., Jack, J.W., Jan, L.Y., and Jan, Y.N. (1987). Transformation of sensory organs by mutations of the *cut* locus of *Drosophila melanogaster*. *Cell* **51**, 293-307.
- Bosher, J.M., Dufourcq, P., Sookhareea, S., and Labouesse, M. (1999). RNA interference can target pre-mRNA: Consequences for gene expression in a *Caenorhabditis elegans* operon. *Genetics* **153**, 1245-1256.
- Bowerman, B., Eaton, B.A., and Priess, J.R. (1992a). *skn-1*, a maternally expressed gene required to specify the fate of ventral blastomeres in the early *C.elegans* embryo. *Cell* **68**, 1061-1075.
- Bowerman, B., Tax, F. E., Thomas, J. H., and Priess, J. R. (1992b). Cell-interactions involved in development of the bilaterally symmetrical intestinal valve cells during embryogenesis in *Caenorhabditis elegans*. *Development* **116**, 1113-1122.
- Bowerman, B., Draper, B.W., Mello, C. C., and Priess, J.R. (1993). The maternal gene *skn-1* encodes a protein that is distributed unequally in early *C.elegans* embryos. *Cell* **74**, 443-452.
- Bowerman, B. (1998). Maternal control of pattern formation in early *Caenorhabditis elegans* embryos. *Current Topics in Developmental Biology* **39**, 73-117.
- Boxem, M., Srinivasan, D.G., and van den Heuvel, S. (1999). The *Caenorhabditis elegans* gene *ncc-1* encodes a *cdc2*-related kinase required for M phase in meiotic and mitotic cell divisions, but not for S phase. *Development* **126**, 2227-2239.
- Brantjes, H., Roose, J., van de Wetering, M., and Clevers, H. (2001). All Tcf HMG box transcription factors interact with Groucho-related co-repressors. *Nucleic Acids Research* **29**, 1410-1419.
- Brenner, S. (1974). The genetics of *Caenorhabditis elegans*. *Genetics* **77**, 71-94.
- Britton, C., McKerrow, J.H., and Johnstone, I.L. (1998). Regulation of the *Caenorhabditis elegans* gut cysteine protease gene *cpr-1*: Requirement for GATA motifs. *Journal of Molecular Biology* **283**, 15-27.
- Brunner, E., Peter, O., Schweizer, L., and Basler, K. (1997). *pangolin* encodes a Lef-1 homologue that acts downstream of Armadillo to transduce the Wingless signal in *Drosophila*. *Nature* **385**, 829-833.
- C.elegans* sequencing consortium (1998). Genomic sequence of the nematode *C.elegans*: A platform for investigating biology. *Science* **282**, 2012-2018.

- Cadigan, K.M. and Nusse, R. (1997). Wnt signaling: a common theme in animal development. *Genes & Development* **11**, 3286-3305.
- Calvo, D., Victor, M., Gay, F., Sui, G., Luke, M.P.S., Dufourcq, P., Wen, G. Y., Maduro, M., Rothman, J., and Shi, Y. (2001). A POP-1 repressor complex restricts inappropriate cell type-specific gene transcription during *Caenorhabditis elegans* embryogenesis. *EMBO Journal* **20**, 7197-7208.
- Campbell, S.D., Sprenger, F., Edgar, B.A., and O'Farrell, P.H. (1995). *Drosophila* Wee1 kinase rescues fission yeast from mitotic catastrophe and phosphorylates *Drosophila* CDC2 *in vitro*. *Molecular Biology of the Cell* **6**, 1333-1347.
- Carmena, M., Riparbelli, M.G., Minestrini, G., Tavares, A. M., Adams, R., Callaini, G., and Glover, D. M. (1998). *Drosophila* Polo kinase is required for cytokinesis. *Journal of Cell Biology* **143**, 659-671.
- Chalfie, M. and White, J. (1988). The nervous system. In *The Nematode Caenorhabditis elegans* (ed. Wood, W.B.), pp. 337-391. Cold Spring Harbor Laboratory Press, Cold Spring Harbor, NY.
- Chalfie, M., Horvitz, H.R., and Sulston, J.E. (1981). Mutations that lead to reiterations in the cell lineages of *C. elegans*. *Cell* **24**, 59-69.
- Chasc, D., Serafinas, C., Ashcroft, N., Kosinski, M., Longo, D., Ferris, D.K., and Golden, A. (2000). The Polo-like kinase PLK-1 is required for nuclear envelope breakdown and the completion of meiosis in *Caenorhabditis elegans*. *Genesis* **26**, 26-41.
- Chen, G.Q., Fernandez, J., Mische, S., and Courey, A. J. (1999). A functional interaction between the histone deacetylase Rpd3 and the corepressor Groucho in *Drosophila* development. *Genes & Development* **13**, 2218-2230.
- Clark, S.G., Lu, W.X., and Horvitz, H.R. (1994). The *Caenorhabditis elegans* locus *lin-15*, a negative regulator of a tyrosine kinase signalling pathway, encodes two different proteins. *Genetics* **137**, 987-997.
- Clucas, C., Cabello, J., Bussing, I., Schnabel, R., and Johnstone, I.L. (2002). Oncogenic potential of a *C.elegans* *cdc25* gene is demonstrated by a gain-of-function allele. *The EMBO Journal* **21**, 665-674.
- Cohen-Fix, O., Peters, J.M., Kirschner, M.W., and Koshland, D. (1996). Anaphase initiation in *Saccharomyces cerevisiae* is controlled by the APC-dependent degradation of the anaphase inhibitor Pds1p. *Genes & Development* **10**, 3081-3093.
- Coqueret, O., Berube, G., and Nepveu, A. (1998). The mammalian Cut homeodomain protein functions as a cell-cycle dependent transcriptional repressor which downmodulates p21^(WAF1/CIP1/SDI1) in S phase. *EMBO Journal* **17**, 4680-4694.

- Crenshaw, D.G., Yang, J., Means, A.R., and Kornbluth, S. (1998). The mitotic peptidyl-prolyl isomerase, Pin1, interacts with Cdc25 and Plx1. *EMBO Journal* **17**, 1315-1327.
- Cubitt, A.B., Heim, R., Adams, S.R., Boyd, A.E., Gross, L.A., and Tsien, R.Y. (1995). Understanding, improving and using green fluorescent proteins. *Trends in Biochemical Sciences* **20**, 448-455.
- Denich, K.T.R., Schierenberg, E., Isnenghi, E., and Cassada, R. (1984). Cell lineage and developmental defects of temperature-sensitive embryonic arrest mutants of the nematode *Caenorhabditis elegans*. *Wilhelm Roux's Archives of Developmental Biology* **193**, 164-179.
- Draetta, G. and Eckstein, J. (1997). Cdc25 protein phosphatases in cell proliferation. *Biochimica et Biophysica Acta-Reviews on Cancer* **1332**, M53-M63.
- Dunphy, W.G. and Kumagai, A. (1991). The Cdc25 protein contains an intrinsic phosphatase activity. *Cell* **67**, 189-196.
- Edgar, B.A. and O'Farrell, P.H. (1990). The 3 postblastoderm cell-cycles of *Drosophila* embryogenesis are regulated in G2 by String. *Cell* **62**, 469-480.
- Edgar, B.A. and Orr-Weaver, T.L. (2001). Endoreplication cell cycles: More for less. *Cell* **105**, 297-306.
- Edgar, L.G. and McGhee, J.D. (1986). Embryonic expression of a gut-specific esterase in *Caenorhabditis elegans*. *Developmental Biology* **114**, 109-118.
- Edgar, L.G., Wolf, N., and Wood, W.B. (1994). Early transcription in *Caenorhabditis elegans* embryos. *Development* **120**, 443-451.
- Egan, C. R., Chung, M.A., Allen, F.L., Heschl, M.F.P., Vanbuskirk, C.L., and McGhee, J.D. (1995). A gut-to-pharynx tail switch in embryonic expression of the *Caenorhabditis elegans* *ges-1* gene centers on 2 GATA sequences. *Developmental Biology* **170**, 397-419.
- Fay, D.S. and Han, M. (2000). Mutations in *cye-1*, a *Caenorhabditis elegans* cyclin E homolog, reveal coordination between cell-cycle control and vulval development. *Development* **127**, 4049-4060.
- Fire, A. (1986). Integrative transformation of *Caenorhabditis elegans*. *EMBO Journal* **5**, 2673-2680.
- Fire, A., Albertson, D., Harrison, S., and Mocrman, D. (1991). Production of antisense RNA leads to effective and specific inhibition of gene expression in *C.elegans* muscle. *Development* **113**, 503-514.
- Fire, A., Xu, S. Q., Montgomery, M.K., Kostas, S.A., Driver, S.E., and Mello, C. (1998). Potent and specific genetic interference by double-stranded RNA in *Caenorhabditis elegans*. *Nature* **391**, 806-811.

- Francis, G.R. and Waterston, R.H. (1985). Muscle organization in *C. elegans*: Localization of proteins implicated in thin filament attachment and I-band organization. *Journal of Cell Biology* **101**, 1532-1549.
- Francis, R., Maine, E., and Schedl, T. (1995). Analysis of the multiple roles of GLD-1 in germline development - interactions with the sex determination cascade and the GLP-1 signalling pathway. *Genetics* **139**, 607-630.
- Fraser, A.G., Kamath, R.S., Zipperlen, P., Martinez-Campos, M., Sohrmann, M., and Ahringer, J. (2000). Functional genomic analysis of *C.elegans* chromosome I by systematic RNA interference. *Nature* **408**, 325-330.
- Fukushige, T., Hawkins, M.G., and McGhee, J.D. (1998). The GATA-factor *elt-2* is essential for formation of the *Caenorhabditis elegans* intestine. *Developmental Biology* **198**, 286-302.
- Furnari, B., Rhind, N., and Russell, P. (1997). Cdc25 mitotic inducer targeted by Chk1 DNA damage checkpoint kinase. *Science* **277**, 1495-1497.
- Galaktionov, K., Jessus, C., and Beach, D. (1995). Raf1 interaction with Cdc25 phosphatase ties mitogenic signal transduction to cell-cycle activation. *Genes & Development* **9**, 1046-1058.
- Galaktionov, K., Chen, X. C., and Beach, D. (1996). Cdc25 cell-cycle phosphatase as a target of c-myc. *Nature* **382**, 511-517.
- Goldstein, B. (1992). Induction of gut in *Caenorhabditis elegans* embryos. *Nature* **357**, 255-257.
- Goldstein, B. (1993). Establishment of gut fate in the E-lineage of *C.elegans* - the roles of lineage-dependent mechanisms and cell-interactions. *Development* **118**, 1267-1277.
- Goldstein, B. (1995a). An analysis of the response to gut induction in the *C.elegans* embryo. *Development* **121**, 1227-1236.
- Goldstein, B. (1995b). Cell contacts orient some cell division axes in the *Caenorhabditis elegans* embryo. *The Journal of Cell Biology* **129**, 1071-1080.
- Gonczy, P., Echeverri, C., Oegema, K., Coulson, A., Jones, S.J.M., Copley, R.R., Duperon, J., Oegema, J., Brchm, M., Cassin, E., Hannak, E., Kirkham, M., Pichler, S., Flohrs, K., Goessen, A., Leidel, S., Alleaume, A. M., Martin, C., Ozlu, N., Bork, P., and Hyman, A.A. (2000). Functional genomic analysis of cell division in *C.elegans* using RNAi of genes on chromosome III. *Nature* **408**, 331-336.
- Grewal, S.I. and Elgin, S.C. (2002). Heterochromatin: new possibilities for the inheritance of structure. *Current Opinion in Genetics & Development* **12**, 178-187.
- Grishok, A., Tabara, H., and Mello, C.C. (2000). Genetic requirements for inheritance of RNAi in *C.elegans*. *Science* **287**, 2494-2497.

- Guo, S. and Kemphues, K.J. (1995). *par-1*, a gene required for establishing polarity in *C. elegans* embryos, encodes a putative Ser/Thr kinase that is asymmetrically distributed. *Cell* **81**, 611-620.
- Han, M. (1997). Gut reaction to Wnt signaling in worms. *Cell* **90**, 581-584.
- Heald, R. and McKeon, F. (1990). Mutations of phosphorylation sites in Lamin-A that prevent nuclear Lamina disassembly in mitosis. *Cell* **61**, 579-589.
- Hedgecock, E.M. and White, J.G. (1985). Polyploid tissues in the nematode *Caenorhabditis elegans*. *Developmental Biology* **107**, 128-133.
- Heim, R., Prasher, D.C., and Tsien, R. Y. (1994). Wavelength mutations and posttranslational autoxidation of green fluorescent protein. *Proceedings of the National Academy of Sciences of the United States of America* **91**, 12501-12504.
- Heim, R., Cubitt, A.B., and Tsien, R.Y. (1995). Improved Green Fluorescence. *Nature* **373**, 663-664.
- Henikoff, S., Jackson, J.M., and Talbert, P.B. (1995). Distance and pairing effects on the *brown* Dominant heterochromatic element in *Drosophila*. *Genetics* **140**, 1007-1017.
- Henikoff, S. (1996). Dosage-dependent modification of position-effect variegation in *Drosophila*. *Bioessays* **18**, 401-409.
- Herman, M.A. (2001). *C.elegans* POP-1/TCF functions in a canonical Wnt pathway that controls cell migration and in a noncanonical Wnt pathway that controls cell polarity. *Development* **128**, 581-590.
- Herman, R. K. (1988) Genetics. In *The Nematode Caenorhabditis elegans* (ed. Wood, W.B.), pp. 17-46. Cold Spring Harbour Laboratory Press, Cold Spring Harbour, NY.
- Herrmann, G.J., Leung, B., and Priess, J.R. (2000). Left-right asymmetry in *C.elegans* intestine organogenesis involves a LIN-12/Notch signaling pathway. *Development* **127**, 3429-3440.
- Hernandez, S., Hernandez, L., Bea, S., Cazorla, M., Fernandez, P.L., Nadal, A., Muntane, J., Mallofre, C., Montserrat, E., Cardesa, A., and Campo, E. (1998). Cdc25 cell cycle-activating phosphatases and c-myc expression in human non-Hodgkin's lymphomas. *Cancer Research* **58**, 1762-1767.
- Hershko, A. (1997). Roles of ubiquitin-mediated proteolysis in cell cycle control. *Current Opinion in Cell Biology* **9**, 788-799.
- Hirsh, D., Oppenheim, D., and Klass M (1976). Development of the reproductive system of *C.elegans*. *Developmental Biology* **49**, 200-219.
- Hochstrasser, M. (1996). Protein degradation or regulation: Ub the judge. *Cell* **84**, 813-815.

- Hodgkin, J. (1985). Novel nematode amber suppressors. *Genetics* **111**, 287-310.
- Hodgkin, J. (1997) *Genetics*. In *C.elegans II* (eds. Riddle, D.L., Blumenthal, T., Meyer, B.J and Priess, J.R.), pp. 881-1047. Cold Spring Harbor Laboratory Press, Cold Spring Harbor, NY.
- Hodgkin, J. and Herman, R. K. (1998). Changing styles in *C.elegans* genetics. *Trends in Genetics* **14**, 352-357.
- Hoffmann, I., Clarke, P.R., Marcote, M.J., Karsenti, E., and Draetta, G. (1993). Phosphorylation and activation of human Cdc25C by Cdc2 CyclinB and its involvement in the self amplification of MPF at mitosis. *EMBO Journal* **12**, 53-63.
- Hoffmann, I., Draetta, G., and Karsenti, E. (1994). Activation of the phosphatase-activity of human Cdc25A by a cdk2 Cyclin-E dependent phosphorylation at the G(1)/S transition. *EMBO Journal* **13**, 4302-4310.
- Hong, Y., Roy, R., and Ambros, V. (1998). Developmental regulation of a cyclin-dependent kinase inhibitor controls postembryonic cell cycle progression in *Caenorhabditis elegans*. *Development* **125**, 3585-3597.
- Howell, A.M., Gilmour, S.G., Mancebo, R.A., and Rose, A.M. (1987). Genetic analysis of a large autosomal region in *Caenorhabditis elegans* by the use of a free duplication. *Genetical Research* **49**, 207-213.
- Huang, L.S., Tzou, P., and Sternberg, P.W. (1994). The *lin-15* locus encodes two negative regulators of *Caenorhabditis elegans* vulval development. *Molecular Biology of the Cell* **5**, 412-
- Hunter, C. P. and Kenyon, C. (1996). Spatial and temporal controls target *pal-1* blastomere-specification activity to a single blastomere lineage in *C.elegans* embryos. *Cell* **87**, 217-226.
- Hutter, H. and Schnabel, R. (1995). Specification of anterior-posterior differences within the AB lineage in the *C.elegans* embryo - a polarizing induction. *Development* **121**, 1559-1568.
- Ishitani, T., Ninomiya-Tsuji, J., Nagai, S., Nishita, M., Meneghini, M., Barker, N., Waterman, M., Bowerman, B., Clevers, H., Shibuya, H., and Matsumoto, K. (1999). The TAK1-NLK-MAPK-related pathway antagonizes signalling between beta-catenin and transcription factor TCF. *Nature* **399**, 798-802.
- Izumi, T., Walker, D.H., and Maller, J.L. (1992). Periodic changes in phosphorylation of the *Xenopus* Cdc25 phosphatase regulate its activity. *Molecular Biology of the Cell* **8**, 927-939.
- Jack, J., Dorsett, D., Delotto, Y., And Liu, S. (1991). Expression of the Cut Locus in the *Drosophila* wing margin is required for cell type specification and is regulated by a distant enhancer. *Development* **113**, 735-747.

- Jessus, C. and Ozon, R. (1995). Function and regulation of *cdc25* protein phosphate through mitosis and meiosis. *Progress in Cell Cycle Research* **1**, 215-228.
- Johnsen, R.C. and Baillie, D.L. (1997) Mutation. In *C. elegans II* (eds. Riddle, D.L., Blumenthal, T., Meyer, B.J and Priess, J.R.) pp. 79-95. Cold Spring Harbor Laboratory Press, Cold Spring Harbor, NY.
- Johnstone, I.L., Shafi, Y., and Barry, J.D. (1992). Molecular analysis of mutations in the *Caenorhabditis elegans* collagen gene *dpy-7*. *The EMBO Journal* **11**, 3857-3863.
- Johnstone, I. L. (1999) Molecular biology. In *C.elegans. A Practical Approach* (ed Hope, I.A.), pp. 201-225. Oxford University Press. New York.
- Kadyk, L.C. and Kimble, J. (1998). Genetic regulation of entry into meiosis in *Caenorhabditis elegans*. *Development* **125**, 1803-1813.
- Kelly, W. G., Xu, S.Q., Montgomery, M.K., and Fire, A. (1997). Distinct requirements for somatic and germline expression of a generally expressed *Caenorhabditis elegans* gene. *Genetics* **146**, 227-238.
- Kemphues, K.J. and Strome, S (1997) Fertilization and Embryonic Polarity. In *C. elegans II* (eds. Riddle, D.L., Blumenthal, T., Meyer, B.J and Priess, J.R.) pp335-359. Cold Spring Harbor Laboratory Press, Cold Spring Harbor, NY.
- Kennerdell, J.R. and Carthew, R.W. (1998). Use of dsRNA-mediated genetic interference to demonstrate that *frizzled* and *frizzled 2* act in the wingless pathway. *Cell* **95**, 1017-1026.
- Ketting, R.F., Haverkamp, T.H.A., van Luenen, H.G.A.M., and Plasterk, R.K.H. (1999). *mut-7* of *C.elegans*, required for transposon silencing and RNA interference, is a homolog of Werner syndrome helicase and RNaseD. *Cell* **99**, 133-141
- Kimble, J. and Hirsh, D. (1979). The postembryonic cell lineages of the hermaphrodite and male gonads in *Caenorhabditis elegans*. *Developmental Biology* **70**, 396-417.
- Kimble J.E. (1981). Strategies for control of pattern formation in *C. elegans*. *Philosophical Transactions of the Royal Society of London* **295B**, 539-551.
- Kimble, J.E. and White, J.G. (1981). On the control of germ-cell development in *Caenorhabditis elegans*. *Developmental Biology* **81**, 208-219.
- Kipreos, E.T., Landcr, L.E., Wing, J.P., He, W.W., and Hedgecock, E.M. (1996). *cul-1* is required for cell-cycle exit in *C. elegans* and identifies a novel gene family. *Cell* **85**, 829-839.
- Kipreos, E. T., Gohel, S. P., and Hedgecock, E. M. (2000). The *C.elegans* F-box/WD-repeat protein LIN-23 functions to limit cell division during development. *Development* **127**, 5071-5082.

- Knight, J.K. and Wood, W.B. (1998). Gastrulation initiation in *Caenorhabditis elegans* requires the function of *gad-1*, which encodes a protein with WD repeats. *Developmental Biology* **198**, 253-265.
- Kondo, K., Makovec, B., Waterston, R.H., and Hodgkin, J. (1990). Genetic and molecular analysis of 8 transfer RNA^{TIP} amber suppressors in *Caenorhabditis elegans*. *Journal of Molecular Biology* **215**, 7-19.
- Kornbluth, S., Sebastian, B., Hunter, T., And Newport, J. (1994). Membrane localization of the kinase which phosphorylates p34(cdc2) on threonine-14. *Molecular Biology of the Cell* **5**, 273-282.
- Kotani, S., Tugendreich, S., Fujii, M., Jorgensen, P. M., Watanabe, N., Hoog, C., Hieter, P., and Todokoro, K. (1998). PKA and MPF-activated polo-like kinase regulate anaphase-promoting complex activity and mitosis progression. *Molecular Cell* **1**, 371-380.
- Kramer, J.M., French, R.P., Park, E.C., and Johnson, J.J. (1990). The *Caenorhabditis elegans* *rol-6* gene, which interacts with the *sqt-1* collagen gene to determine organismal morphology, encodes a collagen. *Molecular and Cellular Biology* **10**, 2081-2089.
- Krause, M., Harrison, S.W., Xu, S.Q., Chen, L.S., and Fire, A. (1994). Elements regulating cell-specific and stage-specific expression of the *C.elegans* MyoD family homolog *hlh-1*. *Developmental Biology* **166**, 133-148.
- Krek, W., Marks, J., Schmitz, N., Nigg, E.A., and Simanis, V. (1992). Vertebrate p34(Cdc2) phosphorylation site mutants - effects upon cell-cycle progression in the fission yeast *Schizosaccharomyces pombe*. *Journal of Cell Science* **102**, 43-53.
- Kumagai, A. and Dunphy, W.G. (1991). The CDC25 protein controls tyrosine dephosphorylation of the CDC2 protein in a cell-free system. *Cell* **64**, 903-914.
- Kumagai, A. and Dunphy, W.G. (1992). Regulation of the Cdc25 protein during the cell-cycle in *Xenopus* extracts. *Cell* **70**, 139-151.
- Kumagai, A. and Dunphy, W.G. (1996). Purification and molecular cloning of Plx1, a Cdc25-regulatory kinase from *Xenopus* egg extracts. *Science* **273**, 1377-1380.
- Kumagai, A., Yakowec, P.S., and Dunphy, W.G. (1998). 14-3-3 proteins act as negative regulators of the inducer Cdc25 in *Xenopus* egg extracts. *Molecular Biology of the Cell* **9**, 345-354.
- Kumagai, A. and Dunphy, W.G. (1999). Binding of 14-3-3 proteins and nuclear export control the intracellular localization of the mitotic inducer Cdc25. *Genes & Development* **13**, 1067-1072.
- Labouesse, M. and Mango, S.E. (1999). Patterning the *C.elegans* embryo - moving beyond the cell lineage. *Trends in Genetics* **15**, 307-313.

- Larminie, C.G.C. and Johnstone, I.L. (1996). Isolation and characterization of four developmentally regulated cathepsin B-like cysteine protease genes from the nematode *Caenorhabditis elegans*. *DNA and Cell Biology* **15**, 75-82.
- Larminie, C.G.C. (1995) PhD Thesis. University of Glasgow, UK.
- Leung, B., Hermann, G.J., and Priess, J.R. (1999). Organogenesis of the *Caenorhabditis elegans* intestine. *Developmental Biology* **216**, 114-134.
- Lin, R.L., Thompson, S., and Priess, J.R. (1995). *pop-1* encodes an HMG box protein required for the specification of a mesoderm precursor in early *C.elegans* embryos. *Cell* **83**, 599-609.
- Lin, R. L., Hill, R.J., and Priess, J.R. (1998). POP-1 and anterior-posterior fate decisions in *C.elegans* embryos. *Cell* **92**, 229-239.
- Liu, S., Mcleod, F. And Jack, J. (1991). 4 distinct regulatory regions of the *cut* locus and their effect on cell type spccification in drosophila. *Genetics* **127**, 151-159.
- Liu, F., Stanton, J.J., Wu, Z.Q., and Piwnica-Worms, H. (1997). The human Myt1 kinase preferentially phosphorylates Cdc2 on threonine 14 and localizes to the endoplasmic reticulum and Golgi complex. *Molecular and Cellular Biology* **17**, 571-583.
- Liu, S. And Jack, J. (1992). Regulatory interactions and role in cell type specification of the malpighian tubules by the Cut, Kruppel, and Caudal genes of *Drosophila*. *Developmental Biology* **150**, 133-143.
- Liu, Z. and Ambros, V. (1989). Heterochronic genes control the stage-specific initiation and expression of the dauer larva developmental program in *Caenorhabditis elegans*. *Genes & Development* **3**, 2039-2049.
- Lu, K.P., Hancs, S. D., and Hunter, T. (1996). A human peptidyl-prolyl isomerase essential for regulation of mitosis. *Nature* **380**, 544-547.
- Lundgren, K., Walworth, N., Booher, R., Dembski, M., Kirschner, M., and Beach, D. (1991). Mik1 and Wee1 cooperate in the inhibitory tyrosine phosphorylation of Cdc2. *Cell* **64**, 1111-1122.
- MacMorris, M., Broverman, S., Greenspoon, S., Lea, K., Madej, C., Blumenthal, T., and Spieth, J. (1992). Regulation of vitellogenin gene-expression in transgenic *Caenorhabditis elegans* - short sequences required for activation of the *vit-2* promoter. *Molecular and Cellular Biology* **12**, 1652-1662.
- Maduro, M.F., Meneghini, M.D., Bowerman, B., Broitman-Maduro, G., and Rothman, J.H. (2001). Restriction of mesendoderm to a single blastomere by the combined action of SKN-1 and a GSK-3 beta homolog is mediated by MED-1 and-2 in *C.elegans*. *Molecular Cell* **7**, 475-485.

- Maduro, M.F. and Rothman, J. H. (2002). Making worm guts: The gene regulatory network of the *Caenorhabditis elegans* endoderm. *Developmental Biology* **246**, 68-85.
- Mailand, N., Falck, J., Lukas, C., Syljuasen, R.G., Welcker, M., Bartek, J., and Lukas, L. (2000). Rapid destruction of human Cdc25A in response to DNA damage. *Science* **288**, 1425-1429.
- Mango, S.E., Thorpe, C.J., Martin, P.R., Chamberlain, S.H., and Bowerman, B. (1994). 2 maternal genes, *apx-1* and *pie-1*, are required to distinguish the fates of equivalent blastomeres in the early *Caenorhabditis elegans* embryo. *Development* **120**, 2305-2315.
- McCarter, J., Bartlett, B., Dang, T., and Schedl, T. (1997). Soma-germ cell interactions in *Caenorhabditis elegans*: Multiple events of hermaphrodite germline development require the somatic sheath and spermathecal lineages. *Developmental Biology* **181**, 121-143.
- McCarter, J., Bartlett, B., Dang, T., and Schedl, T. (1999). On the control of oocyte meiotic maturation and ovulation in *Caenorhabditis elegans*. *Developmental Biology* **205**, 111-128.
- McDowall, J. S. and Rose, A. M. (1997a). Genetic analysis of sterile mutants in the *dpy-5 unc-13* (I) genomic region of *Caenorhabditis elegans*. *Molecular & General Genetics* **255**, 60-77.
- McDowall, J. S. and Rose, A.M. (1997b). Alignment of the genetic and physical maps in the *dpy-5 bli-4* (I) region of *C. elegans* by the serial cosmid rescue of lethal mutations. *Molecular & General Genetics* **255**, 78-95.
- McGowan, C.H. and Russell, P. (1995). Cell-cycle regulation of human WEE1. *EMBO Journal* **14**, 2166-2175.
- McKim, K. S., Starr, T., and Rose, A. M. (1992). Genetic and molecular analysis of the *dpy-14* region in *Caenorhabditis elegans*. *Molecular & General Genetics* **233**, 241-251.
- Mello, C. and Fire, A. (1995) DNA Transformation. In *Caenorhabditis elegans. Modern Biological analysis of an organism* (eds. Epstein, H.F. and Shakes, D.C.), pp. 451-482. Academic Press. San Diego
- Mello, C.C., Kramer, J. M., Stinchcomb, D., and Ambros, V. (1991). Efficient gene-transfer in *C.elegans* - extrachromosomal maintenance and integration of transforming sequences. *EMBO Journal* **10**, 3959-3970.
- Mello, C.C., Draper, B. W., and Priess, J.R. (1994). The maternal genes *apx-1* and *glp-1* and establishment of dorsal-ventral polarity in the early *C.elegans* embryo. *Cell* **77**, 95-106.
- Mello, C.C., Schubert, C., Draper, B., Zhang, W., Lobel, R., and Priess, J.R. (1996). The PIE-1 protein and germline specification in *C.elegans* embryos. *Nature* **382**, 710-712.
- Meneghini, M.D., Ishitani, T., Carter, J.C., Hisamoto, N., Ninomiya-Tsuji, J., Thorpe, C.J., Hamill, D.R., Matsumoto, K., and Bowerman, B. (1999). MAP kinase and Wnt pathways

- converge to downregulate an HMG- domain repressor in *Caenorhabditis elegans*. *Nature* **399**, 793-797.
- Millar, J.B.A. and Russell, P. (1992). The Cdc25 M-phase inducer - an unconventional protein phosphatase. *Cell* **68**, 407-410.
- Moerman, D.G. and Waterston, R.H. (1984). Spontaneous unstable *unc-22* IV mutations in *C.elegans* var Bergerac. *Genetics* **108**, 859-877.
- Molin, L., Mounsey, A., Aslam, S., Bauer, P., Young, J., James, M., Sharma-Oates, A., and Hope, I.A. (2000). Evolutionary conservation of redundancy between a diverged pair of forkhead transcription factor homologues. *Development* **127**, 4825-4835.
- Montgomery, M.K., Xu, S.Q., and Fire, A. (1998). RNA as a target of double-stranded RNA-mediated genetic interference in *Caenorhabditis elegans*. *Proceedings of the National Academy of Sciences of the United States of America* **95**, 15502-15507.
- Morton, D.G., Shakes, D.C., Nugent, S., Dichoso, D., Wang, W. F., Golden, A., and Kcmphues, K. J. (2002). The *Caenorhabditis elegans* *par-5* gene encodes a 14-3-3 protein required for cellular asymmetry in the early embryo. *Developmental Biology* **241**, 47-58.
- Moskowitz, I.P.G., Gendreau, S.B., and Rothman, J.II. (1994). Combinatorial specification of blastomere identity by GLP-1- dependent cellular interactions in the nematode *Caenorhabditis elegans*. *Development* **120**, 3325-3338.
- Mueller, P.R., Coleman, T.R., Kumagai, A., and Dunphy, W.G. (1995a). Myt1 - a membrane-associated inhibitory kinase that phosphorylates Cdc2 on both threonine-14 and tyrosine-15. *Science* **270**, 86-90.
- Mueller, P.R., Coleman, T.R., and Dunphy, W.G. (1995b). Cell-cycle regulation of a *Xenopus* Wee1-like kinase. *Molecular Biology of the Cell* **6**, 119-134.
- Newman-Smith, E.D. and Rothman, J.H. (1998). The maternal-to-zygotic transition in embryonic patterning of *Caenorhabditis elegans*. *Current Opinion in Genetics & Development* **8**, 472-480.
- Ngo, H., Tschudi, C., Gull, K., and Ullu, E. (1998). Double-stranded RNA induces mRNA degradation in *Trypanosoma brucei*. *Proceedings of the National Academy of Sciences of the United States of America* **95**, 14687-14692.
- Nigg, E.A. (1998). Polo-like kinases: positive regulators of cell division from start to finish. *Current Opinion in Cell Biology* **10**, 776-783.
- Nishiwaki, K., Sano, T., And Miwa, J. (1993). *emb-5*, a gene required for the correct timing of gut precursor cell-division during gastrulation in *Caenorhabditis elegans*, encodes a protein similar to the yeast nuclear-protein SPT6. *Molecular & General Genetics* **239**, 313-322.

- Norbury, C., Blow, J., and Nurse, P. (1991). Regulatory phosphorylation of the p34cdc2 protein kinase in vertebrates. *EMBO Journal* **10**, 3321-3329.
- O'Connell, K.F., Leys, C.M., and White, J.G. (1998). A genetic screen for temperature-sensitive cell-division mutants of *Caenorhabditis elegans*. *Genetics* **149**, 1303-1321.
- Okamoto, H. and Thomson, J.N. (1985). Monoclonal antibodies which distinguish certain classes of neuronal and support cells in the nervous tissue of the nematode *C. elegans*. *Journal of Neuroscience* **5**, 643-653.
- Okumura, E., Fukuhara, T., Yoshida, H., Hanada, S., Kozutsumi, R., Mori, M., Tachibana, K., and Kishimoto, T. (2002). Akt inhibits Myt1 the signalling pathway that leads to meiotic G2/M-phase transitions. *Nature Cell Biology* **4**, 111-116.
- Paradis, S. and Ruvkun, G. (1998). *Caenorhabditis elegans* Akt/PKB transduces insulin receptor-like signals from AGE-1 PI3 kinase to the DAF-16 transcription factor. *Genes & Development* **12**, 2488-2498.
- Park, M. and Krause, M. W. (1999). Regulation of postembryonic G(1) cell cycle progression in *Caenorhabditis elegans* by a cyclin D/CDK-like complex. *Development* **126**, 4849-4860.
- Patra, D., Wang, S. X., Kumagai, A., and Dunphy, W. G. (1999). The *Xenopus* Suc1/Cks protein promotes the phosphorylation of G(2)/M regulators. *Journal of Biological Chemistry* **274**, 36839-36842.
- Peng, C.Y., Graves, P.R., Thoma, R. S., Wu, Z. Q., Shaw, A.S., and Piwnicka-Worms, H. (1997). Mitotic and G(2) checkpoint control: Regulation of 14-3-3 protein binding by phosphorylation of Cdc25C on serine-216. *Science* **277**, 1501-1505.
- Peter, M., Nakagawa, J., Doree, M., Labbe, J. C., and Nigg, E. A. (1990). *In vitro* disassembly of the nuclear lamina and M phase-specific phosphorylation of lamins by cdc2 kinase. *Cell* **61**, 591-602.
- Pickart, C. M. (2001). Ubiquitin enters the new millennium. *Molecular Cell* **8**, 499-504.
- Platt, H. M. (1994) Forward. In *The phylogenetic systematics of free-living nematodes* (ed. S.Lorenzen), pp. i-ii. The Ray Society, London.
- Powell-Coffman, J.A., Knight, J., and Wood, W.B. (1996). Onset of *C. elegans* gastrulation is blocked by inhibition of embryonic transcription with an RNA-polymerase antisense RNA. *Developmental Biology* **178**, 472-483.
- Priess, J.R. and Thomson, J.N. (1987). Cellular interactions in early *C.elegans* embryos. *Cell* **48**, 241-250.
- Riddle, D.L. (1988) The Dauer Larva. In *The nematode Caenorhabditis elegans*. (ed. W.B.Wood), pp. 393-412. Cold Spring Harbor Laboratory, Cold Spring Harbor, NY.

- Riddle, D. L., Blumenthal, T., Meyer, B. J., and Priess, J. R. (1997) Introduction to *C.elegans*. In *C. elegans II* (eds. Riddle, D.L., Blumenthal, T., Meyer, B.J. and Priess, J.R.), pp. 1-22. Cold Spring Harbor Laboratory Press, Cold Spring Harbor, NY.
- Rocheleau, C.E., Downs, W.D., Lin, R. L., Wittmann, C., Bei, Y. X., Cha, Y. H., Ali, M., Priess, J.R., and Mello, C.C. (1997). Wnt signaling and an APC-related gene specify endoderm in early *C.elegans* embryos. *Cell* **90**, 707-716.
- Rocheleau, C. E., Yasuda, J., Shin, T. H., Lin, R. L., Sawa, H., Okano, H., Priess, J. R., Davis, R. J., and Mello, C. C. (1999). WRM-1 activates the LIT-1 protein kinase to transduce anterior posterior polarity signals in *C.elegans*. *Cell* **97**, 717-726.
- Roose, J., Molenaar, M., Peterson, J., Hurenkamp, J., Brantjes, H., Moerer, P., van de Wetering, M., Destree, O., and Clevers, H. (1998). The Xenopus Wnt effector XTcf-3 interacts with Groucho-related transcriptional repressors. *Nature* **395**, 608-612.
- Roose, J. and Clevers, H. (1999). TCF transcription factors: molecular switches in carcinogenesis. *Biochimica et Biophysica Acta-Reviews on Cancer* **1424**, M23-M37.
- Rubin, G.M., Yandell, M.D., Wortman, J.R., Miklos, G.L.G., Nelson, C.R., Hariharan, I.K., Fortini, M.E., Li, P.W., Apweiler, R., Fleischmann, W., Cherry, J.M., Henikoff, S., Skupski, M. P., Misra, S., Ashburner, M., Birney, E., Boguski, M. S., Brody, T., Brokstein, P., Celniker, S.E., Chervitz, S.A., Coates, D., Cravchik, A., Gabrielian, A., Galle, R.F., Gelbart, W.M., George, R.A., Goldstein, L.S.B., Gong, F.C., Guan, P., Harris, N.L., Hay, B.A., Hoskins, R. A., Li, J. Y., Li, Z. Y., Hynes, R. O., Jones, S. J. M., Kuehl, P. M., Lemaitre, B., Littleton, J.T., Morrison, D.K., Mungall, C., O'Farrell, P.H., Pickeral, O.K., Shue, C., Vosshall, L. B., Zhang, J., Zhao, Q., Zheng, X.Q.H., Zhong, F., Zhong, W.Y., Gibbs, R., Venter, J.C., Adams, M.D., and Lewis, S. (2000). Comparative genomics of the eukaryotes. *Science* **287**, 2204-2215.
- Russell, P. and Nurse, P. (1986). CDC25+ functions as an inducer in the mitotic control of fission yeast. *Cell* **45**, 145-153.
- Sambrook, J., Fritsch, E. F., and Maniatis, T. (1989). Molecular cloning: a laboratory manual. Cold Spring Laboratory Press, Cold Spring Harbor, NY.
- Sanchez, Y., Wong, C., Thoma, R.S., Richman, R., Wu, R.Q., Piwnica-Worms, H., and Elledge, S.J. (1997). Conservation of the Chk1 checkpoint pathway in mammals: Linkage of DNA damage to Cdk regulation through Cdc25. *Science* **277**, 1497-1501.
- Sawa, H., Lobel, L., and Horvitz, H.R. (1996). The *Caenorhabditis elegans* gene *lin-17*, which is required for certain asymmetric cell divisions, encodes a putative protein similar to seven-transmembrane protein similar to the *Drosophila* Frizzles protein. *Genes & Development* **10**, 2189-2197.
- Schlesinger, A., Shelton, C.A., Maloof, J.N., Meneghini, M., and Bowerman, B. (1999). Wnt pathway components orient a mitotic spindle in the early *Caenorhabditis elegans* embryo

- without requiring gene transcription in the responding cell. *Genes & Development* **13**, 2028-2038.
- Schnabel, R. and Priess, J. R. (1997) Specification of cell fates in the early embryo. In *C. elegans II* (eds. Riddle, D.L., Blumenthal, T., Meyer, B.J and Priess, J.R.), pp. 361-382. Cold Spring Harbor Laboratory Press, Cold Spring Harbor, NY.
- Schnabel, R., Hutter, H., Moerman, D., and Schnabel, H. (1997). Assessing normal embryogenesis in *Caenorhabditis elegans* using a 4D microscope: Variability of development and regional specification. *Developmental Biology* **184**, 234-265.
- Schroeder, D.F. and McGhee, J.D. (1997). Anterior-posterior patterning of the *Caenorhabditis elegans* endoderm. *Developmental Biology* **186**, S3-S3.
- Shen, M. H., Stukenberg, P. T., Kirschner, M. W., and Lu, K. P. (1998). The essential mitotic peptidyl-prolyl isomerase Pin1 binds and regulates mitosis-specific phosphoproteins. *Genes & Development* **12**, 706-720.
- Shi, Y. and Mello, C. (1998). A CBP/p300 homolog specifies multiple differentiation pathways in *Caenorhabditis elegans*. *Genes & Development* **12**, 943-955.
- Shirayama, M., Zachariae, W., Ciosk, R., and Nasmyth, K. (1998). The polo-like kinase Cdc5p and the WD-repeat protein Cdc20p/fizzy are regulators and substrates of the anaphase promoting complex in *Saccharomyces cerevisiae*. *EMBO Journal* **17**, 1336-1349.
- Siddiqui, S. S., Aamodt, E., Rastinejad, F., and Culotti, J. (1989). Anti-tubulin monoclonal-antibodies that bind to specific neurons in *Caenorhabditis elegans*. *Journal of Neuroscience* **9**, 2963-2972.
- Siegfried, K. R. and Kimble, J. (2002). POP-1 controls axis formation during early gonadogenesis in *C.elegans*. *Development* **129**, 443-453.
- Slatis, H. M. (1955). Position effects at the *brown* locus in *Drosophila melanogaster*. *Genetics* **40**, 5-23.
- Smardon, A., Spoerke, J. M., Stacey, S.C., Klein, M. E., Mackin, N., and Maine, E.M. (2000). EGO-1 is related to RNA-directed RNA polymerase and functions in germ-line development and RNA interference in *C.elegans*. *Current Biology* **10**, 169-178.
- Solomon, M.J., Lee, T., and Kirschner, M.W. (1992). Role of phosphorylation in p34cdc2 activation - identification of an activating kinase. *Molecular Biology of the Cell* **3**, 13-27.
- Sternberg, P.W. and Horvitz, H.R. (1988). *lin-17* mutations of *Caenorhabditis elegans* disrupt certain asymmetric cell divisions. *Developmental Biology* **130**, 67-73.
- Stinchcomb, D.T., Shaw, J.E., Carr, S.II., and Hirsh, D. (1985). Extrachromosomal DNA transformation of *Caenorhabditis elegans*. *Molecular and Cellular Biology* **5**, 3484-3496.

- Sulston, J. and Brenner S. (1974). The DNA of *C.elegans*. *Genetics* **77**, 95-104.
- Sulston, J. and Horvitz, H.R. (1977). Post-embryonic cell lineages of the nematode *Caenorhabditis elegans*. *Developmental Biology* **56**, 110-156.
- Sulston, J. and Horvitz, H.R. (1981). Abnormal cell lineages in mutants of the nematode *C. elegans*. *Developmental Biology* **82**, 41-55.
- Sulston, J. and Hodgkin, J. (1988) Methods. In *The Nematode Caenorhabditis elegans* (ed. Wood, W.B.), pp. 587-606. Cold Spring Harbor Laboratory Press, Cold Spring Harbor, NY.
- Sulston, J.E. and White, J.G. (1980). Regulation and cell autonomy during postembryonic development of *C. elegans*. *Developmental Biology* **78**, 577-597.
- Sulston, J.E., Schierenberg, E., White, J.G., and Thomson, J.N. (1983). The embryonic-cell lineage of the nematode *Caenorhabditis elegans*. *Developmental Biology* **100**, 64-119.
- Sundaram, M., and Han, M. (1996). Control and integration of cell signaling pathways during *C. elegans* vulval development. *Bioessays* **18**, 473-480.
- Sunkel, C.E. and Glover, D.M. (1988). *polo*, a mitotic mutant of *Drosophila* displaying abnormal spindle poles. *Journal of Cell Science* **89**, 25-38.
- Tabara, H., Grishok, A., and Mello, C.C. (1998). RNAi in *C.elegans*: Soaking in the genome sequence. *Science* **282**, 430-431.
- Tabara, H., Sarkissian, M., Kelly, W.G., Fleenor, J., Grishok, A., Timmons, L., Fire, A., and Mello, C.C. (1999). The *rde-1* gene, RNA interference, and transposon silencing in *C.elegans*. *Cell* **99**, 123-132.
- Talbert, P.B., LeCiel, C.D., and Henikoff, S. (1994). Modification of the *Drosophila* heterochromatic mutation *brown*Dominant by linkage alterations. *Genetics* **136**, 559-571.
- Tenenhaus, C., Schubert, C., and Seydoux, G. (1998). Genetic requirements for PIE-1 localization and inhibition of gene expression in the embryonic germ lineage of *Caenorhabditis elegans*. *Developmental Biology* **200**, 212-224.
- Thacker, C., Peters, K., Srayko, M., and Rose, A.M. (1995). The *bli-4* locus of *Caenorhabditis elegans* encodes structurally distinct *kex2*/subtilisin-like endoproteases essential for early development and adult morphology. *Genes & Development* **9**, 956-971.
- Thorpe, C.J., Schlesinger, A., Carter, J.C., and Bowerman, B. (1997). Wnt signaling polarizes an early *C.elegans* blastomere to distinguish endoderm from mesoderm. *Cell* **90**, 695-705.
- Thorpe, C.J., Schlesinger, A., and Bowerman, B. (2000). Wnt signalling in *Caenorhabditis elegans*: regulating repressors and polarizing the cytoskeleton. *Trends in Cell Biology* **10**, 10-17.

- Timmons, L. and Fire, A. (1998). Specific interference by ingested dsRNA. *Nature* **395**, 854-854.
- Timmons, L., Court, D., and Fire, A. (2001). Ingestion of bacterially expressed dsRNAs can produce specific and potent genetic interference in *Caenorhabditis elegans*. *Gene* **263**, 103-112.
- Toyoshima-Morimoto, F., Taniguchi, E., and Nishida, E. (2002). Plk1 promotes nuclear translocation of human Cdc25C during prophase. *EMBO Reports* **3**, 341-348.
- Wang, W.F. and Shakes, D.C. (1997). Expression patterns and transcript processing of *ftt-1* and *ftt-2*, two *C.elegans* 14-3-3 homologues. *Journal of Molecular Biology* **268**, 619-630.
- Ward, S. and Carrell, J.S. (1979). Fertilisation and sperm competition in the nematode *Caenorhabditis elegans*. *Developmental Biology* **73**, 304-321.
- Watanabe, N., Broome, M., and Hunter, T. (1995). Regulation of the human WEE1HU CDK tyrosine 15-kinase during the cell-cycle. *EMBO Journal* **14**, 1878-1891.
- Waterhouse, P.M., Graham, H.W., and Wang, M.B. (1998). Virus resistance and gene silencing in plants can be induced by simultaneous expression of sense and antisense RNA. *Proceedings of the National Academy of Sciences of the United States of America* **95**, 13959-13964.
- Waterston, R., Sulston, J., and Coulson, A. (1997) The Genome. In *C.elegans II* (eds. Riddle, D.J., Blumenthal, T., Meyer, B.J and Priess, J.R), pp. 23-46. Cold Spring Harbour Laboratory Press, Cold Spring Harbour, NY.
- White J (1988) The anatomy. In *The Nematode Caenorhabditis elegans* (ed. Wood WB), pp. 81-122. Cold Spring Harbor Laboratory Press, Cold Spring Harbor, NY.
- White, J.G., Southgate E, Thomson JN, and Brenner S (1986). The structure of the nervous system of the nematode *C.elegans*. *Philosophical Transactions of the Royal Society of London* **314B**, 1-340.
- Williams, B.D., Schrank, B., Huynh, C., Shownkeen, R., and Waterston, R.H. (1992). A genetic-mapping system in *Caenorhabditis elegans* based on polymorphic sequence-tagged sites. *Genetics* **131**, 609-624.
- Williams, B.D. and Waterston, R.H. (1994). Genes critical for muscle development and function in *Caenorhabditis elegans* identified through lethal mutations. *Journal of Cell Biology* **124**, 475-490.
- Williams, B.D. (1995). Genetic mapping with polymorphic sequence-tagged sites. In *Caenorhabditis elegans: Modern Biological Analysis of an Organism* (eds. Epstein, H.F. and Shakes, D.C.), pp81-96. Academic Press. San Diego.

- Wilson, M.A., Hoch, R.V., Ashcroft, N.R., Kosinski, M.E., and Golden, A. (1999). A *Caenorhabditis elegans wee-1* homolog is expressed in a temporally and spatially restricted pattern during embryonic development. *Biochimica et Biophysica Acta-Gene Structure and Expression* **1445**, 99-109.
- Wodarz, A. and Nusse, R. (1998). Mechanisms of Wnt signaling in development. *Annual Review of Cell and Developmental Biology* **14**, 59-88.
- Wood W.B. (1988) Introduction to *C.elegans* Biology. In *The Nematode Caenorhabditis elegans* (ed. W.B.Wood), pp. 1-16. Cold Spring Harbour Laboratory Press, Cold Spring Harbor, NY.
- Yaffe, M.B., Schutkowski, M., Shen, M.H., Zhou, X.Z., Stukenberg, P. T., Rahfeld, J.U., Xu, J., Kuang, J., Kirschner, M.W., Fischer, G., Cantley, L. C., and Lu, K. P. (1997a). Sequence-specific and phosphorylation-dependent proline isomerization: A potential mitotic regulatory mechanism. *Science* **278**, 1957-1960.
- Yaffe, M.B., Rittinger, K., Volinia, S., Caron, P.R., Aitken, A., Leffers, H., Gamblin, S.J., Smerdon, S.J., and Cantley, L.C. (1997b). The structural basis for 14-3-3: phosphopeptide binding specificity. *Cell* **91**, 961-971.
- Zamore, P.D., Tuschl, T., Sharp, P.A., and Bartel, D.P. (2000). RNAi: Double-stranded RNA directs the ATP-dependent cleavage of mRNA at 21 to 23 nucleotide intervals. *Cell* **101**, 25-33.
- Zhu, J. W., Hill, R.J., Heid, P.J., Fukuyama, M., Sugimoto, A., Priess, J.R., and Rothman, J.H. (1997). *end-1* encodes an apparent GATA factor that specifies the endoderm precursor in *Caenorhabditis elegans* embryos. *Genes & Development* **11**, 2883-2896.
- Zhu, J. W., Fukushige, T., McGhee, J.D., and Rothman, J. H. (1998). Reprogramming of early embryonic blastomeres into endodermal progenitors by a *Caenorhabditis elegans* GATA factor. *Genes & Development* **12**, 3809-3814.